OUR COVER

Actual photograph taken underwater of an operating laser transmitter designed at ASD Burlington for the Navy in order to study underwater laser transmission characteristics (described in paper by Okoomian, this issue). The transmitter is a self-contained, battery-powered, coherent green radiation source, housed in a container designed to operate at a depth of up to 1,000 ft. It is fitted with cable connections to permit remote operation and recharging of batteries. The laser beam, of noncircular cross-section, has 1-milliradian-minimum and 3-milliradian-maximum angular spread. (Photograph provided through courtesy of C. W. Haney, Trenton, N.J.; cover art direction, J. Parvin.)

Product Engineering

Recently I joined the Product Engineering group and have had an interesting time becoming acquainted with my new associates and their activities. I believe you also will find this of interest. In charge of this staff activity is Mr. D. F. Schmit. Mr. Schmit has been with RCA for over forty years. During this time he has made many friends and has become well acquainted with the various businesses within our Corporation. Through his staff and by personal involvement, he has provided many kinds of assistance to RCA's operating divisions, and done much to promote the professional status of RCA engineers.

One of the activities within Product Engineering is managed by Mr. W. O. Hadlock. All of you know something of Bill and his staff because they publish this magazine. What you may not know is that they are responsible for many other things that help you. Do you not like the ease with which you can get the pertinent facts about an RCA technical report from just the title page? Have you used the *RCA Technical Reports Index?* These are just two things that have come from the Publications group.

Mr. J. P. Veatch, with offices in Washington, D.C., heads up the RCA Frequency Bureau for Mr. Schmit. Jim and his associates staff the Frequency Bureau offices in Washington, D.C., Camden, N.J., and New York, N.Y. Many facets of our business are concerned with the radio frequency spectrum and our Frequency Bureau is constantly working to protect RCA's interest in this area. They also help represent the United States in international frequency allocations and utilization conferences. In addition, they can help you interpret the FCC rules, obtain a station license, or get type approval on a new transmitter.

Another member of Mr. Schmit's staff is Mr. H. E. Schock. Harvey specializes in the area of product assurance. He is well informed on quality assurance techniques used by industry, as well as the many groups within RCA. He spends much of his time keeping our Quality Assurance groups informed of new developments and works with them to solve problems in this area.

A relatively new activity within Product Engineering is managed by Mr. J. W. Wentworth. John and his staff are taking some impressive steps in the area of continued education for engineers. You will be reading more about the pioneering efforts of this team and their CCSE Program in the future.

Corporate Standardizing, under Mr. S. H. Watson, is a portion of the activity with which you should be well acquainted. Sam and his associates guard the integrity of the RCA drawing system and work closely with divisional groups to provide up-to-date standards with a minimum of duplication. You will find that excellent service will be provided when you request a drawing showing any standard item. In addition this group can be helpful when trying to locate old drawings.

Another member of our staff is Mr. G. A. Kiessling. George and his associates are concerned with a wide variety of activities that include education of engineers, professionalism, and communications. George provides liaison between our Company and several outside information sources. He plans and develops a number of very effective information exchange programs for our engineering supervision. He also is responsible for that popular publication *Trend*.

This is the Product Engineering organization together with a sampling of the services offered. It is a staff activity and, therefore, available to aid you. We invite you to take full advantage of our service.

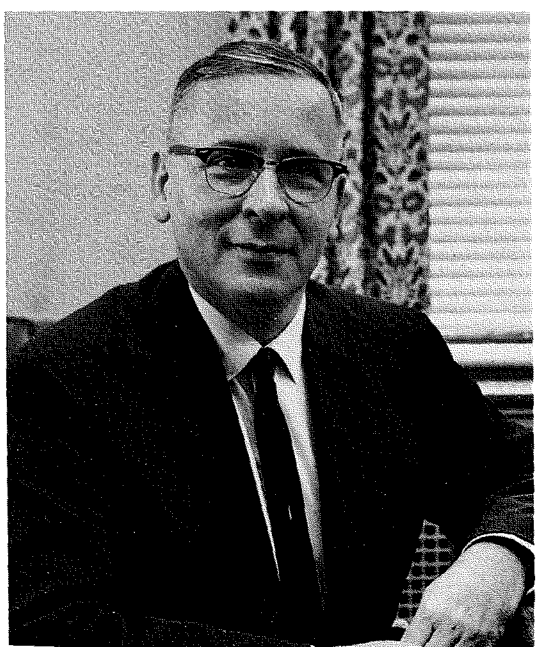

W. C. Morris

W. C. Morriso
Director, Product Engineerin
Research and Engineer n
Camden, N.

RCA ENGINEER

VOL. 12, NO. 3
OCT.-NOV., 1966

CONTENTS

PAPERS

NOTES

DEPARTMENTS

A TECHNICAL JOURNAL PUBLISHED BY **RADIO CORPORATION OF AMERICA,** PRODUCT ENGINEERING 2-8, CAMDEN, N. J.

● *To disseminate to RCA engineers technical information of professional value.* ● *To publish in an appropriate manner important technical developments at RCA, and the role of the engineer.* ● *To serve as a medium of interchange of technical information between various groups at RCA.* ● *To create a community of engineering interest within the company by stressing the interrelated nature of all technical contributions.* ● *To help publicize engineering achievements in a manner that will promote the interests and reputation of RCA in the engineering field.* ● *To provide a convenient means by which the RCA engineer may review his professional work before associates and engineering management.* ● *To announce outstanding and unusual achievements of RCA engineers in a manner most likely to enhance their prestige and professional status.*

RCA ENGINEER articles are indexed annually in the April-May Issue and in the "Index to RCA Technical Papers."

THE engineer's formal means of professional communication consists largely of technical reports, published papers, and oral presentations. Logically, a written report should always come first, since this can be the most comprehensive of the group. From this base, both the professional paper and the oral presentation can easily be derived. An understanding of the techniques and procedures of the professional writer, and of the basic differences between reports, papers, and talks, can be of great help to the engineering author.

One does not become an accomplished writer or speaker after reading one paper about these subjects. However, it could help. This paper concentrates on *practical* advice and counseling for potential authors who are anxious to improve their capabilities.

The Engineer and the Corporation

THE ENGINEER AND HIS PROFESSIONAL COMMUNICATION

I. M. SEIDEMAN, Mgr.
Astro-Electronics Division
Reports and Proposals
Princeton, N. J.

YOUR TECHNICAL REPORT

The present nature of engineering at RCA dictates a rapid pace for everything we do. Professional writers can turn out quite satisfactory reports in very little time. If you, the engineering author, learn the basic techniques and procedures for professional writing, you can make your own lot easier, and avoid the cost or schedule overruns often resulting from a wrong start.

The approach to writing a report is basically the same as that for solving an engineering problem. It is necessary to move in an orderly manner: to analyze, classify, and synthesize. Even when a piece of electronic equipment must be designed in a hurry, you still do not lay out the chassis before you select the circuitry. If you can find standard, state-of-the-art circuits for your design, you use those rather than unproven, exotic configurations—even though the latter may seem intriguing and impressive. And if you knew an engineer with experience in the equipment you were designing, you probably would discuss your plans with him, to get the benefit of his advice. Very much the same thing applies to report writing. No matter how great the rush, you should:

1) Plan your report in advance.
2) Use specific and straightforward language.
3) Get advice or help from your Publications Support group.
4) Read, remember, and use the techniques and procedures adopted by professional writers.

When Write is Wrong

The last thing to do first is to write. When you suddenly realize that work on the report can no longer be put off, sit quietly for a few seconds to settle your nerves and then ask yourself these questions:

1) Who am I writing for?
2) What will I say?
3) How much do I have time to say?
4) In what order will I say it?
5) How will I say it?
6) What don't I want to say?
7) What help can I get—and how soon?

You already know the answers to some of these questions; the information in this paper will help you answer the others. When you have settled on satisfactory answers, you will not only be able to write with speed and certainty; you will also have greatly reduced the chances that an editor or a reviewer will ask for a rewrite or prolonged explanatory sessions.

To help you arrive at the right answers, let's examine the import of these questions.

Who Am I Writing For?

If you are writing only for the information of your supervisor, you can assume that he knows the project background, its special language, and how isolated events fit into the general context of the project's progress: in this case, write as though you were talking to him. But if your report is to go to management or the customer (via your publications group), then you must avoid laboratory jargon, and include the necessary background and explanations to make what you say comprehensible to the technical layman (i.e., any engineer who doesn't know as much as you do). Abbreviations, coined or borrowed words, and general terms (such as "tested satisfactorily") should be explained. The relation of smaller portions of the project, or equipment, to the over-all project should be noted. This is the time, too, to discover if a writing or publication specification has been invoked. If this is the case, get an explanation of its effect from your publications group.

But doesn't all this take *more* time instead of less? Not in the long run. Time spent to plan and to establish a firm base of understanding permits faster progress in the later stages of writing. And less time is taken if you freely accept this approach instead of mentally protesting at every step.

One other point. You are also writing for a typist. She is in short supply and overworked. Pity the poor girl, and speed up the processing of your work by anticipating her problems. Double-space your handwritten manuscript. Dot your *i*'s and cross your *t*'s—these are important clues in her isolating little groups of graphite ripples into *m*'s, *n*'s, *u*'s and *w*'s. Distinguish *beta*'s from capital *B*'s—a note in the margin that you have started on the Greek alphabet helps. Print new and unusual words the first time they appear. And remember that the typist types what she sees; don't print in capital letters if the typed draft is to be lowercase.

IRVING M. SEIDEMAN received his BS degree in Physics from Carnegie Institute of Technology in 1941. He then joined the RCA-Victor Division in Camden, N. J. as a member of the Publications Section of the Special Apparatus Group. In 1946, he became an advertising copy writer for the International Division of RCA. He left RCA in 1947 for work in industrial advertising and electronic equipment sales, but returned to the Missile and Surface Radar Division in Moorestown in 1956 as a Publications Engineer on the TALOS and BMEWS programs. When the Astro-Electronics Division was formed in 1958, he transferred to this activity and handled publications for the TIROS, RELAY, NIMBUS, and other spacecraft projects. He was promoted to Leader, Publications Engineers in 1962, and became Manager, Reports and Proposals, in January 1964. He also has been an Editorial Representative for the RCA Engineer since 1963.

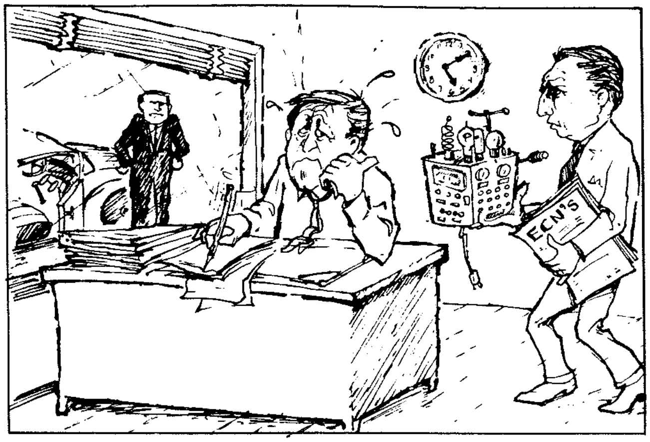

Fig. 1—Most reports are written in a hurry.

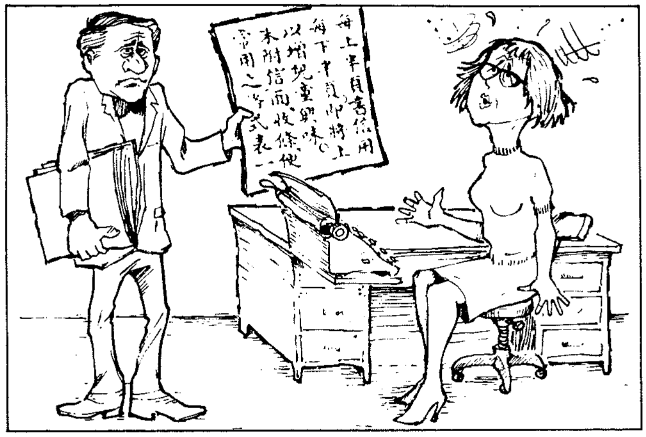

Fig. 2—You are also writing for a typist.

What Will I Say?

The specifics of what to say depends on the project and the type of report. However, it always helps to first list the most important topics, then the next most important, etc. Then develop a continuity for each topic, for example, discussing in turn: 1) the design concept, 2) the established design, 3) the equipment construction, 4) its test, and 5) its acceptance—or 1) the delivery of a vendor item, 2) its test, rejection and return to the vendor, and 3) its redelivery, test, and acceptance. Whatever the sequence, follow through to a disposition that doesn't leave the reader hanging.

A published report of a similar type might be helpful as a reference in organizing your report; ask your publications group to look for a suitable one that might be borrowed.

How Much Do I Have Time to Say?

Words must be equated to time and money. The size and scope of the report should be established (if it has not been previously), based on customer requirements and the project budget. If the report is to consist of several sections, consider the relative importance of each and—before you start writing—ration your word-count accordingly. You may not want to repeat what is in previous or subordinate reports; a summary statement and a reference may do. The extent of detail to be presented must be considered: mathematical derivations often can be shortened, and typical or summary data tabulations can be given in place of comprehensive tabulations. But do not try to telescope three thoughts into one (thus risking ambiguity) or omit articles, adjectives and conjunctions (the reader may think you have just learned English).

In What Order Will I Say It?

For a small project, reporting events in chronological order is a quick and easy way to proceed. For a larger project, each subdivision in turn can be reported this way. If the project involves several phases (e.g., early development, design, prototype production, test, final production), these may be logical basic subdivisions for the report. Parallel study or development of several subsystems may dictate subdivision into these. Whatever method you choose, be consistent, unless compelling reasons dictate a deviation. And be sure the information reported in each subdivision is relevant, logical, and coordinated. Information which may apply equally to more than one subdivision may be reported either in the first or in the one where it is most vital to continuity, and this location referenced at other locations where the information is pertinent.

When you have decided upon your reporting sequence, write it down. This becomes your outline. Then review it to see that all topics are covered. You might want to expand it to include more detail. Use the outline as a checklist or milestone chart. If you have to leave your work for a while, the outline can be used as an index to show where to begin again.

How Will I Say It?

Use simple, direct language to report your information. It takes will power and deliberate effort to think through each sentence as you write it, instead of relying on technical clichés and prefabricated phrases, used like a set of patch cords for any and every purpose. Don't hesitate to cross out an unfinished sentence and start over. More than any other fault, sentences which are started before the ending is thought out

Fig. 3—Use simple, direct language to report your information.

Fig. 4—Assembling a tricycle seems complicated if one has never done it before.

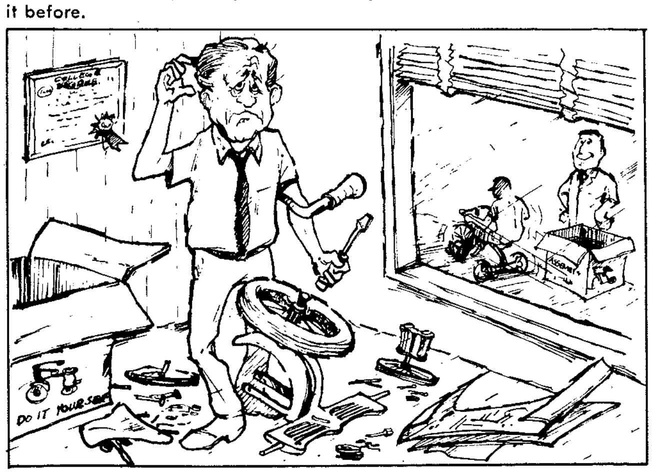

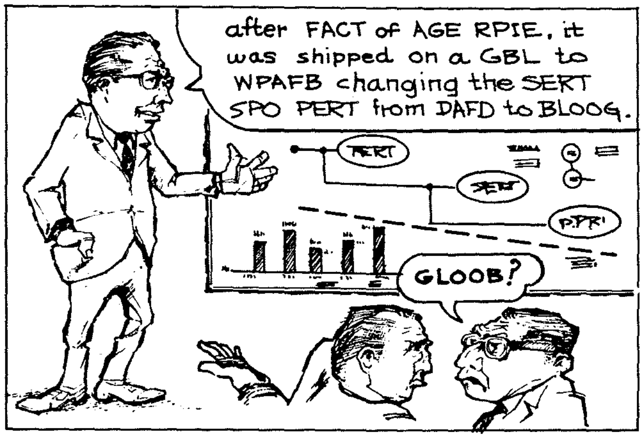

Fig. 5—Do not use abbreviations or acronyms in your talk.

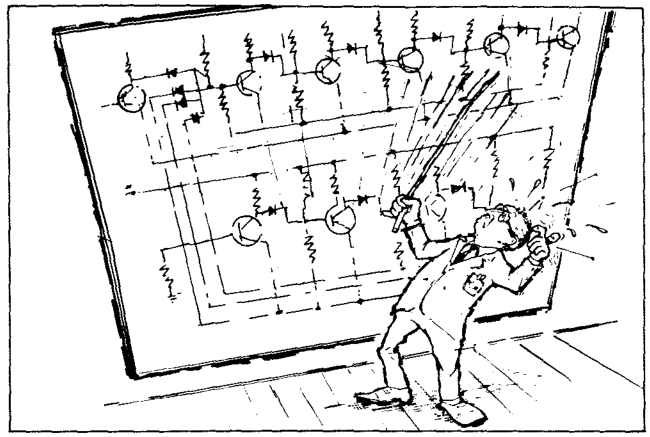

Fig. 6—There are other delays involved . . . such as your own search for a particular part to point to.

tend to slow down both the writer and the reader. Use of abstract words in a sentence often make it difficult to convey an exact thought. *"Implementation of the work was effected"* is an obscure substitute for *"Work was done."* Trying to include afterthoughts in a started sentence most often ends in a confusing statement. Again, rewrite when you rethink.

What Don't I Want To Say?

Although the reader of a report will want to know what went wrong as well as what went right, he is not interested in emotional detail. In short, do not complain and do not blame. Also, do not philosophize. There is a difference between coming to conclusions based on the results of study and research, and giving opinions based on intuition or your personal inclinations.

Don't report implicity. For instance, the statement: *"the video display chassis was transferred from the model shop to the assembly and wiring area"* probably means that *"fabrication of the chassis was completed and assembly of parts on the chassis was started."* The latter statement is specific, and it should be used if that is what is meant. Of course, if a subsystem is shipped to another contractor for integration, this is in itself a milestone, and should be reported.

Don't abbreviate the names of companies or other RCA divisions without spelling them out at frequent intervals. Don't refer to locations only, such as RCA-Lancaster, RCA-Camden; state the division name. There may be more than one division of RCA at a particular location, and vice versa.

What Help Can I Get—And How Soon?

One of the unfortunate facts of life is that a large proportion of an engineering report must be written by the author. This is in contrast to an operating or maintenance handbook, a test plan, and several other types of documents which can, in large part, be ghost written by a technical writer. Among the reasons for this are the fact that a great deal of the report information has never before been communicated; and even if it has been recorded, it is in the form of skeleton notes which can be reconstructed only by the author. Also, the author knows best the degree of success of his work, and he is usually the person best qualified to draw conclusions and make recommendations.

But there is more to a report than the author's first manuscript. If funding is provided for publications support, call them in early. They can help with your outline, interpret any specifications invoked, start the drawings necessary, and take or prepare photographs for the illustrations. They will check your work for coherence and continuity, edit it, type it in "repro" form (that is, the "clean" copy required preparatory to printing), proofread it, make up the Table of Contents, List of Illustrations and Covers, add page numbers, make up an assembly list showing how text and illustrations fit together, print it, collate it, bind it with covers, verify the accuracy of the work, and see that it is distributed to the customer and within RCA. They will then file the text and illustration material and have it available for revisions or a reprint.

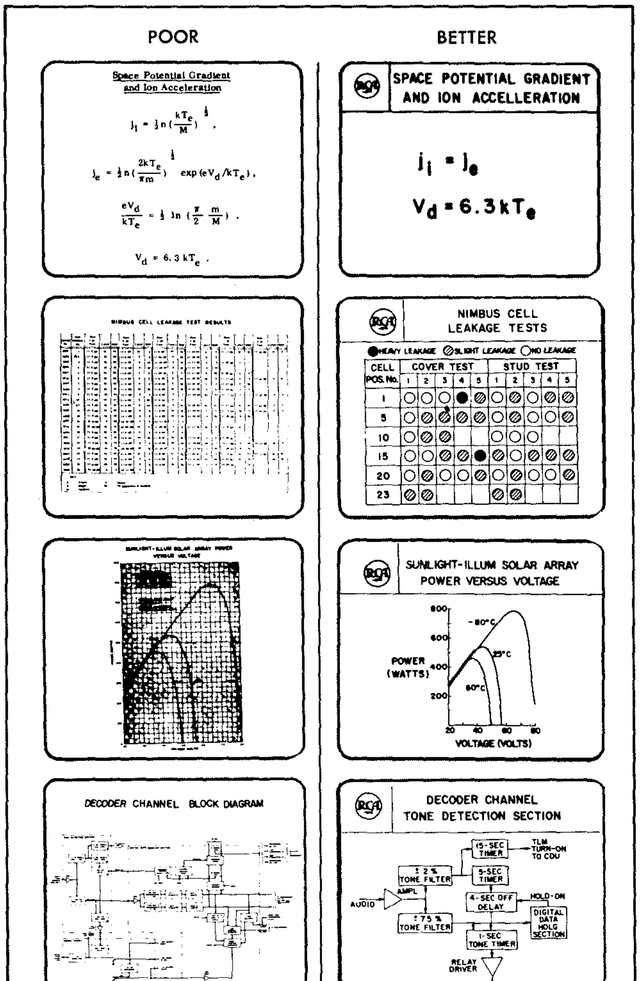

Fig. 7—Examples of slides.

Fig. 8—Make certain that the slide projector provided will take your size slides.

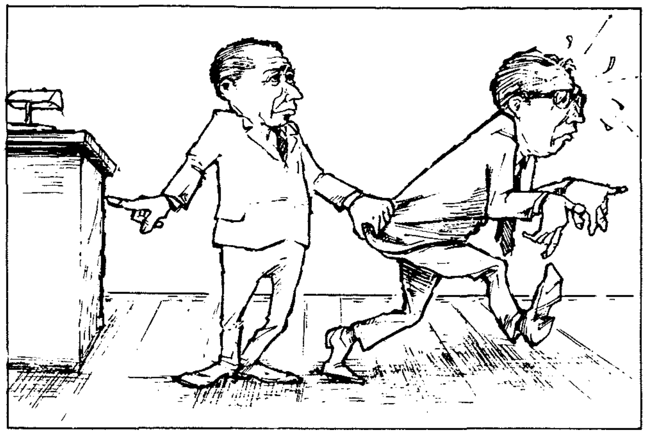

Fig. 9—The idea is not to let your nervousness show.

Practice is Necessary

This writing plan may seem complicated to the harried author whose deadline looms just over the weekend. He should remember that the instructions for assembling a tricycle also seem complicated if one has never done it before. But after going through the procedures once or twice, they suddenly become simple.

When There is Time . . .

The author who has more time to prepare a report may indulge in the luxury of over-writing and then cutting back his material. He may want to review his first manuscript as many as three times: once to delete redundant or extraneous material, once to rephrase what is left, and—if he is an experienced author—once more to refine and polish his sentences, to add sparkle and interest to his manner of expression.

He may want to include more illustrations or discuss his illustrations in more detail instead of leaving their relation to the text implicit. He may want to add references to related work. He may want to add appendixes with detailed supporting information. And he may want to schedule more time for publications editing and production.

YOUR TECHNICAL TALK

An invitation to deliver a talk at a technical meeting implies that the papers committee thinks you have information of current interest and significance to your professional colleagues which would be enhanced by oral delivery. The same information could have been—and might subsequently be—published in a professional journal. Obviously, then, something different than the mere reading of a report or a paper is expected of you when you stand before your audience and speak to them.

Differences Between Talks and Papers

Whether or not you anticipate publication of your paper, you should consider two versions—one suitable for printing, the other suitable for oral presentation. *Why should there be a difference?*

Recent research relating to machine recognition of human language[1] reveals some deep and interesting differences between the hearing and reading processes of the human being. We hear sound in a serial fashion, but we read (or, at least comprehend) a group of words in parallel. Further, the listener depends on much more than hearing a sequence of words to understand the speaker's meaning.

The reader can proceed at his own pace; the listener must keep up with the speaker's. The reader can scan, can reread, can refer from text to illustrations and back, and can stop to consult a basic text or a dictionary; the listener depends on the speaker to make everything clear in logical sequence. The sentences of a talk should be short and straightforward, the audience is unlikely to grasp the complex relationships in long sentences with many explanatory and restrictive modifiers. A paper for publication may be of almost any length (the journal editor can run it in two parts, or may negotiate on its final size); a talk must be carefully planned not to exceed the pre-established time allocated for its presentation. There should *not* be a one-to-one correspondence in detailed content between a talk and a paper; the author often may assume his audience will read his detailed paper in published proceedings of the meeting.

Organization Of Your Talk

A talk should be developed from your completed report or paper, or from a detailed outline of the information to be presented. It should have an introduction and a conclusion, and maintain continuity inbetween. Although the meeting program may carry an abstract of your talk, assume that the listener has not read it or will not be able to recall it as you begin speaking.

To put your audience at ease (and, perhaps, yourself too), use the first 200 words, more or less, to tell the audience what you are going to talk about. You may occasionally wish to withhold a salient point in your work for a later dramatic impact, but remember that suspense in a technical paper generally is in poor taste.

You will then have your listener anticipating, and receptive to, the main body of your talk. Develop your theme, but assume that the listener believes what you say to be true. Do not try to present detailed analyses or verifications of your work in your talk. Keep mathematical supporting data to a minimum.

An audience needs an occasional amount of relaxation. This may be accomplished by a quip, repetition of a phrase, statement of a familiar fact, or a second or two of silence.

Do not use abbreviations or acronyms in your talk. There are a few notable exceptions: those which are universally known and, perhaps, more easily recognizable in the short form, such as AC, FM, NASA, TIROS, and PERT. With proper emphasis (such as display on a slide) you may get the audience to remember one or two abbreviations or acronyms for long or involved expressions. Indiscriminate usage, however, may have the same effect on your audience as the use of Russian nouns and Arabic verbs; the barrier to understanding is not worth risking.

The use of symbols (other than those well known within the

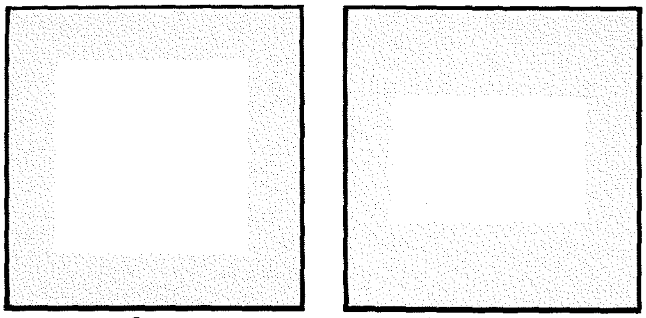

Super 2" x 2" 38 x 38 mm

Standard 35 mm 2" x 2" 23 x 34 mm

Fig. 10—Comparison of image areas of the 2 x 2 super slide and the 35-mm slide.

context of the subject matter) without continual identification can "lose" large portions of your audience. In addition to the phonetic similarity of many symbols (e.g., *b* and *v*, or *c* and *z*), the parameter definitions themselves often are unfamiliar and will bear repeating.

Your talk should have a formal conclusion. You may wish to emphasize the usefulness or the value of the results, the plans or need for additional work, or (if your talk was descriptive) to recapitulate your subtopics. Don't introduce new topics in your conclusion.

The length of your talk will be governed by the time allotted; plan to stay within this time limit. A good figure to use in calculating average talking speed is 140 words per minute. Thus, a 20-minute talk with no planned breaks would consist of about 2,500 words. However, you must reduce this number somewhat if you plan to show slides.

Several elements contribute to the time allotment for slides. The considerate speaker waits for a few seconds after a slide is displayed before he discusses it. The audience will examine it anyway, to the exclusion of the speaker's concurrent remarks, and may then not be able to follow the remaining discussion. There are other delays involved, such as the switching of room lights, occasional aligning of individual slides, and your own search for a particular part of the slide to point to. (A flashlight-type pointer permits you to stand further away from the screen and minimizes this last delay.) It is wise to deduct 15 seconds from your talking time for each slide; 12 slides, for example, would then cut your narrative by three minutes, or approximately 400 words.

Illustrating Your Talk

If you use slides, or other projected-image illustrations, plan to show a few at a time, and have the auditorium lights turned up in between. A prolonged period of darkness provides a choice environment for slumber or departure.

Avoid showing multiple curves, complex tabulations, etc. unless you want merely to impress the audience with their general complexity. Identify each curve by name; do not use letters or numbers and a separate keyed descriptive list. Hold block diagrams to seven blocks or less.

Transparencies

Art work for transparencies must be arranged to ensure legibility of the projected image. Lettering size should be at least one-twentieth the height of the projected area; if the slide is predominantly text, ten lines of printing is the maximum that is comfortable to view. Color adds to contrast, and tends to reduce glare. However, black-and-white is visible at a greater distance from the screen (for the same light intensity at the projector). The illustration of legible, well-designed slides compared to illegible and crowded slides should make the importance of proper layout obvious.

Large-area transparencies (such as Vu-Graphs) offer advantages in cost and preparation time. In many cases they can be prepared by the author. (Instructions for preparing these are given in the *Appendix* at the end of this paper.)

Some professional societies specify slide size and orientation; your RCA Editorial Representative or publications group can advise you on most requirements. Slide projectors (and even motion-picture projectors) usually are available to accommodate standard or specified characteristics.

Art work prepared for slides usually is suitable for illustrating your printed paper; the reverse, however, is seldom true.

Preliminary Arrangements At The Meeting

Plan to arrive early at the auditorium or meeting room. Contact the session chairman or person in charge of arrangements, let him know you are ready, and confirm the availability of facilities you will need.

1) Is there a public address system? Is there a neck or lavalier microphone available, or do you use a (fixed) podium microphone?
2) Is there a slide projector? Will it take your size slides?
3) Is there a pointer available for you to use when slides are projected? (You may wish to bring your own flashlight-type, if one is available to you).
4) If possible, arrange to have someone at the back of the hall signal to you during your talk if your voice is too loud or inaudible.

Facing the Audience

When you first come to the podium and face your audience, are you nervous? Most speakers are. The idea is not to let your nervousness show. Don't duck your head, rearrange your clothing, or take a tight grip on the podium. *And don't rush into the first sentence of your talk.* Stand quietly for a moment, move your feet a few inches apart, loosen your knee muscles (bend your knees just a bit), and drop your hands loosely to your sides. *RELAX!* Look two or three people in the audience right in the eye (move your head slowly to do this), and then begin with your first sentence.

Try to remain aware of your talking speed. Over-emphasize the explosive consonants (*d*, *t*, *p*, etc.) and hold on to the humming ones (*m* and *n*). That will help the audience to understand you and will keep you from building up speed.

Move around (unless you are dependent on a non-mobile microphone). Do not stride or walk continuously, but change your location from time to time. Your audience will then follow you instead of inventorying the chandeliers to relieve their neck muscles. You may continue to speak while you're moving. However, return to the podium for your conclusion; it will be easier for the session chairman to find you there.

If there is a question and answer session, repeat each question before you answer it. It will verify that you have heard the question correctly, and it will ensure that your entire audience hears both question and answer.

ACKNOWLEDGEMENT

Much of the material on graphic aids was made available by the kind cooperation of S. Skarlatos, Manager of Graphic Arts Production for the Astro-Electronics Division.

APPENDIX: VISUAL AIDS

Several types of visual aids for a speaker are in general use. Each type has advantages and disadvantages, depending upon such things as the audience size, the type of meeting hall, and the facilities available. Those which can be readily prepared in-house are:

Flip Charts

These consist of pads of paper, 28 x 34 inches in size, often containing a faint background grid. Lettering, charts, and simple illustrations are drawn on the sheets, using felt-tip markers, tapes, or other means of drawing black or colored lines. The pad is supported on an easel, and each sheet is "flipped" to the rear as the next becomes of current interest. Either the author or a professional artist can prepare flip charts. They may be considered equivalent to free-hand sketches.

Presentation Boards

These can be procured in any size that is convenient to handle (a practical limit is 30 x 40 inches). Generally, lettering and art work are prepared by a professional artist who uses mechanical aids to produce a high quality of illustration. They may be stacked on an easel, and removed one-by-one as the talk proceeds. They also are more suitable for small audiences.

Projection Transparencies

This category is subdivided by sizes: the smallest and most popular is the 35-millimeter slide; a larger size, known by various trade names (e.g., Vu-Graph, Tekni-fax), has an image area of 7½ x 9½ inches.

35-Millimeter Slides

These slides afford the opportunity for a high-quality display of line drawings, photographs, and text on screens large enough for virtually any size audience. They can be prepared in both black-and-white or color; color "trim" may be used to enhance black-and-white illustrations. Line sharpness and contrast on these slides are good, and subtle variations in shade and color come through well. However, the cost of preparation is relatively high, and more time is required for their preparation than for other types of visual aids. A newer variation of this size is the Superslide, which has a somewhat larger image area with square corners. However, some 35-millimeter projectors will cut off the edges of these slides.

Larger Transparencies

These are large enough to accommodate full-size illustrations as they appear on an 8½ x 11 inch document page. They may be prepared in a great variety of ways. The simplest, perhaps, is through use of a clear acetate medium on which the subject matter is drawn with a grease pencil, broad-stroke pen, or adhesive tape. More commonly, however, art work is transferred to them by simple techniques similar to those used in making prints from engineering drawings. Elaborate preparation, using color, is possible. Because of the larger size and projection technique, portions of the image area may be masked during the initial projection, and then sequentially unmasked to "build up" a picture for the viewers.

Fig. 11—Three booklets in use at the Astro-Electronics Division to assist engineers.

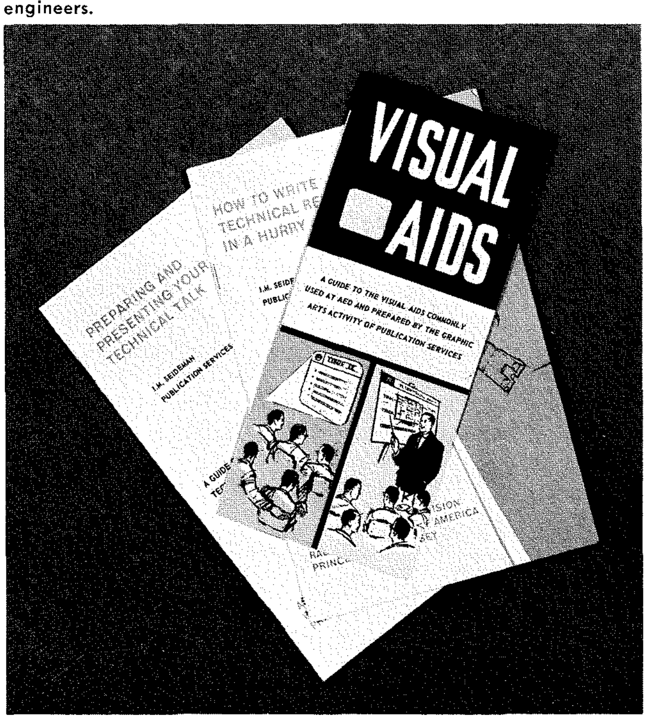

A pre-printed form has been prepared by the Astro-Electronics Division Graphic Arts Group to facilitate the preparation of text or art for these transparencies. The horizontal format is assumed, because it conforms to the aspect ratio of most screens. The large area at the top (see Fig. 12) is provided for the caption; a monogram or other identifying symbol may be inserted at the left. For minimum acceptable quality, free-hand lettering with a soft lead pencil or a black ballpoint pen can be used. For sharp lines and a neater appearance, a sketch should be submitted for redrawing by a professional artist. Material may be typed on this form if the impression is a heavy black.

For reproduction of graphs and charts, the curves or bars should be drawn on the reverse of the graph paper, and only the significant grid lines redrawn.

This size transparency can be the most economical and the fastest to prepare, and consideration should be given to these virtues when a presentation is being planned.

BIBLIOGRAPHY

1. Nilo Lindgren, "Machine Recognition of Human Language, *"IEEE Spectrum* Volume 2, No. 3, p. 114, March 1965.
2. *Aesop's Fables,* Chapt.: "The Hare and the Tortoise," P 34, Grosset and Dunlap, 1946.
   (An early PERT analysis, with some practical results of interest to engineering authors.)
3. Reginal O. Kapp, *The Presentation of Technical Information,* The Macmillan Co., 1948.
   The author presents clearly the difference between "imaginative" and "functional" (i.e., technical) writing; how to *convey* meaning, rather than merely *express* it; and how to avoid saying what you don't mean. The material is taken from a post-graduate course given at University College, London. It is short; it is readable; it has current application.
4. Eugene Ehrlich and Daniel Murphy, *The Art of Technical Writing,* Bantam Books, 1964 (paperback).
   A recent text combining instruction in technical and scientific writing with a handbook of usage and style. The authors seem quite familiar with the conduct of electronic and aerospace projects, and much of the material is directly applicable to current programs at RCA.
5. William Strunk, Jr. and E. B. White, *The Elements of Style,* The Macmillan Co., 1959 (Paperback Edition, The Macmillan Co., No. 107, 1962).
   Small, easy-to-read, text book with specific instructions and examples of the most important elements of style in any type of writing. Wholly applicable to technical reports.
6. Theodore M. Bernstein, *"Watch Your Language,"* Antheneum, New York, 1958.
   An editor of the New York Times compiles from his paper examples of good and bad writing, especially with respect to word usage. Contains many examples of how to say it precisely with a minimum number of words. An eleventh printing, in 1965, confirms its present worth.
7. Robert L. Webb, *Grammar for People Who Wouldn't Have to Worry About it if They Didn't Have Children,* Crowell-Collier Press, 1963.
   In spite of the facetious title and light writing style, this book is an excellent refresher course on parts of speech—for adults.

Fig. 12—Standard Vu-graph format at Astro-Electronics Division.

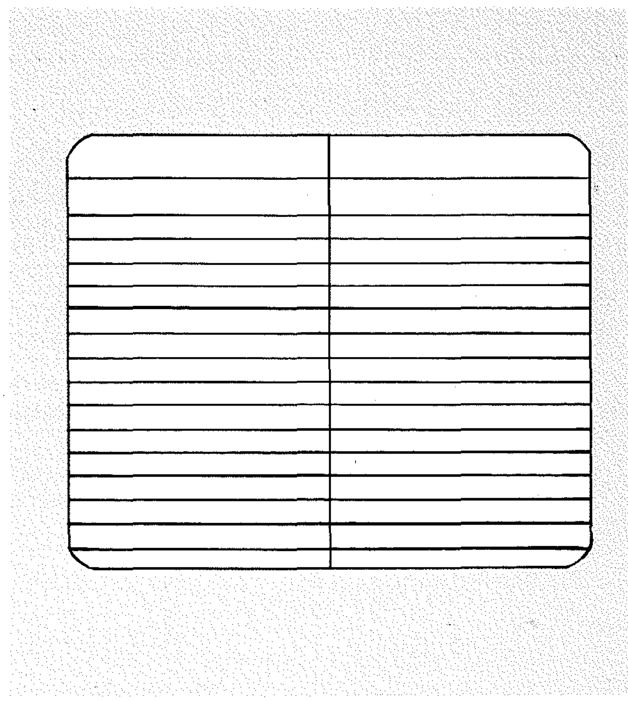

LASERS AND RCA

The laser, now seven years old, has stimulated an extraordinary amount of technical and popular interest. Where does this new development fit into the interests and needs of RCA? What part is RCA playing in the research area? Where is it likely to make use of lasers as a part of a system or in process control, and what will it manufacture? This paper attempts to answer these and other questions concerning lasers in a general manner, while other papers in this issue present details on laser work at: RCA Labs, Princeton; RCA Victor Research Labs, Montreal; Electronic Components and Devices, Somerville; Aerospace Systems Division, Burlington; Astro-Electronics Division, Princeton; and Applied Research, Camden.

Dr. R. B. JANES, Mgr.
Advanced Development
ECD Technical Programs Staff
Electronic Components and Devices, Somerville, N. J.

IN THE seven years since the laser (or optical maser) was first developed, there have been enormous advances in both its technology and its application. The laser is having a pronounced impact on the science of optics, where it has put new life into a somewhat moribund field. It has sparked a great deal of work in the materials area, and the suggested range of applications is ever widening. However, its use in industry is still small, and it remains more a promise than a reality.

ROD-TYPE LASERS

The laser principle was first demonstrated with a rod of ruby crystal. Ruby still remains the most commonly used material for the rod type of laser, which is distinguished by its ability to emit pulses of very high peak powers with modest average power. *Where does RCA fit into this area?*

Much excellent work has been done at RCA Laboratories on new materials for rod lasers. This work includes extensive investigation of calcium fluoride host crystals doped with rare earths, doped calcium tungstate, and yttrium-aluminum-garnet (YAG) host crystals doped with neodymium. YAG is a practical cw crystal laser which is of particular interest in the field of communication. When a YAG laser is properly modulated (e.g., with a gallium arsenide electro-optic crystal), a communications link with a bandwidth wide enough for TV can be designed. However, the rod type of laser must compete with the much more easily modulated and more efficient injection laser.

None of the new materials developed for rod-type lasers compete with ruby for high peak power output. *Where, then, will RCA make use of this work?* There are no plans for RCA to develop and sell laser crystals, nor to make equipment using rod lasers for commercial sale. In the defense area, RCA will have an interest in the new materials for possible use in development of a communications system that can be part of a very large contract. However, this application may be better accomplished with an injection laser. RCA defense engineering activities are also using ruby rod-type lasers for various military applications, including distance-measuring equipments for the army, missile-tracking systems, and special radar transmitters. For such applications, the peak power of the ruby laser permits ranges of several miles. Both the gas laser and the injection laser may be serious contenders in this area, however, particularly for shorter distances.

Final manuscript received August 23, 1966.

ROBERT B. JANES received the B.S. degree in physics from Kenyon College in 1928. He did graduate work in physics at Harvard and at U. of Wisconsin where he received a Ph.D. in 1935. From 1929 to 1931 he taught physics at Colgate U. and from 1931 to 1935 was research assistant at the U. of Wisconsin. From 1935 to 1943, Dr. Janes was an engineer at RCA, Harrison, N. J. where he worked on television camera tubes and phototubes. In 1943 he went to the Tube Division of RCA at Lancaster, Pa. He was in charge of the development and design of television camera tubes until 1950 when he was appointed Manager of the Development Group responsible for camera tubes, storage tubes, and phototubes. In 1953, he was appointed Manager, Color Design, of the Color Kinescope Engineering activity. He became the Manager of the Design activity in the Semi-conductor Division in 1956, and is now Manager, Advanced Development, ECD Technical Programs Staff. Dr. James is a member of Sigma Xi and a Fellow of IRE.

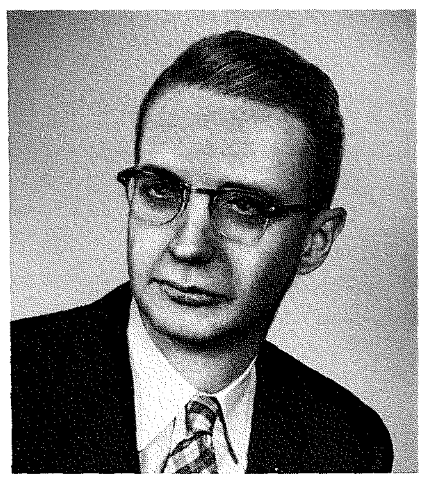

For the future, development of the rod laser appears to be of great importance to RCA in two areas. One is in materials research, where the "fallout" of the work can be of value to the luminescent materials used in color picture tubes. The improved red-emitting phosphor in color tubes has its origin in material research for lasers. The second area is in the use of ruby laser equipment as a tool. This new device may be used for welding fine structures, burning lines in photoresists, and other delicate operations. A ruby laser equipment is now being tested in EC&D as a means of repairing open welds in glass receiving tubes. If the distance between the open leads is not too large, a satisfactory weld can be made by directing the laser beam through the glass onto the leads. The difficulties experienced thus far include a sizable amount of maintenance and cracking of the glass where the hot metal from the weld strikes the bulb. Although both of these problems appear to be solvable, they point up the fact that such equipment has until now been used for experimenting, rather than for actual production.

GAS LASERS

Originally, gas lasers were considered as a source of highly coherent light with a narrow line width but rather low power. This type of laser has been chosen for work in optical fields such as interferometry, and is an excellent research tool. Gas lasers have for some time been able to put out continuous, though low, power. This power output is now being increased very rapidly into the range of several hundred watts. The most powerful gas laser, the CO_2 laser, has a wavelength of 10 micrometers. Although this region is of great interest, suitable detectors must be developed for it.

What about gas lasers and RCA? The gas laser is being used in many scientific investigations. Perhaps the most interesting to RCA is the new area of holography. This method of producing pictures, or some outgrowth of it, is of intense interest to a "picture device" company such as RCA. Because the gas laser can readily be made to emit in the visible region, it is also of great interest for producing TV pictures by new methods. One possibility is to use an electro-optical crystal for horizontal scanning and some mechanical means for vertical scanning. Modulation might possibly be accomplished with an electro-optical crystal such as gallium phosphide.

The best known of the gas lasers is the He-Ne laser, which has an output in the red region. Although argon is a very attractive gas because it lases in the blue region, to date such lasers have had a very short life. RCA Laboratories has recently developed an argon laser with a very long life, and there are plans for EC&D to make this laser on a development basis. In spite of its high power, the gas laser will probably be primarily a research tool for some time to come because of its bulkiness and fragility.

INJECTION LASERS

The semiconductor injection laser is the newest of the lasers, with a history of only four years. The first injection lasers used a p-n junction in gallium arsenide, with the cavity formed by shaping of the junction. The first lasers would operate only at low temperatures (77°K) with high-current pulses. Gradually the efficiency has been improved and the threshold current for laser action has been reduced. RCA Laboratories has made a major contribution to this field in the development of solution epitaxy to form the p-n junction. Today junction lasers can be made to operate under pulsed conditions at room temperature and can operate continuously at 77°K. The best individual lasers can deliver peak powers of 10 watts at room temperature with a current pulse of 40 amperes. The average power can be as high as 0.1 watt. Because injection lasers are extremely small (typically 2 mils by 5 mils by 10 to 20 mils long), a great many can be packed into a small area to create a very bright light source.

The injection laser and its companion, the non-lasing optical diode, are natural devices for RCA to manufacture. They are semiconductor devices, an area in which RCA is already in the marketplace, and they use gallium arsenide, an area in which RCA has made a large investment in technology. Both devices have been in development for four years by a small group in EC&D and for even a longer time by a larger group at RCA Laboratories. This work has been so successful that a new product group has been set up to exploit these devices in the Industrial Tube and Semiconductor Division of EC&D.

The compatibility of this semiconductor approach with EC&D's other work is undeniable. *However, what is the market for these devices?* The optical or non-lasing diode can be used for applications in which a continuous emission is needed at room temperature. If lasing diodes can be made to operate continuously at room temperature and low current levels, they would be preferable for such applications because of their higher efficiency. However, such operation appears to be a long way off. The optical diode can also find a large market in data-processing systems as the light source for card readers. Gallium arsenide is a suitable material for such diodes because it emits in the infrared region, where a silicon diode is an efficient detector. As compared to other light sources, the optical diode has the advantages of very small size, indefinite life (if processed correctly), and capability of being modulated at very high rates.

An optical diode that can emit in the visible region opens up new applications. Such a diode (of rather low efficiency) can now be made to emit in the red region by use of alloy materials of gallium arsenide and phosphide. A great deal of work is in process to improve the efficiency of such diodes by use of RCA's new vapor epitaxial growth process. These diodes can be used as very-long-life indicator lights. Another possible application which is being investigated is alpha-numeric arrays. It appears possible for optical diodes to compete directly with the present "nixie" tubes in this area. Diode arrays not only have the potential of low cost, but also, because of their low-voltage operation, can be driven easily by transistors or integrated circuits.

Where does the semiconductor injection laser fit? To date, there have been two major applications. The first is as a light source for a short-range optical communications system. For this purpose, one or a group of lasers can be operated at room temperature using some sort of pulsed code communication. The equipment can be made very small and rugged, and requires only a small power supply. The second application is as a very bright light source that can be pulsed. Because it is possible to put as many as hundreds of lasers in a very small area, a very bright, powerful light source can be obtained. The efficiency of such a source can be greatly improved by cooling. (An article[1] by M. F. Lamorte gives a more complete review of optical diodes and injection lasers.)

Neither of these applications of the injection laser needs the coherent light of the laser. The narrow angle of emission of the lasing diode, which greatly enhances the brightness (usually given in watts/cm^2/steradian), is the important item. The semiconductor laser is not a particularly good laser because there is always a good deal of non-coherent light emited, the angle of emission is rather large for a laser and there are usually many modes. However, the tremendous advantages of small size, high efficiency, and low voltage make it a very practical tool. It will not be useful in very-high-peak-power applications where the ruby laser fits, and will not supplant the gas laser as a scientific tool. In the future, however, it will find much use in applications requiring large numbers of lasers. With more development its lasing properties will improve, it may be possible to achieve continuous operation at room temperature, and its cost will rapidly fall.

CONCLUSION

Any attempt to prophesy the future in such a new and rapidly changing field is full of pitfalls. Although this paper has pointed out a few of the growing number of applications for lasers, it is more than possible that new uses which fit into RCA's pattern of business may soon outweigh any or all of the functions described.

BIBLIOGRAPHY

1. M. F. Lamorte, "P-N Junctions as Optical Sources," RCA ENGINEER, *this issue.*

P-N JUNCTIONS AS OPTICAL SOURCES

Although RCA traditionally has been in the business of producing and selling light sources, in most cases the devices were designed for electronic rather than illumination functions. While advances made in the past have been remarkable, today the light-source industry may be on the verge of a revolution. Just as the p-n junction revolutionized the amplifying and switching device areas of the electronic components industry, the light-emitting p-n junction may revolutionize the light-source industry, both in types of devices that will be produced and in the scope of their applications. The most dramatic advances during the past 5 to 10 years have been made in gas, insulator-type, and semiconductor laser devices.

M. F. LAMORTE

Electronic Components and Devices

Somerville, N.J.

At present, the most widely used types of solid-state optical sources are the tungsten filament and the electroluminescent phosphors employed in cathode-ray tubes and television screens. The former is a black-body radiator and uses only a portion of the continuous spectrum in any one applications. In the latter an electron beam is used to excite the phosphor, and a series of intense lines is produced rather than a continuum. The tungsten lamp has found little application in electronic functions because of the poor frenquency response of its radiation to high-frequency electrical signals. Electroluminescent phosphors exhibit a frequency response several orders of magnitude higher. Laser-type devices and p-n junction light emitters exhibit even higher frequency response, approaching 1 GHz. Although this paper discusses optical sources as applied to electronic functions, these electronic-type optical sources may also be useful for general illumination applications. The illumination market is well in excess of $1 billion per year.

Final manuscript received August 23, 1966

TYPES OF LIGHT SOURCES

For many years scientists have worked to obtain all-solid-state light sources to perform such electronic functions as transmitting information over light beams and to serve as efficient, inexpensive sources that might replace the cathode-ray type and other types of displays. Although the electron beam as an exciting medium offers some attractive features, low-voltage operation and flat or mural-type display are desirable at price and performance levels which would be competitive with present-day devices.

One type of all-solid-state source which has been under intensive study is the high-field AC and DC electroluminescent device. At the present stage of development, these devices have the disadvantages of low efficiency, poor operating-life characteristics, and high-voltage operation (which makes them incompatible with silicon transistors). If improvements can be made in these areas, however, this type of device would be attractive in some applications for mural displays.

Perhaps the most attractive all-solid-state light source is the p-n junction luminescent diode.[1] Diodes fabricated from many of the varied crystals that exhibit electroluminescence may also be placed in the stimulated-emission mode. The use of this device provides the advantages of high external efficiency in both the incoherent and coherent modes,

MICHAEL F. LAMORTE received the BS from Virginia Polytechnic Institute in 1950 and the MEE from the Polytechnic Institute of Brooklyn in 1951. He held a Teaching Fellowship in 1950-51 and a Research Fellowship in 1951-52 at the latter institution. He was an Adjunct Professor in the E. E. Graduate School of University of Pittsburgh. From 1952 to 1955 he was at the Signal Corps Engineering Labs, Fort Monmouth, N. J., in study of fundamental properties of semiconductors. From 1955 to 1959 he was with the Westinghouse Electric Corp., investigating device theory and technology. Special contributions were made to high-power silicon devices, crystalline material and diffusion studies. In October 1959, he joined the RCA Semiconductor and materials Division at Somerville, N. J., where he has been Engineering Group Leader in Advanced Development, responsible for R&D on varactor diodes and GaAs solar cells up to 1963. Author of several papers, he is a member of the American Physical Society, the IEEE and IEEE-PTGD, Phi Kappa Phi, Tau Beta Pi, and Eta Kappa Nu.

long operating life, and compatibility with driving circuit employing silicon devices. In addition, the high external efficiency reduces the driving-power requirements, and may make possible the use of low-cost silicon integrated circuits. In some cases, the same technology may be employed for different crystals, and the further advantage of greatly reduced development cost results. The diodes which have been reported cover the near-infrared and visible portions of the spectrum. The light intensity may be modulated at frequencies approaching 1 GHz.

Applications for p-n junction light emitters range from electroluminescent displays to such electronic functions as card reading, character recognition, sensing, electro-optical switching, optical ranging, illumination, metrology, communication, intrusion alarms, control circuits, and warning devices. The non-laser diode appears to have a substantial advantage over the laser in present-day devices for display applications; however, the laser diode has distinct advantages for electronic-function applications.

In the following section, the nature of p-n junction luminescence is discussed, and the various crystal materials used in light-emitting diodes are classified according to the portion of the spectrum in which each emits energy.

LIGHT-EMITTING DIODES

In general, light is emitted from a p-n junction when the diode is forward-biased. Minority carriers are injected into the opposite-conductivity-type material, and a nonequilibrium condition is created which causes the carriers to recombine radiatively. External efficiency is proportional to the injection efficiency of the junction. Because the injection efficiency may approach unity when the junction is properly designed, the external efficiency may also approach unity.

There are many known semiconductor materials, and probably many unknown at this time, which emit light when properly fabricated into diodes. Fig. 1 shows various crystal materials and the portion of the spectrum in which they emit radiation. Table I lists these materials and indicates those which also provide laser action. With the exception of SiC, the materials fall into three groups: the III-V group and the II-VI group of the periodic table and lead salts. The lead salts emit radiation toward the far-infrared portion of the spectrum, while the III-V and II-VI groups cover the near-infrared and visible portions of the spectrum. The latter two groups exhibit considerable

TABLE I—Listing of p-n Junction Light Emitting Diodes

Crystal	*Macrometers*	*Laser Action*	*Remarks*	*References*
PbSe	8.5	Yes	direct	2
PbTe	6.5	Yes	direct	2, 3
InSb	5.2	Yes	direct	4
PbS	4.3	Yes	direct	2
InAs	3.15	Yes	direct	5
$(In_x Ga_{1-x}) As$	0.85-3.15	Yes	direct	6
$In (P_x As_{1-x})$	0.91-3.15	Yes	direct	7
GaSb	1.6	No		8
InP	0.91	Yes	direct	9
GaAs	0.90	Yes	direct	10, 11, 12
$Ga (As_{1-x} P_x)$	0.55-0.90	Yes	direct	13
CdTe	0.855	No	homojunction	14
$(Zn_x Cd_{i-x}) Te$	0.59-0.83	No	homojunction	15
$CdTe\text{-}Z_oTe$	0.56-0.66	No	heterojunction	16
BP	0.64	No	indirect	17
$Cu_2Se\text{-}ZnSe$	0.40-0.63	No	heterojunction	18
$Zn (Se_x Te_{1-x})$	0.627	No	homojunction	19
ZnTe	0.62	No	barrier	20
Ga P	0.565	No	indirect-band gap	21
	0.68	No	indirect-oxygen line	
Si C	0.456	?	-SiC homojunction	22

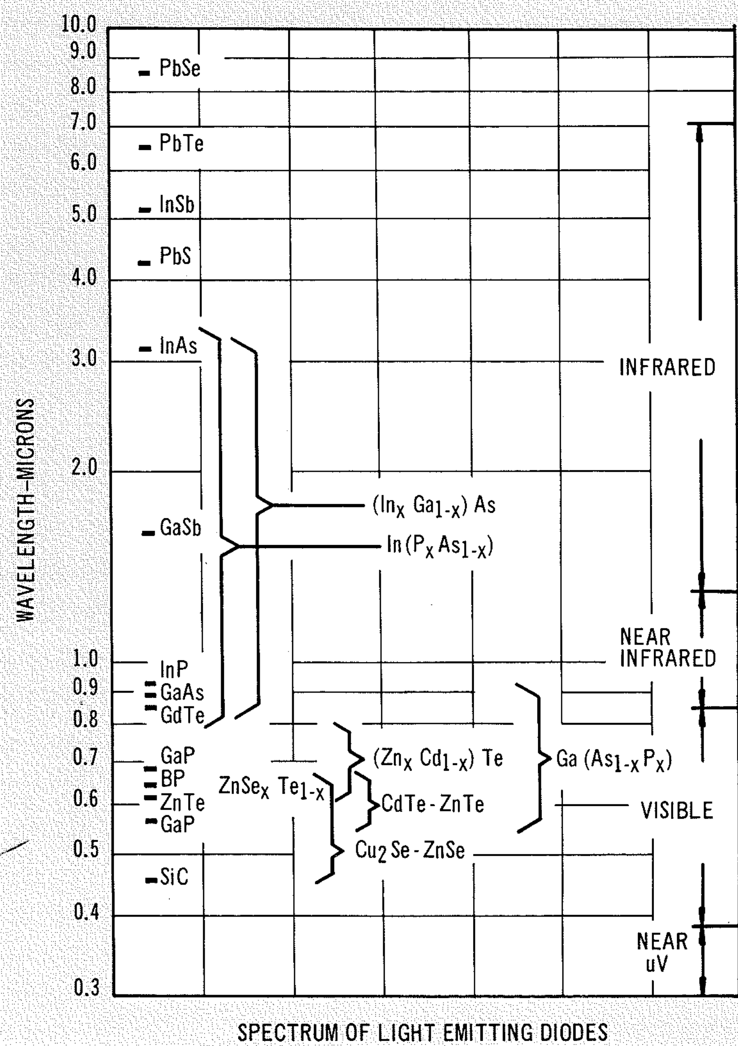

Fig. 1—Various crystal materials and the portion of the spectrum in which they emit radiation.

overlap. Continuous coverage of the spectrum from the blue to the near-infrared region can be obtained by use of mixed crystals.

Generally, any one diode emits one strong line that has width in the order of 300 angstroms. The portion of the spectrum in which the diode emits depends on its forbidden-band energy and/or the position that the dopant takes in the forbidden band. Each semiconductor, including the mixed crystals, possesses a unique bandgap energy and emits a characteristic wavelength. With the crystals shown in Table I, the entire spectrum from 0.45 to 3.1 micrometers can be covered. Further investigation will probably extend this coverage out to 8.5 micrometers. If the II-VI compounds do not adequately cover the spectrum in the blue and near-ultraviolet regions, another group of materials will have to be investigated for this region.

GaAs light-emitting diodes have received more attention than other types for several reasons:

1) Existing military and industrial applications require this type of infrared-emitting device.
2) The emission of GaAs devices matches the peak response of both silicon detectors and photodevices that have an S-1 response.
3) More advanced technology for GaAs crystal growth and device fabrication existed at the time that the most intensive studies on p-n junction light sources were conducted.
4) An ample supply of high-quality GaAs crystal is available from commercial establishments.
5) A certain amount of confidence in fabrication techniques exists as a result of previous experience on other GaAs devices.

In addition, many of the problems associated with increasing the external efficiency of p-n junction light sources are similar to those encountered on other GaAs devices. Therefore, GaAs affords a convenient vehicle for investigation of these problems and improvement of light-emitting devices.

PERFORMANCE OF P-N JUNCTION DIODES

The performance of a light-emitting device is determined in large measure by the quality of the p-n junction. It is difficult to form high-injection-efficiency junctions in some crystals. In the lead salts and the III-V compounds, both n- and p-type crystals may be obtained easily; therefore, homojunctions of high quality may be obtained. In the II-VI compounds, however, n- and p-type crystals of the same crystalline material are not always possible; as a result, heterojunctions must be employed. Because heterojunctions are usually inferior to homojunctions, particularly with respect to injection efficiency, the II-VI compounds are used as a last resort.

Crystalline defects are introduced during the construction of heterojunctions as a result of the mismatch (however small) in the crystalline structure of two different types of crystal. These defects produce energy levels in the band gap at the junction region of the diode. In most cases, depending on the defect density and its activation energy, these defect energy levels adversely affect the internal radiative recombination efficiency. The most probable result is that the defect levels cause a nonradiative recombination process which tends to reduce the radiative recombination efficiency. Moreover, heterojunctions usually require more complex technology, are more difficult to control, and are more difficult to obtain reproducibly. If a choice exists, therefore, homojunctions are more desirable.

A disadvantage of using wide-band-gap materials for luminescent diodes is that low contact resistance is more difficult to obtain. These materials (particularly SiC and GaP) cannot be operated at high-current-density values because of their high contact resistance, coupled with the higher thermal resistance of diatomic and ternary compounds. These resistances serve to reduce the brightness of the emitted radiation. In addition, the impurity atoms assume energy levels within the band gap somewhat removed from the band edges, and result in large activation energies. This condition may lead to carrier freeze-out at low temperatures and render the diodes inoperative at such temperatures. However, improvements in technology and crystalling quality may minimize and perhaps even eliminate these problems.

GaAs diodes exhibit higher efficiencies than any other light-emitting diodes. This greater efficiency can be attributed to the higher crystal quality and more advanced fabrication techniques. Improvements must be made in other materials to match the performance of GaAs diodes. In principle, there is nothing to prevent any of the light-emitting diodes from attaining an internal quantum efficiency of unity. The external efficiency is usually low because of reabsorption and a small critical angle in most semiconductor materials.

BIBLIOGRAPHY

1. J. I. Pankove and M. J. Massouli, "Injection Luminescence from Gallium Arsenide," *Bull. Am. Phys. Soc. 7,* 98 (1962)
2. J. F. Butler and A. R. Calawa, "Magneto-Emission Studies of PbS, PbTe and PbSe Diode Lasers"
3. J. F. Butler, A. R. Calawa, R. J. Phelan, Jr., T. C. Harman, A. J. Strauss, and R. H. Rediker, "PbTe Diode Laser" *Appl. Phys. Lett. 5,* 75 (1964)
4. R. J. Phelan, A. R. Calawa, R. H. Rediker, R. J. Keyes, B. Lax, "In Sb Diode Laser," *Appl. Phys. Lett. 3,* 143 (1963)
5. I. Melngailis, "Maser Action in InAs Diodes," *Appl. Phys. Lett. 2,* 176 (1963)
6. I. Melngailis, A. J. Strauss and R. H. Rediker, "Semiconductor Diode Masers of $(In_x Ga_{1-x})$ As," *Proc. IEEE 51,* 1154 (1963)
7. F. B. Alexander, V. R. Bird, D. R. Carpenter, G. W. Manley, P. S. McDermott, J. R. Peloke, H. F. Quinn, R. J. Riley and L. R. Yetter, "Spontaneous and Stimulated Infrared Emission from In $(P_x As_{1-x})$ Diodes," *Appl. Phys. Lett. 4,* 13 (1964)
8. A. R. Calawa, "Injection-Luminescence in Ga Sb." *J. Appl. Phys. 34,* 1660 (1963)
9. R. Weiser and R. S. Levitt, "Stimulated Light Emission from In P," *Appl. Phys. Lett. 2,* 178 (1963)
10. M. I. Nathan, W. P. Dumke, G. Burns, F. H. Dill, Jr., and G. J. Lasher, "Stimulated Emission of Radiation from GaAs p-n Junctions," *Appl. Phys. Lett. 1,* 62-64 (1962)
11. R. N. Hall, G. E. Fenner, J. D. Kingsley, T. J. Soltys, and R. O. Carlson, "Coherent Light Emission from GaAs Junctions, *Phys. Rev. Lett. 9,* 366-78 (1962)
12. T. M. Quist, R. H. Radiker, R. J. Keyes, W. E. Krag, B. Lax, A. L. McWhorter, and H. J. Zeiger, "Semiconductor Maser of GaAs," *Appl. Phys. Lett. 1,* 91-92 (1962)
13. J. J. Titejen and S. A. Ochs, "Improved Performance of Ga (Asi-x Px) Laser Diodes," *Proc. IEEE,* 1965
14. G. Mandel and F. F. Morehead, "Efficient Electroluminescence from p-n Junctions in Cd Te at 77° K," *Appl. Phys. Lett. 4,* 143 (1964)
15. F. F. Morehead and G. Mandel, "Efficient Visible Electroluminescence from p-n Junctions in $(Zn_x Cd_{1-x})$ Te," *Appl. Phys. Lett. 5,* 53 (1964)
16. M. V. Kot and A. E. Tsurkan, "Recombination Radiation in p-n Junctions of Crystals of the Cd Te—Zn Te System," *Sov. Physics, Solid State 7,* 2304 (1966)
17. R. J. Archer et al., "Optical Absorption, Electroluminescence, and the Band Gap of BP," *Phys. Rev. Lett. 12,* 538 (1964)
18. M. Aven and D. A. Cussano, "Injection Electroluminescence in ZnS and ZnSe," *J. Appl. Phys. 35,* 606 (1964)
19. M. Aven, "Efficient Visible Injection Luminescence from p-n Junctions in Zn $(Se_x Te_{1-x})$ *Appl. Phys. Lett. 7,* 146 (1965)
20. N. Watanake, S. Usui, and Y. Kanai, "Injection Luminescence in Zn Te Diodes," Japan. *J. Appl. Phys. 3,* 427 (1964)
21. M. Gershenzon and R. M. Mikulyak, "Light Emission From Forward-Biased p-n Junctions in Ga P," *Solid-State Electronics 5,* 321 (1962)
22. L. B. Griffiths "SeC, Diode Laser," *Proc. IEEE 51,* (1963)

LASER STUDIES AT
RCA VICTOR RESEARCH LABORATORIES, MONTREAL

A Review

Laser research has been in progress for several years in the Montreal Laboratories of the RCA Victor Company, Ltd. This work has emphasized gas laser studies, and was a rather natural extension of the interests and technologies already existing as part of the extensive gaseous plasma physics activities in the laboratory. This paper describes laser investigations which have been undertaken in the fields of spectroscopy, interferometry and plasma diagnostics. Also presented is recent work involving the use of lasers for altering the population distributions in gas discharges. Results of several experiments on new, high-power carbon dioxide lasers constructed in the laboratory are also given. These devices have been used to generate watts of cw power with high efficiencies in the infrared and are of interest for several applications. In addition a summary is given of recent work on lithium-drifted silicon photodiodes for fast, high-sensitivity laser detectors.

Dr. A. I. CARSWELL, Director
Optical and Microwave Physics Lab.
Research Laboratories
RCA Victor Company, Ltd., Montreal, Canada

LASER research has been in progress for several years in the Montreal Laboratories of the RCA Victor Company, Ltd. This work has emphasized gas lasers and was a rather natural extension of the interests and technologies already existing as part of the extensive gaseous plasma physics research activities in the laboratory.[1] Much of the laser work has centered on the plasma properties of lasing discharges and on the use of lasers as high-frequency coherent electromagnetic wave generators for plasma diagnostic applications. Lasers now provide sources having coherence properties comparable to sources previously existing in the microwave region, so that many of the conventional microwave diagnostic methods can be reapplied at optical frequencies. In addition, at the higher frequencies, new and important phenomena can be observed.

Associated with this work has been a continuing effort to improve the properties and operating characteristics of various solid state photon detectors in the visible and infrared spectral regions. Since the advent of lasers, much of the detector work has been directed towards optimizing certain detector properties (e.g. response time and spectral sensitivity) for particular laser systems.

Final manuscript received August 1, 1966

In this paper the work in these several areas is summarized, and some of the more recent investigations are described in detail.

He-Ne AND CO_2 GAS LASERS

Much of the initial work at RCA Victor in Montreal involved the use of helium-neon lasers. The gas discharge technology existing in the laboratory permitted the assembly of a variety of systems for the construction and assessment of lasing He-Ne discharges. A considerable portion of the early work was devoted to an investigation of the dependences of the oscillation properties on the various discharge parameters (i.e. current, pressure, mixture ratio, etc.) For this work a number of gas discharge tube configurations have been employed, involving electrodeless, as well as hot and cold cathode tubes and excitation by direct current and by RF and 60-Hz AC.

As one outcome of this work, RCA Victor has developed a low-cost (under $400) He-Ne laser designed for teaching and demonstrating optics in secondary schools and universities. A photograph of this RCA Victor Educational

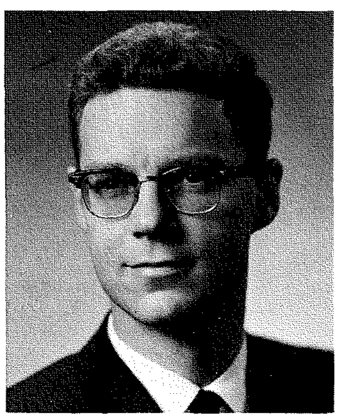

DR. ALLAN I. CARSWELL graduated with honors in 1956 from the University of Toronto with a BASc in Engineering Physics. In the same year he entered the graduate school of the University of Toronto to study molecular physics. In 1960 he received his PhD. In 1960-61, Dr. Carswell studied at the Institute of Theoretical Physics of the University of Amsterdam on a Canadian National Research Council Fellowship. Dr. Carswell joined RCA Victor Co. Ltd. Research Laboratories on his return to Canada in 1961, and since that time has studied the interaction of electromagnetic waves with plasma systems—including microwave scattering from supersonic plasma flow fluids, and studies of the properties of ionized gas flow systems. Recently, Dr. Carswell has been actively engaged in a study of the properties and applications of gas lasers and coherent optical frequency radiation. He is a member of the Canadian Association of Physicists, the American Institute of Physics, and the Canadian Aeronautics and Space Institute.

Laser is shown in Fig. 1. The unit incorporates Brewster angle windows and adjustable mirrors to permit access to the resonant cavity for more advanced experimentation. A dark plastic cover reduces the side light from the discharge tube while still permitting visible observation of the interior parts when the laser is turned on. The laser output is from both ends of the tube in two equal intensity beams (approximately 1 mW). This permits two independent experiments to be performed simultaneously with a single unit.

The advanced plasma tube design incorporates a concentric gas reservoir for long life and has unheated electrodes so that a simple power supply can be employed. The tube operates on either high voltage 60-Hz AC or on direct current which is provided from a power supply enclosed in the base. These lasers have been in use for an extended period in our laboratory and a number have been marketed in Canada. Typical tube lifetimes appear to be in excess of six months and several hundred hours of operation. When necessary, tube replacement can be carried out in a few minutes and at a very low cost. With optional modifications, operation can be achieved at any of the three main neon frequencies (i.e. 0.63, 1.15, or 3.39 micrometers).

These lasers can be invaluable for teaching optics as well as for general laboratory application. Fig. 2 illustrates with unretouched photographs how well the laser can be used to demonstrate ray tracing in geometrical optics. The optical components shown in the photographs are fabricated with transparent plastic which has sufficient internal scattering to make the beam visible and smoke is introduced in the air paths to make the photographs. With the intense coherent laser beam it is also easy to demonstrate phenomena associated with polarization, diffraction and interference. A kit of such experiments has been assembled to be marketed with the laser unit.

More recently, much of the research effort on gas lasers has been directed towards an investigation of the high power carbon dioxide laser. Laser oscillation in carbon dioxide was first observed[2] in mid 1964 and by the end of 1965 it had been found that with the addition of nitrogen and helium to the carbon dioxide, very-high-power high-efficiency laser action would be attained. Continuous power outputs of several hundred watts at efficiencies up to about 20% have recently been reported and under pulsed (Q-switched) conditions peak powers of 50-75 kW have been demonstrated. When compared to other gas lasers these values represent and increase in CW power of one or two orders of magnitude and in efficiency of more than two orders of magnitude.

Because of this high power and efficiency, many possible applications for this laser are apparent. The principal output wavelength of the laser is in the infrared at about 10.6 micrometers in the middle of the 8-to-14-micrometer atmospheric "window".[3] In this wavelength region, absorption by the atmospheric gases is very small ($\simeq$ 0.1 db/km) and scattering by dust and aerosol particles is considerably less than at shorter wavelengths, so there is considerable interest in the CO_2 laser for ground-based communications and radar applications.

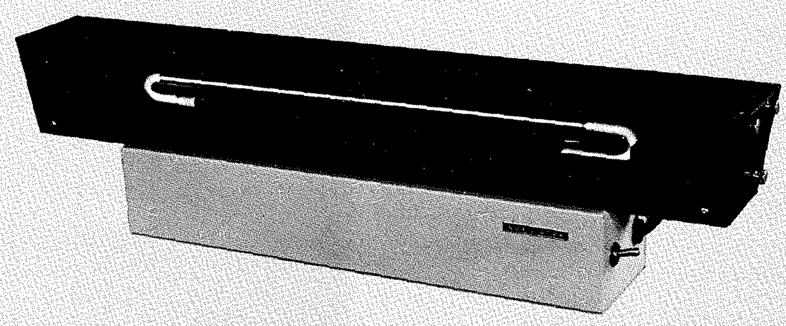

Fig. 1—Low-cost He-Ne laser for teaching and laboratory use developed by RCA Victor Research Labs, Montreal.

In Fig. 3 is shown a schematic energy-level diagram for CO_2 and N_2 to illustrate the mechanism whereby the highly efficient laser oscillation is brought about. There is an almost exact coincidence ($\Delta E = 18$ cm^{-1}) in energy of the first vibrational level of molecular nitrogen with the upper level of the CO_2 laser transition. This leads to a very large probability (cross-section) for the transfer of energy between these two levels. This N_2 level is metastable in that electric dipole transitions to the N_2 ground state are not allowed and as a result sizeable populations of this level are built up leading to a greatly increased population of the upper CO_2 laser level. Coupled with this is the advantageous effects of the metastable states in the added helium on the desired population inversion.[4]

Sample displays of the output spectrum of a CO_2-N_2-He laser are shown in Fig. 4. The three different scans are for identical discharge conditions, but for slightly different mirror separations in the cavity (e.g. produced by thermal drift). It is seen from these results that the oscillation typically occurs simultaneously on a number of the rotational lines in the *P*-branch of the vibrational band. (*P-branch transitions* are those in which the rotational quantum number J changes by $+1$; i.e. $\Delta J = +1$. In the *Q*-branch, $\Delta J = 0$; and for the *R*-branch, $\Delta J = -1$.) These lines, as mentioned above, are in the region of 10.6 micrometers and have a separation of about 0.02 micrometers (200 angstroms).

As the cavity is tuned slightly, very large changes in the relative intensities of these lines can be obtained. The reason for this behavior is shown in Fig. 5 by comparing the typical CO_2 laser oscillator conditions with those of the well-known visible He-Ne laser (0.6328 micrometers). For the case of an optical cavity length (separation between mirrors) of $L = 1.5$ meters, the axial modes of the cavity are separated by a frequency of $c/2L = 100$ MHz. For the visible He-Ne transition, the Doppler broadened profile of the line over which amplification can occur is about 1,500 MHz so that several axial modes will oscillate simultaneously unless special efforts are made to suppress some of them.

At the CO_2 laser frequency of 10.6 micrometers, however, the Doppler width of the line is only about 50 MHz (since the width is inversely proportional to the wavelength) and single mode operation can be readily obtained if the cavity resonance can be set within this 50-MHz width. However, since amplification can occur on several of the rotational lines as indicated in Fig. 5, the relative outputs of these will depend upon the "matching" of the cavity resonance to the particular rotational line. As shown in Fig. 5, when the cavity is tuned for maximum output on one, it may be at a minimum of another, etc. Hence in an unstabilized laser, the

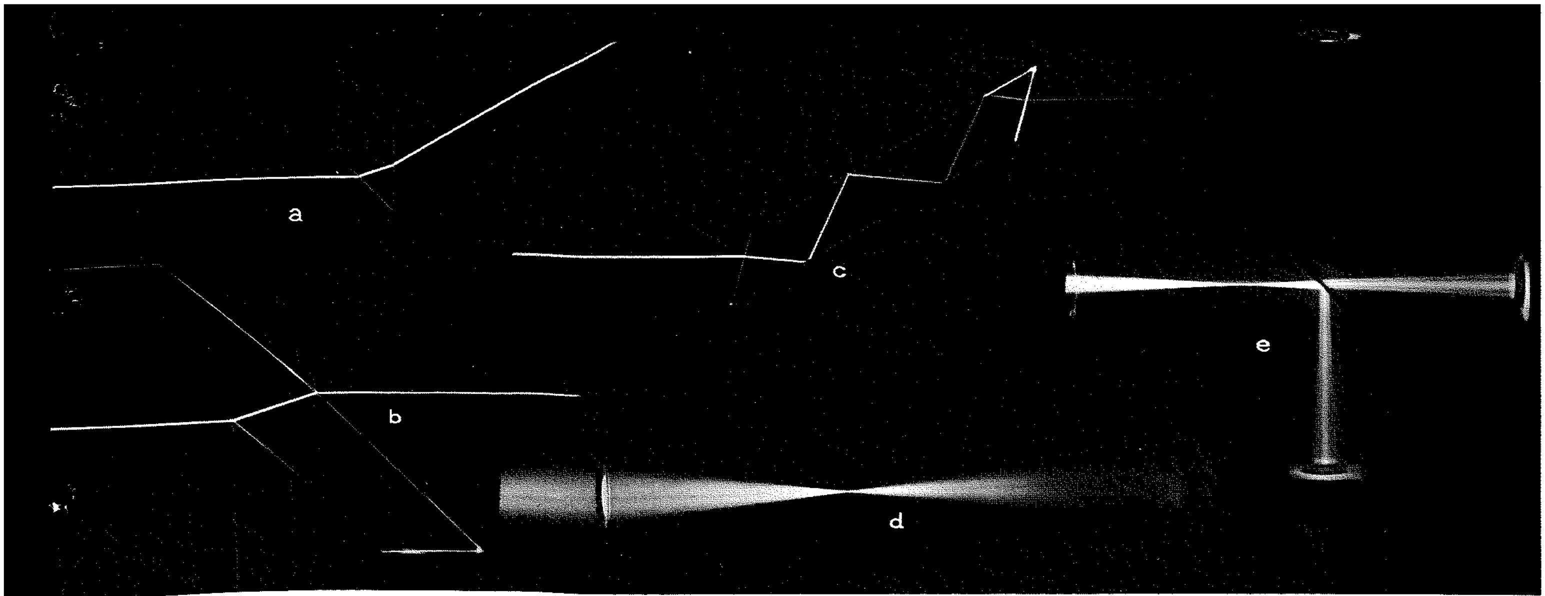

Fig. 2—Sample photographs illustrating the usefulness of the Educational Laser for demonstrating optical phenomena. (a) Prism refraction and reflection (internal and external). (b) Multiple refraction and reflection in a thick plate. (c) Multiple internal reflection in a rhomb. (d) Focussing by a simple lens. (e) Ray paths in a focussed-beam Michelson interferometer.

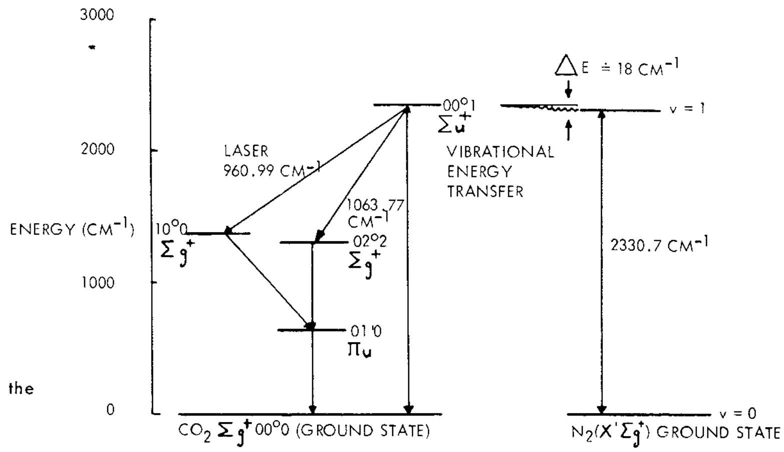

Fig. 3—Energy levels of CO_2 and N_2 involved in the operation of the high-power carbon dioxide laser.

Fig. 4—Sample output spectra of the CO_2 laser for different cavity mode settings. Emission occurs on several rotational lines of the P-branch of the 10.6 μm band. Simultaneous oscillation in the R-branch can also occur but with much lower intensity.

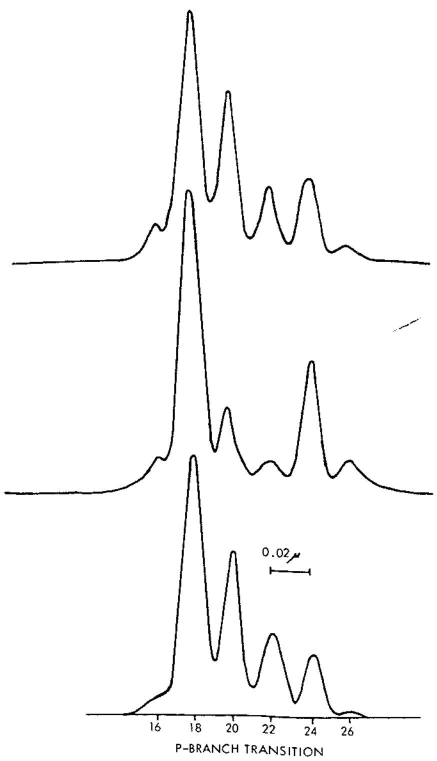

Fig. 5—Comparison of the longitudinal mode spectra of the visible He-Ne and infrared CO_2 lasers in a 1.5-meter cavity ($C/2L = 100$ MHz). (a) Neon gain curve and resonator frequencies. (b) Multimode output spectrum of He-Ne laser. (c) Gain curves for 3 sample rotational levels in CO_2 and the associated resonator frequencies. (d) Single mode output on each of the 3 rotational transitions.

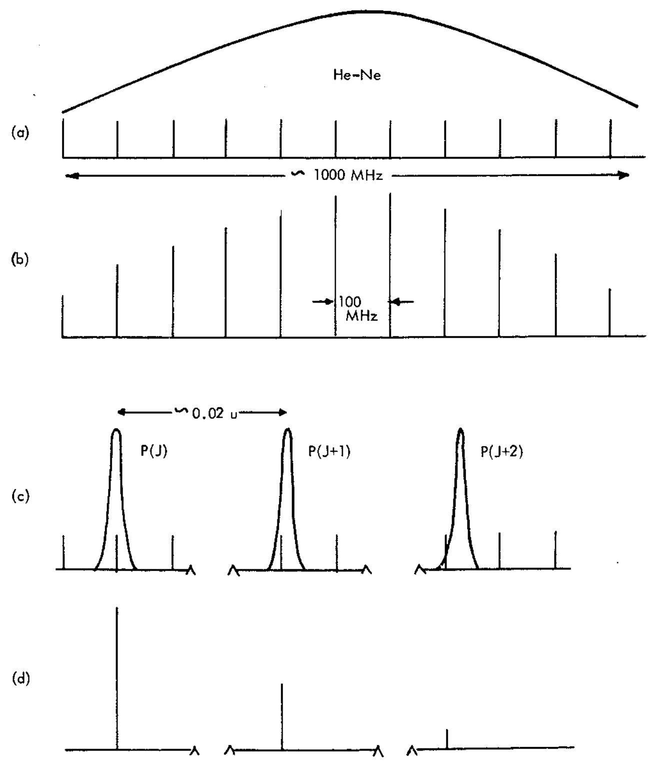

thermal drift can cause frequency and output variations such as those shown in Fig. 4. These variations can be controlled, however, by using appropriate methods to stabilize the optical cavity and to select the desired frequency.

Fig. 6 shows sample variations of the output power of a CO_2-N_2-He laser as a function of the current through the DC discharge at several pressures. Fig. 7 shows a photograph of the laser used to obtain the data of Fig. 6. The tube is 2 inches ID and has internal mirrors in the plane-parallel configuration separated by about 1.5 meters. Output coupling is by diffraction through a circular hole in one mirror. Typical optical power levels in the cavity are of the order of 100 watts with efficiencies between 5% and 10%. The same unit can be excited by 60 Hz AC.

As an indication of the power levels available, a 10-watt beam from this unit (obtained by using an output coupling aperture of only 6 mm diameter) unfocussed will ignite paper or wood across the room (10 to 20 ft). At distances up to 2 to 3 ft, an unfocussed 10-watt beam will penetrate asbestos and other refractory materials. The coarse tuning of the laser is most easily achieved by observing the brightness changes of the white-hot spot created as the beam impinges on a fire-brick. (Brightness temperatures measured with a pyrometer of the order of 2,000 degrees are typical.)

Fig. 8 shows a sample plot of the laser output power as a function of the pressure. For the gas mixture used here (approx. 10% CO_2, 10% N_2 and 80% He), Figs. 6 and 8 show that oscillation is attainable over a wide range of discharge conditions.

Since beginning work on the CO_2 laser a variety of discharge configurations have been used. Tube diameters between about 1.5 cm and 5 cm at lengths from 1.5 to 2.5 meters have been investigated and combinations of internal and external mirror systems have been employed. The system shown in Fig. 7 is air-cooled with only modest facilities for cavity stabilization. This unit is used as shown to examine the plasma effects on the laser oscillation. A 16-GHz microwave interferometer (seen in Fig. 7) is used to measure the electron density in the laser tube simultaneously with the other parameters (e.g. output power, current, pressure etc.) The interferometer can record phase shifts as small as 0.1° and permits electron density measurements down to densities of the order of $10^9/cm^3$ in the laser.

A typical plot of the electron density is shown in Fig. 9 for current and pressure variations. It is interesting to note that the electron densities are of the order of 10^{10} with total particle densities of about 10^{17} showing that the degree of ionization in the laser is very small (of the order of 10^{-7}). This again demonstrates the efficiency of the system since energy present as ionized species represents a loss to the laser output.

In addition to the investigations described above, present work on the CO_2 laser includes spectroscopic studies of the discharges using conventional and stimulated transition spectroscopy (described in the following section). For this work both steady state and pulsed discharges are employed. Propagation through the atmosphere and plasma is also being investigated.

LASER SPECTROSCOPY

The Laboratory has been involved for some time with the study of the spontaneous sidelight emission of gas lasers. As a result of this work it has been shown recently[5,6] that the strong optical frequency field generated by a laser is capable of producing a significant change in the population distribution of the excited atoms in a gas discharge. Although the primary change in population occurs for those levels which have an energy difference corresponding to the laser frequency, changes of population will also occur for other levels that are connected to the "primary" levels via radiative transitions or via nonradiative collisional transitions.

The changes in population of the various levels can be readily detected by the changes in the intensity of the spontaneous emission. Using a modulated laser beam and a phase-sensitive detection system it is posssible to measure very small changes in the spontaneous emission and hence very small changes in the population of the various energy levels involved.

This technique of using a laser to alter populations in a gas discharge and of studying the resultant changes in the spontaneous emission from the

Fig. 6—Sample variation of CO_2-N_2-He laser output power as a function of discharge current for several pressures.

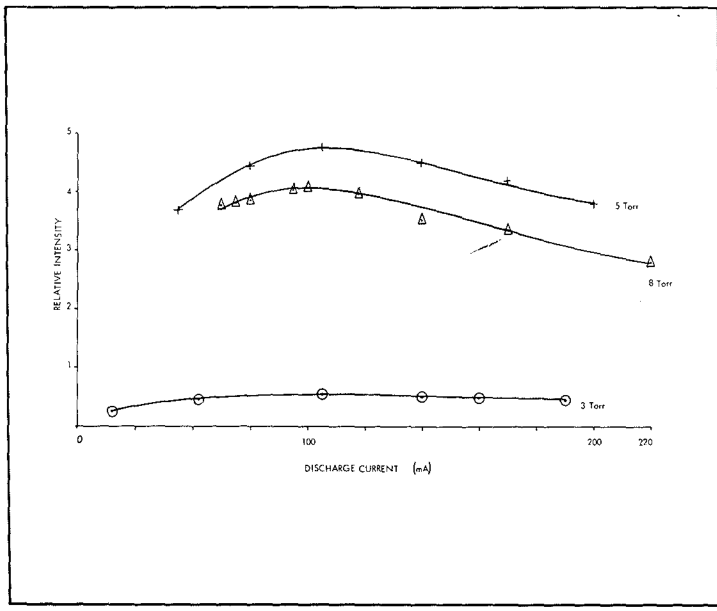

Fig. 7—Photograph of a CO_2 laser system and associated microwave interferometer.

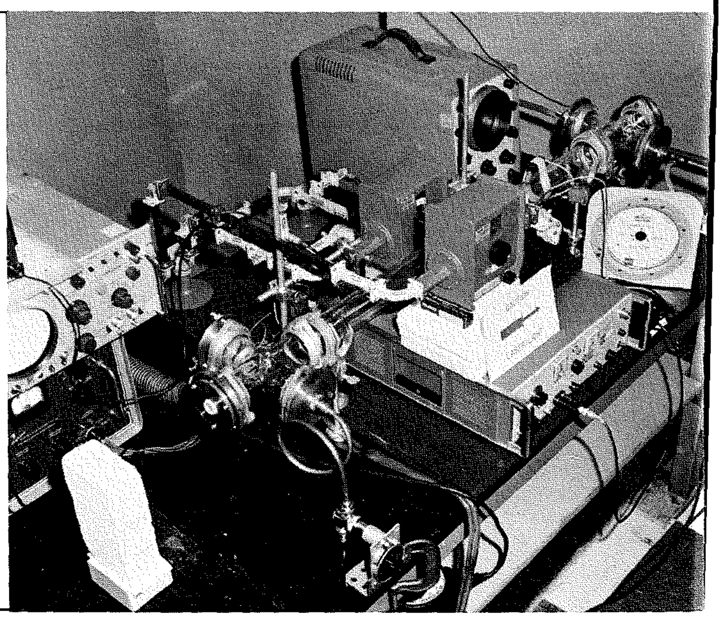

various levels with phase sensitive technique shall be referred to for brevity, as *stimulated transitions spectroscopy* (STS). This technique, although similar in some ways to *fluorescence spectroscopy* differs in several respects. The STS can involve either stimulated emission, or absorption caused by the laser field, depending on the relative populations of the upper and lower "primary" levels. The method can be applied for the study of a variety of radiative and collisional processes in any gas discharge in which there are primary energy levels which are "resonant" at a laser frequency. Because of the "cascading" processes resulting from the change in the population of the primary levels, STS can provide information about energy levels separated by sizeable energy differences (e.g. several e.v.) from the primary levels. The use of the phase sensitive detection system also provides a direct indication of direction of the change in the population (i.e. an increase or a decrease) from the sign ($+ve$ or $-ve$) of the signal with reference to the laser beam.

The usefulness of the STS method has been demonstrated by its application to the well-known competition between the 0.6328-micrometer and 3.39-micrometer transitions in a He-Ne laser.

The apparatus arrangement used is shown schematically in Fig. 10. A He-Ne gas discharge tube (approximately one meter long) with Brewster-angle windows is positioned between the mirrors in a conventional laser configuration and oscillation is obtained at the desired frequency (0.6328 or 3.39 micrometers). The laser beam is chopped at a convenient frequency (between 10 and 100 Hz) by a rotating chopper inside the optical cavity and a monochromator is positioned to receive (using a lens-mirror arrangement) the spontaneous emission from the side of the discharge tube over a small length (ΔL). The chopper blade material is selected to ensure that the laser beam is interrupted with minimum perturbation to the other optical frequency fields in the cavity.

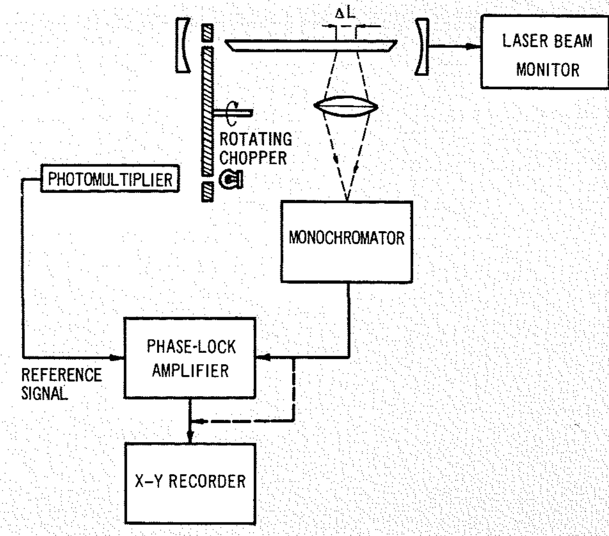

Fig. 10—Schematic diagram of the apparatus used for Stimulated Transition Spectroscopy of a laser discharge.

The output of the monochromator is fed into a phase-lock amplifier together with a reference signal produced by the chopper. The resultant output signal from the phase-lock amplifier is displayed on an *X-Y* recorder or oscilloscope. Using this arrangement it is possible to detect the small changes in the spontaneous emission (sidelight) from the discharge brought about by the switching off and on of the laser beam.

Provision is also made to allow the monochromator signal to by-pass the phase-lock amplifier and to go directly into the recorder to provide a conventional display of the sidelight spectrum. The system is arranged so that a positive signal from the phase-lock system indicates an increase in the sidelight emission when the laser is on, while a negative signal means a decrease in the sidelight intensity when the laser is on. The system can be made to oscillate at either 0.6328 or at 3.39 micrometers separately, or at both frequencies simultaneously by introducing appropriate filters into the optical cavity.

Fig. 8—Sample variations of CO_2 laser output power with pressure.

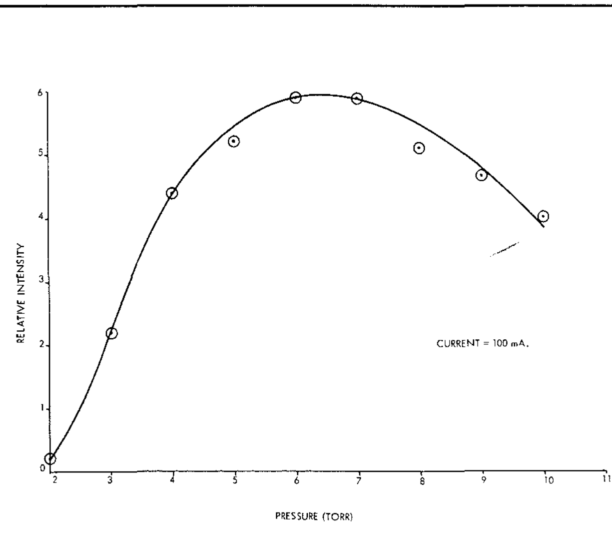

Fig. 9—Electron density variations in a CO_2-N_2-He laser discharge, as a function of the discharge current.

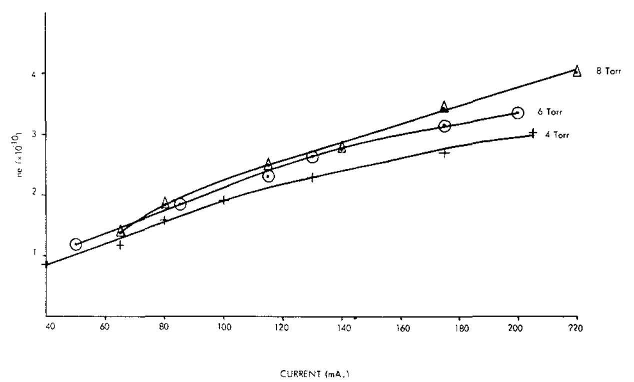

With the laser oscillating only at 0.6328 micrometers, a spectrum of the spontaneous emission from the side of the discharge tube as recorded by the phase-lock system is shown in Fig. 11a. As indicated above, the positive peaks in Fig. 11 represent spontaneous transitions that are increased in intensity as a result of the laser beam whereas the negative peaks show transitions that are reduced because of the laser field, hence the positive peaks can be expected to arise from transitions originating from levels whose populations have been increased by the action of the laser field. Conversely, the negative peaks will be associated with transitions from levels whose populations have been decreased.[5,6]

The information of Fig. 11 can be more meaningfully summarized in the form of the energy level diagram shown in Fig. 12. In this figure, the primary laser transition is shown as a heavy wavy line. The transitions corresponding to the positive peaks in Fig. 11 are indicated by solid lines and those corresponding to the negative peaks by dashed lines.

In Fig. 11b a sample low dispersion phase-lock spectrum of the spontaneous sidelight emission is shown for the laser oscillating at 3.39 micrometers under the same discharge conditions as for the 0.6328-micrometer oscillation.

It will be observed that many of the positive and negative peaks shown in Fig. 11a have reversed polarity in Fig. 11b. This is because of the competition between the 0.6328-micrometer and 3.39-micrometer laser cascades (illustrated in Fig. 12) which have a common upper level.

The sample results presented here illustrate the effectiveness of the STS technique for examining population changes in gas discharges. It has been found that the method is useful for detecting changes in levels which are separated by sizeable energy differences from the "primary" levels stimulated by the laser field. As shown in Fig. 12, population changes resulting from three- and four-step radiative processes are readily detectable by this method. Although the above illustration involves the analysis of a gas discharge in which lasing action is occurring, the method can be applied to any gas discharge system having energy levels resonant with the laser frequency. These systems can be placed either internal or external to the optical cavity of the laser used to provide the primary field. We are at present using the STS method on a variety of gas discharges external to the laser cavity and have found that, by

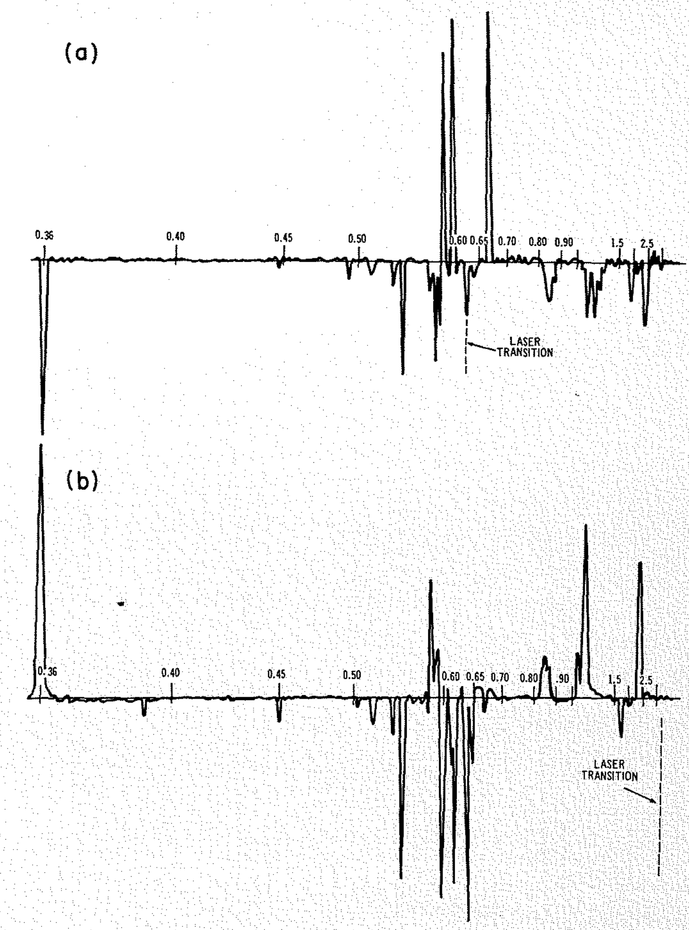

Fig. 11—Sample spectra obtained from the phase-lock system in the wavelength range from 0.35 μm to 3.5 μm for laser oscillation at (a) 0.6328 μm, and (b) 3.39 μm.

Fig. 12—Neon energy level diagrams showing the more prominent transitions observed in Fig. 11. The solid lines indicate spontaneous emissions increased by the laser field (+ve peaks in Fig. 11) and the dashed lines indicate emission decreased by the laser field. Laser oscillation is at (a) 0.6328 μm, and (b) 3.39 μm.

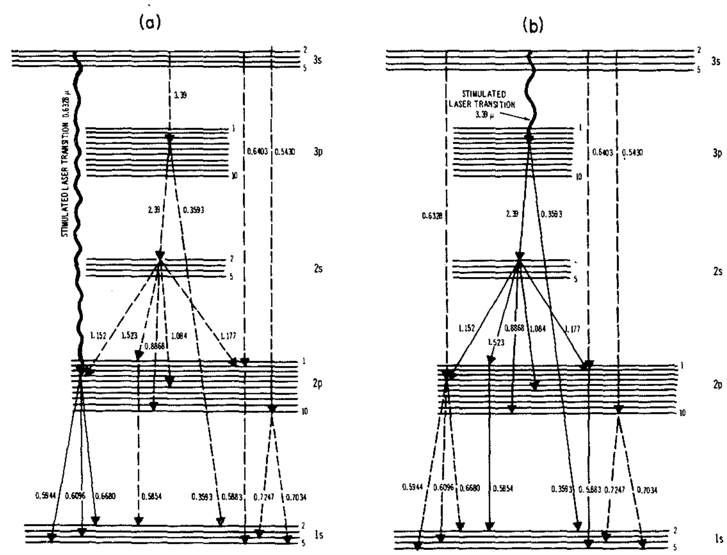

focussing the laser field it is readily possible to measure the population changes. Most of the present work is being done with CO_2, N_2, and He discharges because of our interest in the carbon dioxide lasers.

One of the main advantages of the STS method lies in the fact that, because of the phase sensitive detection, only those levels undergoing population changes (via radiative or collisional mechanisms) are recorded in the spectra and the direction of the population change is unambiguously determined from the sign of the output signal. As a result, it is known that any emissions recorded by this method, indicate transitions from only those levels which are interacting with the primary "stimulated" levels. In this way, one is in effect "tagging" the atoms or molecules which undergo the stimulated transition and then observing their redistribution throughout the whole cascade of accessible energy levels. Measurements of the intensity changes in the spontaneous emission recorded by the STS method can be used to provide quantitative information regarding collision cross sections and Einstein coefficients in the discharges but for accurate work of this type it is essential to take into account all of the transitions affecting the populations of the levels involved. For energy levels two or three "steps" below the primary levels, the effects of several competing transitions on the population may be difficult to assess.

One final feature of the method should also be pointed out. Since, in the present studies it is shown that the modulation (chopping) of the laser beam intensity is manifested as a modulation of the laser sidelight at a variety of frequencies, any one of these frequencies could be used to monitor variations in the laser signal. For example, the strongly modulated emission at 0.3593 micrometer can be used to measure variations in the 3.39-micrometer laser intensity. This is an advantage since the detectors available at 0.3593 micrometer (e.g. photomultipliers) are more sensitive than those available at 3.39 micrometers. This approach could be used to generalize the plasma diagnostic technique involving a three-mirror laser interferometer system described recently by Ashby and Jephcott.[7] Using a laser which was oscillating at both 0.6328 and 3.39 micrometers, these authors used the variations in the 0.6328 micrometer laser emission to monitor the variations in the 3.39 micrometer signal in the interferometer. However, the 0.3593 micrometer spontaneous emission could equally well have been used with oscillation at 3.39 micrometers only.

PLASMA DIAGNOSTICS

There are several possible methods of applying lasers for plasma diagnostics. The most straightforward approach is to use a laser source in an interferometer system to measure the refractive index of the plasma and from this to deduce the plasma properties. For an electromagnetic wave of wavelength λ, traversing a path length L in a plasma with refractive index n, it is known that the phase shift, $\Delta\phi$ of the wave (in radians) with respect to a vacuum path of the same length is given by:

$$\Delta\phi = \frac{2\pi L}{\lambda}(n-1). \qquad (1)$$

The quantity $(n - 1)$ is the "refractivity" of the plasma, and is in general, a property dependent upon all of the plasma constituents, i.e. electrons, ions and neutral atoms. In fact it is possible to write the refractivity as a sum of terms of the form:

$$\begin{aligned}&(n-1)_{\text{plasma}}\\ &= (n-1)_{\text{electron}} + (n-1)_{\text{ion}}\\ &+ (n-1)_{\text{molecule}} + (n-1)_{\text{atom}}\end{aligned} \qquad (2)$$

where each term can be expressed in terms of the basic plasma properties. For example, at high frequencies the refractivity of the free electrons is given by:

$$(n-1)_{\text{electron}} = \frac{-\omega_p^2}{2\omega^2} \qquad (3)$$

where ω is the angular electromagnetic wave frequency ($\omega = 2\pi f$) and ω_p is the plasma frequency defined by:

$$\omega_p^2 = N_e \frac{e^2}{m\varepsilon_o} \qquad (4)$$

with N_e = electron density, e = electron charge, m = electron mass, and ε_o = permittivity of free-space. Inserting appropriate values of the constants, gives for the electron refractivity the result:

$$(n-1) = -4.47 \times 10^{-14}\lambda^2 N_e \quad (5)$$

where λ is in cm and N_e is electrons/cm^3.

For the atoms (and molecules) it is possible to express the refractivity in terms of the polarizability, α, which is related to the separation of the bound charges in the atom (or molecule) brought about by the applied electric field. The result is of the form

$$(n-1) = 2\pi N_o \alpha \qquad (6)$$

where N_o is the number density of the atomic (or molecular) species.

For the ions in the plasma the establishment of the refractivity by either theory or experiment is quite difficult. In many cases of interest the ion value is found to be of the same order as that for the corresponding neutral atom and the usual practice is often to set them equal.

Substitution of Equations 2 through 6 in Equation 1 gives for the total phase shift in the plasma:

$$\Delta\phi = \frac{2\pi L}{\lambda}\left[\sum_i 2\pi N_i\alpha_i - 4.47 \times 10^{-14}\lambda^2 N_e\right] \qquad (7)$$

where the summation is over the several atomic, molecular, and ionic species in the plasma. It is seen from Equation 7 that the electrons shift the phase in the opposite direction, to the other plasma constituents and this fact can be utilized to extract the electron effects from the others.

In the microwave region the electron refractivity is the dominant term and the electron density can be determined to a good approximation by retaining only the final term on the RHS of Equation 7. At optical frequencies, however, this is not the case.

Most common neutral gases at NTP have optical refractivities of the order of:

$$(n-1) = 2 \times 10^{-4} \approx 5 \times 10^{-24} N_o \qquad (8)$$

For an optical wavelength of 1 micrometer (10^{-4} cm) the electron refractivity of Equation 5 would be

$$(n-1)_{electron} \approx 5 \times 10^{-22} N_e \quad (9)$$

Equations 8 and 9 show that the refractivity per particle is generally much larger for electrons than for the other species. Since the minimum optical phase shifts detectable in practice are of the order of 3° (0.01 fringe) it is apparent that for experimental systems the condition $[L(n-1)/\lambda] > 0.01$ must be satisfied. For a wavelength of 10^{-4} cm and a path length of 1 cm, this results in the condition that the refractivity must be greater than 10^{-6} (for L = 100 cm the refractivity need only be greater than 10^{-8}). The required densities of neutral gas and electrons to satisfy this condition can be derived from equations 8 and 9 and are given in Table I.

In most plasmas of laboratory interest the degree of ionization is low so that N_e is generally less than 0.1 N_o. Hence the sample calculations above illustrate why all constituents of the plasma must be included in the analysis of laser interferometry of plasmas. Also, it is apparent that even for rather sizeable path lengths, electron densities can only be measured with any accuracy at optical frequencies if they exceed about $10^{13}/cm^3$.

This minimum measurable density can be reduced by using longer wavelengths in the infrared region. In considering this approach, however, it is to be noted that although the refractivity increases as λ^2, the phase shift only increases as λ, for a given path length L in the plasma, since there are fewer of the longer wavelengths in the plasma. This wavelength dependence can also be used to separate the electron contribution to the refractivity from the other contributions listed in Equation 2.

In our laboratory, at present the above interferometric techniques are being applied at visible, infrared and millimeter wavelengths to several plasma systems. Of particular interest are plasmas generated in the various laboratory flow facilities[1] designed to simulate re-entry and rocket exhaust plasmas. These plasmas in general exhibit properties which change rapidly in space as well as in time (e.g. turbulence) and in good resolution available with laser beams is a great advantage. Experimentally, however, problems are encountered with the systems at optical frequencies because of the need to suppress all extraneous vibrations in the interferometer before accurate measurements can be made.

Another laser technique for plasma diagnostics involves the measurement of the scattering of laser light by a plasma system. The scattering of light by elastic or acoustic waves is a well known technique[8] for measuring the properties of the waves and the medium involved. Brillouin[9] in 1922 showed that the angular frequency ω_i of the incident light is shifted to ω_s and the frequency shift ω is given by the equation

$$\omega \equiv \omega_i \pm \omega_s = 2\Gamma v \sin \theta/2 \quad (34)$$

TABLE I—Particle Densities for Detectable Phase Shift

L(cm)	N_o/cm^3	N_e/cm^3
1	2×10^{17}	2×10^{15}
100	2×10^{15}	2×10^{13}

where Γ is the wave number of the light in the medium along its incident direction (equal to the refractive index of the medium times $[\omega_i/c]$) and v is the velocity of the acoustic waves in the medium: θ is the angle of scattering measured with respect to the incident light.

One may similarly obtain scattering of light from a plasma medium in which electrons have an inherent frequency spectrum of longitudinal oscillations. The scattering of light by electrons is known as Thomson scattering. Since in a plasma, the longitudinal oscillation frequency ω of the medium can be anywhere between zero and an upper limit of the order of the plasma frequency, the laser frequency shifts also exhibit this spectrum, with corresponding changes in the direction of the beam. This phenomenon is the cause of "Doppler broadening" of a laser beam in a plasma medium. The Thomson scattering of light by plasma electrons is very difficult to observe experimentally unless an extremely bright monochromatic laser and a high density plasma interact, because the cross-section for Thomson scattering is very small. Great care must be taken to reduce the stray scattering of the laser beam in the apparatus so that the plasma scattering can be measured.

Theoretically, a detailed examination of the laser-plasma interaction shows that the scattering cross-section in a plasma medium is not given only by the Thomson scattering cross-section (applicable to free electrons), but by a very complicated relation.[10]. The scattering is a function of plasma parameters such as electron and ion temperatures and densities, and of the laser frequency, the angle of scattering, the frequency shift of the scattered radiation, the bandwidth of the detector and the solid angle subtended at the receiver.

At Montreal, considerable theoretical work on laser scattering by plasma has been carried out by Dr. Shkarofsky[10]. In addition to a detailed analysis of the Thomson scattering, Dr. Shkarofsky has investigated a variety of ways in which a scattered laser beam can be utilized to measure the statistical single particle distribution functions for plasmas in the density range from 10^8 to 10^{13} charge-carriers/cm^3. Starting with with an investigation of the Thomson scattering off ambient plasma oscillations, the work has been extended to consider multiple-beam scattering systems in which the laser beam is scattered off oscillations induced in the plasma. It is planned to undertake the experimental investigation of these phenomena in the near future.

STUDIES OF FOCUSSED COHERENT BEAMS

As part of our laser research program there has been an active investigation of some of the special properties of highly focussed coherent beams. The interest in the focal properties of coherent beams arises on the one hand from a desire to know more about the ultimate in "resolution" attainable with focussed laser beams and on the other by the desire to utilize focussed laser radiation for the generation of optical frequency fields with extremely high field strengths and energy densities.

In such studies we have found it extremely useful to examine the focal properties at millimeter-wave frequencies instead of at the optical frequencies. In the microwave wavelength range between about 2 and 8 mm, 150-GHz to 35-GHz "optical" systems can be set up (i.e. systems whose dimensions are much greater than the wavelength) and the electromagnetic fields can be probed directly for amplitude and phase information much more accurately than at optical frequencies. Two such recent investigations are described below.

Resolving Power of Focussing Systems with Coherent Illumination

In any real focussing system, the image of each source point is a diffraction pattern of finite extent whose shape and dimensions depend on the geometry of the system and the wavelength of the radiation.

Where the source points are completely incoherent, the resultant intensity pattern in the focal plane is obtained by the direct summation of the individual intensities at each point. In

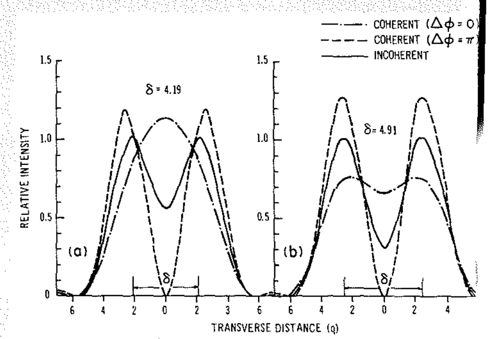

Fig. 13—Sample theoretical curves showing focal plane intensity distribution for two overlapping diffraction patterns.

this case, it has been found convenient to apply the so-called Rayleigh criterion for the limit of resolution. This criterion states that two source points are resolvable when their image separation is greater than the separation between the central intensity maximum and the first minimum in the diffraction pattern of either image.

If the energy radiated by the source points is coherent, the composite pattern in the focal plane can only be obtained by summing (vectorally) the individual field amplitudes, taking into account the phase relations existing between them[11,12]. The resultant is then squared to give the true intensity distribution. When this is done, it is found that sizeable variations in the limit of resolutions can be obtained depending on the relative phases of the source points.

The variation of the resolving power of a focussed system has been examined theoretically for the three following cases:

1) two incoherent source points,
2) two in-phase coherent source points,
3) two antiphase coherent source points.

This was done by computing the resultant intensity pattern in the focal plane from two image diffraction patterns of unit maximum intensity of properties corresponding to the three above cases, for various separation distances between the individual patterns.

Fig. 13 shows two of a series of composite plots corresponding to separation distances δ of 4.19 and 4.91 respectively which illustrate clearly the effects of coherent sources on resolving power. It is observed that while the resultant pattern for incoherent source points is well resolved, that for the coherent ones is still unresolved. On the other hand, it is apparent that the antiphase coherent sources because of the symmetry of the system will always produce a zero intensity image at the midpoint ($q = 0$) of the pattern and in this respect, will always be resolved no matter how small δ is made.

The large variations in the resultant of the coherent energy patterns caused by side lobe effects are evidenced in Fig. 13. For $\delta = 4.91$ the main lobe of one pattern coincides closely with the first side lobe of the other. With uniform illumination the amplitude of the first side lobe is only 0.132 for a contribution of about 2% to the total intensity. In the case of coherent sources, the side lobe effects are much more pronounced. For in-phase sources, the overlapping lobes are 180 degrees out of phase and the resultant intensity is given by $(1 - 0.132)^2 \approx 0.75$ showing a 27% reduction from the corresponding incoherent intensity. Conversely, for antiphase coherent sources the effect of the side lobe is additive and the resulting intensity is increased by 26% over that of the incoherent case.

It is apparent from the results that, the in-phase coherent source points are not resolved as easily as the incoherent ones. This situation is clearly illustrated in Fig. 14 where the value of the intensity I_m at the central minimum of the composite intensity pattern is compared to the intensity I_p of the side maxima as function of separation δ. A pattern is defined as resolved when $(I_m/I_p) < 1$, and the smaller the ratio, the better the resolution. [For antiphased sources, $(I_m/I_p) \equiv 0$.] One can observe that for a given resolution the minimum achievable δ separation values are always less in the case of incoherent source points.

In an effort to examine how well the foregoing simple theory would describe the conditions attainable in a real focussing system, experimental measurements of the resolving power of a single lens system were conducted using coherent electromagnetic waves at microwave frequencies (34.45 GHz, wavelength 8.7 mm).

The system used for the measurement is shown schematically in Fig. 15. From a single klystron source the transmission line divides into two flexible branches terminated by open ended waveguide antennas that can be symmetrically positioned on either side of the system axis. Calibrated variable attenuators and 360° phase shifter inserted at appropriate positions provide accurate adjustment of signal intensities and variation of relative phase.

Two series of experimental measurements were carried out. One with the in-phase sources ($\Delta\phi = 0$) and one with the antiphase sources ($\Delta\phi = 180°$). Sample results are shown in Fig. 16 for two different separation distances (δ) in the case of in-phase sources. The agreement with theoretical computations is very good. The effects of the side lobes on the composite patterns are readily apparent in the experimental curves where the intensity at the peaks of the composite plot is about 30% lower than the intensity of the individual sources because of the overlapping of oppositely phased main lobe and side lobes.

The results obtained with antiphase sources show similar effects and also a close agreement with the theoretical computations. In addition, measurements were made for several values of the relative phase between the two above extremes. As would be expected, the results present effects intermediate to those described.

Fig. 14—(a) Sample of a resolved pattern, (b) comparison of the resolution for coherent and incoherent source points as a function of their separation δ.

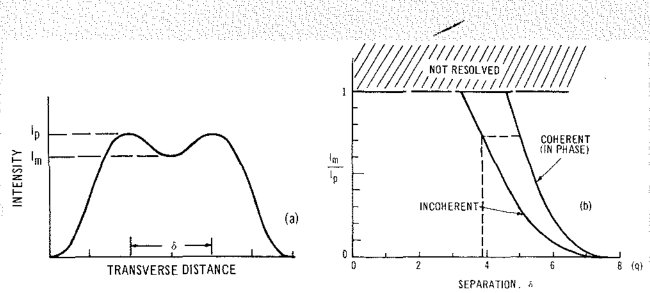

Fig. 15—Schematic diagram of the microwave system (34.5 GHz).

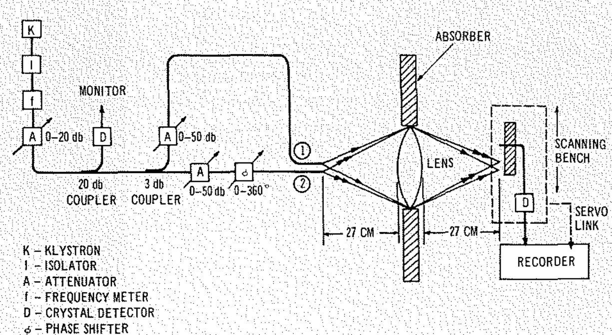

Longitudinal Electromagnetic Field at the Focus of a Coherent Beam

In a recent paper, Boivin and Wolf[13], have published a detailed theoretical analysis of the structure of the electromagnetic field in the region of the focus of a coherent beam which emerges from an aplanatic imaging system. Since their analysis was not limited to a scalar diffraction theory, they were able to exhibit the vectorial features of the focussed beam. As a result, it was found that the field has a strong longitudinal component in certain regions in the neighborhood of the focus. An experimental examination of this phenomena was undertaken in the laboratory and the measurement of this longitudial component in a wide-aperture microwave lens system has been achieved[14].

The apparatus used was a simplification of that shown in Fig. 15. The orientation of the receiving waveguide could be adjusted to detect either the longitudinal or transverse electric field intensity (I_L and I_T, respectively), by coupling to the TE mode of the waveguide. The angle subtended by the lens at the focus was 46° (i.e., in the notation of (Reference 13, $\alpha = 23°$). The test was conducted at a microwave frequency of 34.5 GHz (8.7-mm wavelength).

In Fig. 17, superimposed results are shown for scan of the transverse and longitudinal field intensities in the focal plane. The scan was made in the direction of the incident-field electric vector (i.e., $\phi = 0$ in Reference 13). The field intensities I_T and I_L (proportional to the squares of the electric field amplitudes) are shown, on a decibel scale, as a function of the transverse position in the beam.

Since Boivin and Wolf have given computations only for $\alpha = 45°$ and the experiments are for $\alpha = 23°$, it is not possible to make a complete comparison, but, in general, the results (e.g. Fig. 17) are in good agreement with the theoretical predictions. The measured "dipole" nature of the field contours[14] is essentially identical to that computed theoretically. The longitudinal field intensity is seen to have a "zero" value at the focus and in the $\phi = \pi/2$ direction, but to show a series of peaks symmetrically placed on opposite sides of the optic axis in the $\phi = 0$ direction.

Scaling the results of Reference 13 for the present system indicates that the maximum value of I_L should occur in the $\phi = 0$ direction at about 0.9 wavelengths from the axis, and this is very close to the experimentally measured position shown in Fig. 17. The relative positions of the maxima and minima of I_T and I_L shown in Fig. 17 are also in agreement with the theory.

Similar good agreement between the theory and experiment is found in the relative peak magnitudes of I_T and I_L. The peak longitudinal field amplitude computed by Boivin and Wolf is about 28% of the peak transverse field amplitude and the measured value is −11 dB which gives a longitudinal field amplitude about 29% of the transverse field. This excellent agreement may be somewhat fortuitous since the computations were for a wider aperture system, and the experimental measurements will undoubtedly show some errors arising from field perturbations caused by the receiver. However, the results demonstrate clearly the existence of the strong longitudinal field in the focal region.

In addition to the results shown, some measurements have been made with sources having nonuniform amplitude distribution across the lens. Since the microwave beams can be "shaped" rather conveniently, measurements at microwave frequencies can be used to obtain information on the longitudinal field distribution for focussed laser beams having more complex amplitude distribution.

SILICON PHOTODIODE LASER DETECTORS

Both the mesa and planar types of silicon diode developed in these laboratories make excellent photodiodes for a wide variety of applications in the visible part of the spectrum. However, with the advent of near-infrared lasers there has been an increasing need for fast detectors in the 0.7 to 1.15 region, and the conventional photodiode is not especially suitable for this purpose for three reasons, all of which hinge on the relatively very thin depletion layer attainable. Firstly, a thin depletion layer gives a high capacitance per unit area which, particularly for large-area devices reduces a system's high frequency performance; and secondly, at these near-infrared wavelengths the absorption coefficient of silicon be-

Fig. 16—Sample comparison of experimental and theoretical field distributions in the focal plane for two coherent, in-phase source points.

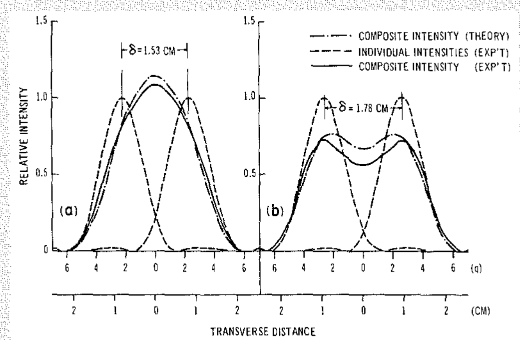

Fig. 17—Measured variations in the transverse and longitudinal electric field intensities I_T and I_L in the focal plane. Scan is in direction of E-vector of the source.

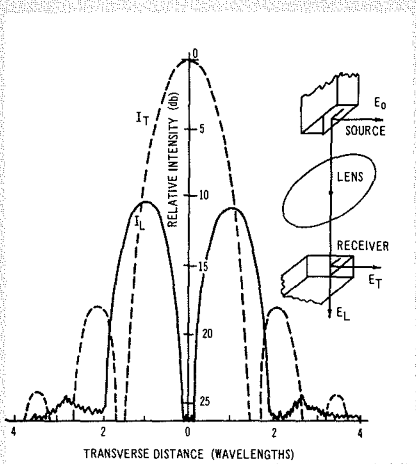

Fig. 18—Quantum efficiency of a conventional silicon p-n diode and lithium drifted diode as a function of wavelength.

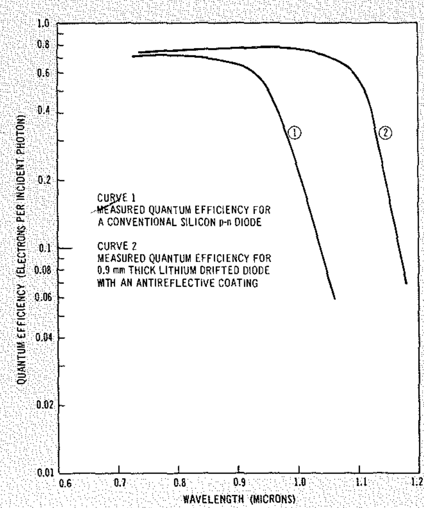

comes small, causing poor quantum efficiency unless the absorbing region is relatively wide. Thirdly, unless the total thickness of the conventional device is very small it cannot be fully depleted, so that the residual base material acts as an undesirable series resistance which again handicaps the device's speed of response. For certain applications, restriction of the area of conventional photodiodes to about 2 cm^2 (for technological reasons) is also undesirable.

These limitations have now been overcome in our laboratory by the development of a special type of thin-window lithium-drifted diode fabricated from a *p*-type silicon wafer about 1 mm thick having an area up to 4 cm^2. After performing a shallow diffusion of boron on one side, lithium is diffused into the opposite side and then drifted through to the boron layer. The diode is then encapsulated in such a way that radiation can enter through the boron-diffused surface. Since the entire body of the device is compensated, the depletion layer created by a reverse bias extends completely across from the n^+ layer to the p^+ layer, resulting in good quantum absorption, low capacitance, and negligible series resistance. Such photodiodes, when antireflection coated, have quantum efficiencies exceeding 80% at 0.7 and 0.9 micrometers 60% at 1.06 micrometers, and 20% at 1.15 micrometers with a collection time of less than 40 ns, a leakage current of about 1 μA/cm^2 and a capacitance of 10 pF/cm^2. Sample spectral response of these devices is shown in Fig. 18 and response time data is given in Fig. 19.

This new form of photodiode also enables multi-element devices such as arrays or four-quadrant configurations to be readily made by ultrasonically cutting into the depletion layer from the lithium-diffused (rear) surface, as shown in Fig. 20. This technique gives excellent electrical isolation between elements together with remarkably narrow blur widths (as little as 0.1 mm) and yet no dead space between elements. Photographs of completed units are shown in Fig. 21.

Another feature of the device is that if it is reversed before encapsulation, the inherently thick dead layer met by radiation entering through the lithium-diffused surface results in a narrow wavelength region of sensitivity (about 0.1 micrometer wide, centered on 1.06 micrometers. This aspect becomes important if the device is used to detect radiation from the 1.06-micrometer neodymium laser in the presence of strong background, such as sunlight.

Fig. 19—Silicon photodiode depletion layer transit time variations for different intrinsic layer thicknesses and applied voltages.

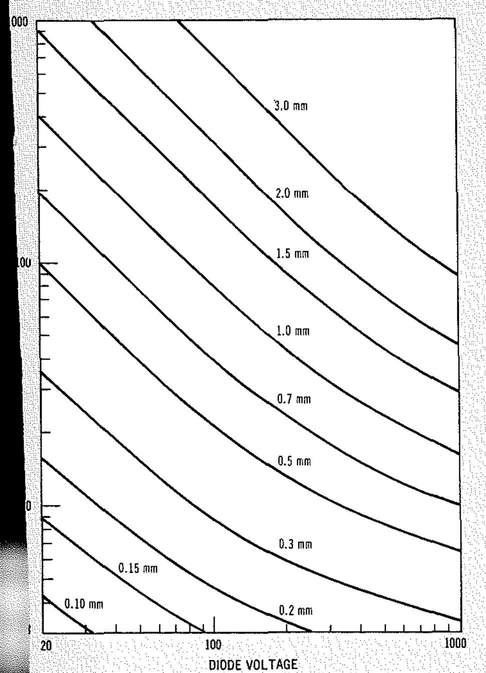

Fig. 20—Cross-section of thin-window Si(Li) photodiode showing the slot which separates the four sensitive regions of a quadrant detector.

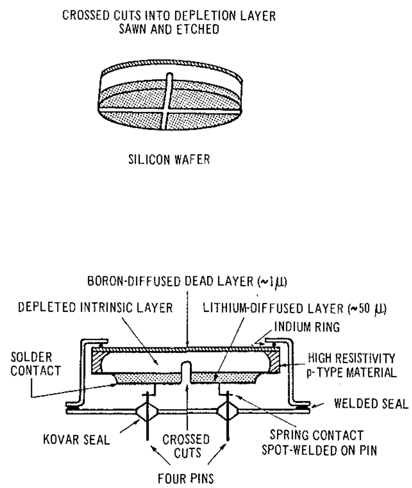

Fig. 21—Encapsulated four-quadrant thin-window Si(Li) photodiode. Note absence of "dead spaces" on the front of the detector.

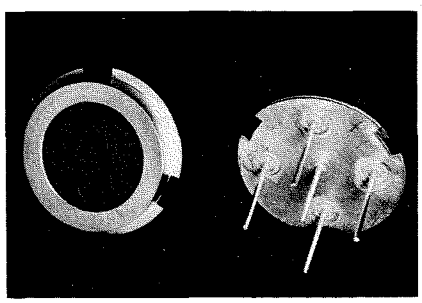

CONCLUSION

This article has outlined a number of areas of laser research currently being undertaken at the RCA Victor Research Laboratories in Montreal. Because of the rapid state of development in the whole laser field it is difficult to predict with any accuracy the fields of greatest activity in the future. However, as far as gas lasers are concerned it is evident that in the next few years, there will be a considerable effort made to develop more and better molecular lasers with frequencies extending further out into the infrared and submillimeter range.

ACKNOWLEDGEMENTS

The author wishes to acknowledge the support of the Canadian Defense Research Board Directorate of Industrial Research in much of the work described. The assistance of Dr. A. Crane, Dr. H. Pullan, Dr. I. P. Shkarofsky, Mr. A. Waksberg and Mr. J. I. Wood in the preparation of this manuscript is gratefully acknowledged.

BIBLIOGRAPHY

1. *Plasma Physics Research & Engineering—Eighteen Technical Papers by RCA Scientists and Engineers;* RCA Reprint PE-263. (Reprinted from RCA ENGINEER *11*, 4, Dec. 65-Jan. 66.)
2. C. K. N. Patel, *Phys. Rev. 136*, A1187 (1964).
3. H. J. Moody, H. Buizert, A. Waksberg, and A. Crane, RCA Victor Rept. 3-900-2 (July 66).
4. G. Moeller, and J. D. Rigden, *Appl. Phys. Lett. 7*, 274 (1965).
5. A. L. Waksberg, and A. I. Carswell, *Appl. Phys. Lett. 6*, 137, (1965).
6. A. L. Waksberg, and A. I. Carswell, *Measurements of Laser Induced Population Changes in Gas Discharges,* RCA Victor Res. Rept. TM7-801-018.
7. D. Ashby, and D. Jephcott, *Appl. Phys. Lett. 3*, 13, (1963).
8. W. J. Comley, *Contemporary Physics 4*, 15, (1962).
9. L. Brillouin, *Ann de Physique 17*, 88, (1922).
10. I. P. Shkarofsky, *RCA Victor Quarterly Reports to ARL/WPAFB,* 1965-66.
11. A. I. Carswell and C. Richard, *Focussed Microwave Systems for Plasma Diagnostics,* RCA Victor Rept. 7-801-32, Dec. 1964.
12. A. I. Carswell and C. Richard, *Appl. Optics 4*, 1329, (1965).
13. A. Boivin, E. Wolf, *Phys. Rev. 138* B1561 (1965).
14. A. I. Carswell, *Phys. Rev. Lett. 15*, 647, (1965).

QUANTUM ELECTRONICS RESEARCH AT RCA LABORATORIES

An Introduction

Dr. H. R. LEWIS, Director

Electronic Research Laboratory
RCA Laboratories, Princeton, N. J.

SEVERAL years ago in an introductory article on laser research it was necessary to try to explain how the laser works. In one way, that was fortunate because at that time there were few working laser devices and even fewer applications. In the absence of anything more concrete, discussions of the physics of quantum electronics, of "promising" new materials and of rather grand applications—a thousand TV channels carried on a single light beam—were in order. Today, however, the situation is quite different. Technical people are accustomed to the laser and are prepared to use it without necessarily understanding in detail how it works. Literally hundreds of different laser devices are now available with a wide variety of operating characteristics. A very encouraging aspect is the undiminished rate of progress in devices; for example, in the past 18 months a gas laser (CO_2) has been developed with an efficiency 2 orders of magnitude better than that previously available. Time, and the availability of better devices have provided some specific applications and the issue in which this article appears contains accounts of a number of applications of interest to RCA. Thus we can afford to abandon background material and discuss meatier topics.

One role of the Laboratory in quantum electronics has been to supply basic knowledge and specific devices to the operating divisions of RCA for application. The applications which have come along earliest are in the military field because in that area a very small margin of improvement can be well worth exploiting. The more difficult problem of commercial applications is being pursued largely at the Laboratory, but here there is less which can be currently discussed. This is a result both of the proprietary nature of such work and of the slower rate of progress towards more difficult goals. It is interesting to speculate, however, on the apparent decrease in discussion of commercial laser applications in the public press in the past year. It may very well mark the transition from dream-applications, which can be freely discussed, to real ones.

A good example of the Laboratories' role in Corporate work in quantum electronics lies in the injection laser. A technique of liquid-phase epitaxy developed by H. Nelson produces superior laser diodes for room-temperature applications; the technique itself has been adopted for production at the Somerville plant by Lamorte. At the same time devices developed by J. I. Pankove, H. Nelson, and G. C. Dousmanis have been incorporated into novel communications and radar systems by W. J. Hannan and his co-workers at DEP Camden. With superior diodes DEP has been able to get increased government support for its development work. To hold this kind of advantageous position the Laboratory must continue to explore new techniques for producing still better injection lasers. One possibility is in the use of vapor-phase growth of alloys emitting at shorter wavelengths; J. Tietjen, I. J. Hegyi, H. Nelson, and J. I. Pankove are investigating this possibility with $GaAs_xP_{1-x}$.

In the components field, K. G. Hernqvist and J. R. Fendley have developed a superior argon gas laser that offers substantially better life than any announced by our competitors. It has given RCA Lancaster the opportunity to enter into the laser field with a new and valuable device. Z. J. Kiss, R. C. Duncan, and R. J. Pressley have produced a new optically pumped laser, the first in which pump efficiency is improved by "cross-relaxation." In this kind of device an ion with appropriate absorption bands (trivalent chromium) absorbs energy from a mercury lamp and then transfers it to a different ion (trivalent neodymium) with a favorable emission line for laser purposes. The host material for these ions is yttrium aluminum garnet from which a device has been made which generates an average of 10 watts of power in the infrared. Detection of infrared radiation still presents problems because the conventional photoconductive detector is either insensitive or slow. H. S. Sommers and E. K. Gatchell have demonstrated that greatly improved detectors can be achieved by using a microwave bias for the photoconductor.

Starting with some ideas which were an outgrowth of the work on optically pumped lasers, C. H. Anderson and E. S. Sabisky have produced an optically-pumped, low-noise microwave amplifier. This work represents the first new development in some years in the first of the quantum-electronic devices, the maser. L. Morris, at Applied Research Camden is currently carrying out further experiments to evaluate its practical promise.

In the applications area, H. J. Gerritsen, D. L. Greenaway, and E. G. Ramberg have been working for some time with holograms, to evaluate their potential for display systems. Similarly, D. Vilkomerson and R. Mezrich have been interested in hologram memories for computers.

Many other commercial applications of the laser are possible. To realize them, we need not only better lasers, but improved components of all kinds to go with them. These components include modulators, detectors, and new recording media. In the future, the Laboratory will continue to look for new ways to improve and use these components. At the same time, it will expand its use of the laser as a very advanced tool for new scientific studies.

Final manuscript received July 25, 1966

DR. HENRY R. LEWIS received AB, MA, and PhD degrees from Harvard University in 1948, 1949, and 1956 respectively. In 1950 and 1951 he was a teaching fellow in physics at Harvard. His PhD thesis was a study of distortions observed in nuclear resonances using the molecular beam technique. From 1951 to 1953, and for a year after receiving the doctorate, he worked with the Operations Evaluation Group of the Massachusetts Institute of Technology on various problems in naval warfare. Dr. Lewis joined the Technical Staff of RCA Laboratories in 1957 and worked on new paramagnetic materials for masers. In 1960 he became head of the Quantum Electronics Group whose projects included masers, lasers, and associated devices. He is now Director of the Electronic Research Laboratory.

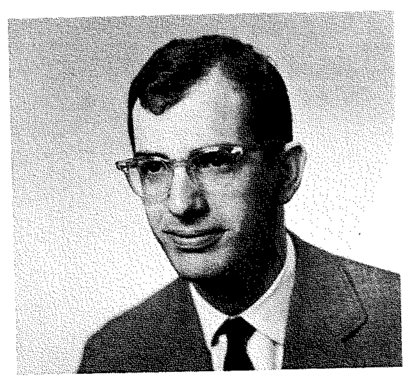

ARGON LASERS

In argon lasers excited ions produce the laser radiation. From the laser physics point of view there are several advantages in using charged particles for lasing. The associated laser tube construction problems have recently been overcome, making it possible to manufacture reliable, long life argon lasers. In spite of the low efficiencies presently attainable, several promising applications are being studied where the continuous-duty argon laser operation in the visible wavelength region is made use of.

DR. K. G. HERNQVIST
RCA Laboratories
Princeton, N. J.

IN gas lasers, excitation of atoms for lasing is due to impact by fast electrons. The interaction takes place in a gas discharge type plasma. Such a plasma consists of neutral atoms, ions, and fast moving electrons. A characteristic, and for laser operation very important, property of such plasmas is the *high electron temperature,* which may be several orders of magnitude higher than the temperature of the neutral gas or the ions.

GAS LASERS USING THE NEUTRAL GAS FOR LASING

In one class of gas lasers, of which the famous He-Ne laser is a member, the excited *neutral* atoms do the lasing. These lasers yield only low power and, except for the He-Ne laser, are limited to wavelengths in the infrared region. The limitations of this type of gas laser are exemplified by the energy level scheme sketched in Fig. 1. Generally, electrons excite ground-state atoms both to the upper and lower laser level. For population inversion to occur the lifetime of the upper level must be much longer than that of the lower level. This means that the radiative transition probability from state u to state g must be low and that corresponding to the transition l to g must be high. In order to overpopulate the upper level the opposite would be desirable for the probability of impact excitation by the electrons. Unfortunately a correlation exists between the radiative transition probability and the impact excitation probability. If one is high the other is high. Another difficulty concerns the reabsorption of radiation corresponding to the l-g transition (resonance radiation). Not only must the lifetime of state l of the individual atoms be low but the radiation must immediately leave the plasma region. This requirement sets limits on the neutral gas pressure and thus on the number of available lasing atoms.

Final manuscript received July 6, 1966

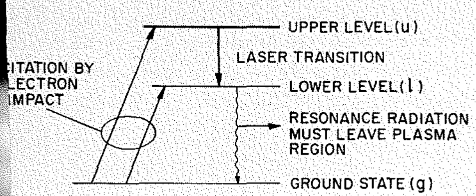

Fig. 1—Energy level diagram illustrating gas laser operation.

GAS LASERS USING THE IONIZED GAS FOR LASING

Both of the above discussed limitations are alleviated in the more recently discovered ion lasers.[1] Here the *ions* are excited to do the lasing. Excitation is achieved by electron impact. Since this excitation interaction takes place between two *charged* particles, Coulomb forces affect the excitation probability. It is then possible to have a *high excitation probability* and a *low radiative transition probability.* Another advantage of having the lasing particles charged has to do with the outlet of resonance radiation from the plasma. The ions can be preferentially accelerated by electric fields to give the equivalence of a high ion temperature which broadens the lines and minimizes the absorption of the resonance radiation corresponding to the transition below the lower lasing level. A price has to be paid for these advantages in terms of a more difficult tube-building technology. Since the ions are in effect a continuously produced "lasing gas," a high plasma density is called for to obtain a sufficient number of lasing particles. This high density plasma has a destructive influence on the plasma-confining structure as will be discussed further below.

The "ion gas" produced in these lasers has electronic properties quite different from those of the neutral gas. These properties and the above-mentioned ad-

DR. KARL G. HERNQVIST received the Ph.D. in Electrical Engineering from the Royal Institute of Technology, Stockholm, Sweden, in 1959. He worked on radar and microwave instrumentation in the Royal Swedish Air Force in 1945 and 1946. From 1946 to 1952 he was concerned with electron-tube research at the Research Institute of National Defense, Stockholm. He was an American-Scandinavian Trainee at RCA Laboratories in 1949. In 1952 he joined RCA Laboratories, where he has worked on microwave tubes, electron guns, and gas-discharge devices. In 1956 he independently conceived and reduced to practice the thermionic energy converter. He is presently doing research on gas lasers. Dr. Hernqvist has gained an international reputation for his work. He has been the recipient of two RCA Achievement Awards for outstanding work in research. He has authored several dozen technical papers and holds 15 patents. He is a Senior Member of IEEE and a member of the American Physical Society and Sigma Xi.

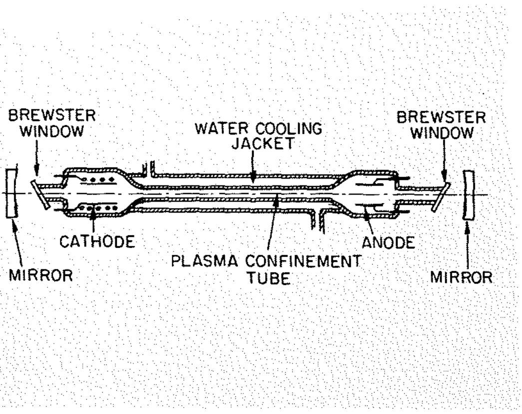

Fig. 2—Typical gas laser configuration.

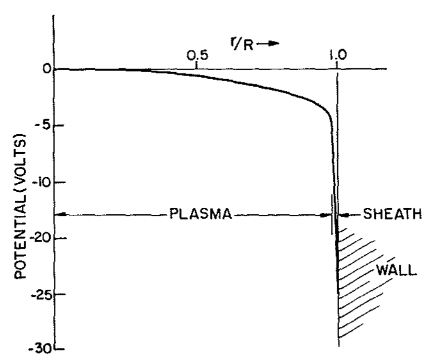

Fig. 3—Radial potential distribution within plasma and space charge sheath.

vantages have made possible a large number of new gas laser transitions throughout the visible part of the spectrum. Many gases and metal vapors have been made to lase in the ionized state. From the tube construction point of view, the noble gases are easiest to handle. Of the different gases argon is the most efficient in lasing.

PROPERTIES OF LOW PRESSURE LASER DISCHARGES

The most common type of discharge tube used for gas lasers is shown schematically in Fig. 2. It consists of a thermionic cathode and an anode separated by the long plasma confinement structure. The confinement structure constricts the discharge into a narrow straight column allowing line of sight passage between the two Brewster angle windows and along the axis of the tube. The two external mirrors form the optical resonator.

The type of discharge taking place in the argon ion laser is characterized by a very high current density (500 to 1,000 A/cm^2) in the narrow bore and a relatively low gas density (corresponding to an equivalent pressure of a few hundredths of a torr). This type of low pressure discharge was studied in detail by Tonks and Langmuir.[2] One significant consequence of the low pressure operation is a long ion mean free path. Ions generated in the plasma travel quickly to the walls and very rarely make collisions with the neutral gas atoms. For typical laser operation the electron plasma temperature is about 50,000°K. The potential distribution established in the plasma confining structure corresponds to a uniform axial gradient and a transverse distribution as shown schematically in Fig. 3. The axial field is very weak compared to the average transverse field so that ions formed in the plasma are accelerated towards the wall. Typically there is a potential difference of about 5 volts between the axis and the periphery of the plasma column. There exists an approximately 20-volt potential drop in a thin space-charge sheath separating the plasma from the wall. Ions formed at the axis thus have an impact energy at the wall of about 25 volts. As a consequence of the potential drop *within* the plasma there exists a large radial velocity spread for the ions. This velocity spread increases in magnitude towards the periphery of the plasma. Because of the Doppler shift this large radial velocity spread minimizes the self-absorption of the resonance radiation, which is so important for efficient laser operation. Since the axial ion velocity is not affected by the transverse field, the linewidth of the laser radiation (viewed along the laser axis) remains small, corresponding to the thermal velocity of the ions. Thus the ion gas has properties equivalent to a high "radial temperature" but a low "axial temperature."

LASER TUBE CONSTRUCTION PROBLEMS

As discussed above, the high density, low pressure plasma offers several advantages as a laser medium. However, the intense ion bombardment creates severe problems in tube construction. The ion energies are near threshold for sputtering of many common tube construction materials. Two methods of construction of the plasma confining structure have been tested.

One type of construction uses a long, unbroken water-cooled insulator tube made of quartz or a ceramic material as shown schematically in Fig. 2. This type of construction suffers from several drawbacks. The intense ion bombardment of the wall causes sputtering decomposition. As a consequence, cathode poisoning gases accumulate in the tube and residues are left on the tube walls. These residues may lead to formation of "hot-spots" on the wall. Secondly, the gas-pumping effects of the plasma cause a pressure gradient in these long tubes, preventing the operation of the whole length of discharge tube at optimum pressure. Thirdly, the poor heat conductivity of most insulators causes severe limitations in power density, thus limiting the attainable efficiencies. From several points of view a more satisfactory type of construction[3] uses a series of short bored metal discs lining the inside of a large diameter quartz tubing shown in Fig. 4. Since a voltage gradient exists along the plasma column these discs must be electrically isolated from each other. The wall potential follows the uniform axial potential in a step-wise fashion. This type of construction eliminates many of the drawbacks of the insulator tube construction, such as the freeing of the cathode poisoning gases, pressure nonuniformity (separate gas return is provided for each section), and the poor heat transport properties. Using metal discs, however, one is still faced with the sputtering problem which results in gas clean-up and electrode erosion.

A recent development at RCA Laboratories has greatly alleviated some of these problems. In a joint program by J. R. Fendley, Jr. and the author, it has been found that high purity graphite has outstanding properties as a construction material for the plasma confining structure.[4] In a comparison test, tantalum and molybdenum were seriously damaged by sputtering but graphite was unaffected. In a successful 1,000-hour

Fig. 4—Laser construction using sectioned metal bore.

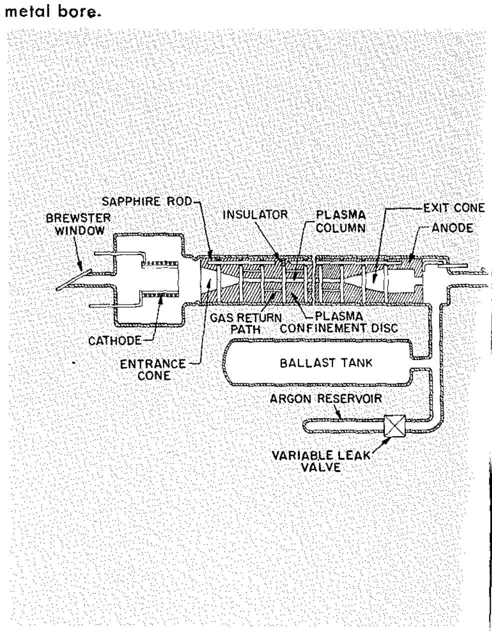

life test only slight sputtering damage was observed for a graphite structure.

A typical graphite construction of a long-life argon laser is shown schematically in Fig. 4. The cathode is a barium impregnated tungsten matrix cathode. To reduce noise and instabilities a symmetrical construction is chosen and the cathode is placed relatively close to the plasma confining structure. A gradual transition to the main bore size is provided both at the cathode end and at the anode end to minimize sputtering effects. The graphite structure operates at about 1,000°C during use, and the dissipated heat radiates through the large diameter quartz tubing.

Two types of argon reservoirs are employed as shown in Fig. 4. One is a ballast tank communicating with the main part of the tube. It serves to smooth out the pressure variations during start-up periods and also to extend the time between refilling the tube. A manually or electrically operated leak valve is used to replenish argon lost due to the clean-up effect. An automatic refill system is contemplated to assure constant pressure in the discharge tube.

Using these construction techniques it is possible to manufacture reliable argon lasers having life expectancy of a thousand hours or more. Several such laser tubes constructed at RCA Laboratories range in power output from 50 mw (Fig. 5) to 1.5 watts (Fig. 6). The heat can radiate directly into the room or it can be captured on water-cooled plates (Fig. 6). An axial magnetic field needed for optimum output can be obtained using permanent magnets as shown in Fig. 6.

PERFORMANCE CHARACTERISTICS OF ION LASERS

Noble-gas ion lasers yield continuous duty oscillations at wave-lengths throughout most of the visible spectrum as shown in Fig. 7. The most efficient is the 4,880-angstrom line of argon. Generally, oscillation at the krypton and xenon lines is less efficient than that of the principal argon lines. Neon lines have been made to oscillate in the ultraviolet region. Of the different oscillating lines for a particular gas several may oscillate simultaneously. Wavelength selection can be made by means of a prism in the cavity.

In general, the output power of a particular line increases approximately as the square of the current. Output powers as high as several tens of watts have been reported. Ultimate limits appear not to have been reached yet.

Efficiency is the most unsatisfactory performance parameter of noble gas ion lasers. Typically for power outputs of the order of one watt, the efficiency is less than a tenth of a percent. The useful laser oscillation is a volume effect and the losses (mostly power transported to the plasma confining structure by the particles) are surface effects. Therefore, for a given discharge current density the efficiency tends to increase as the volume to surface ratio of the plasma region increases. That is to say, the larger the device the higher is the efficiency. Presently attainable efficiency limits are not of fundamental nature, but are inherent in the particular discharge configuration used. Considerable future improvements in efficiency should therefore not be surprising.

APPLICATIONS OF ARGON LASERS

Due to its present low efficiency the noble gas ion laser is not a serious competitor in applications where heating effects of the radiation is of primary concern. However, where high density continuous duty quantum delivery in the energy range 2 to 4 eV is desired, the ion laser is unique among presently available lasers.

Generally, quantum detectors have higher sensitivity in the visible wavelength range than in the infrared region where more efficient lasers are available. This is the reason why argon CW lasers are seriously considered for ranging and space communications. In applications where direct visual read-out is required, the noble-gas ion lasers are capable of almost complete color coverage. A large-screen laser display built for the Air Force by Texas Instruments was demonstrated at a recent IEEE Convention. This system used electromechanical scanning and electro-optic modulator to display a picture.

Several applications using an argon laser to produce photochemical effects are presently being studied. Examples of these are hologram exposure and read-out, photo-resist exposure, photobleaching, and polymerization.

BIBLIOGRAPHY

1. W. B. Bridges and A. N. Chester, *IEEE J. Quantum Electronics, QE-1*, 66 (1965).
2. L. Tonks and I. Langmuir, *Phys. Rev. 34*, 876 (1929).
3. E. F. Labuda, E. I. Gordon, and R. C. Miller, *IEEE J. Quantum Electronics QE-1*, 273 (1965).
4. K. G. Hernqvist and J. R. Fendley, Jr., "Construction of Long Life Argon Lasers," *submitted for publication* to *IEEE J. Quantum Electronics.*

Fig. 7—Typical noble-gas ion laser wavelengths shown in their relation to human eye color perception.

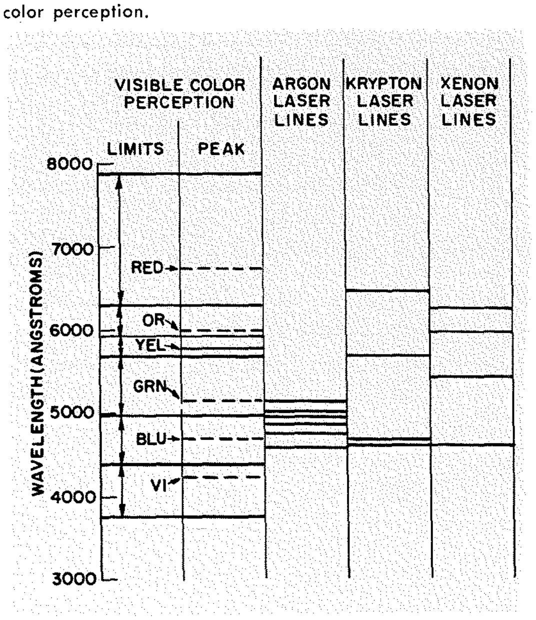

Fig. 5—Argon laser, 50 mW.

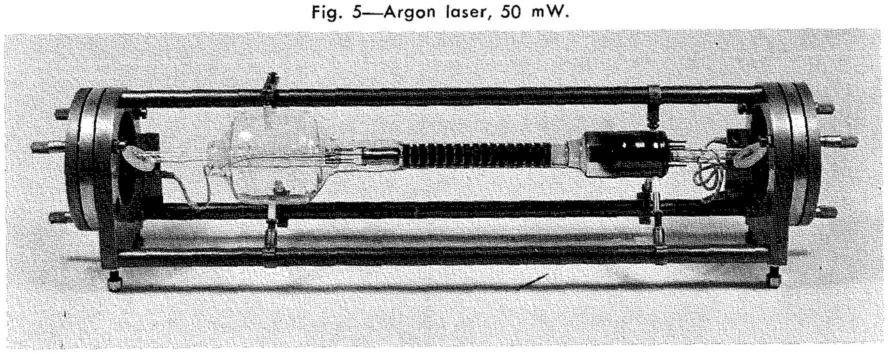

Fig. 6—Argon laser, 1-W.

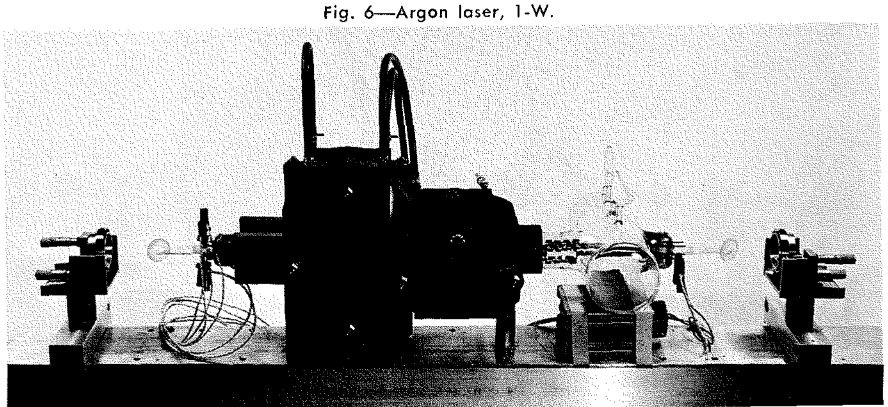

Nd:Cr:YAG
HIGH-EFFICIENCY HIGH-POWER SOLID-STATE LASER SYSTEM

Following the initial success of Kiss and Duncan of the RCA Laboratories in demonstrating that the Nd^{3+}:YAG laser could be improved by incorporating Cr^{3+} as an energy transfer agent,[1,2] a systematic study of the parameters and characteristics of this system was undertaken. This led to an optically pumped laser system with an average output of 10 watts at 10,640 angstroms. This paper discusses the theoretical limits imposed on any optically pumped laser system, outlines the experimental approach taken to optimize the Nd:Cr:YAG system and presents the operating characteristics of a Nd:Cr:YAG system representing the current state of the art.

Dr. R. J. PRESSLEY
RCA Laboratories, Princeton, N.J.

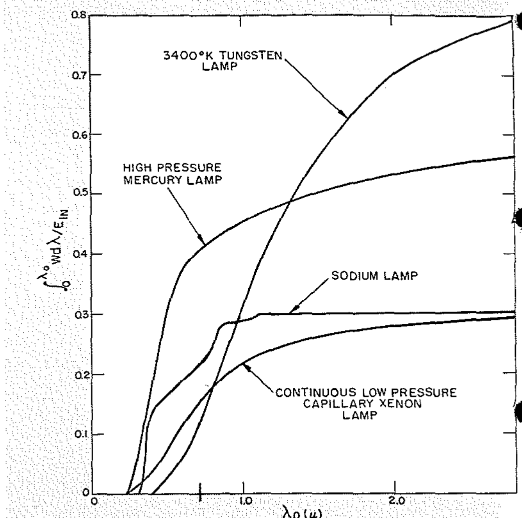

Fig. 1—First estimate of overall efficiency limits set by using conventional broadband optical pumps.

ALL OPTICALLY pumped laser systems have an inherent energy loss, since the pump photons must be of higher energy than the emitted radiation. This loss can in principle be minimized by using a monochromatic optical pump at an energy only marginally greater than the laser. Such monochromatic pumps are at present relatively inefficient, of limited intensity and available at only a few wavelengths. The usual situation is a broad band emitter and a laser material having an absorption spectrum that can utilize only a fraction of the energy emitted by the pump.

THEORY

A first estimate of the overall efficiency limits set by using conventional broad band optical pumps is shown in Fig. 1. This plots the fraction of the electric energy input that is emitted at wavelengths shorter than any given wavelength. For long wavelength laser systems, a tungsten lamp is the most efficient pump as its integrated optical output is typically 90% of electrical input. This is considerably higher than the 60% obtained with Hg lamps or the 30% available with continuous xenon and sodium lamps. The Hg and Na sources, however, have considerably greater output in the shorter wavelength region and are correspondingly better for pumping systems with outputs in the near infrared and visible. The high pressure mercury lamp is theoretically the most efficient pump lamp for systems with absorption over the visible region.

There are, of course, other losses in the laser operation. In order to achieve the limiting efficiencies of Fig. 1 it is necessary that 1) all of the pump energy is imaged on the crystal; 2) all of this energy is absorbed and passes through

Final manuscript received July 28, 1966.

The research reported here was sponsored by the Electronic Technology Division, Air Force Avionics Laboratory, Research and Technology Division, Air Force Systems Command, Wright-Patterson Air Force Base, Ohio, under Contract No. AF33-(615)2645 and RCA Laboratories, Princeton, New Jersey.

Fig. 2—Absorption spectrum of Nd^{3+}:YAG at 300°K from 0.3 to 0.9 micrometer.

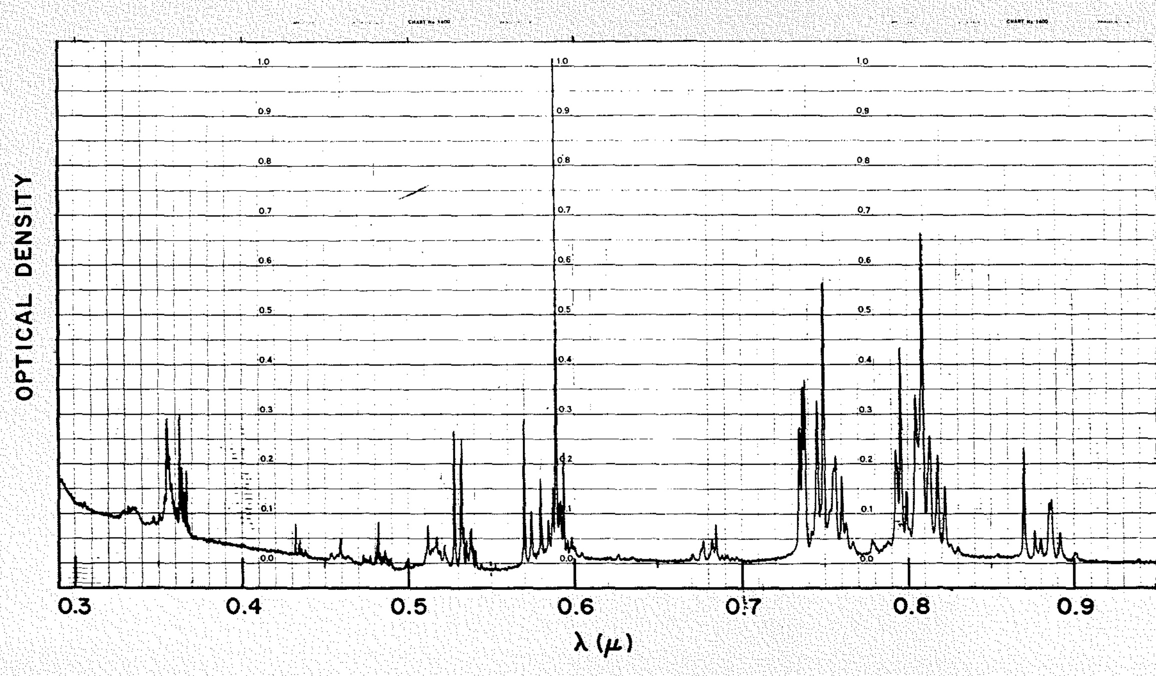

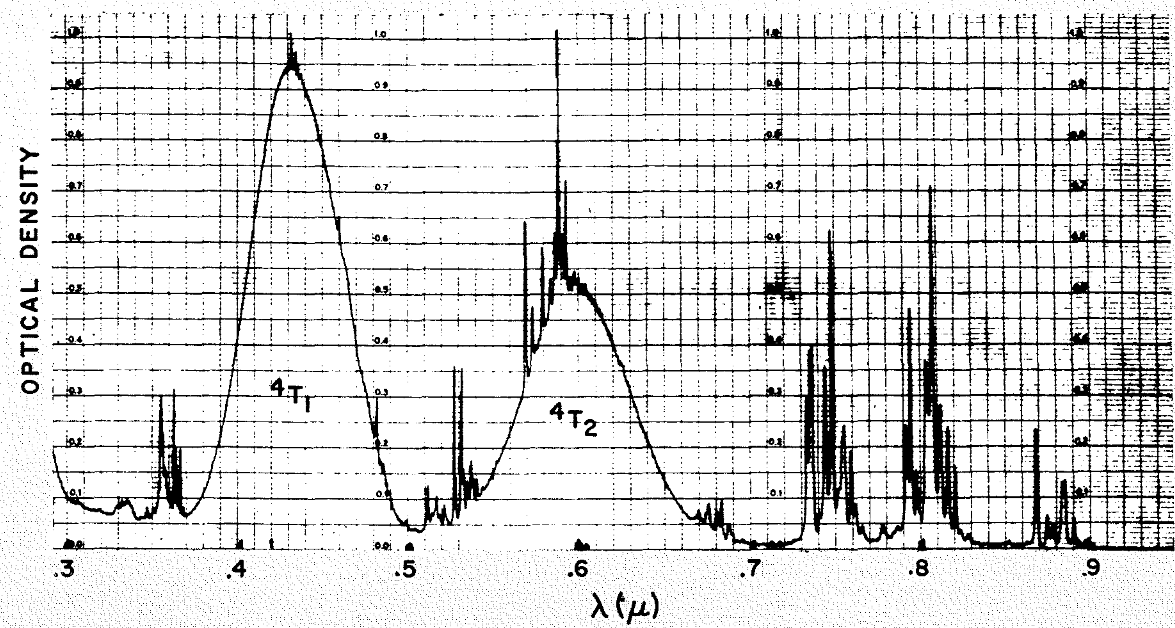

Fig. 3—Additional bands introduced by Cr^{3+}.

the upper metastable laser level; 3) operation is sufficiently above threshold that stimulated emission predominates over spontaneous emission and 4) the output coupling is large enough so that internal scattering and absorption losses are negligible.

Items 1), 3), and 4) can be approached experimentally, since linear ellipses or other optical systems for coupling the lamp and crystal image more than 50% of the lamp output on the crystal depending on the relative dimensions of the lamp and crystal and the complexity and size that one is willing to design into them. Fluorescent efficiencies approaching 100% have been measured and thresholds in the infrared are low enough so that operation at levels as high as ten times threshold are easily obtainable with output coupling losses much larger than all internal losses.

The most serious limitation on the laser efficiency is in 2), the absorption of the broadband pump emission by the crystal. Fig. 2 shows the absorption of Nd:YAG alone while Fig. 3 shows the additional bands that the Cr^{3+} introduces.

The additional pumping that this Cr^{3+} introduces depends upon the Cr^{3+} concentration as well as crystal size and pump lamp. In order to give an estimate of the improvement for various pump lamps, Table I combines the efficiencies of the various steps with the maximum theoretical emission from various optical pumps to give theoretical laser power and efficiency for Nd:Cr:YAG lasers and various lamps. The entries in Table I are explained as follows:

Line 1—The efficiency of conversion of electrical-to-optical output at wavelengths shorter than the laser output.

Line 2—The efficiency of conversion of electrical input to optical output in the Nd^{3+}YAG absorption bands assuming side pumping of a typical 3-mm rod of 1.5% Nd^{3+} doping.

Line 3—The efficiency of conversion of electrical input to optical output in the

Dr. ROBERT J. PRESSLEY received his BS in 1954 from Michigan State University, majoring in physics. He joined RCA Laboratories in 1954 as a member of the research training program. Following this he engaged in research on infrared sensitive photoconductive surfaces for imaging systems. Upon receipt of a David Sarnoff Fellowship in 1956, he took a leave of absence and entered Princeton University Graduate School. He received his MA in 1958 and his PhD in 1962, both in physics. During this time he also returned to RCA on projects involving ammonia gas masers, communications systems studies, and optical beating experiments in sodium vapor. His thesis research was an investigation of the interaction of electron spins and nuclear magnetic moments in very pure lithium metal, an experimental investigation using simultaneous ESR and NMR monitoring of the same sample in thousand-gauss fields. During the 1961-62 academic year, Dr. Pressley served as an instructor at Princeton University setting up laboratory courses in optics and electromagnetic theory. He returned to RCA Laboratories in 1962 and has been associated with the Quantum Electronics Group. He has worked in optical masers with the emphasis upon laser operation and characteristics, in particular, the optimization of the CaF_2:Dy and the Nd:Cr:YAG systems. He has also been active in preparing and testing of new materials particularly in the organic laser field investigating various rare earth chelates. This work has resulted in several new organic laser systems. He is a member of the American Physical Society, and the Society of Sigma Xi.

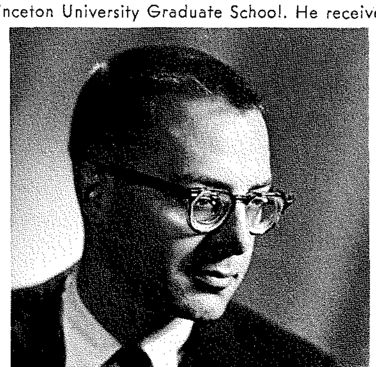

Fig. 4—Number of excited ions versus time.

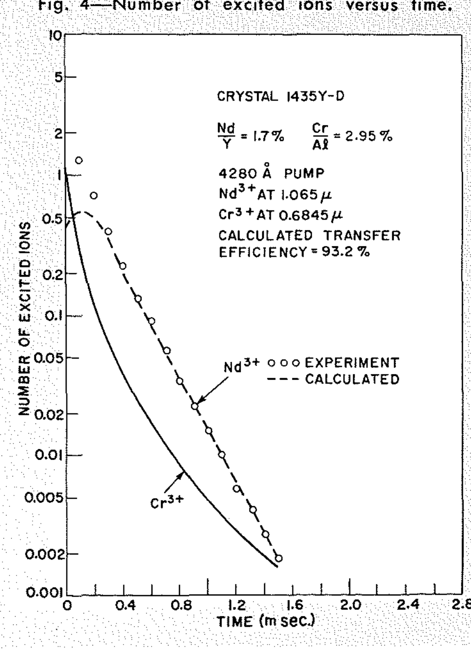

TABLE I—Overall Laser Efficiency

LINE		TUNGSTEN	DC XENON	MERCURY HIGH PRESSURE	SODIUM HIGH PRESSURE
		3400°K blackbody	blackbody	non-blackbody	non-blackbody
1	Total optical output efficiency Optical Watts ÷ electrical Watts	35%	22%	45%	30%
2	Optical efficiency into Nd:YAG bands	3.5%	3.5%	<1%	?
3	Optical efficiency into Cr:YAG bands	6.1%	3.5%	20%	25%
4	Imaging efficiency of linear ellipse	50%	50%	50%	50%
5	Nd:YAG absorption to Nd:YAG emission efficiency	80%	80%	80%	80%
6	Cr:YAG absorption to Nd:YAG emission efficiency	60%	60%	50%	60%
7	Overall ideal Nd:YAG efficiency 2x4x5	1.4%	1.4%	<1%	?
8	Overall ideal Cr:YAG efficiency 3x4x6	2.5%	1.4%	>5.0%	7.5%
9	7 + 8—overlap	3.5%	2.6%	5.5%	7.5%
10	Maximum total emission of 2 mm diam x 5 cm long source	600 W	1000 W	3000 W	400 W
11	Maximum laser output using above source	21 W	26 W	165 W	30 W

Cr^{3+}:YAG absorption bands for a similar crystal with 1.5% Cr^{3+} concentration.

Line 4—Typical imaging efficiency of a linear ellipse with 5-cm source and 5-cm laser.

Line 5—Average energy conversion efficiency from Nd absorption lines to laser ouput (different photon energies).

Line 6—Average energy conversion efficiency from Cr absorption bands to laser output (different average photon energy).

Line 7—The overall ideal efficiency for a side pumped Nd^{3+}:YAG crystal is obtained by multiplying lines (2)×(4)×(5).

Line 8—Ideal Cr^{3+} efficiency for a side-pumped Nd^{3+}:Cr^{3+}:YAG crystal is obtained by multiplying lines (3)×(4)×(6).

Line 9—Gives the overall total ideal efficiency for a Nd:Cr:YAG laser obtained by adding lines (7) and (8) and subtracting a small factor for the overlap of the absorption lines. This assumes 100% Cr^{3+} to Nd^{3+} transfer.

Line 10—One factor of importance for total output is the total power that can be emitted for a lamp of the same dimensions as the laser rod (2 mm x 5 cm). The value for sodium lamps is uncertain as they are not yet well developed. It could be a good bit higher.

Line 11—Gives the total output power that can be achieved using these different sources to pump an ideal Nd:Cr:YAG laser in a linear ellipse.

LASER PREPARATION

A very important parameter in laser operation is the quality of the laser rod itself. It must have low scattering losses, low strain, and no absorption at the laser frequency. The ends must be polished to high optical quality with the desired geometry, and the dielectric reflectors must have the desired reflectivity and low loss.

Since we were dependent upon outside suppliers for the laser material, we procurred it in as large boules as possible and selected the regions with the lowest optical losses to cut into laser rods. The techniques of optically polishing the ends were developed in the optical polishing shop at the Laboratories to a degree considerably higher than was available outside. These techniques, combined with commercially available dielectric coatings, gave laser rods that consistently gave high output power and low thresholds.

ENERGY TRANSFER

One requirement that is important in this double doped system is that the transfer time from the excited Cr^{3+} to the Nd^{3+} be short compared with the Cr^{3+} fluorescent decay time. This transfer time is found to decrease with an increase in either the Nd^{3+} or Cr^{3+} concentration at a rate characteristic of a dipole-dipole interaction between both the $Cr^{3+} \rightarrow Cr^{3+}$ neighbors and the $Cr^{3+} \rightarrow Nd^{3+}$ neighbors. This transfer time can be measured by observing the buildup and decay of the Nd^{3+} fluorescence when the excitation is only in the Cr^{3+} absorption bands.

Fig. 5—Experimental arrangement.

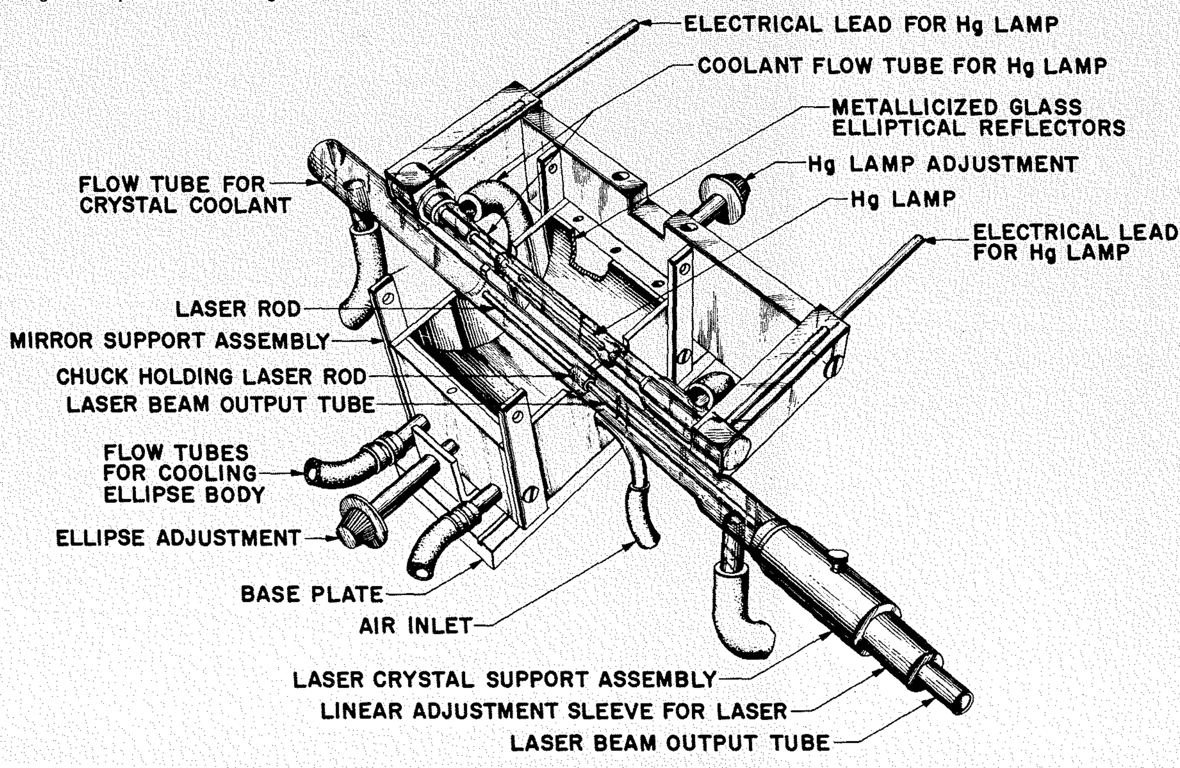

Typical experimental data for this type of measurement is shown in Fig. 4 where both the Cr^{3+} and Nd^{3+} fluorescent time dependences are shown. The transfer efficiency in this crystal is 93% indicating that this concentration of Cr^{3+} meets the requirements of an absorber that transfers energy well to the active Nd^{3+} ion. The discrepancy between experiment and theory in the first 200 μs is due to some direct excitation of the Nd^{3+} ions by the pump lamp.

POWER

The experimental arrangement is shown in Fig. 5. It uses a right cylindrical ellipse for coupling the Hg pump lamp to the laser crystal. Using this equipment and water for cooling we were consistently able to obtain powers greater than 1 watt and efficiencies of a few tenths of a percent. The best results were obtained with a laser rod doped with 1.5% Nd^{3+} and 0.5% Cr^{3+}. This is also the largest high quality Nd:Cr:YAG rod that we have obtained. It is 2.00 inches long by 0.187 inch in diameter and is polished with flat ends. Fig. 6 shows the power output vs. pump power for this rod for both 3% and 8% output couplings with a 4-kW Hg pump lamp and at 3% output coupling with a 3-kW lamp. A maximum power of 10 W was obtained with a 4-kW lamp operated at 3 kW. At this level the differential efficiency was 1%. However, since the lamp output spectrum is changing as the electrical input to the lamp is increased some of this may be due to an increasingly good match between the mercury output and the Cr^{3+} absorption. This is probably what gives rise to the superlinearity in the output. The overall efficiency at 10-W output was 0.33%. Higher powers and efficiencies could be obtained if the Hg lamps could be operated at their nominal ratings for any length of time.

Again, the shorter 3-kW lamp gave a higher overall efficiency of 0.36%. The laser was operated at the 7.5 W level with less than 2.1 kW into this lamp. In all of these runs 85% of the power output was in the forward beam and 15% out the back due to the reflectivity on the back surface being too low.

Since this rod had only 0.5% Cr^{3+} it did not fully absorb the Hg pump light and also did not transfer it to the Nd^{3+} with full efficiency. Considerable improvement toward the 5% efficiency predicted in Table I should be possible with smaller-diameter more heavily doped rods.

Fig. 6—Power output vs. pump power.

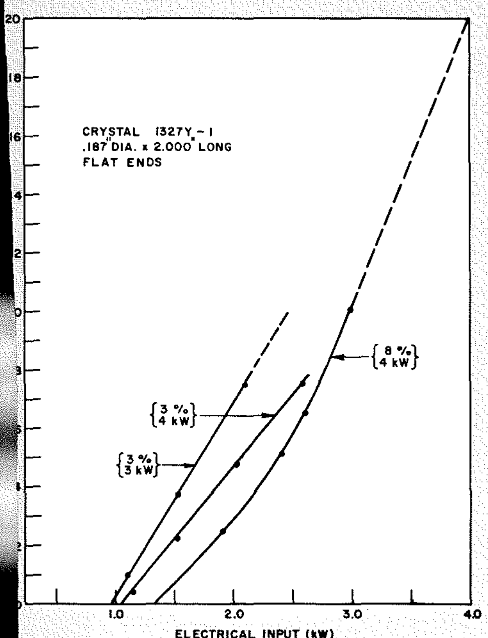

TIME DEPENDENCE

The time dependence of the laser output may be of two forms for Nd:Cr:YAG rods. Either there is a ripple superimposed upon a continuous output or else there is a train of regular spikes. The particular mode depends upon the radius of curvature of the ends, the diameter of the crystal, and the doping.

This ripple has a characteristic frequency of from 50 to 100 kHz depending upon how much above threshold the laser is operating. If the same laser crystal is operated with flat reflectors and a higher output coupling its output consists of a series of regular spikes with a repetition rate at this same ripple frequency. Fig. 7 shows the repetitive trace of this spiking for a crystal operating at 10-W average power. The time scale is 10 μs per division and goes from right to left. The smearing out of the top of the spikes is due to incomplete filtering in the power supply leaving residual 60-Hz ripple on the lamp. The width of the spikes at half amplitude is 0.6 μs and the time between spikes is 10 μs; this gives a ratio of peak to average power of 16. The output is then a train of 160-W spikes of 0.6-μs half-width at a 100-kHz rate.

This laser system can also be operated at elevated temperatures, with only a 50% reduction in power with a coolant at 80°C. This could be important if the system is to be radiatively cooled.

SUMMARY

Incorporation of the Cr^{3+} makes possible a more efficient, higher gain, higher power laser system. The advantages of higher efficiency and power are obvious, but the higher gain also makes the use of this system for frequency doubling much easier. In order to obtain frequency doubling a nonlinear optical material, such as lithium niobate, is placed in the optical cavity and a fraction of the 10,641.6-angstrom radiation is converted to 5,320.8 angstroms. The frequency doubling is proportional to the square of the intensity of the optical field in the doubler. The higher gain of the Nd:Cr:YAG system enables us to achieve high field intensities even with the added losses due to the doubler crystal inserted in the optical cavity. Preliminary experiments have produced 1 mW of continuous output at 5,320.8 angstroms, with several orders of magnitude improvement expected with the system optimized. A further increase in the 5,320.8-angstrom output can also be achieved if the laser is made to operate in a repetitive spiking rather than a continuously operating mode.

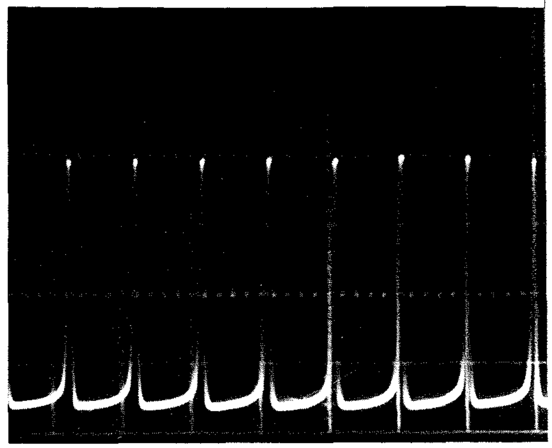

Fig. 7—Repetitive spiking output of Nd:Cr:YAG laser at the 10-W average level. The time scale is 10 μs/div. from right to left.

The repetitive pulse nature of the higher power output at this 100 kHz rate also suggests the possible use of this laser in some form of ranging or 3-D radar system.

This system is still a factor of 5 times less efficient than our theoretical estimates in Table I. The majority of that is due to the Cr^{3+} concentration in our crystal being too low. Not all of the pump light is absorbed and not all of the energy is transferred. If Nd:Cr:YAG with higher Cr^{3+} concentration could be obtained with sufficiently good optical quality, a factor of 2 to 4 improvement should be immediately available.

ACKNOWLEDGMENTS

This research was conducted in collaboration with P. V. Goedertier. The energy transfer was calculated by W. Zernick. The mechanical design work and assistance of C. J. Kaiser were also important factors in achieving these results.

BIBLIOGRAPHY

1. Z. J. Kiss and R. C. Duncan, Jr., *Applied Phys. Lett. 5*, 200 (1964).
2. Z. J. Kiss and R. C. Duncan, RCA ENGINEER, p. 53, Vol. 11, No. 2, August-September 1965.

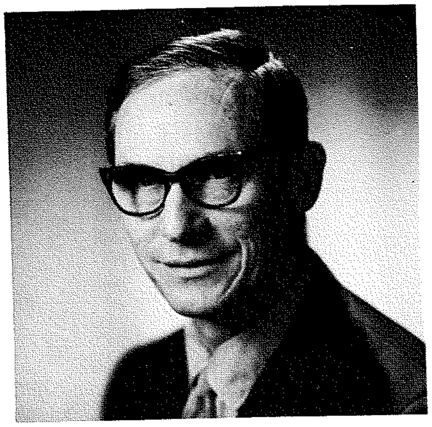

DR. HENRY S. SOMMERS, JR. attended Stanford University in 1933 and 1934, and received his BA in physics from the University of Minnesota in 1936. He was awarded a PhD in Physics in 1941 from Harvard University, where he served as Physics Instructor during 1942. From 1942 to 1945, he was a Staff Member at the MIT Radiation Laboratory, where he made wartime contributions for which he received the Naval Ordnance Development Award in 1945. After the war, Dr. Sommers was appointed Assistant Professor of Physics at Rutgers University. In 1949, he joined the research staff at the Los Alamos Scientific Laboratories in New Mexico, where he carried out fundamental studies on the thermodynamic properties of liquid helium and on the scattering of neutrons by liquid helium. Dr. Sommers joined RCA Laboratories in 1954. His work at RCA has been devoted to the study of electrical properties of insulators and semiconductors, including the development of tunnel diodes for which he received an RCA Achievement Award. He recently returned from a year abroad at Laboratories RCA Ltd. Zurich, and as a Guggenheim Fellow and Fulbright Lecturer at the Hebrew University in Jerusalem. He is the author of many papers in the fields of solid state physics, cryogenics, nuclear physics, chemical kinetics, and instrumentation. He is a Fellow of the American Physical Society and a member of the Federation of American Scientists.

DR. E. K. GATCHELL completed his undergraduate education at Columbia and received his Ph.D. in physics from the University of Rochester in 1956. He joined RCA Laboratories in 1956 where he has worked on infrared imaging and hot electron emission from semiconductors. He is currently working in the area of optical demodulation. He has received an RCA Laboratories Achievement Award. He is a member of Phi Beta Kappa, Sigma Xi and the American Physical Society.

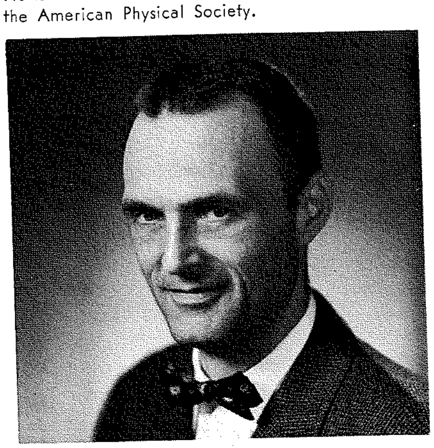

SUPERSENSITIVE LASER LIGHT DETECTOR

Recently the RCA Laboratories have demonstrated a significant increase in the sensitivity of broadband infrared detectors which offers the promise of wideband receivers with signal-to-noise approaching the theoretical limit set by noise-in-signal. Although the work has been concerned with receivers for point-to-point broadband communications, the units also work extremely well as narrowband point detectors which can be modified for problems requiring a low-frequency detector with larger active area.

Dr. H. S. SOMMERS, JR. and Dr. E. K. GATCHELL

RCA Laboratories, Princeton, N.J.

In this work on optical receivers, actually what is under consideration is the performance of the front end of an optical receiver (Fig. 1) of which the optical transducer itself is a small but key part. The latter is a speck of photoconductor cemented between the pole pieces of a re-entrant reflection cavity. The voltage is supplied by exciting the cavity (X band in these studies) with a klystron coupled through a circulator. When the amplitude-modulated signal is focused on the photoconductor, the photoconductance follows the optical modulation; this modulates the cavity Q, which transfers the AM input signal to sidebands of the microwave power reflected from the cavity. There follows an RF amplifier and second detector, whose output is a video signal which reproduces the envelope of the optical input.

The work has concentrated on cavity design and fabrication, mounting of the photoconductive samples and performance studies. Standard microwave plumbing, klystrons, amplifiers, and second detectors have been used so as to evaluate the improvement in optical receivers that can be achieved with commercially available microwave components. The studies consisted of terminal measurements of video output and signal-to-noise. The overall sensitivity and frequency response of the receiver was deduced, as well as the performance of the optical transducer.

The bulk of this paper concerns original work not yet published. For RCA groups, additional data can be found in company-private reports by the same authors available in RCA Libraries, to which the RCA reader is referred for greater detail and for a pertinent bibliography on optical detection with microwave cavities. (Standard works on photoconductivity are listed in the Bibliography at the end of this paper.) The transmission of the TV picture is described in another RCA company-private report by J. Bordogna, W. Hannan, T. Penn, C. Reno, and R. Tarzaiski of Applied Research, Camden.

Final manuscript received August 1, 1966.

PHOTOCURRENT GAIN

A necessary condition for a photoconductor to have high sensitivity is a large ratio of current output to light input, i.e., a high photoconductive gain G:

$$G \equiv \frac{I_s}{\alpha q F}$$

where I_s is the signal current output of the photoconductor and F is the optical signal flux in photons/sec (Fig. 1); α is the quantum efficiency of the detector, and q the fundamental charge. Current gain reduces the noise of the following amplifier, the principal noise source in many important applications.

Conventionally, high-gain photoconductivity is associated with materials in which only one carrier is mobile. In homogeneous materials, single-carrier photoconduction occurs if one carrier of the photo-produced pair is very quickly localized in a deep center while the other remains free to conduct, as in insulating photoconductors like CdS; or if the optical absorption ejects carriers from a deep center that has been incorporated in the lattice by proper doping. An equivalent result is achieved by constructing inhomogeneous regions to localize the pair, as in the phototransistor. None of these single-carrier photoconductors has given a wideband infrared detector as sensitive as junction diodes.

A recent theoretical analysis has shown that a two-carrier photoconductor, with an RF bias instead of the DC bias that is normally applied to photoconductors, can have very high current gain, frequency response, and sensitivity. The rapid reversal of the electric field localizes the induced photo pairs in the sample as effectively as does a deep trapping center or internal barrier. This permits the use of the high purity transistor materials, which have both excellent high-frequency properties and band gaps narrow enough to respond to infrared radiation. With dc bias the high-frequency response of these materials has not been good because their long minority carrier lifetimes limit the gain-bandwidth product.

The photocurrent gain and the gain-bandwidth product of the photoconductor in the RF cavity can be expressed in terms of measureable parameters of the cavity and semiconductor.

$$G = \left[\frac{v_1\tau_1}{(1+\omega^2\tau_1^2)^{1/2}} + \frac{v_2\tau_2}{(1+\omega^2\tau_2^2)^{1/2}}\right]\frac{E}{W^{1/2}}\left[\frac{1}{2\pi R\Delta f}\right]^{1/2}$$

$$G \cdot B = \frac{v}{2\pi}\frac{E}{W^{1/2}}\left[\frac{1}{2\pi R\Delta f}\right]^{1/2}$$

Symbols:

Photoconductor: v_1, v_2 = drift velocities of carriers 1 and 2, τ_1, τ_2 = their photoconductive lifetimes.

Cavity: E = electric field at the position of the photoconductor, W = stored energy, Δf = bandwidth (in Hz).

Amplifier: R = input impedance.

Signal: ω = modulation frequency in radians/sec, B = video bandwidth of demodulator in Hz (assumed less than Δf).

The ratio $(E/W^{1/2})$ is a figure of merit of the cavity, a geometrical parameter describing the interaction of the photoelectrons with the stored energy which is similar to the figure of merit of a klystron.

The desired bandwidth B, a design parameter dictated by the communication problem, determines the characteristics of the following amplifiers. It also prescribes the preferred Δf of the cavity, which should be about $3B$. In practice, however, the klystron frequency largely determines Δf, since with conventional design and matching techniques the loaded Q of the cavity can range only between about 50 and 500.

ALIGNMENT OF RECEIVER

Although *SNR* is the preferred measure of receiver sensitivity, there is a sufficiently close correspondence between the maximum of *SNR* and of photocurrent gain to permit the gain to be used as a check of operational performance. This greatly simplifies the problem of adjusting the front end of the receiver, so that in spite of the extra complexity that one associates with microwave circuits, the receiver alignment is routine. In fact, the only precise step is pointing the optics at the target, a problem not properly associated with the receiver alignment but with operation. (The difficulty of pointing is intensified by the very small angular coverage of high-performance communication receivers, which require high angular resolution to reduce background interference.)

The alignment steps are listed to give some idea of what is involved in a detector with microwave bias. The only monitor needed is the output signal, which indicates the current gain. With a packaged system, these are factory adjustments.

1) Tune klystron to cavity resonance and lock on with AFC.
2) Match cavity to waveguide with adjustable coupling (zero reflected power as indicated by second detector bias).
3) Overcouple cavity to give sufficient reflected power to bias second detector into linear region (about 25 mV DC bias for IN23B crystal). Steps 2) and 3) are simultaneous.
4) Focus infrared onto photoconductor. This requires an appropriate source of chopped light.
5) Adjust microwave power for maximum

Fig. 1—Photoconductive demodulator, front end of optical receiver.

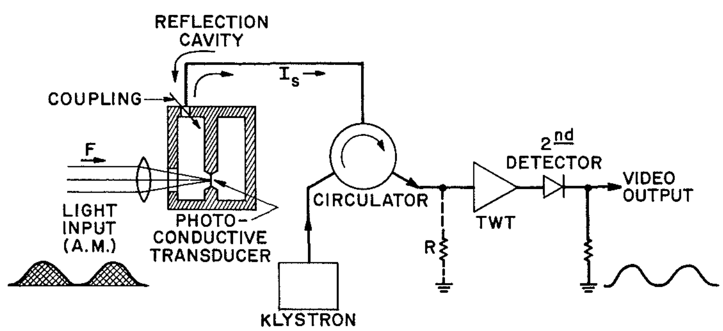

Fig. 2—Response of germanium photoconductor, gain vs modulation frequency.

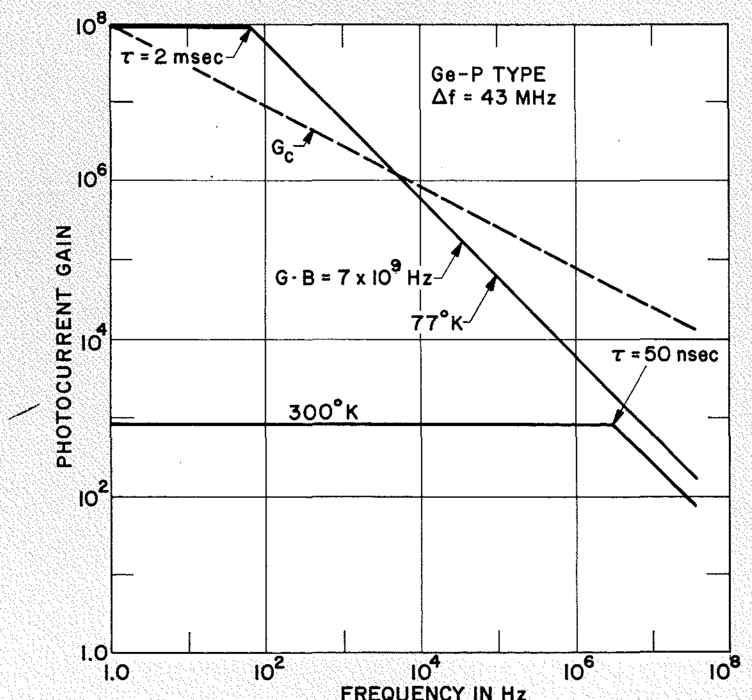

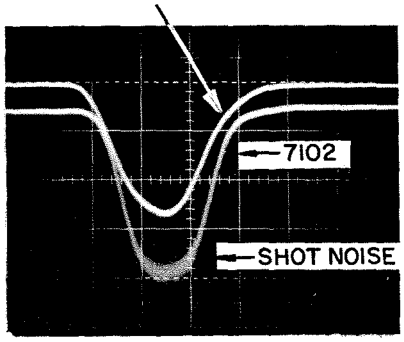

Fig. 3—Comparison of response of InSb photoconductor and 7102 photomultiplier. Pulse risetime = 20 ns; 10^5 photons/pulse; 8,400-angstrom light.

output signal. Required power input to cavity ranges from 50 μW to 10 mW, depending on the photoconductor. Correct adjustment of step 3).

6) Make final trimming by simultaneous adjustments of klystron power and frequency about the cavity resonance.

TYPICAL FREQUENCY RESPONSE OF PHOTOCONDUCTIVE GAIN

A typical frequency response is shown by the measurements on a detector of germanium, which responds to about 1.5 micrometers, shown in Fig. 2. The infrared signal is from a gallium arsenide laser, wavelength 0.84 micrometers. The current gain is plotted against modulation frequency for a pair of curves which show the predicted effect of photoconductive lifetime on the response.

At room temperature, the lifetime of this germanium sample was 50 ns, producing the break at 3 MHz. The low-frequency gain was almost 1,000, and the gain-bandwidth product nearly 10^{10} Hz. It is a good broadband optical transducer over the range where $G \cdot B$ is constant, which means modulation frequency from 1 MHz up to the cavity cutoff (to 20 MHz.) Immersed in liquid air, the only important change is the great increase in photoconductive lifetime to a couple of milliseconds, which enhances the low-frequency response. Now it is an exceedingly high performance detector for modulation bandwidths anywhere from 100 Hz to 20 MHz. (Proper surface treatment of the germanium should give the long lifetime at room temperature.)

On this same graph we have indicated G_c, the gain at each bandwidth needed to reduce the amplifier noise until it is less than the noise-in-signal at unity *SNR*. The gain G_c can be thought of as the minimum condition that the amplifier not degrade the information in any useful signal. The comparison is somewhat arbitrary, but representative of a class of problems in broad-band communications, with amplifier input impedance of 50 ohms and noise figure 3 DB, for which an acceptable signal requires *SNR* of only a few dB. If no other source of noise were present, the germanium in liquid air would be ideal for bandwidths from 1 Hz to 10 kHz, since here the measured gain exceeds G_c; actually, $1/f$ noise in the system precluded the goal of being signal-noise limited at low level. It seems technically feasible to reach this limit with further refinements. Actually this would then count single events, giving a high efficiency photon counter.

Studies with photoconductors of Si, InAs, and InSb give comparable results, covering the range of wavelengths from the visible to beyond 5 micrometers. Extension to the important region of 10 micrometers has not yet been done, but is easily possible. The quality at the longer wavelengths will depend to a large extent on the optical absorption coefficient of available materials.

COMPARISON WITH AVAILABLE HIGH-QUALITY FAST DETECTORS

The easiest demonstration of the improvement offered by the receiver using a microwave cavity is a direct comparison with more familiar infrared detectors. Of these, the most sensitive for the 8,400 angstrom light from a gallium arsenide laser is the 7102 photomultiplier. Its serious disadvantages are a quantum efficiency of only ½% and high dark current. The latter can be greatly reduced by cooling in dry ice.

We have several comparisons with the 7102. Fig. 3 upper trace shows a scope trace of a pulse from an InSb photoconductive detector, which has good high speed response and is sensitive to wavelengths to 5.5 micrometers. The pulse of risetime 20 ns contains 10^5 photons, a high enough intensity so that no noise is apparent with the photoconductor. The lower trace is the 7102, showing considerable noise-in-signal at this light level. Clearly in this case the photoconductive receiver is outperforming the photomulti-

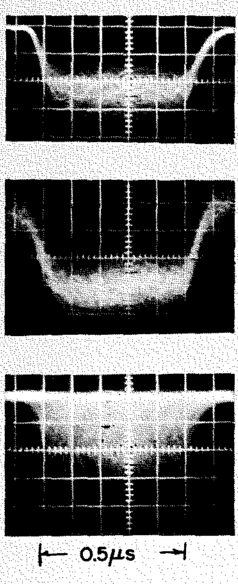

Fig. 4—Comparison of response of germanium photoconductor and 7102 photomultiplier at low signal level. Pulse risetime = 100 ns; 8,400-angstrom light.

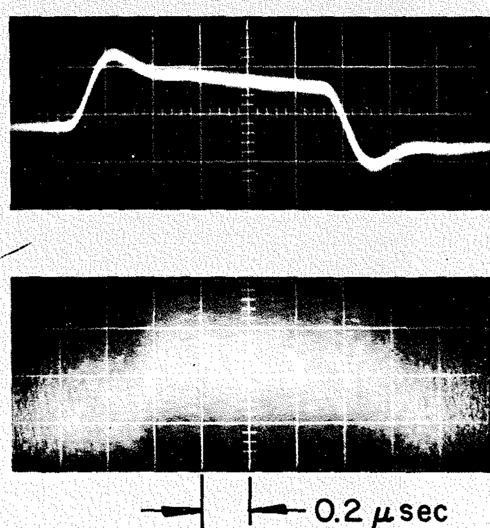

Fig. 5—Comparison of germanium photoconductor and silicon photodiode. Pulse risetime = 200 ns; 10^3 photons/pulse; 8,400-angstrom light.

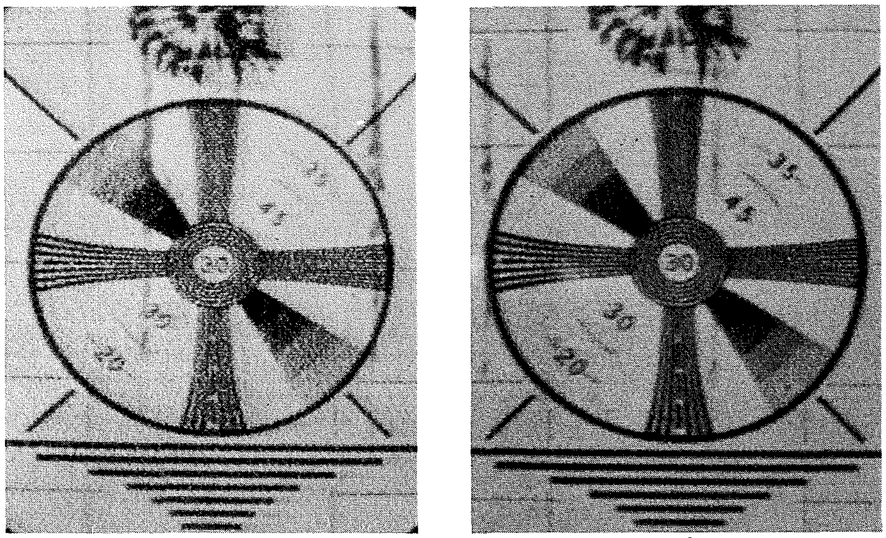

Fig. 6—Comparison of germanium photoconductor (left, 1.8 $\times$ 10^{-9} watts) and InAs photodiode (right, 1.3 $\times$ 10^{-7} watts); 1.15-micrometer light.

plier, its good quantum efficiency overcoming the advantage of the very high noise-free charge multiplication in the 7102. As for any InSb detector, the device was cooled, to liquid air temperature in this photo.

The relative performance of the photomultiplier increases as the light is reduced because its dependence of *SNR* on light is of lower order than for these solid state detectors. Hence the most stringent test of the photoconductor is near the limit of minimum detectable signal. Fig. 4 is such a case; both the photoconductor and the 7102 are cooled to give optimum performance. The middle trace is the response of a germanium crystal to a pulse of ½ μs duration containing about 10^3 photons. The trace shows considerable noise, but has a clearly defined signal whose amplitude can be determined with fair accuracy. Compare this with the lower trace, the cooled photomultiplier with the same input signal; only the presence of a signal is determined, the shot noise being so large that the signal amplitude cannot be estimated ($SNR < 1$). Quality equivalent to the photoconductor requires 50 times as much light (upper trace).

Fig. 5 shows a cooled germanium photoconductive detector and a quality silicon photodiode, Philco L-4501. The diode response is optimized by using a high impedance amplifier so that the effective input impedance is set by the shunt capacitance of the 6 inches of coaxial cable between diode and amplifier. The microsecond pulse here has much higher intensity, for the germanium (top trace) shows no noise. The signal from the Si diode is hardly discernible.

Closer to the interest of RCA is the final example, a TV picture transmitted as a single sideband FM modulation on a 5-MHz subcarrier impressed on the beam of a 1.15-micrometer laser (Fig. 6). The competition is a detector custom-made from the best available components (a Philco L-4530 InAs photodiode mounted in the front end of a low noise preamplifier with 3-dB noise figure and 1,000-ohm input impedance). The photo on the right shows the test pattern received by the diode with 10^{-7} watts of signal. The germanium photoconductor operated at room temperature gives an equivalent signal output with about 2% of the input —left picture. Cooled to 145°K, it would have required 1/10 of this light.

OTHER APPROACHES TO IMPROVED DEMODULATORS

Clearly the photoconductive detector with microwave bias has shown a great improvement in sensitivity of infrared receivers. In its present form it is well suited to wavelengths out to 5 micrometers and to problems in which the incoming signal can be focused on the small area detector. It seems reasonable that design modifications can significantly increase the detector area with no worse effect than the usual trade-off between area and sensitivity (minimum detectable signal varying as the reciprocal root of the area) and to the 10-micrometer region.

One can expect other approaches to give improved detectors. These results with RF bias should precipitate a flurry of work to increase the response of photoconductors with DC bias, which have the inherent advantage of their circuit simplicity. However, a number of factors tend to compensate for the extra cost of the microwave bias. The microwave circuit permits capacitance coupling to the photoconductor, which greatly simplifies the fabrication and mounting and eliminates a troublesome source of low-frequency noise. Also standard high-purity materials can be used, the high concentrations of deep levels which is required with dc bias not being necessary. The presence of these impurities can be expected to enhance the free-carrier trapping, which degrades the high-frequency response. Also there are suggestions that DC bias cannot have as large a gain-bandwidth product, although this theoretical question is not fully resolved. Finally, the pace of development of solid state X-band components promises to reduce the complexity of microwave equipment to the point where the decision between RF and DC bias will be determined by performance.

Another coming detector is the avalanche diode. This photodiode is operated at such a high field that the photocarriers are multiplied by free-carrier generation as they traverse the junction. It promises very fast response, but the difficulty of controlling the multiplication limits it to modest charge gain. As yet, no high performance has been reported for input light longer than 1.5 micrometers. It seems most suitable for very broad bandwidths or extreme modulation frequency in the gigahertz region.

CONCLUSION

The photoconductive detector with microwave bias has given the first low-level infrared receiver offering the promise of a sensitivity approaching the ideal limit set by noise-in-signal. Receivers already demonstrated are point detectors with very high sensitivity for light from the visible to 5 micrometers, and for information bandwidths up to 100 MHz. Future developments should bring their sensitivity close to the ideal limit; extend the spectrum to the 10-micrometer region, and the frequency response to the UHF; and increase the detector area. While it is possible that other classes of devices with simpler circuits will be developed to match this performance, the burden of proof is now definitely on them.

BIBLIOGRAPHY

1. A. Rose, *Concepts in Photoconductivity and Allied Problems,* Interscience Publishers, New York, New York, 1963.
2. R. H. Bube, *Photoconductivity of Solids,* John Wiley and Sons, Inc., New York, New York, 1960. (This book emphasizes insulating photoconductors for visible light.)
3. Kruse, McGlauchlin, and McQuistan, *Elements of Infrared Technology;* Generation, Transmission, and Detection. John Wiley & Sons, Inc.
4. *Applied Optics 4,* (June 1965 issue on Infrared detectors).
5. H. S. Sommers, Jr. and W. B. Teutsch, "Demodulation of Low-Level Broadband Optical Signals with Semiconductors: Part II—Analysis of the Photoconductive Detector", *Proc. IEEE 52,* 144-153, 1964.
6. J. P. Gordon, "Variable Coupling Reflection Cavity for Microwave Spectroscopy", *Rev. Sci. Instr. 32,* 658-661, June, 1961.

UNDERWATER LASER TRANSMISSION CHARACTERISTICS

H. J. OKOOMIAN
Aerospace Systems Division
Burlington, Mass.

Characteristics of the transmission of visual radiation in water are discussed and underwater transmission data applying to extended ranges are presented. Measurements have been made with an intense, narrow-beam, coherent radiation source which has a spectral peak at 5,300 angstroms and a bandwidth of 24 angstroms.

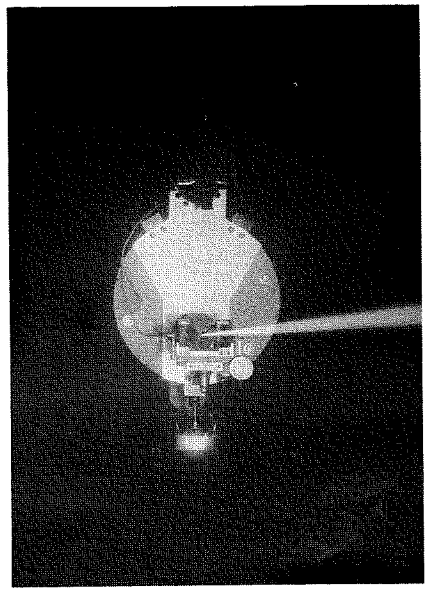

Experimental laser transmitter operating underwater. (Photo courtesy C. W. Haney.)

A GREAT deal of experimental and theoretical work[1,2,3] conducted during the past few decades has contributed significantly to our knowledge of the transmission properties of optical radiation in oceanic and limnetic waters. Measurements have been made with increasingly greater sophistication, and theoretical developments have been increasingly more extensive. Despite important advances and significant contributions, however, our understanding in this area is still severely limited. This becomes particularly evident in the design of underwater optical equipment when one attempts to evaluate the performance of a system. In many such applications, it is only possible to make rough estimates.

The development of high-power, pulsed laser devices operating in the green part of the spectrum where water transmission is maximal, enhances the feasibility of underwater optical systems which heretofore were not practical. This development has, therefore, heightened the interest in such systems and has emphasized the immediate practical need for an improved understanding of transmission of visual radiation in water.

The exposition which follows is essentially divided into two parts. The first part consists of a discussion of the transmission characteristics of visual radiation in water; the second part consists of a description and analysis of a transmission experiment with a high-power, narrow-beam, coherent source.

TRANSMISSION OF VISUAL RADIATION IN WATER

Attenuation Coefficient α

Two attenuation coefficients which characterize the transmission medium will be referred to in the discussion which follows. These coefficients are the same as those generally found in the literature on transmission. For clarification, however, the one denoted by α will be defined under this heading. The second coefficient, denoted by k, will be defined under the next heading.

Let us examine the attenuation in a specific example which is pertinent to the experiment to be described later. Consider a collimated beam with narrow cross section passing through an attenuating medium, and consider the measurement of this radiation with a detector which has an aperture of sufficient size to permit reception of the entire beam. The attenuation determined by measeurments made with the detector over short distances can be expressed in terms of a simple exponential function as is Lambert's law of absorption or Beer's law. That is, if I is the intensity at range R and I_o is the intensity at $R = 0$, then:

$$I = I_o \exp(-\alpha R) \qquad (1)$$

where α is a constant characterizing the medium and usually referred to as the attenuation constant or the volume attenuation coefficient. For analytical purposes, the attenuation constant α can be considered to be the sum of two terms. One term is an indication of the amount of atomic absorption of radiation; the other term is an indication of the amount of radiation scattered out of the beam. Experimentally, however, the components of α are determined indirectly; measurements of the type described here always yield the composite α. There are many experimental data obtained over short ranges supporting the exponential relationship expressed in

Final manuscript received May 9, 1966

HOWARD OKOOMIAN received BA and MA degrees from the University of Connecticut in 1950 and 1957, respectively. In 1951 he was engaged in the development of electronic distance measuring equipment at the U.S. Army Signal Corps Laboratory. Between 1952 and 1955 he was engaged in the development of thermal insulation materials and the development of cold weather tentage at the John B. Pierce Foundation Laboratories. Between 1956 and 1961 he was engaged in applied research at Hermes Electronics Co., developing scientific instrumentation, designing and building UHF-microwave equipment and working in the areas of masers and microwave spectroscopy. During this period he spent three months working with the Physical Science Study Committee of the Massachusetts Institute of Technology. He joined the DEP Aerospace Systems Division of RCA in 1961 and has since been engaged in applied research and the design and development of laser devices and systems. In the area of lasers he has been engaged in the development of advanced techniques in static and Q-switched lasers, and in the generation of high power optical harmonics. He has also performed analysis of laser radars, coherent optical receivers, and the transmission characteristics of water for narrow beam laser transmitters.

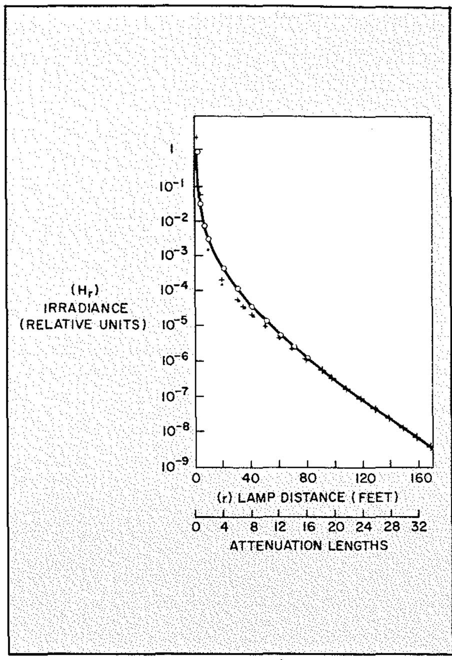

Fig. 1—Total irradiance of a point source versus range.

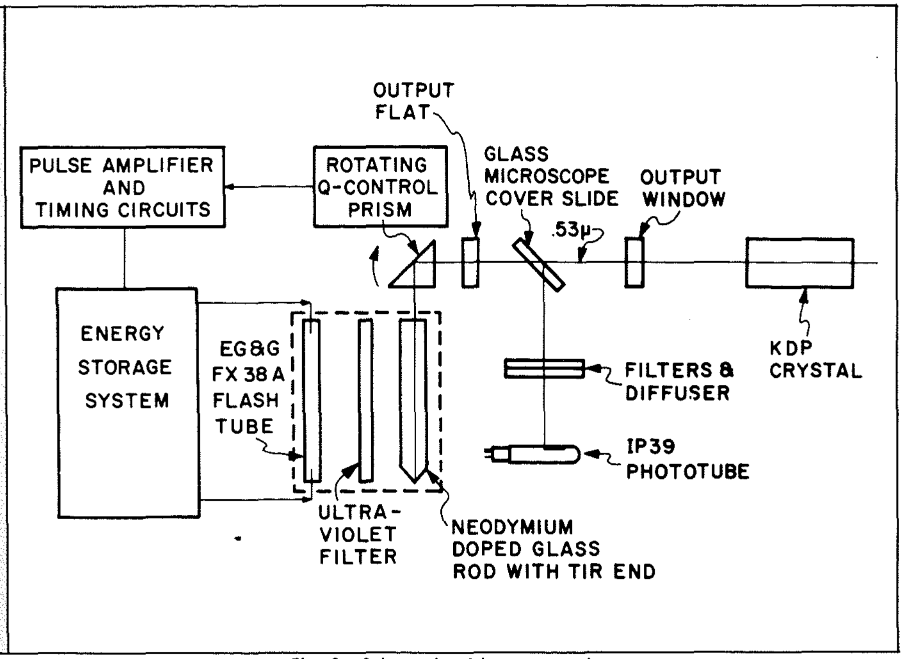

Fig. 2—Schematic of laser transmitter.

Eq. 1. As the range over which measurements are made is increased, however, the experimental data will be found to depart significantly from this relationship. The measured intensities will be considerably higher than those predicted by this formula with the use of an α value determined by measurements over short ranges. The reason for this increase is the presence in the detected radiation of a component which was originally scattered out of the beam and then re-scattered so that it eventually enters the detector aperture. That is, a portion of the radiation which was scattered out of the beam and considered lost, is, in fact, returned to the beam by multiple scattering.

In our experiment, the observed intensity is greater than that predicted by the simple exponential relationship expressed in Eq. 1. For the effect to be observable, however, the path traversed by the radiation must be long enough so that a large number of scattering interactions have taken place.

Monopath and Multipath Irradiance, and Attenuation Coefficient k

It is convenient to discuss transmission characteristics of water in terms of irradiance. Irradiance is defined as the radiation power falling on or crossing a unit area of a plane surface. The total irradiance produced at a surface from an arbitrary light source can be expressed as the sum of two parts, corresponding to radiation which arrives at the surface directly, and the radiation which arrives at the surface indirectly. Direct radiation is not involved in scattering interactions and it travels in a straight line. We shall refer to this type of radiation as monopath radiation. Indirect radiation is involved in many scattering interactions and finally arrives at the detector via a path which consists of a series of nonparallel, connected straight lines.

We shall refer to this type of radiation as multipath radiation. Symbolically:

$$H_r = H_r^{\circ} + H_r^{*} \qquad (2)$$

where H_r is the total irradiance, H_r° is the monopath irradiance and H_r^{*} is the multipath irradiance. For point sources, the functional dependence of H_r° is the product of the inverse square of the range and an exponential of the range; that is,

$$H_r^{\circ} = \frac{J \exp(-\alpha R)}{R^2} \qquad (3)$$

where J is the radiant intensity with dimensions of power per unit solid angle, R is the range or distance from the source and α is the attenuation coefficient defined in Eq. 1.

Neglecting diffraction effects, Eq. 3 holds also for a special kind of idealized point source, namely, a point source which only emits radiation within a specified solid angle which is less than 4π steradians. The expression holds only within the region of this solid angle since, by definition, there is no radiation external to it.

A correspondingly accurate relationship for multipath irradiance has not yet evolved. A number of theories have been proposed and developed to various states of completion, but these appear to have been only partially successful in providing an adequate model. The four most prominent theories of transmission have been briefly summarized in Ref. 1. One of these, the diffusion theory, leads to a particularly simple solution. Motivation for its development came from a recognition of the phenomenological similarities between optical transmission and neutron transmission. Neutron transmission in homogenous materials has been explained successfully by the use of diffusion theory[4], and theorists have suggested that an analogous development in optical transmission would be equally successful. Along with these phenomenological similarities there are differences which make the use of diffusion theory approach questionable. Also, natural hydrosols existing in oceans and lakes are far from uniform. Therefore, any method based on homogenous properties of the medium will be of limited usefulness. Despite these shortcomings, there appears to be sufficient correspondence between the expression derived from the theory and irradiance measurements to warrant its use in estimating underwater transmission.

Inverse range and exponential dependencies are the essential features of the solution obtained for the differential equations of the theory. For a point source, the irradiance is expressed symbolically as:

$$H_r = \frac{Jk \exp(-kR)}{4\pi R} \qquad (4)$$

where k is the second coefficient characterizing the transmission medium, J,

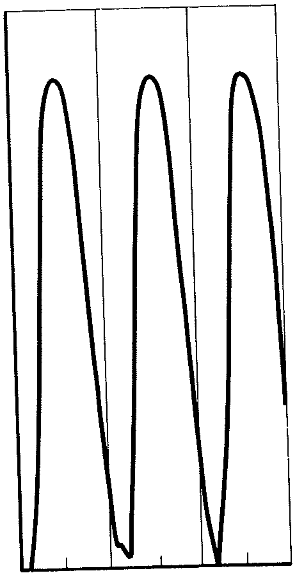

Fig. 3—Spectral mode lines of output radiation.

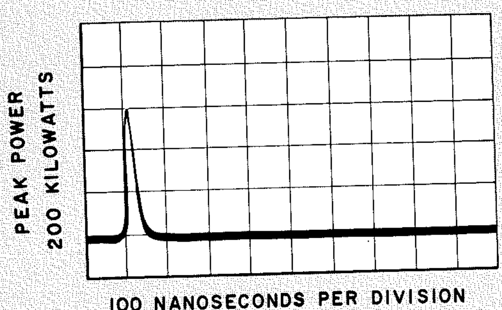

Fig. 4—Temporal waveform of output radiation.

Fig. 5—Spectral character of transmissometer light source.

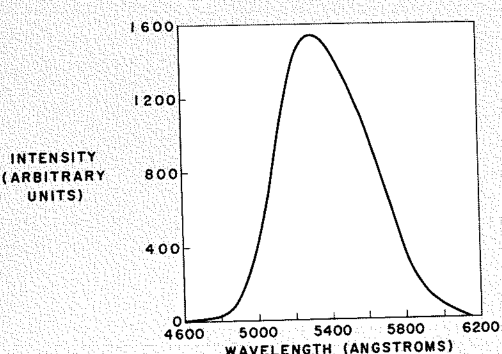

as before, is the radiant intensity and R is the range. We shall refer to k as the multipath attenuation coefficient. The complete expression for the total irradiance due to a point source is:

$$H_r = \frac{J \exp(-\alpha R)}{R^2} + \frac{Jk \exp(-\alpha R)}{4\pi R} \quad (5)$$

Duntley[5] has conducted a series of measurements in lake water to determine the validity of Eq. 5. In water which has an $\alpha = 0.20$ ft^{-1} and $k = 0.057$ ft^{-1}, the agreement is excellent except at the intermediate ranges. This is evident in Fig. 1 which is a plot of the total irradiance data measured by an irradiance photometer; the solid dots are the values computed from Eq. 5. (Fig. 1 has been reproduced here from Ref. 5. An additional scale of attenuation lengths has been added to facilitate comparison with irradiance plots presented later. An attenuation length is defined here in $1/\alpha$.)

In a report on another series of experiments in lake water, Duntley[6] has developed an empirically modified form of the point source equation for sources having beamwidths from 20° to 360°.

Experimental data available for sources which are highly collimated have been reported by Duntley[1] and by Knestrick and Curcio[7] for measurements made over propagation lengths of less than 8 attenuation lengths. The experiment which will be described in the next section has resulted in data from measurements made over a distance of 30 to 50 attenuation lengths, a region characterized by a predominance of the multipath irradiance component of total irradiance. It will be shown that in this region the irradiance due to a highly collimated beam can be expressed by the formula derived for a point source, Eq. 5, with the addition of a multiplicative constant.

EXPERIMENTAL PROGRAM

A measurement program was undertaken in November 1963 at the David Taylor Model Basin in Carderock, Maryland, for the purpose of determining the transmission characteristics of high-power green laser radiation in water. The equipment consisted of a submersible laser transmitter and a submersible receiver. Each unit was held 5 feet below the surface of the water by a support attached to an electrically driven carriage which spanned the channel in which the measurements were made. The range over which the measurements were made could be varied by moving the carriages to any position along the channel. The channel was 20 feet wide and varied in depth from 20 to 10 feet. The water in the channel was filtered Potomac River water.

Transmitter and Receiver

The transmitter is a completely self-contained battery-powered, coherent green radiation source, housed in a waterproof container designed to operate at a maximum depth of 1,000 feet. The unit is fitted with electrical connectors and cables to permit remote operation and remote recharging of the batteries. In addition, an RF coaxial transmission line cable, also connected to the unit, permits a remote photoelectric measurement of a signal from a photocell which monitors the green output power. High-power coherent green radiation pulses are obtained by the generation of second harmonic radiation in a potassium dihydrogen phosphate crystal, utilizing techniques described in Ref. 8. Fig. 2 is a schematic diagram of the transmitter. The fundamental radiation is derived from a Q-switched neodymium-glass laser which has an output centered at 10,600 angstroms. The second harmonic radiation is centered at 5,300 angstroms and consists of 80 evenly spaced mode lines, a few of which are shown by the spectrometer tracing in Fig. 3. The overall spectral width is about 24 angstroms.

The output waveform of the second harmonic radiation consists of a pulse of short duration. Fig. 4 shows a typical 200-kW pulse measured with a calibrated vacuum photodiode and a circuit with a response time of 15 ns.

The beam, which has a non-circular cross section, has maximum and minimum angular spreads of 3 and 1 milliradians, respectively.

The receiver consists essentially of an RCA-IP39 multiplier phototube (S-4 spectral response) mounted in a submersible housing. The collecting area of the receiver is about 1 cm^2. Its field of view is determined by the aperture in a Gershan tube mounted external to the housing. The receiver signals were relayed by a properly terminated transmission line to the input of a wideband amplifier, and then they were displayed on an oscilloscope. When used in this manner, the receiver has a signal-to-noise ratio of one when the radiant signal power incident on the photocathode is 5×10^{-10} watt and there is no background radiation.

Measurement of Attenuation Coefficient α

Attenuation coefficient α of the water in the channel was measured *in situ* with a commercial transmissometer (Marine Advisors, Inc., Model C-2A). The instrument consists essentially of a tungsten light source imaged on a photodetector with a separation between source and detector of one meter. A No. 58 Wratten filter placed over the source aperture results in an output

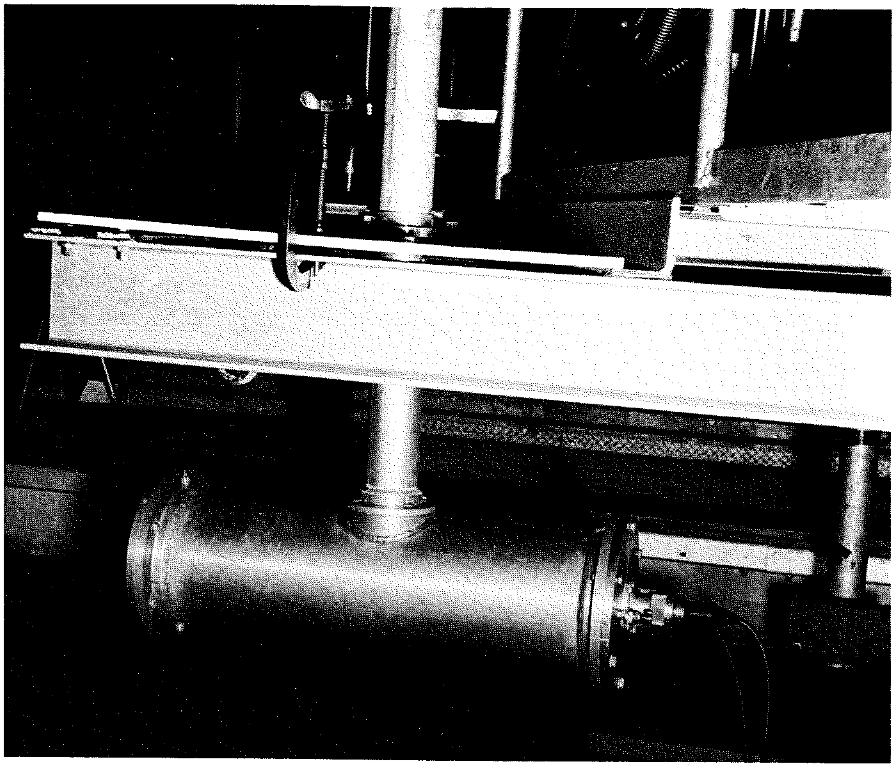

Fig. 6A—Submersible transmitter mounted on carriage (side view).

centered at 5,300 angstroms and characterized by the curve in Fig. 5.

Transmission Measurements with the High Power Source

Measurements were made with the transmitter attached to one of the channel carriages which was kept in a fixed position at one end of the channel. Figs 6a and 6b depict two views of the transmitter mounted on the carriage. The receiver (shown in Fig. 7) was attached to another carriage which was moved along the channel with measurements being taken at 50- or 100-foot intervals. The carriages moved on precision tracks so that the transmitter and receiver remained aligned during the experiment.

Fig. 8 is a photograph of the transmitter 5 feet below the surface of the water in the channel at the David Taylor Model Basin. Scattering from the beam is clearly visible at short ranges.

The peak power output of the transmitter for these measurements was 130 kW which yields a radiant intensity of 3.9×10^{10} watts per steradian for an average beamwidth of 2 milliradians.

Fig. 6B—Submersible transmitter mounted on carriage (end view).

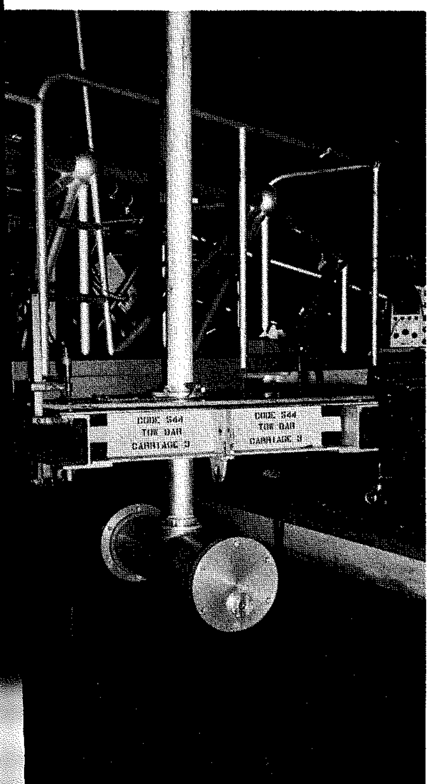

Fig. 7—Submersible laser receiver mounted on carriage.

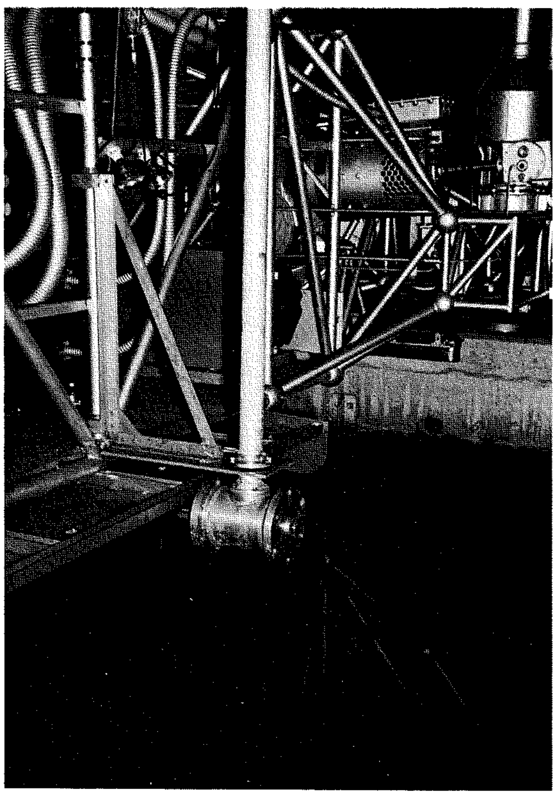

Fig. 8—Laser transmitter operating in water.

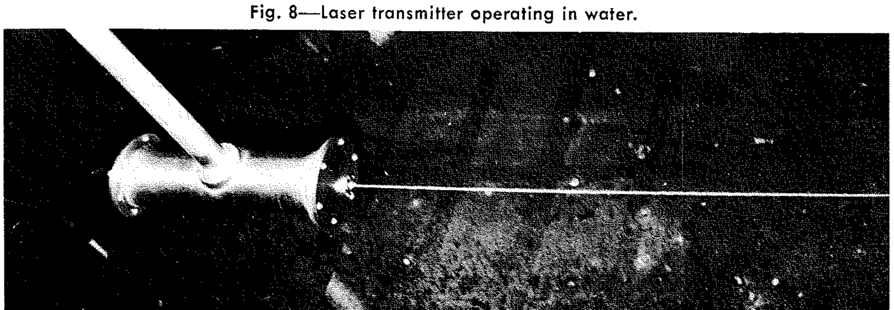

Fig. 9—Signal strength versus range (field of view 26°).

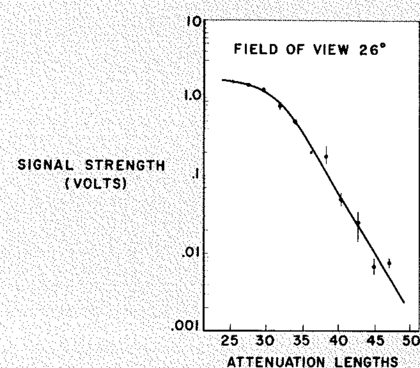

Fig. 10—Signal strength versus range (field of view 2°).

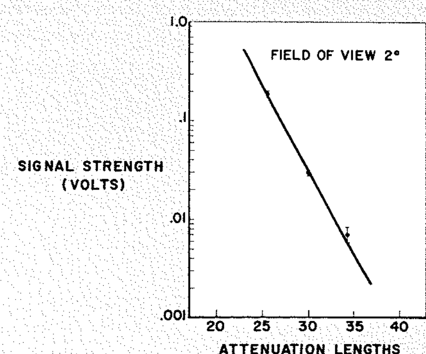

The measurements with the laser were made by photographically recording an oscilloscope trace of the received signal, and at a later time reading the signal amplitudes on the film. Measurements were made for two receiver fields of view: 26° and 36 milliradians. These data are plotted in Figs. 9 and 10 as a function of transmission path length $(1/\alpha)$. The end points of the vertical lines on the graph mark the maximum and minimum readings recorded at each indicated range, and the dots represent the average value of all measurements taken in each case. The cause of the scatter in the measurements has not been established. This uncertainty in the data, which appears to become greater as the signal decreases in amplitude, corresponds to an uncertainty in the deduction of a form for the irradiance function. It is reasonable, however, to expect that as long as α and k do not vary, the relationship must be representable by a smooth and regular curve. The most reasonable curves under these circumstances appear to be the ones displayed in Figs. 9 and 10.

On applying the receiver transfer characteristic to those curves, one obtains a value for the combined monopath and multipath irradiance. The monopath irradiance can be computed from Eq. 3 utilizing the value of α measured with the transmissometer. Since $(H_r \cdot H_r^o) = H_r^*$, the multipath irradiance can also be obtained.

True irradiance should be measured with a receiver having a field of view of $180° \times 180°$ (2π steradians) for there will be some contribution of multipath radiation which is incident on the receiver at angles out to 90°. Duntley[1] has measured radiance characteristics of light scattered from narrow beams of small divergence, and the results seem to indicate that the contribution to true irradiance from radiation which enters the detector at angles of incidence greater than 13° is quite small, and for most cases, negligible. On the other hand, a significant portion of the multipath irradiance will be excluded for a receiver field of view of 2°.

This is evident in Fig. 11, which is a plot of the ratio of monopath to multipath irradiance determined from the measurements made with two different fields of view. Here, one can see that at any given distance the ratio for the 2° field of view is approximately two orders of magnitude greater than the ratio for the 26° field of view.

Another observation of interest is that if the multipath irradiance function (H_r) given in Eq. 4 is multiplied by a constant factor C which is considerably less than one, it can be made to fit the experimentally derived irradiance curve. That this expression must be multiplied by a factor considerably less than one is not surprising if we recall that it was derived for a point source (which emits radiation in all directions). In the experiment, however, the source emits radiation in directions confined only to a small solid angle. It is clear that for this latter source there would be no contribution to the multipath irradiance from primary radiation which, in the case of a true-point source, would be emitted in directions outside the small solid angle. In view of the fit obtained in this manner, it is interesting to examine both the monopath irradiance and the multipath irradiance functions over an extended region. This has been done in Fig. 12 for the 26° field of view for which the appropriate multiplicative constant is $C = 4.08 \times 10^{-3}$.

The total irradiance can be obtained by graphically summing the two curves in Fig. 12. The curves have been normalized for an arbitrary value of J. Additional specific data related to these measurements can be found in Ref. 7. The dashed lines indicate extrapolation; solid lines are based on measurement. Attenuation coefficient k used in these graphs is obtained in the following way. At extended ranges, the total irradiance function H_r is approximately equal to H_r^* and eventually the exponential factor $\exp(-kR)$ becomes the dominant factor. In this region then:

$$k = \frac{\ln H_{r2} - \ln H_{r1}}{R_2 - R_1}$$

where: H_{r2} is the irradiance at a distance R_2 and H_{r1} is the irradiance at distance R_1.

CONCLUSIONS

We have examined the point source multipath irradiance function obtained from diffusion theory with respect to irradiance produced at extended ranges by intense pulses of laser radiation. The correlation between the measured values and the values predicted by the expression modified simply by a multiplicative constant suggests the correctness of the general functional form. A logical extension of this work would be to test the formula for other values of α and to examine the character of constant C as a function of beamwidth.

ACKNOWLEDGEMENTS

The author wishes to acknowledge the work of Thomas Nolan, William White, Nunzio Luce, and Edward Kornstein in the development of the underwater equipment and the experiments.

This work was sponsored by the U. S. Navy, Bureau of Ships, under contract NObsr 87569.

BIBLIOGRAPHY

1. S. Q. Duntley, "Light in the Sea", *J. Opt. Soc. A.* Volume 53, Number 2 pp. 214-233. February 1963.
2. Transmission of Energy within the Sea: Light, J. E. Tyler and R. W. Prusendorfer. *The Sea,* Editor M. N. Hill, Volume I: Physical Oceanography, Interscience Publishers, John Wiley and Sons, Incorporated, 1962 (pages 397-451).
3. E. F. DuPre and L. H. Dawson, *Transmission of Light in Water: An Annotated Bibliography,* NRL Bibliography Number 20, U.S. Naval Research Laboratory, Washington, D.C., April 1961.
4. S. Glasstone and M. C. Edlund, *The Elements of Nuclear Reactor Theory,* D. Van Nostrand Company, Incorporated (1952).
5. S. Q. Duntley, *Measurements of the Transmission of Light from an Underwater Point Source* U.S. Navy Bureau of Ships Contract NObsr-72039 Task 5 Report Number 5-11, October 1960.
6. S. Q. Duntley, *Measurements of the Transmission of Light from an Underwater Source Having Variable Beam-Spread,* Scripps Institution of Oceanography, Visibility Laboratory. U.S. Navy Bureau of Ships Contract NObsr-72092, Project S FOO 1 05 01 November 1960 (S10 Reference 60-57).
7. G. L. Knestrick and J. A. Curcio, "Transmission of Ruby Laser Light through Water". Paper presented at the Opt. Soc. Meeting at Jacksonville March 26, 1963. (Authors are at the U.S. Naval Research Laboratory, Optics Division.)
8. P. A. Franken and J. F. Ward, "Optical Harmonics and Non-Linear Phenomena", *Rev. Mod. Physics,* Volume 35, Number 1, January 1963.
9. H. J. Okoomian, *Proceedings of the Seminar on Acoustic Imaging and Pulsed Light,* held at the 70th meeting of the Mine Advisory Committee, National Academy of Sciences, National Research Council, December 2, 1964. *To be published.*

Fig. 11—Ratio of monopath to multipath irradiance versus range.

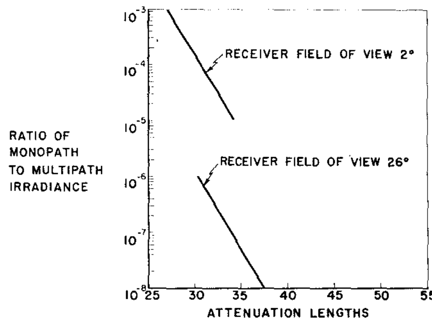

Fig. 12—Logarithm of irradiance versus range.

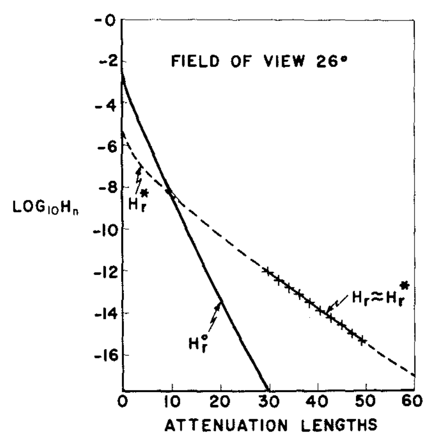

APPLICATION OF INJECTION LASERS TO COMMUNICATION AND RADAR SYSTEMS

This paper describes the application of the GaAs room-temperature laser diode to laser communication and radar systems. Since this GaAs diode requires a threshold drive current of only 10 amperes, simple and reliable drive circuits can be used, while elimination of the need for refrigeration reduces power input, and size and weight.

W. J. HANNAN
Applied Research
DEP, Camden, N. J.

Until RCA achieved laser operation with a GaAs diode at room temperature,[1] the major deterrent to the use of a laser diode was the need to operate it at low temperature. Laser operation can now be achieved with a GaAs diode at room temperature and at a threshold drive current of only 10 A. The low threshold permits simple, reliable drive circuits to be used, while elimination of refrigeration considerably reduces power input, size, and weight.

CHARACTERISTICS OF THE INJECTION LASER

Figs. 1, 2, 3 and 4 show the performance of the RCA laser diode tested during room temperature operation. Fig. 1 is a photograph of a dual-beam oscilloscope trace showing current input to the laser diode and the light output from it. The light pulse emitted from one end of the laser diode is shown in the lower trace and the diode current input is shown in the upper trace. Note that a peak output power of 10 W is achieved at a peak drive current of 40 A. This represents the performance of a typical diode; however, some diodes emit as much as 18 W with the same drive current.

Fig. 2 is a plot of output power radiated from one end of the diode as a function of drive current. The region around the lower knee of the curve, where the slope suddenly changes, represents the laser threshold of the diode. Typically the threshold current I_{th}, is 10 A. For currents above I_{th}, the laser output increases steadily until heating effects cause the output to taper off.

Fig. 3 shows the measured spectrum of the light radiated from the diode. The spectrum consists of four longitudinal modes spaced approximately 6 angstroms apart, in agreement with the mode spacing calculated from the length of the Fabry-Perot cavity formed by the diode. At room temperature, the center of the laser emission spectrum occurs at about 9020 angstroms, with a temperature-dependent shift of about 2 angstroms per degree Celsius, as shown in Fig. 4.

Radiation from the laser diode is collected and focused into the desired beamwidth by a small lens. Fig. 5a shows that when the laser is placed in the focal plane of the lens, the radiation pattern is fan-shaped with an aspect ratio of about 10:1. Fig. 5b shows that by defocusing the lens it is possible to obtain a far-field pattern with a 1:1 aspect ratio. Far field power measurements have shown that defocusing, to the extent that a 1:1 aspect ratio is achieved, does not introduce significant side lobes in the beam.

The laser module shown in Fig. 6 was developed for use in communication and radar systems. This module consists of a laser diode and beam collimating lens, mounted in a cylindrical housing with a precision machined tapered seat. The laser diode and its lens are accurately aligned along the axis of the cylinder, focused for a suitable beam pattern, and then permanently fixed in position. This module fits into a mating precision-tapered hole in the transmitter housing, allowing for easy replacement of the laser emitter without the need for critical optical realignment procedures.

Final manuscript received Sept. 1, 1966

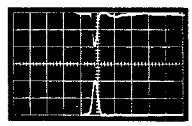

Fig. 1—Light output power vs current input to GaAs laser diode.

WILLIAM J. HANNAN (S'55—M'57—SM'65) was born in New York, N. Y., on February 13, 1929. He graduated from the RCA Institutes in 1951 and was hired by RCA as an engineer in the Industrial Products Division. In this division he contributed to the design of the RCA television system. He received the BSEE from Drexel Institute (evening college) in 1954. He was awarded a Sarnoff Fellowship which he used to obtain the MSEE from the Polytechnic Institute of Brooklyn, N. Y., in 1955. Mr. Hannan has been employed in RCA's Applied Research Department since 1956. His experience includes the design and development of transistor television circuits, digital communication receivers, digital data-processing equipment, and optical communication systems. He is currently leader of a group working on laser communication and radar systems.

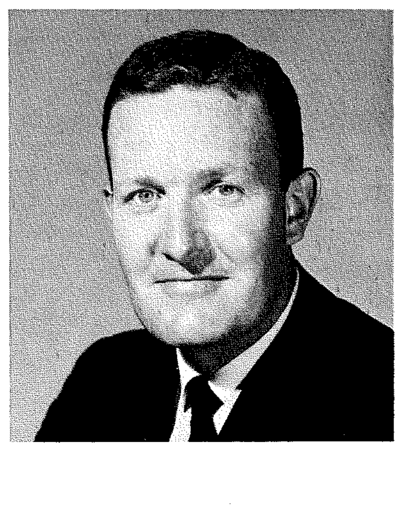

Fig. 2—Light output power vs diode current.

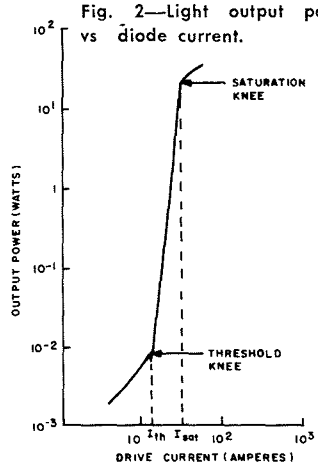

Fig. 3—Spectrum of emission from a GaAs laser diode.

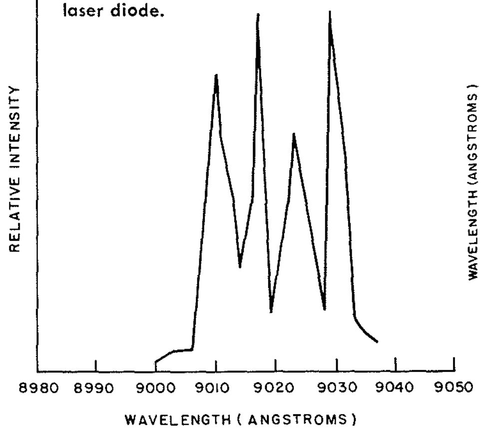

Fig. 4—GaAs laser wavelength vs ambient temperature.

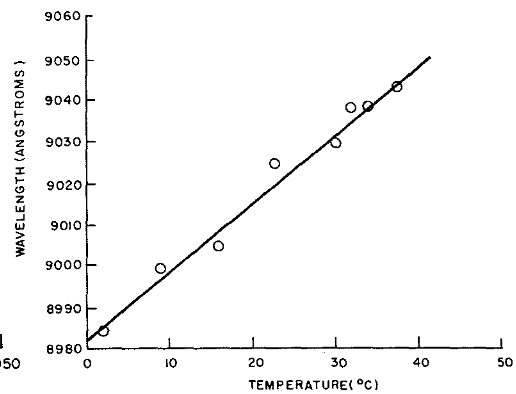

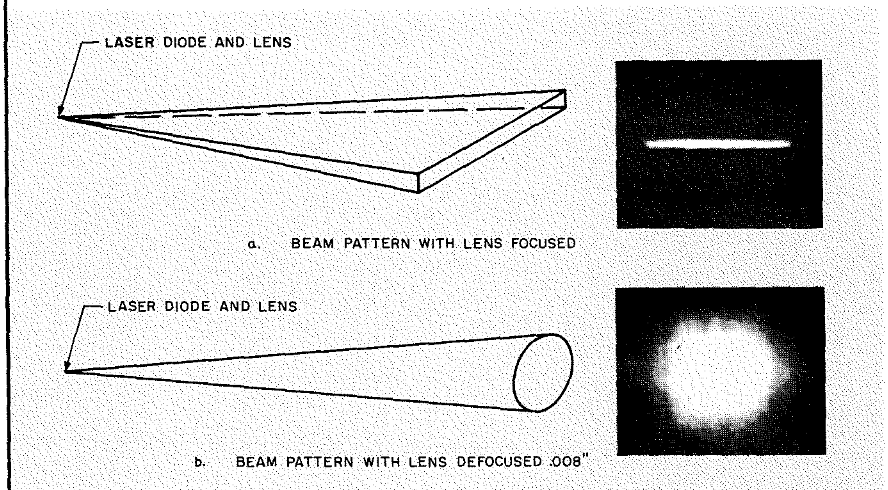

Fig. 5—Effect of defocusing an injection laser beam.

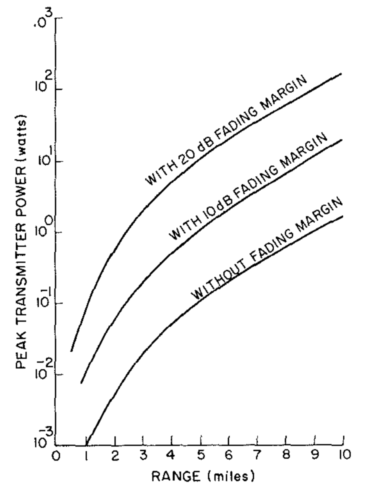

Fig. 8—Required transmitter power-vs-range.

SYSTEM PARAMETERS (Fig. 8)

D_r	4 inches
ρ	0.3 A/W
λ	9020 angstroms
T_o	0.7
B_m	3 kHz
F	2
f	8000 p/s
α_t	3 mrad
α_r	23 mrad
τ	75 ns
B	5 MHz
R_l	1000 Ω
SNR	15 dB
M	0.1 W/m²/angstrom
σ	0.2 km⁻¹
q	0.06%

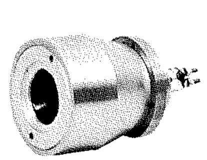

Fig. 6—Laser module.

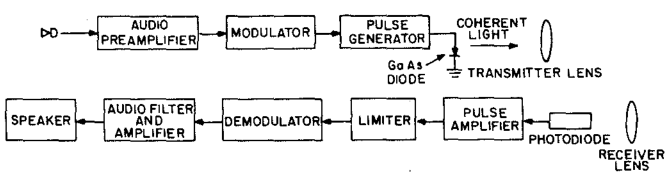

Fig. 7—Major components of laser communications system.

INJECTION LASER COMMUNICATION SYSTEMS

To date, injection laser communication systems have been developed mainly for military applications where the narrow beamwidth, narrow spectral width and non-visible features of the injection laser are exploited to obtain communication security. When the manufacturing cost of the injection laser is reduced, it is expected that this type communication system will also be used for commercial applications such as localized communications for museums, fairs, etc.

A block diagram of an injection laser communication system is shown in Fig. 7. When driven by short, high-current pulses, the GaAs diode emits coherent light in a fan-shaped beam with an angular divergence of less than 15°. The transmitter lens focuses this radiation into the desired beamwidth and voice signals are transmitted over it by pulse frequency modulation.

The received laser beam is collected by a parabolic reflector and focused on a photodiode. The detected pulses are amplified, limited and sent through a pulse-frequency demodulator to produce the audio output signal.

The basic equations which define the performance of a laser communication system are shown in Table I.

Typical parameter values for a state-of-the-art injection laser communication system and the corresponding transmitter power vs range curves (derived from the above the equations in Table I) are given in Fig. 8. This data shows, for example, that a 10-W transmitter will provide a 20-dB fading margin at a range of 5 miles, for the given set of parameters.

Fig. 9 shows three different laser transmitters that have been developed by Applied Research. Fig. 9a shows a miniature laser transmitter developed for an intrusion alarm system; Fig. 9b shows a wide beamwidth transmitter (about 15°) developed for a short range, hand-held communication system; and Fig. 9c shows the transmitter developed for NASA's GEMINI 7 experiment.

TABLE I—Basic Equations for Laser Communications System

$$\frac{S}{N} = \frac{\rho^2 P_s^2 R_l G^2}{2eB\,(\rho P_s + \rho P_b + I_d)\,R_l G^2 + 2FkTB} \qquad (1)$$

$$P_b = \frac{M \alpha_r^2 A_r \xi T_a T_o B_{opt}}{4} \qquad (2)$$

$$T_a = e^{-\sigma R} \qquad (3)$$

$$B = \frac{0.4}{\tau} \qquad (4)$$

$$q = \tau f = 3\tau B_m \qquad (5)$$

$$R_l = \frac{1}{2\pi BC} \qquad (6)$$

$$P_{to} = \frac{P_s \alpha_t^2 R^2}{A_r T_o T_a} \qquad (7)$$

P_{tc} = transmitter power (W)
ρ = responsivity of photodetector (A/W)
P_s = received signal power (W)
P_b = received background power (W)
R_l = load resistance (ohms)
e = charge on an electron (1.6×10^{-19} C)
B = bandwidth (Hz)
F = noise factor of preamplifier
k = Boltzmann's constant (1.38×10^{-23} J/°K)
T = temperature (°K)
I_d = detector dark current (A)
G = internal gain of photodetector
M = solar irradiance
α_r = receiver beamwidth (rad)
A_r = area of receiver optics (m^2)
T_a = transmission of atmosphere
T_o = transmission of optics
B_{opt} = passband of optical filter (Å)
τ = pulse duration (sec)
C = capacitance shunting detector load resistor (ohms)
α_t = transmitter beamwidth (rad)
R = range (m)
σ = atmospheric attenuation coefficient (m^{-1})
q = duty factor of transmitter
B_m = information bandwidth
ξ = reflection coefficient

INJECTION LASER RADAR SYSTEMS

The power output capability of an injection laser is relatively low compared to the power available from a crystal laser (e.g., such as a ruby laser). Moreover, the emission wavelength of the injection laser does not fall within a region where sensitive multiplier phototubes are available. As a result, the maximum operating range of an injection laser radar is relatively short compared to that of a crystal laser radar. On the other hand, the injection laser is much smaller and more efficient than crystal lasers and it can be operated at much higher pulse repetition rates. Hence, there are certain applications where an injection laser radar can be used to advantage.

The basic equations which define the performance of a laser radar are the same as those given for the communication system, (see Table I), except for Eq. 7, which indicates required communications transmitter power P_{tc}. If the target is a diffuse reflector that intercepts the entire laser beam, the required radar transmitter power P_{tr} is:

$$P_{tr} = \frac{\pi P_s R^2}{A_r \xi T_o T_a} \qquad (8)$$

where ξ is the target reflectivity.

Typical parameter values for a state-of-the-art injection laser radar and the corresponding radar transmitter power vs range curves (derived from the Equations 1-6 of Table I and 8 above) are given in Fig. 10. This data shows that a multiplier phototube receiver provides greater operating range than a photodiode receiver and, for the given set of parameter values, the maximum range with a 10-W transmitter is about 300 meters.

It is interesting to note that a multiplier phototube provides best performance in radar systems whereas a silicon photodiode provides best performance in most communication systems. This situation occurs because the field of view of communication receivers is usually much wider than the field of view of radar receivers and, therefore, the communication receiver is plagued by a much higher level of background radiation. For this condition it can be shown that the higher responsivity of the photodiode (at 9,000 angstroms) more than offsets the advantage offered by the multiplier phototube's high, essentially noise free internal gain.

The range measurement accuracy of a pulsed radar is

$$\frac{c}{4B\sqrt{S/N}} \qquad (9)$$

where c is the velocity of light (3×10^8 m/s). This equation indicates that range accuracy can be improved by increasing receiver bandwidth. However, with regard to a room temperature operated injection laser radar, a point of diminishing returns is reached at a bandwidth of about 20 MHz. Beyond 20 MHz the rise time of the pulses remains essentially constant, at a value determined by the rise time of the laser drive circuit.

Further improvement of range accuracy can be obtained only by increasing *SNR*. This can be done by increasing transmitter power, by increasing receiver-sensitivity, or by employing multiple pulse integration. With the latter method, the range accuracy improvement factor is between N and $\sqrt{N}$, depending on the type integrator used, where N is the number of pulses that occur during the integration period. For example, if 100 pulses occur during the measurement period the measurement accuracy could be improved by a factor of 10 or more. Thus it is clear that the high pulse repetition rate capability of the injection laser can be used to advantage in obtaining good range accuracy.

As previously mentioned, the peak output power of a typical injection laser diode is 5 to 10 watts. Larger peak output power can be realized by assembling an array of laser diodes.

Fig. 11 shows peak output power vs array size as a function of transmitter beamwidth, based on state-of-the-art laser diodes which have a peak output power of 10 W and an active width of 0.003 inch. The size of the array increases as the transmitter beamwidth is reduced because the longer focal length lenses (needed to reduce beamwidth) must have larger diameters to collect the 5°x15° fanshaped radiation from the laser diodes. Fig. 12 shows the optics of a laser array designed to generate a peak output power of 280 watts in an 8 mrad beam.

For short range applications that require extremely good range accuracy, the triangulation range finding tech-

Fig. 9—Injection laser transmitters.

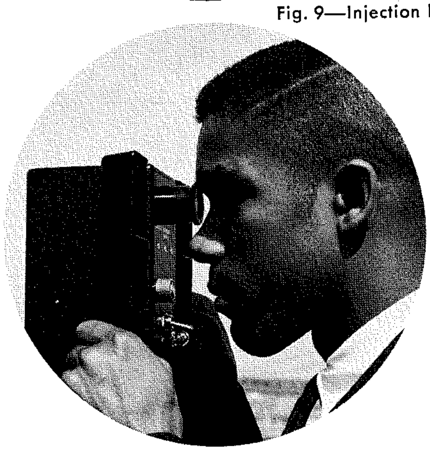

Fig. 10—Transmitter power vs range.

SYSTEM PARAMETERS (Fig. 10)

D_r	4 in.
ρ Diode	0.3 A/W
ρ phototube	3 x 10^{-3} A/W
λ	9020 angstroms
F	2
α_t	1 mrad
α_r	2 mrad
SNR	10 dB
M	0.1 W/m²/angstrom
R_l	1000 Ω
B	5 MHz
τ	75 ns
ξ	0.1
B_{opt} (phototube)	100 angstroms
I_d (phototube)	1 x 10^{-10} ampere

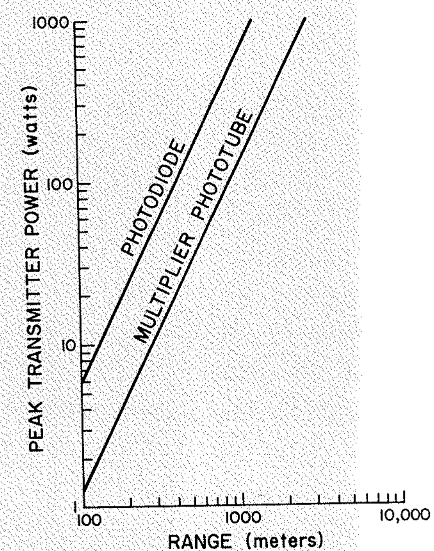

Fig. 11—Peak output power vs size of laser array.

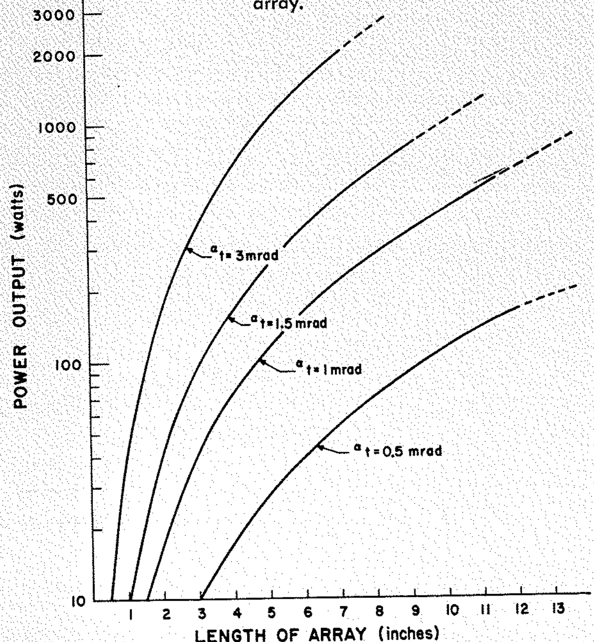

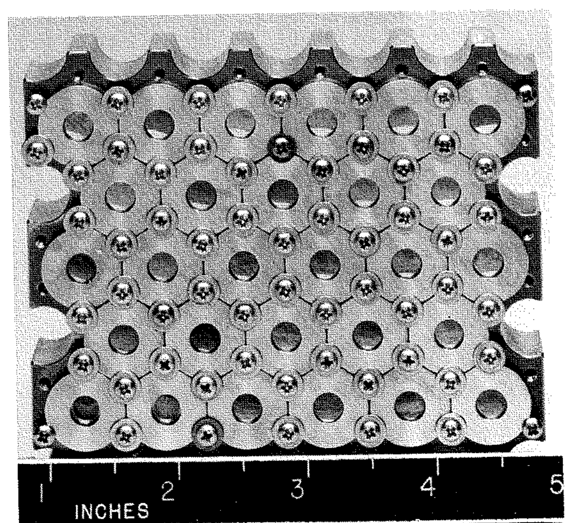

Fig. 12—Optics for a 28 element laser array.

nique illustrated in Fig. 13 offers a possible solution. This technique relies on the fact that a radar return is detected only when a target is within the intersection of the transmitter beam and the receiver field of view. Thus, range can be measured to an accuracy on the order of inches simply by geometric triangulation. Achieving comparable range accuracy with conventional radar calls for measuring time delays on the order of a fraction of a nanosecond, a difficult task requiring large, complex equipment.

Referring to the detailed system geometry shown in Fig. 14, one can show that the range resolution of a triangulation radar is given by

$$\Delta x = \frac{p(2y-A)\left[a+\left(\frac{p-f_o}{f_o}\right)D\right]}{(2y-A)^2-\left(\frac{p-f_o}{f_o}\right)^2 D^2} \qquad (10)$$

The performance that could be expected from a laser triangulation radar is indicated in Fig. 15. For the given set of system parameters, the maximum range measurement error vs range and the signal-to-noise ratio vs range are plotted in Figs. 15a and 15b, respectively.

The range of a laser radar can be extended considerably by mounting a retroreflector on the target. From the simple geometric relationships indicated in Fig. 16, the relationship between transmitted ($P_{tr'}$) and received ($P_{s'}$) power, of a system employing a retroreflector is

$$P_{tr'} = \frac{\pi P_{s'}\alpha_t^2 R^2}{4A_{tar}T_oT_a^2} \qquad R < \frac{D_r}{\phi_d} \qquad (11)$$

$$P_{tr'} = \frac{\pi^2 P_{s'}\alpha_t^2\phi_d^2 R^4}{16A_{tar}A_rT_oT_a^2} \qquad R > \frac{D_r}{\phi_d} \qquad (12)$$

where: ϕ_d = diffraction limited beamwidth of retroflector ($1.22\lambda/d_{tar}$ rad), A_{tar} = area of retroreflector (m^2), and D_r = diameter of receiver optics (m). Using the same parameter values as those given in Fig. 10, one can show that a 1-inch retroreflector can be tracked out to a range of about 5 miles.

ACKNOWLEDGEMENTS

The equipment described here was developed by D. Karlsons, C. Reno, T. Penn and G. Clubine of the Applied Research Laser group. The laser diodes were developed by the Quantum Electronics group (RCAL) under the direction of Dr. H. Lewis.

BIBLIOGRAPHY

1. C. W. Reno, H. Nelson, J. I. Pankove, F. Hawrylo, and G. C. Dousmanis, "High-Efficiency Injection Lasser at Room Temperature," *Proc. IEEE*, 52, pp. 1360-1361 (1964).

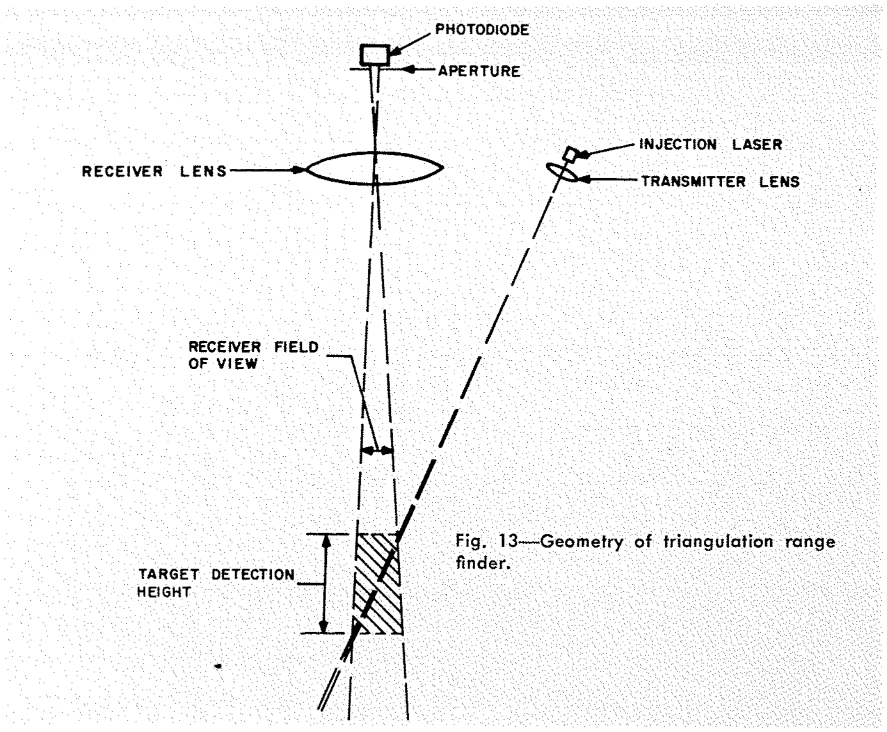

Fig. 13—Geometry of triangulation range finder.

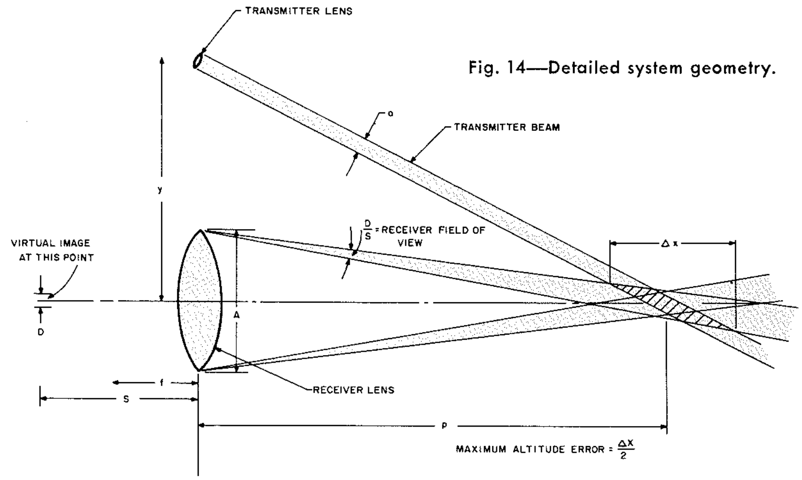

Fig. 14—Detailed system geometry.

SYSTEM PARAMETERS (Fig. 15)

P_{tr}	10 W	τ	80 ns
D_r	3 in	B	5 MHz
T_o	0.8	F	2
ξ	0.1	R_l	1000 Ω
α_t	Æ1 mrad	f	4000 p/s
D	0.01 in	y	12 in
ρ	0.3 A/W	f_o	6 in
		T	300 °K

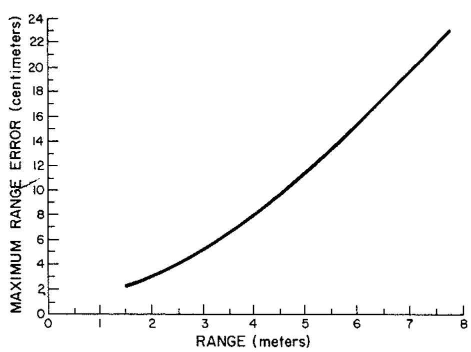

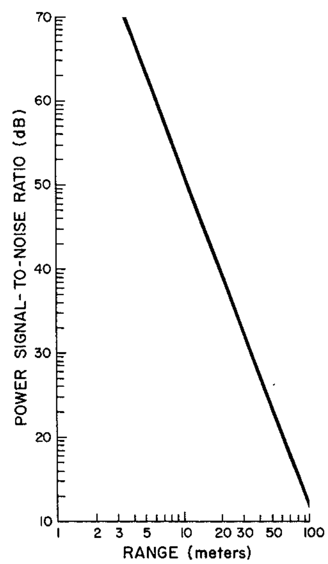

Fig. 15—Performance of laser triangulation radar.

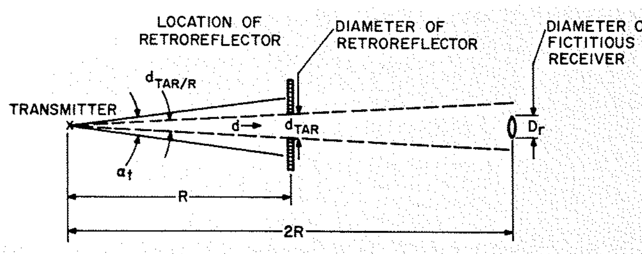

Fig. 16—Equivalent geometry of a retroreflector system.

LASER SPECTROSCOPY

This paper summarizes some main areas of research and technology based upon spectroscopy using lasers. It discusses how the monochromaticity of the laser allows very great precision in line shape and line position measurements. The high light intensity obtainable from lasers offers the possibility of detecting emission lines previously undetectable, and also gives rise to a large group of new phenomena in the field of nonlinear optics.

DR. H. J. GERRITSEN
RCA Laboratories
Princeton, N. J.

SPECTROSCOPY in the usual sense consists of measurements of transmittance of light through a material. The light used contains a narrow spread of wavelengths, obtained by selecting a fraction of the radiant energy from a hot body by means of a dispersing element such as a prism, grating, or Fabry-Perot interferometer.

For the purpose of this discussion, such a definition is too restricted. For example, it is not uncommon that one is interested in the spectral distribution of a hot, emiting body rather than in its transmittance. Other experiments may be designed to measure frequency shifts when light falls on some material as, for example, in the case of Raman spectroscopy.

In what follows we discuss some uses of the laser in these various fields. A somewhat arbitrary division is made between *active spectroscopy* in which deliberate tuning is used, and *passive spectroscopy* in which one detects shifts and broadening, experienced by monochromatic, untuned, laser light when it is scattered by optical density fluctuations in some material.

ACTIVE SPECTROSCOPY

Laser Monochromaticity

If one wants to use a laser as the light source in spectroscopy, the first thoughts that come to mind are the advantages offered by such a very monochromatic source, and the need to tune the frequency of this source. If such tuning is not readily possible, one needs to change the frequency of the substance whose transmittance is to be measured. The latter can be done with electric or magnetic fields. As to the first point, the advantage of monochromaticity of the laser, some caution should be noted. All three major types of lasers, paramagnetic cystals, gases, and injection lasers usually operate at a number of rather independent wavelengths (so-called *modes*) simultaneously. These different modes are individually usually very monochromatic. The reason for the mode multiplicity is that the optical resonant structures used are often so large compared to the wavelength of the laser light, that several resonant modes exist within the emissive bandwidth of the active laser medium.

Sometimes the absorption lines one wants to measure are broad enough that the multimoding is not objectionable. In other cases mode control will be necessary in order to permit the selection of one single wavelength. From the previous discussion, it follows that mode control is easier with the longer wavelengths, and for that reason medium and far-infrared gaseous or semiconducting lasers operate often in a single mode.

The choices for frequency tuning, particularly over a wide range, are at present still rather restricted. Some details about the tuning techniques available follow.

Large Frequency Changes

Nonlinear effects were historically the first to be used in obtaining large shifts in the frequency of a laser.[1,2] Particularly useful in this respect is Raman scattering, which is the process whereby a molecule adds to or subtracts from the incident photon of the laser—a photon corresponding to one of the energy jumps allowed for the molecule either to a lower or a higher energy level. The first case is called an anti-Stokes process, the latter a Stokes process. The emission wavelength of these Raman lines, incidentally, offers a way to identify the nature and temperature of the emitting material,[3] and when powerful lasers are used, should allow one to do spectroscopy of the atmosphere using the Raman component in the backscatter of the

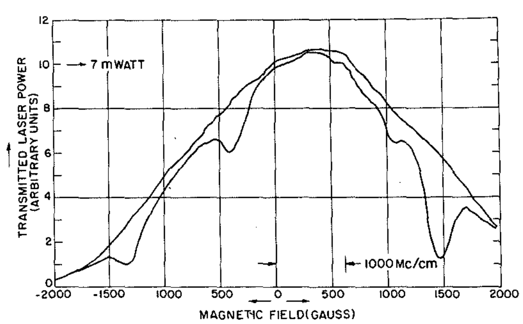

Fig. 1—Tuned laser spectrogram of CH_3F. High reflectivity mirrors were used resulting in a 290 MHz laser width. Path lenght was 15.5 cm, CH_3F pressure was 4 mm; upper curve: empty cell; lower curve: cell filled with CH_3F.

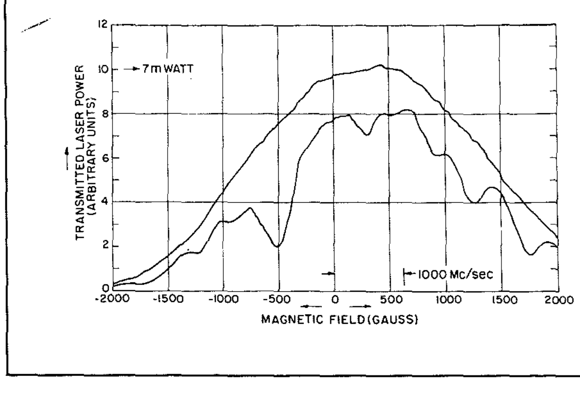

Fig. 2—Tuned laser spectrogram of C_2H_6, using high reflectivity mirrors. Path length was 7.7 cm; C_2H_6 pressure was 11 mm; upper curve: empty cell; lower curve: cell filled with C_2H_6.

Final manuscript received July 20, 1966

laser.[4] It was discovered[5] that when a Raman active material is placed in the beam of a high-power laser, (typically a Q-switch laser with an output of the order of 10 MW/cm^2) stimulated emission occurred at additional wavelengths, separated from the exciting laser wavelength by Stokes or anti-Stokes frequencies. In particular, the stimulated Stokes radiation can be quite strong. It has been reported[6] that 20% of the 6,943-angstrom radiation from the ruby laser can be converted to the Stokes line at 992 cm^{-1} to longer wavelength using benzene. By choosing other liquids such as water, nitrobenzene, cyclohexane, etc., or certain solids, (calcite or diamond), a large variety of new wavelengths has been obtained.[2] This choice of wavelengths permits a discontinuous-type laser spectroscopy that has found use so far in a few isolated cases such as, for example, in measurements of the two-quantum photoionization of Cs and I.[7] For continuous-frequency laser spectroscopy one would have to use one of the methods of fine tuning on the different Raman lines. A listing of different Raman active liquids used for laser tuning appeared recently.[8] Also, if continuous rather than pulsed output is desired, it appears likely that the threshold for stimulated Raman emission can be reached by using high-power CW argon or CO_2 lasers and placing the sample in the focal point of a near concentric laser mirror configuration with highly reflecting mirrors. In passing, it might be mentioned that particularly in the far infrared region the obtainable resolution has usually been low because of the lack of strong light sources and efficient detectors. It is therefore of some significance that it was recently reported[9] that the stimulated Stokes and the laser beam that excited this radiation can be mixed in a nonlinear crystal, here CdS, to give rise to pulses of 0.3 watt at the difference frequency which was in the 10-micrometer region. [*Editor's Note:* the IEEE standard term *micrometer* (10^{-6} meter) is used throughout to denote "micron."]

For active spectroscopy, however, injection lasers are more important because they have the property that the frequency of laser emission can be changed by large amounts if one prepares an alloy. For example, by changing the ratio of InAs to GaAs one can cover the region from 3.11 to 0.84 micrometers.[10] Fine tuning is then possible in a variety of ways such as by changing the temperature of by applying stress[11] or a magnetic field.[12] A spectrometer consisting of a set of alloyed injection lasers to cover the desired frequency range, each tunable over a few cm^{-1} and generating single modes, seems an attractive possibility, perhaps realizable in the future.

More recently, injection lasers of PbS and PbSe were operated whose frequency could be changed from 7 to 11 micrometers in a continuous fashion.[13] A complication is, apart from the fact that these lasers were pulsed and operated at 77°K, that a few modes oscillated simultaneously.

Finally, another large-range tuning technique, based on parametric down-conversion[14] appears quite promising for spectroscopic purposes. In this approach the Q-switch pulse from a neodymium laser was first converted to 5,290-angstrom green light by second-harmonic generation. This light was then used to pump a lithium niobate crystal. The nonlinear crystal gives rise to a coupling between the pump wave and two virtual waves for which the crystal cavity has resonances. In order that the two waves can experience large gain, the sum of their frequencies must equal the pump frequency, and furthermore the beams must move in such directions in the crystal that phase matching can occur, which means that the sum of their momenta equals the pump momentum. Under these conditions the two waves can build up and oscillate. This condition is temperature dependent and frequency tuning in the 9,500-to-12,000-angstrom region was obtained by varying the temperature of the crystal from 50°C to 60°C. The tuning is fairly smooth with occasional jumps of the order of 100 cm^{-1} due to the discrete optical mode structure in the cavity. Additional tuning with a biasing electric field could probably reduce this difficulty. A 0.1% efficiency from laser pump to parametric laser output was reported with very good monochromaticity.

It has been suggested[15] that parametric down-conversion can be used to make a CW tunable oscillator in the 15-to-25 micrometer region using a CW high-power CO_2 laser at 10.6 micrometers as the pump and a tellurium crystal as the nonlinear element. Appreciable powers may be expected.

Fine-Frequency Tuning Methods

Earlier we mentioned that external fields such as magnetic and pressure fields can be used to tune injection lasers. The tuning by magnetic field can also be applied to high-gain gas lasers[16] and was used in one of the early investigations of tuned laser spectroscopy.[17] The tuning range is not large, 1-cm^{-1} tuning requires magnetic fields of the order of 5 kilogauss. Such large fields usually have a deteriorating effect on the power output of the gas lasers. Moreover, they require expensive solenoids.

Another method with an even smaller tuning range is to diffract the light beam by a traveling acoustical wave. The frequency of the diffracted light waves is now increased or decreased by a multiple of the acoustical frequency. Since acoustical waves above about 2 GHz undergo strong attenuation except at low temperatures, tuning beyond 0.1 cm^{-1} is difficult.

The small tuning range mentioned above can in principle also be obtained by *cavity-pulling*, that is, by changing the laser wavelength by making a small change in the distance between the end reflectors. The accuracy obtainable in that case is probably less than if one uses acoustical tuning; nevertheless this method has been used to measure the

Dr. **HENDRIK J. GERRITSEN** received his BS in Physics and Chemistry in 1948 from the University of Leiden. In 1948-1949 he served in the Dutch army and worked there on development of infrared signaling systems. From 1950 to 1955 he was a Member of the Technical Staff of Kamerlingh Onnes Laboratories, Leiden. There he worked in the field of magnetic resonance phenomena at very low temperatures and received his MA degree in 1952 and PhD summa cum laude in 1955. In that same year he joined the newly founded RCA Laboratories in Zurich, where he worked from 1955 to 1957 on photoeffects in insulators. In 1957 he was transferred to the RCA Laboratories in Princeton where he has been working in the field of paramagnetic resonance and microwave masers until the end of 1961. In 1961-62 he was Associate Professor at Chalmers University of Technology, Gothenburg, Sweden, where he lectured in Quantum Electronics and did experimental and theoretical work in crystal field theory. In 1962 he returned to RCA Laboratories where he has since worked on gas lasers, topics in photochemistry and optical processing theory including holograms. He has received two RCA Laboratories Achievement Awards, one in 1957 together with Dr. W. Ruppel for work on photoconductivity in zinc oxide, the other in 1959 together with Dr. H. R. Lewis for paramagnetic resonance and master studies on rutile. Dr. Gerritsen has been granted eight patents and has applied for several others. Among his many papers are recent ones on a cascade laser, publication of the first doubly ionized laser, and three papers on a new principle and its use: tuned laser spectroscopy of gases.

atomic temperature in a xenon gas discharge.[18]

A modest amount of tuning has also been obtained by mixing the laser frequency with a microwave in a nonlinear crystal.[19]

PASSIVE SPECTROSCOPY

In order to discuss the type of new information that has and is expected to come from measurements of the spectral distribution of scattered laser light, let us arrange the resultant shifts in frequency according to increasing magnitude.

Rayleigh Scattering

Rayleigh scattering could be defined in a slightly unfair way as that fraction of the light, scattered by a medium, which before the use of lasers was treated as having the same spectral distribution as the incident light. The pre-laser experiments used the angular spread and depolarization in order to get information, for example, about suspensions of macromolecules in liquids.

H. Z. Cummins and colleagues observed that the Rayleigh scattered light is spectrally broader than the incident laser light[20] and used this information to derive particle size and the presence of local velocities in the liquid. These experiments measured laser line broadenings of the order of 10 Hz, which is a precision far superior to what one could measure with conventional light sources. The detection method used is that of optical heterodyning.

Several articles[20,23] on the Rayleigh effect have since appeared, including investigations near phase transitions in solids and liquids.

The Rayleigh scattering in pure liquids can be understood from a theory by L. Landau and G. Placzek[21] who proposed that sound can be scattered from the optical density fluctuations caused by statistical entropy fluctuations. These entropy fluctuations do not propagate (except in helium-II) and hence the light is not Doppler shifted. The width of the Rayleigh line determines the decay time of fluctuation of that particular wavelength.

Brillouin Scattering

Let us briefly review the theory of lattice modes in solids. If one plots frequency of vibration as a function of the reciprocal of the corresponding wavelength, one finds that there are several branches. From the origin out, one has a longitudinal and two transverse acoustical branches. For a while the lines are straight with a slope corresponding to the velocity of sound propagation but when the wavelength approaches the reciprocal of twice the lattice spacing, the sound velocity changes rapidly.

In addition to the acoustical branches one also has optical branches. Of these the frequency is not strongly dependent upon inverse wavelength but equals approximately the Reststrahl frequency.

In order to obtain information about the wavelength dependence of the sound propagation in the acoustical branches, one can use ultrasound generated by microwaves from a piezoelectric transducer. Ultrasonic measurements are not easy in the first place, and above a few gigahertz are more difficult due to strong absorption in most materials at room temperature. The sound frequency is, in addition, not easy to tune and is, among others, limited by the microwave generators to frequencies so low that appreciable deviation of the sound velocity from the low frequency value is not to be expected.

Rather than study man-made sound propagation, one can study the acoustical properties by measuring effects resulting from thermally excited sound waves. One method for doing this is thermal neutron scattering, although the accuracy is not too good. The other method is scattering of laser light. The scattered light is shifted from the laser frequency by an amount Δf, the Brillouin shift, given by:[22]

$$\Delta f = \pm 2 v_s \frac{n}{\lambda_0} \sin(\theta/2)$$
$$= \textit{phonon frequency}$$

where v_s = sound velocity, n = index of refraction of the medium, λ_0 = laser wavelength in vacuum, θ = angle between incident laser and scattered light. The frequency shift as a function of angle determines the sound velocity at that frequency and the width, $\delta\Delta f$, contains information about the lifetime of that phonon according to:

$$\frac{\delta \Delta f}{\Delta f} = \frac{\alpha}{\pi}$$

where α is the sound absorption coefficient.[23] The authors report a relaxation in toluene by measuring both velocity and absorption versus the wavelength of the hypersonic phonon. Other areas of interest where lattice interactions are important are in phase transitions, in ferroelectricity, in ferro- and antiferromagnetism, and in superconductors.

The measuring technique can be an optical heterodyne method up to perhaps a few hundred megahertz; above that frequency one probably should filter out the direct laser light and use a scanning Fabry-Perot with a photomultiplier and a counter.

Raman Scattering

This process was briefly referred to earlier. In solids Raman scattering is the scattering of light from the optical phonon branch. Recently, Raman scattering was observed from silicon.[24] Since in this experiment the optical phonon energy was determined by surface scattering from an opaque material, one may expect soon to see similar applications in the study of metals and superconductors. The technique in Raman laser work is as follows: one rejects the exciting laser light by painstaking filtering. Since Raman shifts of visible light are typically of the order of 100 angstroms, such filtering is fairly straightforward. The weak scattered Raman radiation is then detected in a spectrometer of sufficient resolution: if the linewidth is desired, usually a high quality Fabry-Perot interferometer is required. Photographic or photoelectric counting techniques can then be used.

NONLINEAR SPECTROSCOPY

When the light fields used to excite the Brillouin or Raman vibrations are very strong, stimulated emission can occur at the Brillouin or Raman shifted frequencies. This phenomenon was already mentioned (under *Active Spectroscopy*) as a means of discontinuous tuning, but is also actively investigated at present for its own sake. More information can be found in the books under references 2 and 23.

SOME USES OF LASER SPECTROSCOPY

It is not feasible in the limited space to cover this subject in great detail. From the previous discussion it is clear that an appreciable increase in our knowledge of materials has and is taking place due to laser spectroscopy. This knowledge is probably opening up new fields of study, such as detailed understanding of liquid-solid phase transitions.

As another application of passive spectroscopy, let us consider the studies of plasmas.

One of the early experiments of this kind[25] was done with the goal to measure plasma density as a function of time during a discharge. This measurement was made by placing the discharge tube inside the laser interferometer. The plasma density could then be determined by counting the number of passing fringes. This method has been developed[26] to the point where plasma densities above 10^{11} electrons/cm^3 can be measured with a 0.25-mm spatial resolution and a time resolution below 1 μs. Also cooperative electrostatic oscillations have recently been observed by measuring the spectral distribution of ruby laser light from a dense plasma.[27] If a laser is used based on gas transitions similar to those occurring in a given discharge, the laser can then serve as a probe to measure, for example, the density of an excited state or temperature as a function of position in a discharge tube.

An example of active laser spectroscopy is the experiment referred to earlier[17] in which line shapes and relative line positions were determined with a high precision. The line shapes measured were used to determine collision diameters in methane and other gases.[17,28] Also information about Stark splitting in gases has been obtained using the same technique.[29] The saturation observed in the experiments leads one to believe that this type of selective excitation may be useful in synthetic chemistry.

One limitation to very high resolution studies is that at room temperature and low enough pressure that collision broadening is negligible (in practice this means less than about 10-torr pressure), the Doppler linewidth of a gas having the density of air is 0.007 cm^{-1}. The natural linewidth of a gaseous absorption line, however, is determined by the spontaneous emission lifetime and is often two orders of magnitude or more below the Doppler linewidth. It was shown by Javan and coworkers[29] that when enough laser power is available to saturate the gaseous absorption line, the frequency width is given by the inverse natural lifetime and not by the much broader Doppler width.

As to some applications of laser spectroscopy, it is evident that it has use in the field of analytical chemistry. Trace amounts of gases can be detected using lasers. Methane can be detected easily at very low concentrations by its absorption, using a HeNe laser.[28] Isotope ratios in tracer experiments may be determined readily. Raman radiation can be used for identification of materials.[3] The laser has also been used as a microprobe. A *Q*-switched laser is focused on a surface and the vapor plume coming off is then excited by passing it through a dischargeable spark gap.[31] Enough light is then available to photograph the spectrum. This method has some advantages and also disadvantages compared with the electron microprobe. Advantages are: it works on heavy as well as light elements and is rather inexpensive. Disadvantages are mainly in the errors involved in absolute concentration measurements and in its rather large ($\sim$ 60 micrometer) spot size.

CONCLUSION

Although certain measurements can be made with greater precision, or have been made possible at all when the laser is used in place of conventional sources, laser techniques have not as yet developed to a stage where they can compete with general-use spectroscopes. Any meaningful evaluation of the technological usefulness of stimulated-type lasers, is still premature. In addition to the possible uses already mentioned in the foregoing text, the following may be noted:

1) A new phenomenon observed is that such intense hypersonic waves can be generated that they often damage the crystals in which they are excited.[30]
2) Anti-Stokes stimulated emission could be useful for sophisticated low-temperature cooling.
3) The possibility of Raman tunability in the *Q*-switched lasers may allow one to make three-dimensional holograms of fast-moving objects at such a wavelength that coincidence can be chosen with an existing cw gas laser for steady-state viewing.

BIBLIOGRAPHY

1. P. A. Franken, A. E. Hill, C. W. Peters and G. Weinreich, "Generation of Optical Harmonics," *Phys. Rev. Letters 7*, 118, 1961.
2. N. Bloembergen, *Nonlinear Optics*, W. A. Benjamin Inc., New York, 1965
3. S.P.S. Porto and D. L. Wood, "Ruby Optical Maser as a Raman Source," *Applied Optics*, 1, 139, 1962.
4. J. Cooney, RCA ENGINEER, *this issue.*
5. E. J. Woodbury and W. K. Ng, "Ruby Laser Operation in the Near IR," *Proc. IEEE 50*, 2367, 1962.
6. G. Eckhardt, R. W. Hellwarth, F. J. McClung, S. E. Schwarz, D. Weiner and E. J. Woodbury, "Stimulated Raman Scattering from Organic Liquids," *Phys. Rev. Letters 9*, 455, 1962.
7. J. L. Hall, "Two Quantum Photoionization of Cs and I," *IEEE QE-2*, 4, 1966, 1966 Quantum Electronics Conf., Abstract 3C-4.
8. J. Eckhardt, "Selection of Raman Laser Materials," *IEEE QE-2* 1, 1, 1966
9. M. D. Martin and E. L. Thomas, "Infrared Difference Frequency Generation," *IEEE QE-2*, 4, 1966, 1966 Quantum Electronics Conf. Abstract IC-4.
10. I. Melngailis, A. J. Stauss and R. H. Rediker, "Semiconductor Diode Masers of In_x (Ga_1-x) As," *Proc. IEEE 51*, 1154, 1963.
11. D. Meyerhofer and R. Braunstein, "Frequency Tuning of a GaAs Laser Diode by Uniaxial Stress," *Applied Physics Letters 3*, 171, 1963.
12. I. Melngailis and R. H. Rediker, "Magnetically Tunable CW InAn Diode Maser," *Applied Phys. Letters 2*, 203, 1963.
13. J. M. Besson, J. F. Butler, A.R. Calawa, W. Paul, and R. H. Rediker, "Pressure-Tuned PbSe Diode Laser," *Appl. Phys. Letters 7*, 206, 1965.
14. J. A. Giordmaine and R. C. Miller, "Tunable Coherent Parametric Oscillation in $LiNbO_3$ at Optical Frequencies," *Phys. Rev. Letters 14*, 973, 1965.
15. C.K.N. Patel, "High Power Molecular Lasers and their Application to Investigation of Non-linear Optical Phenomena in the Infrared," *IEEE QE-2*, 4, 1966, 1966 Quantum Electronics Conf. Abstract 2A-2.
16. R. L. Fork and C.K.N. Patel, "Broad-Band Magnetic Field Tuning of Optical Masers," *Appl. Phys. Letters 2*, 180, 1963.
17. H. J. Gerritsen and S. A. Ahmed, "Measurement of Absolute Optical Collision Diameters in Methane Using Tuned-Laser Spectroscopy," *Phys. Letters 13*, 41, 1964.
18. C.K.N. Patel, "Determination of Atomic Temperature and Doppled Broadening in a Gaseous Discharge with Population Inversion," *Phys. Rev. 131*, 1582, 1963.
19. W. W. Rigrod and I. P. Kaminow, "Wide Band Microwave Light Modulation," *Proc. IEEE 51*, 137, 1963.
20. H. Z. Cummins, N. Knable and Y. Yeh, "Observation of Diffusion Broadening of Rayleigh Scattered Light," *Phys. Rev. Letters 12*, 150, 1964.
21. L. Landau and G. Placzek, "Struktur der Unverschobenen Streulinie," *Phys. Z. Sowjetunion 5*, 172, 1934.
22. L. Brillouin, "Diffusion de la Lumiere et des Rayons X par un Corps Transparent Homogene," *Ann. Phys.* (Paris) *17*, 88, 1922.
23. R. Y. Chiao and P. A. Fleury, "Brillouin Scattering and the Dispersion of Hypersonic Waves," *Physics of Quantum Electronics Conf. Proc.*, Ed. by P. L. Kelley, B. Lax, and P. E. Tannenwald, McGraw Hill Book Co., New York 1966, Page 241.
24. J. P. Russell, "Raman Scattering in Silicon," *Applied Physics Letters 6*, 223, 1965.
25. D.E.T.F. Ashby and D. F. Jephcott, "Measurement of Plasma Density Using a Gas Laser as an Infrared Interferometer," *Appl. Physics Letters 3*, 13, 1963.
26. W. B. Johnson, A. B. Larsen and T. P. Sosnowski, "A Beat Frequency Interferometer for Plasma Diagnostics," *IEEE QE-2*, 4, 1966, 1966 Quantum Electronics Conf., Abstract 8C-8.
27. S. A. Ramsden, R. Benesch, W.E.R. Davies, and P. K. John, "Incoherent Scattering of a Ruby Laser from a Plasma," Second Rochester Conf. on Coherence and Quantum Optics, 6/66.
28. H. J. Gerritsen and M. E. Heller, "A High-Resolution Tuned-Laser Spectroscope," *Applied Optics Supplement 2; Chemical Lasers 73*, 1965.
29. M. S. Feld, H. J. Parks, H. R. Schlossberg and A. Javan, "Spectroscopy with Gas Lasers," *Physics of Quantum Electronics Conf. Proc.*, McGraw Hill Book Co., New York 1966, Page 567.
30. R. Y. Chiao, C. H. Townes and B. P. Stoicheff, "Stimulated Brillouin Scattering and Coherent Generation of Intense Hypersonic Waves," *Phys. Rev. Letters 12*, 592, 1964.
31. Dr. F. Brech, *Private Communication*, Jarrell Ash Co., Newtonville, Mass.

LASER DIGITAL DEVICES

As opposed to most applications in which lasers are used basically as special sources of radiation, this program is concerned with whether laser components could form a new generation of switching circuits for digital computers. This paper describes only laser digital devices in which all of the processing signals are in the form of optical energy. These devices could be used as general-purpose logic circuits in the same way that transistors are presently used for this purpose, except that all of the processing would be done with optical rather than electrical signals. The operation of the laser digital devices is based on a signal gain derived from a laser amplifier and on nonlinear (saturable) interaction of intense optical signals with laser materials. The two basic non-linear processes are quenching of the output of a laser oscillator and saturation of optical absorption. This paper is condensed from the material contained in Ref. 1, plus summaries of some of the recent results obtained under a new contract with Rome Air Development Center. A bibliography of RCA efforts in this area is given by Ref. 2-6.

DR. W. F. KOSONOCKY and R. H. CORNELY
RCA Laboratories, Princeton, N. J.

OPERATION of laser switching devices can be based on amplification of optical signals by a laser amplifier and the two nonlinear processes: saturation of gain (quenching), and saturation of optical absorption. Our present work is centered on the study and development of GaAs inverter circuits whose operation is based on the amplification of an input signal by a laser amplifier and quenching of the output of a laser oscillator. Another class of laser switching device can be constructed by placing saturable absorber material inside a cavity that also contains emissive (laser) material. Depending on the relation between the material constants of the absorber and emitter, these devices can operate either as bistable or monostable circuits. A bistable circuit, operating as a laser oscillator that can be triggered on and off by externally applied optical signals, can be made using semiconductor laser materials. However, it is not very likely that a proper saturable absorber can be found to make semiconductor monostable circuits. We have, however, demonstrated the operation of a monostable circuit, using a ruby laser as the emitter and different solutions of phthalocyanine as the saturable absorber. These ruby laser devices were also operated as relaxation oscillators, more commonly known as passive *Q*-switch lasers.

Final manuscript received July 28, 1966

The research reported in this paper was sponsored by the Air Force Systems Command, Rome Air Development Center, Griffiss Air Force Base, New York, under Contract Number AF30(602)-3169, AF30(602)-3914, and RCA Laboratories, Princeton, New Jersey.

The processes of optical absorption and stimulated emission are distinguishable only because of the difference in the occupation of the energy levels involved in the optical transitions. Therefore, basically the same criteria can be used to estimate the optical signal levels needed to cause an appreciable change in the populations of the energy levels for either of these processes.

The condition of steady state saturation is applicable when the duration of the applied optical signal is longer than the spontaneous recovery times of the material. In this case, the absorption (or the gain) is reduced to one-half its low signal value when the stimulated transition rate becomes equal to the recovery rate associated with spontaneous transitions. For a material with a purely radiative recovery process, the signal flux power density P^1 in watts/cm^2 required to reach this condition can be estimated by:

$$P^1 = \frac{12\, n^2 \Delta\gamma}{\lambda^8} \qquad (1)$$

where λ is the wavelength in micrometers, n is the index of refraction, and $\Delta\gamma$ is the homogenously broadened line width in wave numbers, cm^{-1}. For most available materials, the expression in Eq. 1 must be multiplied by the ratio of the radiative lifetime T_r to the actual recovery time that tends to bring the system towards the steady state condition.

For optical pulse signals whose durations are considerably shorter than the spontaneous recovery time constants of the materials, the minimum energy density W^1 in joules/cm^2 required to reduce the absorption (or the gain) coefficient to 0.37 of its low signal value is:

$$W^1 = \frac{h\gamma}{2\sigma} \qquad (2)$$

where $h\gamma$ is in Joules/photon and the absorption cross sections $\sigma = \alpha/N$ where α is the absorption coefficient in cm^{-1} and N is the density of the absorbing sites. For material with homogenously broadened absorption lines, the energy density W^1 in joules/cm^2 can also be estimated by an expression analogous to Eq. 1:

$$W^1 = \frac{12\, n^2}{\lambda^3} \Delta\gamma\, T_r \qquad (3)$$

Since the radiative lifetimes of optically pumped solid-state lasers are of the order of a millisecond while the radiative lifetimes of semiconductor lasers are of the order of a nanosecond, optically pumped lasers are more suitable as high energy pulse generators. However, semiconductor lasers are the most suitable components for small signal switching devices as the energy density that must be developed within a laser digital device for one switching operation is proportional to the homogeneously broadened linewidth $\Delta\gamma$ and the radiative lifetime T_r of the optical transitions. Although materials with strong optical transitions and short radiative lifetimes also tend to have somewhat wider linewidths, the energy required to cause one switching operation in optically pumped lasers, such as ruby or neodymium lasers, can be estimated to be about five orders of magnitude higher than for GaAs lasers. The upper bound on the switching time of a laser digital device is determined by the effective recovery time toward a steady-state condition. A reasonable estimate of the recovery time for optically pumped solid-state lasers is 10^{-4} seconds in comparison to 10^{-10} seconds for GaAs lasers.

Fig. 1—GaAs laser inverter. (a) pictorial view; (b) schematic of active laser region.

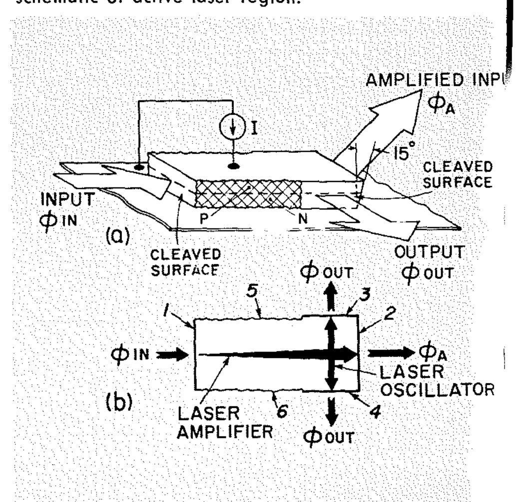

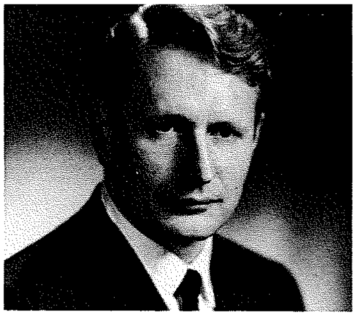

Dr. **WALTER F. KOSONOCKY** received the BS and MS in Electrical Engineering from Newark College of Engineering, Newark, N. J., in 1955 and 1957, respectively. In 1965 he was awarded Sc.D. degree in Engineering by Columbia University, New York, N. Y. Since June 1955 he has been employed at RCA Laboratories, Princeton, N. J., where after one year as a Research Trainee, he became a Member of the Technical Staff in the Computer Research Laboratory. His work has included: development of the ferrite aperture plate memory system, application of transistors in computer circuits, investigation of the use of ferrite cores and micromagnetic techniques for high speed computers, application of tunnel diodes for digital computer logic and memory systems, development of tunnel-diode/transistor high-speed computer circuits, and a study of pattern recognition systems. Since April 1962, Dr. Kosonocky has been engaged in a feasibility study of the use of lasers as digital computer components. He received an RCA Laboratories Achievement Award in 1959 for his contributions related to the application of parametric devices for digital computer logic and memory systems; and in 1963 he received an RCA Laboratories Achievement Award for his contributions to applications of tunnel diodes and transistors for high speed computer systems. He was also awarded the David Sarnoff Fellowship for the academic year 1958-1959. Dr. Kosonocky is an adjunct Professor at Electrical Engineering Department of Newark College of Engineering. He is a member of Sigma Xi, Tau Beta Pi, Eta Kappa Nu, and IEEE.

ROY H. CORNELY received the BSEE from Drexel Institute of Technology in June 1960. As part of the cooperative industry program at Drexel, he was employed by the Teleregister Company, Stanford, Conn. In 1961, he attended the Moore School of Electrical Engineering at the University of Pennsylvania and was a part-time instructor of Physics at Drexel. In 1962, he received an MSEE upon completion of his thesis on the permalloy sheet memory. He is presently engaged in a part-time Doctoral Study Program at Rutgers. In June 1961, Mr. Cornely became a Member of the Technical Staff at RCA Laboratories. His initial assignments were in the magnetics section where he worked on high speed memory and magnetic flux logic devices. He made a basic study of magnetic flux reversal processes in ferrites. Since June 1963, he has been concerned with the application of optical phenomena to new digital devices.

We have experimentally verified the validity of Eq. 2 in a study of the saturation of absorption of an unpumped ruby crystal illuminated by pulses from a ruby laser. Our subsequent experiments with solution of phthalocyanines indicated that the steady state saturation process appropriately describes the response of these solutions when they are illuminated by pulses from a Q-switched ruby laser. The absorption spectra of these solutions are reduced to 50% of their initial values by a laser pulse flux power density of 0.1 to 0.15 MW/cm^2. We are presently studying the large optical signal response of GaAs laser components. Although a detailed description of the large signal response due to band to band transitions would be very complex, our experimental results suggest that essentially the same analysis as that applied to transitions between discrete levels can also be applied in the case of GaAs lasers. Our recent work on the large signal response of the GaAs laser amplifier points out that the gain coefficient in the amplifier also saturates at a flux power density on the order of 0.1 MW/cm^2.

GaAs LASER INVERTER

Basic logic operations such as *or-not* and *and-not* can be performed by a laser digital device that operates as an optical inverter-amplifier. The inverter consists of a laser amplifier wherein part of the amplifier junction area is utilized as an oscillator. The construction and operation of the laser inverter is shown schematically in Fig. 1. In the absence of an input ϕ_{in}, the oscillator section of the device produces an output signal ϕ_{out}. As the input signal ϕ_{in} is increased, the gain in the oscillator section decreases to the point where the output ϕ_{out} of the laser oscillator is quenched. The amplified input signal ϕ_A may be used as an input to another inverter or it can be dissipated in an appropriate termination.

For construction of laser inverters we try to use GaAs laser materials that lase uniformly across the whole junction region. A laser amplifier can be formed between sides 1 and 2 by using nonreflective coatings or by lapping side 2 at a verticle angle with respect to side 1, thus destroying the laser cavity between these two sides. The laser amplifier described is formed by lapping side 2 at a vertical angle of 15°. The laser oscillator is between the cleaved sides 3 and 4. Sides 5 and 6 are roughened by abrasive paper to prevent internal oscillations in the laser amplifier structure. A typical unit is 4 mils high, sides 1 and 2 are 10 mils wide, sides 5 and 6 are 26 mils long, and sides 3 and 4 are 4 mils wide.

The operation of the laser inverter was demonstrated using an external input signal derived from a laser oscillator. Both devices were made from the same GaAs wafer. Lenses were used to refocus the output of the source laser on the active laser region of side 1 of the inverter. The laser devices were individually mounted in two small vacuum chambers on cold fingers cooled by liquid nitrogen. The test results are shown in Fig. 2. The waveforms of the input signal ϕ_{in}, the amplified input ϕ_A, and the inverter output ϕ_{out} are shown in Fig. 2a, b, and c, respectively. The input signal is applied 80 ns after the inverter is energized, so that amplification and quenching take place only during the pulse overlap period. These waveforms

Fig. 2—Inverter signal waveforms, 50 ns/div. (a) Input, Φ_{in}, 100 mW/div; (b) Amplified output, Φ_A, 15 mW/div; (c) Inverter output, Φ_{out}, 4 mW/div.

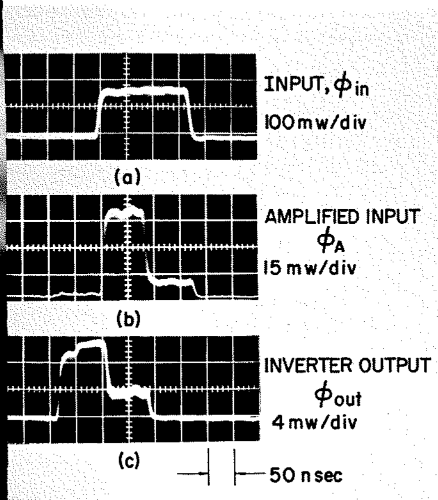

Fig. 3—Dual laser-oscillator. (a) pictorial view; (b) Schematic of active laser region.

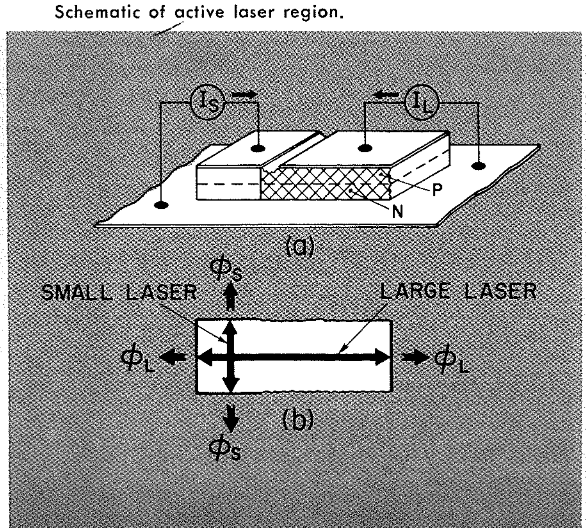

Fig. 4—Etched cross-section of GaAs wafer. Magnification about 700X.

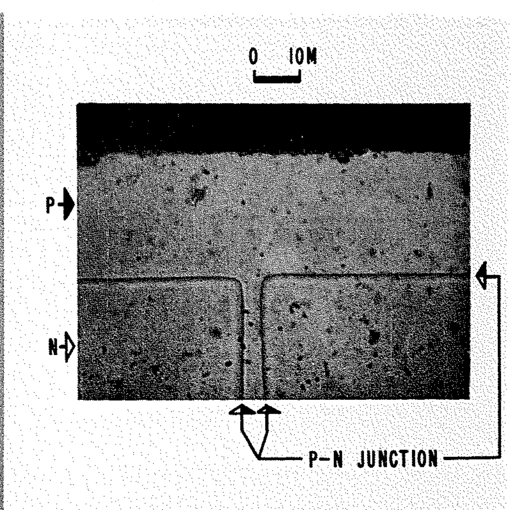

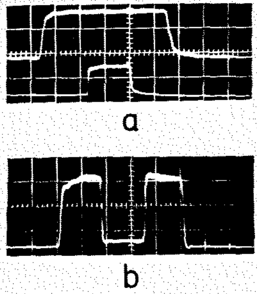

Fig. 5—Waveforms for the dual laser-oscillator, 100 ns/div. (a) I_S (top), 1.6 amperes/div; I_L (bottom), 2 amperes/div; (b) Small laser output, Φ_S, 4 mW/div.

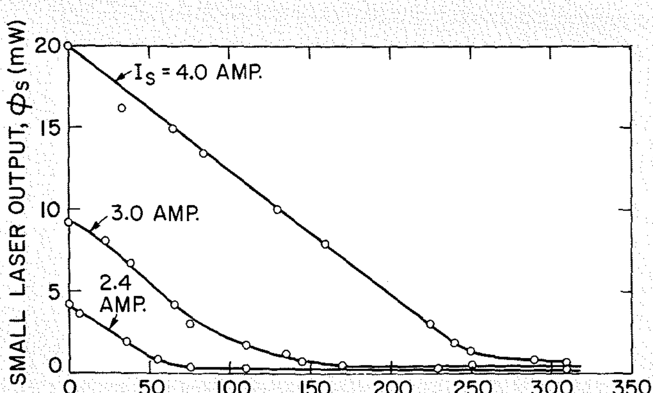

Fig. 6—Operation of the dual laser-oscillator, Φ_S vs. Φ_L.

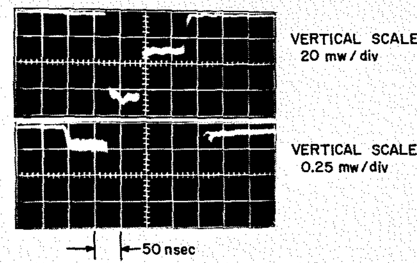

Fig. 7—Output waveforms of a GaAs laser amplifier, (a) Vert. scale: 20 mW/div; (b) Vert. scale: 0.25 mW/div; Horizontal scale for (a) and (b): 50 ns/div.

were detected by an RCA 7102 photomultiplier with an aperture sufficiently large to capture most of the optical signal in each case. The peak intensities of these signals are $\phi_{in} = 150$ mW, $\phi_A = 50$ mW, and $\phi_{out} = 10$ mW. The input signal ϕ_{in} was measured by removing the inverter from the path of the source laser beam. Therefore, the value of ϕ_{in} does not equal the signal actually coupled into the laser inverter, but rather it represents the total signal available from the source laser.

We are studying the quenching characteristics of a GaAs laser oscillator using a dual laser oscillator such as shown in Fig. 3. Typically, the dual laser-oscillator contains two resonators within one laser structure, one 10 by 4 mils and the other 10 by 30 mils. Isolation in the described unit was achieved by sawing a groove through the top metal contact into part of the semiconductor material while monitoring the leakage conductance. The isolation resistance between the two diodes is about one ohm, which is sufficiently large to allow separate electrical control of the two oscillators. However, we can also achieve complete electrical isolation, as well as coupling optical signals between two laser regions, by using a specially prepared laser material in which, as is shown in Fig. 4, a 5-micrometer P-region is sandwiched between two parts of the N-region of a GaAs laser wafer. A tested dual laser-oscillator was made from the same wafer that was used for the laser inverter. The operation of the dual laser-oscillator is illustrated in Figs. 5 and 6. Fig. 5a shows the waveforms of the applied currents to the small oscillator I_S and to the large oscillator I_L. Fig. 5b shows the variation of the output of the small laser as a function of the output of the large laser. Note that: 1) the quenching is a linear process, and 2) excluding coupling losses, the amplifier portion of the laser inverter must provide a signal gain of more than 10 for complete quenching of the inverter output and a fanout of two. We have found that in the case of certain specially prepared GaAs laser materials the quenching ratio, defined as the slope $\Delta\phi_S/\Delta\phi_L$ in Fig. 6, can approach a value of 0.5. In our opinion, the quenching ratio is determined by the ratio of the effective thickness of the inverted population region to the thickness of the optical beam guided by the GaAs laser. Thus materials with wider inverted population regions would tend to have more efficient quenching characteristics. Our study of radiation confinement in GaAs lasers points out that at 77°K the optical beam is about 1 micrometer wide. This result based on near-field emission measurements is also consistent with the diffraction limited far-field emission pattern of GaAs lasers.

GaAs LASER AMPLIFIERS

Typical performance of the amplifier part of the inverter is illustrated by the waveforms of Fig. 7. In this test special care was taken to detect only the output signal of the amplifier. The laser amplifier dimensions were 5 by 30 mils. Its output facet was lapped at a 15° vertical angle. The output spectrum of the source laser overlapped the peak of the amplified fluorescence spectrum of the amplifier. The output of the source laser was focused onto the input facet of the amplifier using the experimental setup shown in Fig. 8. The devices were operated at 77°K. Both units were driven by equal 120-ns-duration and 8.0-ampere-amplitude partially-overlapping current pulses. There is a ratio of 80 between the scales in part a and part b. Both parts of the figure, however, show the same detected output signal. The detected output signal, therefore, consists of three different output levels. The first portion of the output S_1, which is clearly visible in the lower photograph, represents the transmission of the source signal when no current is applied to the laser amplifier. The second output level S_2 represents the amplified input signal. The third output level S_3 is due to super-radiance of the amplifier. The detected signal amplification defined as $(S_2\text{-}S_3)/S_1$ was found to be as high as 500. The net transmission signal gain, defined as $(S_2\text{-}S_3)/S_o$ where S_o is the total output of the source laser, was about unity for large input signals and approached a value of only 5 for very low input signals.

To achieve better signal coupling between the oscillator and the amplifier, we have constructed directly coupled GaAs laser devices in which the separation (on the order of one micron) between the oscillator and the amplifier is made by cleaving. A photograph of the side view of such an oscillator-amplifier pair is shown in Fig. 9. In the tests of the directly coupled amplifier, a net signal gain of about 20 for low input signals (of about 10 mW) was obtained. The gain coefficient saturates to one-half of its low signal value at a signal flux power density in excess of 0.1 MW/cm^2. The saturation of the gain coefficient can be observed from the measurement of the transmission gain and from the reduction of the amplifier fluorescent spectrum due to the application of an input signal.

The GaAs laser amplifier is expected to have a very large gain-bandwidth product. The delay time for passing a signal through the amplifier can be esti-

Fig. 8—Experimental setup for the testing of GaAs laser amplifiers and inverters.

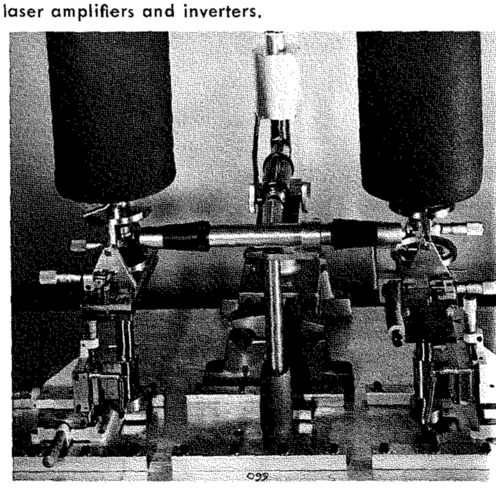

mated to be on the order of 10^{-12} second. A simplified theory of the operation of GaAs laser amplifiers predicts a signal gain as high as 10^4 for an amplifier current that is 8.5 times larger than the laser threshold current for an equivalent laser oscillator. However, on the basis of our measurements, we expect that a signal transmission gain between 10 to 100 is a more realistic figure due to the gain-saturation effects associated with amplified fluorescence. One of the main limitations of a GaAs laser amplifier, which in true for laser amplifiers in general, is that it has a very large noise signal due to amplified fluorescence. Since the signal amplified by the amplifier portion of the inverter is not used directly as an output signal, the GaAs laser inverter is an example of a device that takes advantage of the high gain characteristics of the laser amplifier while it still discriminates against the noise signal.

GaAs LASER INVERTER SWITCHING CIRCUITS

The GaAs laser inverter is most suitable for performing *or* and *or-not* logic functions. It is generally recognized that the transfer characteristic of a digital circuit must have a threshold level, which will prevent the circuit from responding to either low level or noise signals, and a saturation region into which the circuit switches to produce a fixed output level when the applied signal is well above the threshold level. A closer inspection of digital devices points out that both threshold and saturation are needed only for the noninverting devices. An inverter, however does not require threshold for low signals if it has a good cut-off region. This point is illustrated by the sketches in Fig. 10. A network of three cascaded levels of laser inverters is shown in Fig. 10a. The remaining parts b, c, and d give the signal transfer curves for the input signal P_1 through one, two, and three levels of inverters. The GaAs laser inverter has a natural capability for a fan-out of two and a fan-in of one. Two approaches for allowing more than one input, without sacrificing the isolation properties of two perpendicular light beams, are shown in Fig. 11.

Presently, we are attempting to establish the basic feasibility of GaAs laser inverter circuits by: 1) using high precision optical equipment, as shown in Fig. 8, for the coupling of signals between laser devices, and 2) by developing techniques for direct coupling of optical signals as, for example, is illustrated in Fig. 9. With these approaches, however, we expect to be able to interconnect only a small number of gates. The only realistic approach is to develop techniques for integrated GaAs laser digital devices. Then, one could visualize an array of active laser circuits in the form of a pattern of strips of high-gain laser amplifiers made into inverters by a set of reflecting boundaries. These inverters, in turn, would be interconnected by low-gain (or low-loss) laser amplifier transmission lines to form logic circuits. The major technological problem that would have to be solved to make this concept a practicality is to find means for making reflecting boundaries which could change part of a laser amplifier into a laser oscillator without physically separating the laser oscillator from the whole GaAs wafer.

At least in principle, semiconductor laser digital devices have several very attractive characteristics for high-bit-rate batch-fabricated digital circuits. The optical interconnections are free from inductive and capacitance effects. There is a natural impedance match between the active device and the transmission medium (both of which may be in the form of semiconductor laser components). The delay time constants associated with any mismatches can be made very short, on the order of 10^{-11} second. A single plane crossing of two optical signals should be possible if the planar dimensions of the optical waveguides are large as compared to the wavelength of light. Finally, switching times on the order of 10^{-10} to 10^{-11} second are possible with GaAs laser digital devices. The only major disadvantage, in terms of the present state of development of GaAs lasers, is that even at liquid-nitrogen temperature a current on the order of an amp is required for a device having planar dimensions of several hundred square mils. The power requirements per logic element will have to be reduced by at least a factor of 100 in order that laser digital devices be competitive with transistor technology. To accomplish this, a monolithic technology for the fabrication of the GaAs laser devices with planar dimensions on the order of one mil for an individual component must be developed.

ACKNOWLEDGMENT

The authors wish to express their appreciation to W. H. Bleacher and W. Romito for their contributions in preparation of GaAs materials and devices.

BIBLIOGRAPHY

1. RADC-TR-65-238, *Laser Digital Devices,* Final Report prepared under Contract AF33(602)-3169 by RCA Laboratories, Princeton, New Jersey, September, 1965.
2. RADC-TDR-64-123, *Neuristor Logic Technology,* Final Report prepared under Contract AF30(602)-2761 by Applied Research Dept., RCA Defense Electronic Products, Camden, New Jersey, June, 1964, pp. 147-150.
3. Kosonocky, W. F., "Feasibility of Neuristor Laser Computers," *Proc. of Optical Processing of Information Symposium,* October 23-24, 1962, Washington, D. C. Spartan Books, Ins., Baltimore, Maryland, 1963.
4. Reimann, O. A. and Kosonocky, W. F., "Progress in Optical Computer Research," *IEEE Spectrum,* Vol. 2, No. 3, pp. 181-195, March 1965.
5. Kosonocky, W. F., "Laser Digital Devices," *Proc. of Symposium on Optical and Electro-Optical Information Processing Technology,* November 9-10, 1964, Boston, Massachusetts. MIT Press, 1965.
6. Kosonocky, W. F., Cornely, R. H., and Marlow, F. J., "GaAs Laser Inverter," *Digest International Solid-State Circuits Conf.,* February 17-19, 1965, Philadelphia, Pennsylvania.

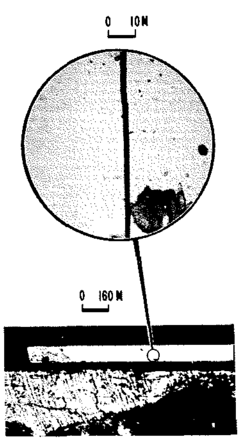

Fig. 9—Laser oscillator directly couples to laser amplifier.

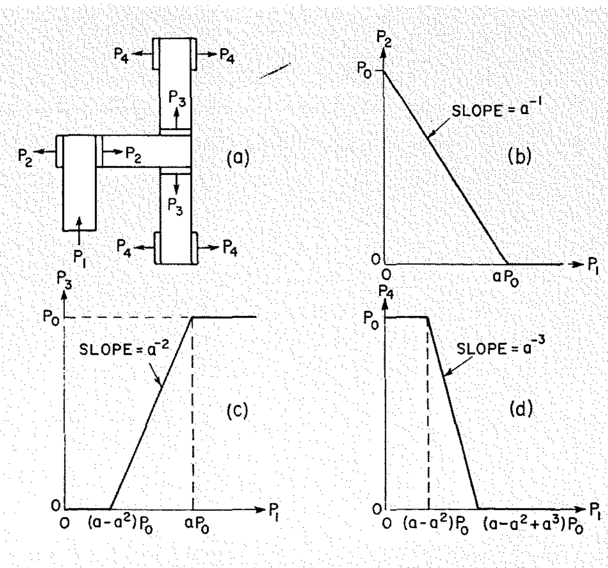

Fig. 10—Three stages of GaAs laser inverters. (a) schematic of the circuits. (b) P_2 vs. P_1. (c) P_3 vs. P_1. (d) P_4 vs. P_1.

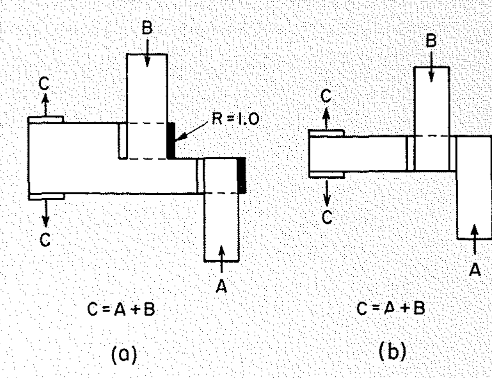

Fig. 11—Two approaches for obtaining multiple inputs for GaAs laser inverter circuits.

THE SIGNIFICANCE OF THE LASER IN MEDICINE AND BIOLOGY

L. E. FLORY
Physical Research Lab.
Astro-Electronics Division
Princeton, N.J.

The demonstration of a new and unique form of radiant energy usually results in an immediate speculation as to its possible use in Medicine and Biology. Only a few months after the discovery of the X-ray it was already being used for diagnostic purposes. High frequency diathermy and various nuclear radiations are further examples. Laser radiation is no exception. Unfortunate experience with X-rays in the early days demonstrated the importance of understanding the biological effects of radiation as a means of protecting those who may be exposed to it in the course of their experiments. An enormous amount of information has been accumulated on the biological effects of microwaves, X-rays and other forms of electromagnetic radiation primarily in the study of protective measures.

In the case of the laser, this background was of considerable help in approaching the study of the significance of laser energy in Medicine and Biology. There are three areas of interest:

1) An understanding of the hazards of laser radiation,
2) The possible use of the laser beam as a tool in Medicine and Biology, and
3) The direct interaction of laser radiation with biological materials with a view to its possible therapeutic effects.

Final manuscript received July 20, 1966

HAZARDS

The laser forms the most concentrated source of energy available to man. Power densities many times that found at the surface of the sun can be produced. It is this tremendous flux density that creates the greatest hazard. The possibility of damage when a laser beam falls on the surface of tissues can depend upon several factors:

1) The pigmentation of the tissue—the more concentrated the pigmentation, the more absorption.
2) The available blood circulation which acts as a coolant and will tend to prevent damage due to temperature rise.
3) The spectral absorption of the tissue. If the tissue is of a color that will selectively absorb the specific wavelength being radiated, the possibility of damage will be correspondingly greater.

When a laser beam contacts the skin the immediate effect is an eruption from the surface due to a rapid heating. This in itself would produce only superficial surface damage. However, deep-seated damage has been observed which is out of proportion to the observable damage on the surface. True, the relative transparency of the skin may allow half or more of the radiation to be absorbed at a deeper level. It has been suggested, however, that the primary cause of deep seated lesions is the generation of a pressure wave which inflicts mechanical damage rather than the more obvious thermal effects. This pressure wave might be generated in three ways:

1) Eruption on first contact ejected material at high velocity. Conservation of momentum would account for the generation of an inward pressure wave.
2) Transient heating would result in thermal expansion.
3) Transient heating would generate trapped gases in the interior of the tissue.

In any case, the result seems to be the generation of a shock wave which progresses through the tissues breaking down the cell walls.

The organs of the body are susceptible to specific damage to varying degrees. By far the most sensitive is the eye. The lens and cornea are transparent to the laser radiation and, in addition, can

LESLIE E. FLORY received his BSEE at the University of Kansas in 1930. From 1930 to 1942 he was a member of the research division of RCA Manufacturing Company in Camden, N.J. During that time he was engaged in research on television pickup tubes and related electronic problems, particularly in the development of the iconoscope. In 1942, he was transferred to RCA Laboratories Division, Princeton, N.J., continuing to work on electronic tubes and special circuit problems, including electronic computers, infrared image tubes and sensory devices. From 1949 to 1953, he was in charge of work on storage tubes and industrial television at RCA Laboratories. Since 1953, he has continued in charge of work on industrial television with emphasis on transistor circuitry and has supervised the work on Electronic Vehicle Control and Medical Electronics. Mr. Flory, a Fellow of the Technical Staff, RCA Laboratories, has been affiliated with Astro-Electronics Division since 1965. Recently, he was appointed consultant to the RCA Team co-operating with Hoffman-LaRoche to develop new medical electronic devices. He has published numerous articles in the field of Television and Medical Electronics. Mr. Flory is a Member of Sigma Xi; a Fellow of the IEEE; a Member of the SMPTE; and is Secretary General of the International Federation for Medical Electronics and Biological Engineering. Forty U.S. Patents have been issued in his name.

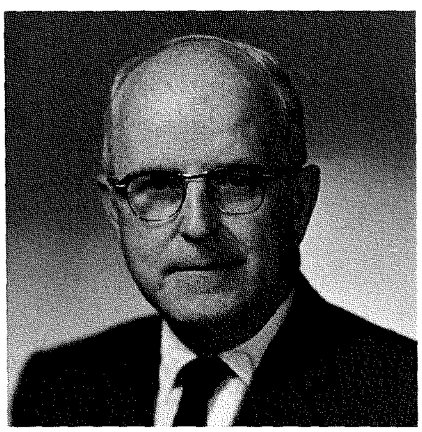

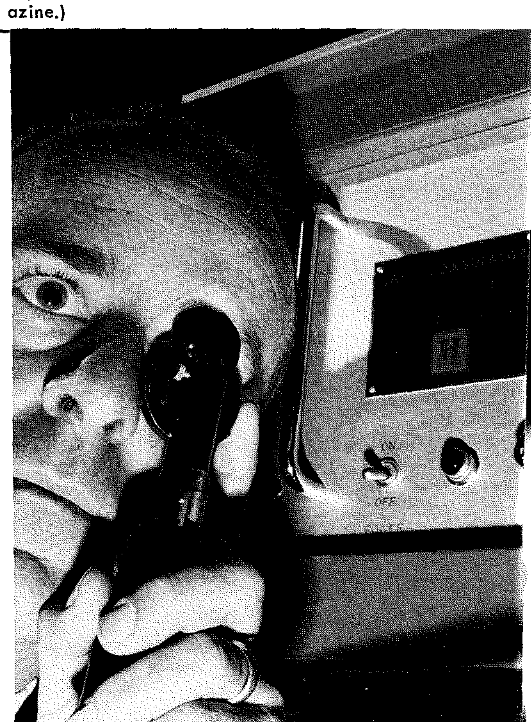

Fig. 1—Laser coagulator. (Photo courtesy *Laser Focus* magazine.)

concentrate the energy several fold by the normal focusing action onto the surface of the retina where it can do the most damage. Direct exposure to the primary beam is not the only hazard in the case of the eye. Specular reflections from objects in the path of the beam by chance or reflection from a lens surface can be equally dangerous.

Much attention is being given the hazards of laser use and rules of safety concerning their operation, and the permissible thresholds are in a state of constant evaluation and updating.

THE LASER AS A TOOL

The high concentration of energy in the laser beam makes it attractive as a tool in certain biological and medical procedures. The most highly publicized use to which it has been put is in photocoagulation at the retinal surface of the eye, (Fig. 1) commonly utilized to correct a detachment of the retina. The laser has been used as a photocoagulator with success in many cases. It has not been clearly established, however, that it is superior for this purpose to other sources of light. Some dangers exist in its use because of the high absorption of other parts of the eye such as the iris. It would appear for the moment that the laser as a photocoagulator is useful because it is a convenient source of high intensity light and not because of its unique property of coherence.

Other uses as a tool in cellular studies also make use of the extremely small area into which tremendous power can be concentrated. For example by focusing the beam through a microscope it is possible to reduce the spot to subcellular size. It can thus be used as a probe to selectively hemolyze individual cells for study of their constituents.

THERAPEUTIC USES OF LASERS

One of the more exciting aspects of the use of lasers in medicine is the possibility of selective destruction of tumor cells. A number of experimenters have worked in this area, irradiating both natural and transplanted tumors in animals (Fig. 2) and natural tumors in humans. Tumor tissue is destroyed by laser radiation but this mechanism is not yet understood. A localized thermal effect accounts for a part of the action, but several workers have reported an apparent build up of an effect which may destroy the tumor over a period of days after irradiation even though the immediate effect may be minimal. They speculate on a possible change in the enzyme activity in the material or the generation of a toxic material which causes the tumor to regress over a period of time. Another possibility is the formation of an antigenic material by action of the radiation on protein constituents of the tissue. While these effects, which are not understood, are extremely interesting, one researcher stated that the observations were reported with "suppressed enthusiasm" because as yet there are so many unknowns and the experiments have not been well controlled.

Whether, again, the effects on tumor tissue are thermal, mechanical or due to the high degree of monochromaticity and coherence of the radiation, specific effects are being produced which account for the observed results. Electron spin resonance experiments have been conducted with biological material being irradiated by laser radiation in vitro. The results indicated that free radicals were being produced by the laser radiation. The effects of such action in a living tissue are not yet known.

CONCLUSION

As is often the case with a new technique, the early reports of the uses of lasers in medicine were, in many cases, optimistic. A selective means of simply destroying malignant tumors would be so important that every encouraging result is apt to be reported out of proportion to its significance.

At the moment, it appears that the laser is an important tool in microsurgery, and it does appear that there are non-thermal effects in the reaction of laser radiation with tissues. Some of these non-thermal effects have shown some relation to the post-radiation regression of tumors. A large number of competent workers are exploring the field with the latest equipment, with greater emphasis placed on the control of both the equipment and the experiments. The results are certain to be exciting.

Fig. 2—Laser irradiation of tumor. (Photo courtesy *Laser Focus* magazine.)

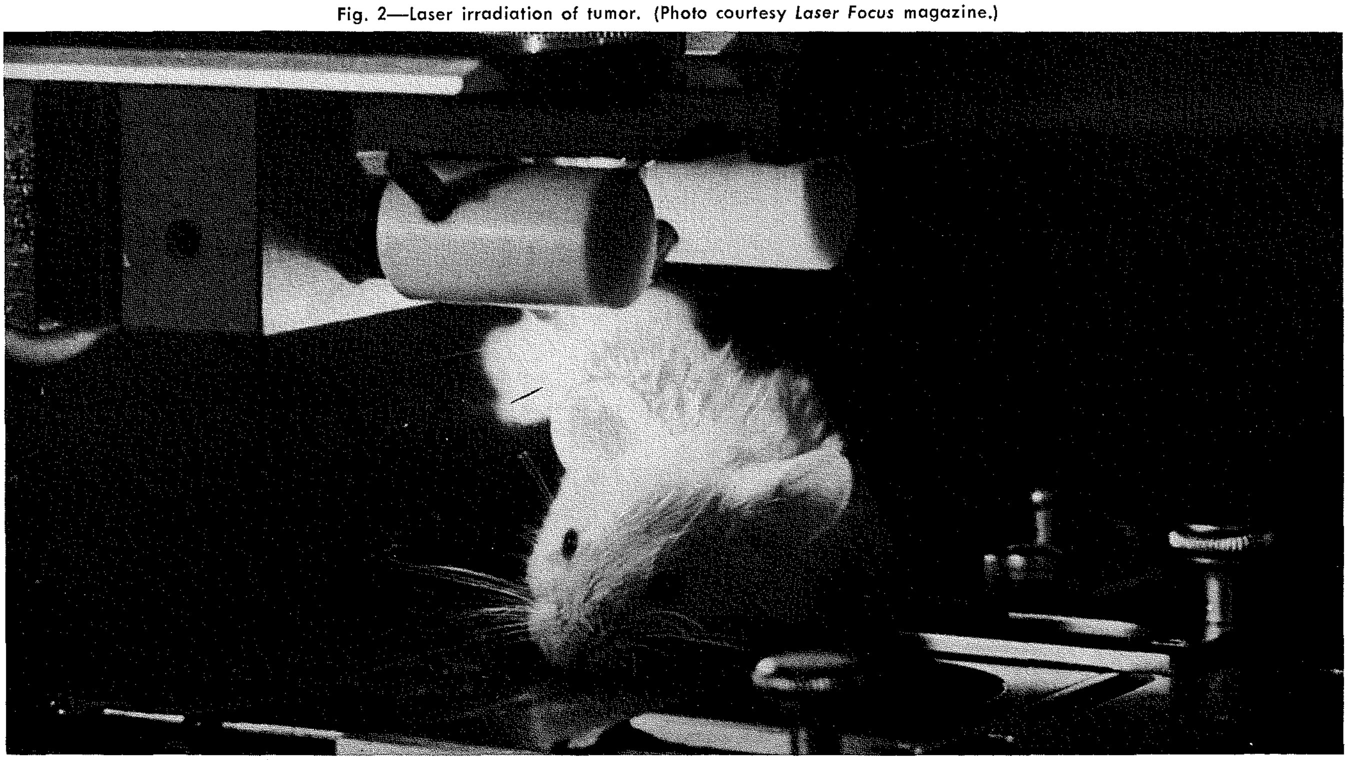

LASER SAFETY CONSIDERATIONS

Described here is a program of safety to provide adequate safeguards against the potential hazards of the laser. The program considers matters of sight hazards, since the radiance of a laser can exceed the level which the human eye can safely tolerate. It also considers other factors involving cases where focused or unfocused laser beams can produce burns on tissue or vaporize certain materials. A bibliography of references on laser safety is included.

P. BROWN, JR.
RCA Laboratories
Princeton, N. J.

OVER the past decade, the laser has evolved from its initial position of experimental device to its present position of well-established, highly versatile tool of technology and research. The species of lasers has expanded from the first solid state laser, ruby, to encompass gas lasers and semiconductor lasers. Their frequency range extends from the infrared to the ultraviolet. Generally, either pulsed or continuous mode operation is available; however, some lasers can be operated in both modes. The available power ranges from a few milliwatts to a few hundred watts for continuous wave operation, and up to one gigawatt for pulsed operation.

Lasers are unique sources of light that produce beams characterized by high intensity, high monochromaticity, and divergences of a few milliradians. It is these properties that make the laser such an effective tool for welding, drilling, photocoagulation, photocauterization, ranging, and the other myriad applications that exploit its capabilities. These remarkable benefits, however, are not available without attendant potentially severe hazards to improperly trained operators. Its radiance, already many times greater than that of the sun at the same wavelength, exceeds the level that the unaided human eye can safely tolerate. Laser beams, both focused and unfocused, can produce burns on tissue and can vaporize certain materials so quickly that the beam must not be permitted to impinge on explosive substances.

Much of the literature dealing with the hazards encountered in work with lasers concentrates on the provision of protection against eye injury.[1-12] A program of eye protection from laser radiation should have two aspects: 1) *provision of protective eye shields*, and 2) *institution of a hazards control procedure*. Goggles are available that have been designed specifically for protection of the eyes from the light emitted by the commonly used lasers. Great care should be taken to use *only* the goggle that is appropriate protection against the particular laser being used. Several optical equipment manufacturers, such as Bausch & Lomb and the American Optical Company, make these "ANTI-LASER" goggles. Special attention must be given to the necessity of screening out the harmful ultraviolet light produced by the argon laser in addition to attenuating the visible lasing frequencies. Glass and many plastics are almost opaque to emission from the carbon dioxide laser. In fact, it is convenient to enclose both ends of the laser tube in a plexiglass enclosure. A useful listing of laser emission is contained in Reference 13.

Specification of the required optical

PAUL BROWN, JR. received his B.S. in Physics from Howard University in 1959. He then joined RCA at DEP in Camden, New Jersey. In 1960 he left RCA to join the Signal Corps where he was Project Officer, Signal Corps, Research and Development Laboratories, from 1960 to 1962. He worked on atomic frequency standards and worldwide synchronization of atomic clocks project. In 1962 he joined RCA Laboratories, and since that time has had assignments in the Electronics Research Laboratory, and in the Materials Research Laboratory. For the past year he has been a member of the Technical Administration Section and has responsibility for laboratory safety.

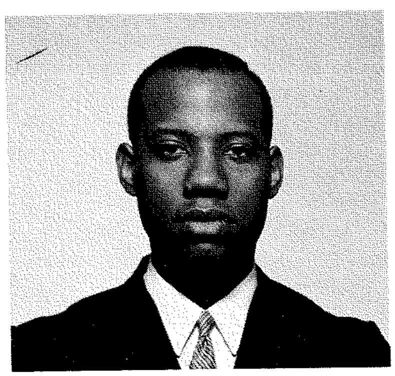

Final manuscript received July 8, 1966.

density of the goggle filter at the laser wavelength is the most critical criterion for assuring adequate protection. This optical density should be available in a relatively flat region of the filter absorption characteristic, and not at a point where the filter absorption changes rapidly. In addition to satisfying this criterion, the filter must not craze under impact of radiation from high-power lasers. The choice of a value of optical density will depend upon a selection of a safe dosage of radiation for eye exposure. Unfortunately, there is not general agreement on where this level should be set.[5,6] To select as this level the minimal radiation dosage that just produces a retinal lesion—lowered by an appropriate safety factor—would seem a reasonable choice. However, the wide variance in the absorption properties of the retinas of different individuals, the incomplete understanding of the effects induced by an apparent breakdown of reciprocity, lack of a determination of any possible chronic effects arising from long-term, repeated low-dosage exposures, and insufficient data to cover the complete species of lasers make it difficult to establish such a level. An upper level of 0.5 mW/cm^2 incident on the eye is suggested for continuous wave emission. For pulsed operation—durations of milliseconds and shorter—the same level is suggested, but the level now refers to peak power per square centimeter.

The second aspect of the program of eye protection can be formulated in accordance with some of the following general guidelines:

1) Never view an insufficiently attenuated laser beam or its specular reflection.
2) Wear *appropriate* protective goggles.
3) Keep laser apparatus completely enclosed whenever possible.
4) Keep specular reflectors out of the path of the laser beam.
5) Never leave an operating laser unattended.
6) Avoid work environments with low ambient room illumination.
7) Post signs alerting others to the presence of laser radiation.
8) Use count down techniques when firing high-power pulsed neodymium lasers so that room occupants may look away from the direction of the beam.

Although not much attention has been directed toward the hazards associated with semiconductor lasers, such as gallium arsenide, gallium arsenide-phosphide, and indium antimonide, some preliminary observations suggest that the intense 8,400-Angstrom emission from gallium arsenide produces excitation of the eye.[14,15] It is recommended, therefore, that these laser beams not be viewed with the unaided eye. Image converters can be used to make observations on these lasers. The focused image of the junction of a semiconductor laser has produced charring of paint, hence extreme caution should be exercised when working with optical systems that produce a sharply focused image of the laser junction.[16] Experiments that produce lasing in semiconductors by electron bombardment can also produce X-ray intensities in excess of the maximal permissible dosage. Adequate shielding must be provided for these setups, and X-ray warning signs posted.

High-energy neodymium and ruby lasers with exit energies in excess of a few joules have produced superficial burns on human skin.[17] Investigation of the effects of repeated laser exposures of varying dosages is just now being started, and although the studies are far from complete, preliminary findings indicate that the avoidance of exposure of the skin to any pulsed laser radiation is not too extreme a precaution. It is noted that the susceptibility of the skin to damage increases with increases in its pigmentation.

The interaction of high intensity laser radiation with matter is very often accompanied by the generation of pressure waves in solids, photohydraulic effects in liquids—both of which may result in formation of plumes and sprays—and dielectric breakdown.[18,19] Shattering of the material or rupture of the containing vessel can occur in the presence of the first two effects, and arcing of high voltage terminals as well as disruptive gas breakdown in instances of the third.

A program of safety that takes into account the laser safety considerations just discussed as well as the more detailed ones treated in the references should provide adequate safeguards against the potential hazards of the laser.

BIBLIOGRAPHY

1. M. M. Zaret, "Analysis of Factors of Laser Radiation Producing Retinal Damage," *Proc. of the 1st Annual Conf. on Biological Effects of Laser Radiation;* The Federal Proc., Vol. 24, No. 1, Part III, Supplement No. 4, Jan.-Feb. 1965, pg. S-62.
2. H. W. Straub, "Use of Protective Goggles in Areas of Laser Radiation," *Proc. of the 1st Ann. Conf. on Biological Effects of Laser Radiation;* Op. Cit., pg. S-78.
3. H. W. Straub, "Protection of the Human Eye from Laser Radiation," *Annals of the N.Y. Academy of Science;* Vol. 122, Art. 2, pg. 773, May 28, 1965.
4. "Harmful Effects of Laser Irradiation," *Electronics,* Vol. 38, March 22, 1965, pg. 128.
5. C. H. Swope and C. J. Koester, "Eye Protection Against Lasers," *Applied Optics,* Vol. 5, pg. 523, May 1965.
6. J. C. Kaufman, "Protect Your Sight from Laser Light," *Microwaves,* April 1966, pg. 38.
7. M. M. Zaret, "Safeguarding Lasers," *National Safety News,* Feb. 1965, pg. 23.
8. *Investigating Laser Eye Protection,* Hazards Control Quarterly Report, UCRL 7571, pg. 24.
9. *Eye Protection Criteria for Laser Radiation,* Hazards Control Quarterly Report, UCRL 7811, Jan.-March 1964, pg. 14.
10. *Comment on Eye Protection Criteria for Laser Radiation,* Hazards Control Quarterly Report, UCRL 12004, pg. 37.
11. A. Kohtiao, et al., "Hazards and Physiological Effects of Laser Radiation," *Annals of the N.Y. Academy of Science,* Op. Cit., pg. 77.
12. D. A. Patrician, *Safety Precautions—Lasers,* (a company rules paper), RCA, 2-2, Camden, N.J.
13. J. J. McCormick, "A List of Visible Laser Wavelengths," *Private Communication,* Jan. 12, 1965, RCA Laboratories.
14. R. J. Keyes and T. M. Quist, "Recombination Radiation Emitted by Gallium Arsenide," *Quantum Electronics III,* Columbia University Press, Vol. II, 1964, pg. 1825.
15. Y. Nannichi, "On the Visibility of 8,400-Angstrom Light from GaAs Laser Diodes," *Japan Journal of Applied Physics,* Vol. 4, 1965, pg. 308.
16. R. L. Bloom, *Quantum Electronics III,* Op. Cit., 1878.
17. L. Goldman, "Comparison of the Biomedical Effects of the Exposure of Human Tissue to Low and High Energy Lasers," *Annals of the N.Y. Academy of Science,* Op. Cit., pg. 802.
18. J. F. Ready, "Development of Plume of Material Vaporized by Giant-Pulse Laser," *Applied Physics Letters,* Vol. 3, No. 1, July 1963, pg. 11.
19. J. F. Ready, "Effects of Laser Radiation," *Industrial Research,* Vol. 7, Aug. 1965, pg. 44.

DRILLING OF MICROSCOPIC HOLES IN METALS BY LASER BEAM

This paper investigates the feasibility of drilling microscopic holes in metal by using a beam of light from a laser. A series of experiments on different materials that can be so ablated determined the energy and power required to remove a given volume of target material. The character of the resulting hole was studied, including shape, precision of location, and the repeatability of shapes.

B. R. CLAY
Aerospace Systems Division
Burlington, Mass.

THE high-intensity radiation from lasers can be utilized to ablate structural material and produce holes or cavities. It is possible to drill holes smaller than 0.001 inch in diameter in metal as hard as tungsten with precision and without injurious heating of the metal. This technique of drilling should be particularly useful in fabricating extremely compact micro-energy memory units for computers, electron-gun apertures, high-resolution optical targets, and micro-diffusion orifices.

DESCRIPTION OF LASER EQUIPMENT

Source

The laser chosen for the experiments was a small ruby rod 0.2 inch in diameter and 2.5 inches long.[1] Ruby was selected for its ease of use. Its output wavelength is in the visible region of the spectrum (6,943 angstroms) and its output energy is high relative to other materials.

The ruby was clad in sapphire (0.4-inch outside diameter) and was pumped by an FX-42 lamp with pulses 400 μs in duration. The elliptical cavity was 2 inches in diameter and 3 inches long with ½-inch interfocal separation. A 17-inch long interferometer configuration was terminated by a 50% reflector on the output end and by a 99.5% multilayer dielectric reflector directly deposited on the plane ruby face at the other end (see Fig. 1).

Final manuscript received July 12, 1966

Attenuators

Small holes are of interest, so the laser beam must be focused to a fine spot on the specimen resulting in high energy density on a small area. While high energy density is desirable for drilling holes through thick metals it is undesirable for thin metals and deposited film targets.

A method for adjusting incident energy was therefore essential. One method considered was the adjustment of laser output by variation of the input pump power. This method has limited application because the output from the ruby is still quite high at the threshold of oscillation (i.e., the least energy of excitation at which laser action can occur). Also, the range of output energies obtainable by variation of pump input energy is not great enough for the anticipated needs.

Another means considered for adjusting incident energy was the use of an attenuator. A problem arising from the use of commercially available precision attenuators is lack of durability. At laser energies, some transmission attenuators burn through with one or more exposures; others lose calibration with extended use. Iris diaphragms can suffer damage as their leaves become burned through or welded together. Liquid optical attenuators with an absorbing dye can be used, but they are subject to bleaching or non-linear action.

Neutral density filters, unless especially constructed for this application, might be completely destroyed by the blast from a single shot. Optical filters in general become non-linear at extreme values of incident energy. This non-linear effect has been found useful in saturable absorber Q-switch applications but was avoided in this case.[2]

A good absorber for high intensity ruby emission was found to be an aqueous solution of cupric sulfate. Four liquid cell absorbers using this material were fabricated and tested. The cells were found to be linear over the range of intensities to be used in this series of experiments. They were calibrated at lower light levels using a spectrometer and then checked at the high end of the range with a laser as the source.

The low range accuracy was estimated to be ±0.5% and the high range accuracy to be ±1.5%. The filter transmission percentages are:

Cell 1:	4.5%	Cell 3:	13.0%
Cell 2:	5.2%	Cell 4:	7.4%

Additional attenuation was obtained by use of geometric redistribution of the laser beam cross section. By the arrangement of lenses shown in Fig. 1, the direct output was expanded and recollimated. The beam expander entrance pupil was 5 mm and the beam expanded objective focal length was 32 mm. The beam expanded secondary lens had a focal length of 182 mm. The exit pupil diameter D_E is given by:

$$D_E = \frac{l_2}{l_1} D_o$$

where l_1 is the focal length of the first lens, l_2 is the focal length of the second lens of the beam expander, and D_o is the diameter of the entrance pupil; D_E is seen to be 5.7 times that of the entrance pupil. The energy density ratio is the square of the entrance to exit pupil diameter ratio or 32.5. By adjusting the lenses so as to be confocal, the emergent radiation was made parallel.

The expanded beam was reduced further in intensity by combinations of the four liquid-cell absorbers.

Aperture

To obtain fine continuous adjustment of the beam intensity, an aperture adjust-

BURTON R. CLAY received his BS in Physics from the Indiana University in 1949. He joined RCA's Color Television Development Section in Camden in 1950. His activities there included circuit design and optical instrument development. Also he studied the effect of magnetic environments on color TV receivers and developed corrective devices. In 1959, he joined the Data Processing Section to participate in the development of peripheral equipment for industrial control computer systems and a fiber-optics analog-to-digital converter for computer input use. Mr. Clay transferred to the Aerospace Systems Division in 1961 to work on laser electro-optical and electronic design problems. He investigated mode-selection methods and laser coupling means, and made major contributions to the design of moderate and high power Q-spoiled ruby lasers for ranging applications. He provided the mechanical-optical design and integration for the receiving system of a high power, high resolution laser radar and served as optical adviser and consultant for several programs. Mr. Clay is a Senior Member of the IEEE; he holds twelve U.S. patents.

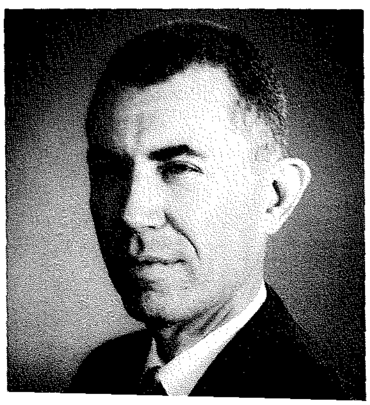

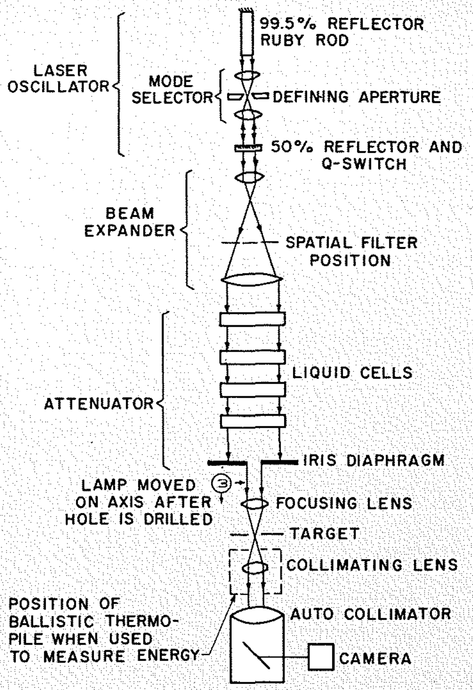

Fig. 1—Optical arrangement for hole drilling.

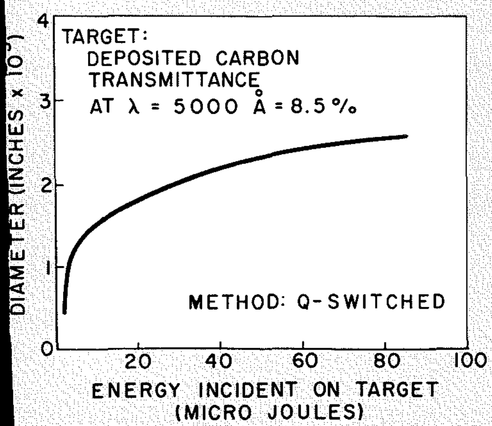

Fig. 2—Diameter as function of energy.

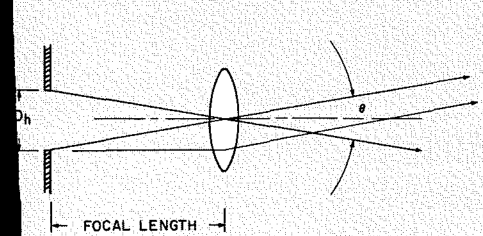

Fig. 3—Hole diameter measurement arrangement.

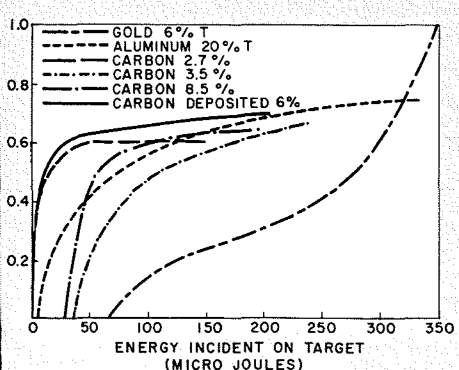

Fig. 4—The effect of statically fired pulses on various target materials.

ment was used. An iris diaphragm was placed in the expanded beam. Its effective open-to-closed area ratio was approximately 20:1. This diaphragm was protected by the liquid cells and by the beam expanded as a safeguard against accidental welding or burn-through of the iris leaves.

By using the liquid filters in combination, a transmission ratio of 2×10^{-5} was possible. The iris diaphragm extended this range by a factor of 20 so that the full range after beam expansion was about one million to one.

MEASUREMENT OF ABLATED VOLUME

To relate the incident energy to the volume of material removed by a laser blast, a suitable means of determining volume had to be found. This could be done by weighing the target before and after the shot and computing the volume, or by measuring the hole diameter and depth. The latter method was adopted for convenience.

A great simplification could be realized if the hole were made circular and the target thin. If the target were very thin, the hole could be assumed to be the same diameter throughout and no correction for a tapered or complex shape need be made. This configuration was implemented by using vacuum-deposited thin films on glass substrates. Various metals and carbon were deposited on glass slides to a thickness which gave a few percent optical transmission at $\lambda = 550$ angstroms. Each slide had a unique transmission and was thus identifiable. The transmission was also a rough check on the film thickness. Actual thickness measurements were made by interferometry. Fig. 2 shows the relationship of energy to hole size.

The hole diameters were measured by the collimator arrangement shown in Fig. 3, using a microscope objective lens with accurately known focal length. The ablated hole was located in the principal focal plane of the objective. The angular diameter θ of the hole was read in the collimating lens which resolved better than 0.5 second of arc.

As in Fig. 3, the hole diameter D_h was related to the angular diameter by $D_h = f\theta$, where f was the focal length of the lens and θ was read in the auto collimator directly and photographed by an attachable Polaroid camera. Deviations from circularity were thus recorded. Diameters of ablated areas were determined by *1)* direct measurement of circular holes or *2)* by calculation of equivalent diameters of irregular areas measured by a planimeter. The results of these computations are shown in Figs. 4 and 5.

As the energy was increased beyond that required to ablate a hole of given size, the radiation first ablated the hole and the remainder passed through the hole. The duration of the laser pulse had an effect on the energy vs hole area relationship and upon the physical nature of the hole.

When the laser was *Q*-switched, its pulse was of much shorter duration than when it was statically fired (see Figs. 6a and 6b). The peak power for a given energy output is inversely proportional to the pulse duration. The *Q*-switched single pulse was approximately 40×10^{-9} second long and the conventionally or statically fired pulse was approximately 200×10^{-6} second long, a time ratio of about one to 5,000. For the same energy then, the power is 5,000 times greater with the *Q*-switched pulse. The effect of a static pulse on target is shown in Figs. 7a and 7b to be one of central penetra-

Fig. 5—The effect of Q-switched pulse on various target materials.

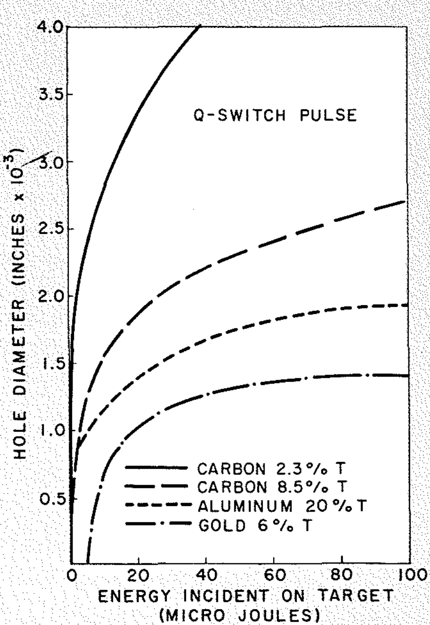

Fig. 6—Waveforms of laser pulses.

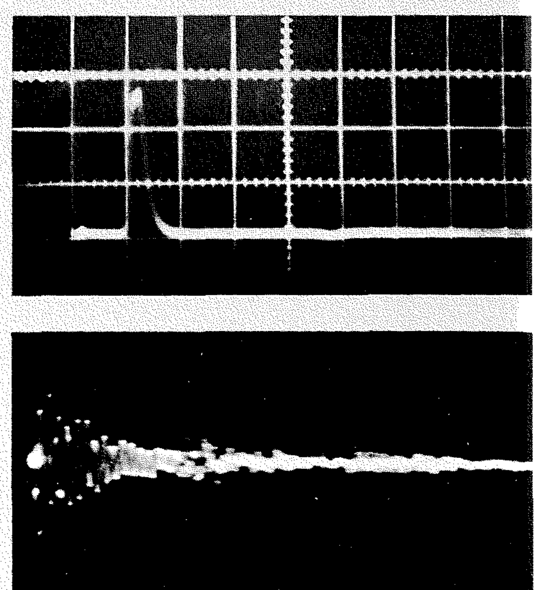

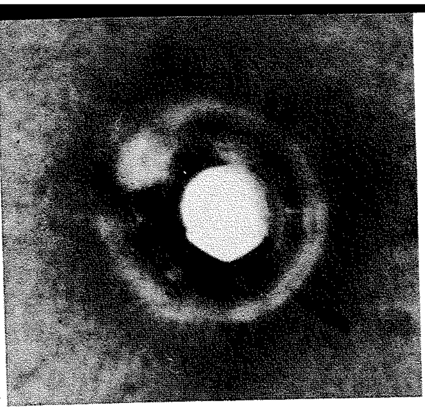

a

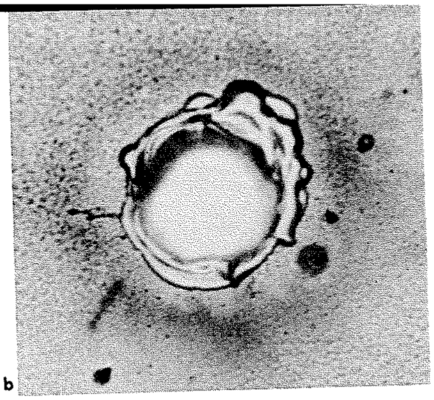

b

Fig. 7—Example of laser drilling in nickel. a) Hole of 0.0005-inch diameter produced by non Q-switched laser in 0.003-inch thick nickel. Microscope is focussed at upper surface in order to determine shape of entrance hole and crater. Hole photographed with microscope using illumination from above and below specimen simultaneously, and b) Same as a) above except microscope focussed on lower surface of 0.003-inch thick nickel in order to determine shape of exit hole. (Upper and lower illumination).

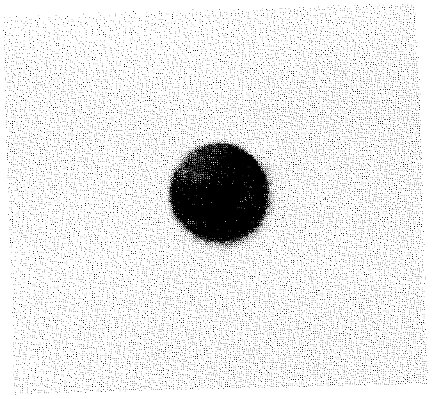

Fig. 8—Hole of 0.0005-inch diameter produced in 0.003-inch thick nickel by Q-switched laser. Note the circular shape and absence of crater. (Illumination from above.)

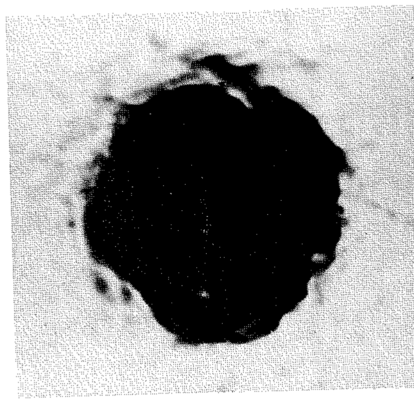

Fig. 10—Hole of 0.002-inch diameter mechanically drilled in 0.002-inch thick nickel. (Microscope illuminated from above.)

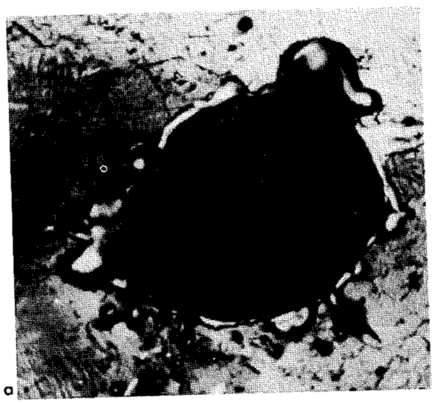

a

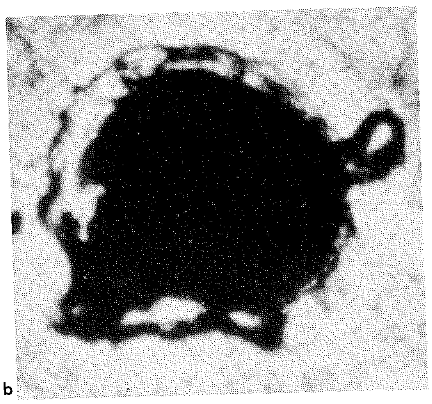

b

Fig. 9—Example of laser drilling in nickel. a) Hole of 0.002-inch diameter produced by non-Q-switched laser in 0.002-inch thick nickel, upper illumination. (Pulse 50% larger than used for Fig. 6b); and b) Hole of 0.002-inch diameter produced by non-Q-switched laser in 0.002-inch thick nickel, upper illumination. (Pulse 50% shorter than used for Fig. 6b).

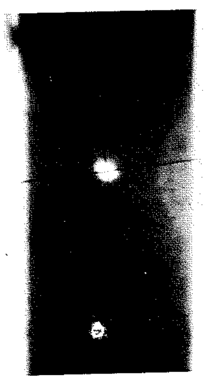

Fig. 11—Hole of 0.00048-inch diameter drilled in human hair of 0.0042-inch diameter. This was made with a non-Q-switched laser. The accuracy in hole location is seen by noting that the collimator cross hairs were placed at the coordinates of the desired hole center. The laser was then fired and the hole was found to be well centered at the cross hair intersection.

tion leaving a molten crater edge (which quickly solidifies). However, when the shorter Q-switched pulse is used, the higher power causes a blasting effect and penetration is not accompanied by a crater nor any structural evidence of heating around the edge of the hole (see Fig. 8). This latter effect was observed on thicker targets while the former was observed on both the thin-film targets as well as on the thicker ones. The effect of pulse length on size is shown in Figs. 9a and 9b. For comparison, a hole drilled mechanically is shown in Fig. 10.

Some materials such as mu-metal and certain ferrites are altered structurally and magnetically by drilling with conventional drills or with electron beam boring devices. This unfortunate consequence of state-of-the-art drilling methods limits the application of these materials to magnetic cores for memories and transducers. A Q-switched laser, however, offers promise of drilling holes without disturbing the magnetic properties of the material.

DETERMINATION OF DRILLING ACCURACY

To designate a location for a hole and to pre-define its diameter, solutions to the following problems had to be developed:

1) the shape of the hole was not perfectly round in every case.
2) the shape of the hole was not repeatable in successive shots even when attempting to hold all parameters constant.

These problems were found to be caused by the changing distribution of energy in the cross section of the laser beam. Off-axis modes were developing which were different between successive shots. This effect was overcome by devising a mode selector as shown in Fig. 1.

The lens has at its focus an opaque disk with a small hole in its center; another lens, confocal with the first, also contains the small hole at its focus. The radiation from the laser is approximately parallel entering the selector and more nearly parallel leaving it. This device is inserted inside the oscillator cavity, i.e., the Fabry-Perot interferometer.

If an off-axis mode begins to build up within the oscillator, its rays will not come to focus at the center of the mode selector defining aperture. They will be focused at a point near or at the edge of the hole. The light thus obstructed will be attenuated and so oscillations are prevented from building up along this path. That path with the greatest gain will be along the optical axis which contains the center of the mode selector aperture. Oscillations tend to build up to their final strength along the optic axis, encouraging the pure axial mode in the ruby.

The tendency to burn the edges of the defining aperture is minimized because the off-axis modes which can damage the aperture do not build up sufficiently in the system.

The defining aperture and its associated lenses were chosen to provide a beam of smaller angular divergence than that formed by the focusing lens (Fig. 1) and the unmasked hole diameter. When this condition was met, the holes were circular, and the holes were repeatable in diameter for given input conditions. An example of the accuracy obtainable is seen in Fig. 11—note that the hole is accurately centered in a human hair.

If the defining aperture in the mode selector is not circular, then, of course, the hole made in the target will not be circular. Square holes and long narrow slits have been ablated in sheet metal by placing appropriate masks in the system.

The shape of the defining mask is related to that of the hole by several factors:

1) The placement of the mask in the system.
2) The distribution of gain (hot filaments) in the ruby (ruby optical quality and pump configuration contribute).
3) The accuracy of system alignment.

A more convenient placement for the mask was found to be after, rather than within, the selector. The convenience in using a larger mask or spatial filter area is that the energy density is less than enough to destroy the mask. The spatial filter shape however is the approximate Fourier transform of the energy distribution desired in the target plane, and bears little resemblance to the hole shape desired.

In practice a determination of the mutual intensity function for quasimonochromatic coherent light falling on a transparent object (the desired hole) is made.[3] A transparency is made from this set of determinations which has a pattern of areas of varying density. This plate may be made by hand if the values are known or it may be made photographically by Gabor's technique.[4]

If the mask were placed at the defining aperture position, its shape would be that of the desired hole in the target.

The coordinates of the hole center can be predetermined to an accuracy of ±0.0001 inch by using a precision micromanipulator to translate the target. The laser beam output direction—in a well-aligned oscillator cavity with an appropriate mode selector—has an uncertainty of about this amount. Thus, excellent accuracy and repeatability are obtained.

DRILLING OF THICK METAL TARGETS

Targets of various thickness were drilled both by the static and Q-switched methods. The metal used was 301 stainless steel in thicknesses from 0.002 to 0.010 inch. The results are plotted in Fig. 12. A factor contributing to the non-linearity of the curve is that the hole is slightly tapered and the incremental volume per unit length of penetration decreases with depth (see Fig. 13). Another factor is that for deeper penetration, the beam evidently passes through a cloud of metal vapor and particles produced as penetration progresses. This may scatter and absorb some photons.

Refractory metals such as tungsten, molybdenum, and platinum were drilled, and, as might be expected, required more energy from static firing than less dense materials of the same thickness.

A striking effect, however, is the relative independence of material density or other characteristics on energy when the Q-switched pulse is used. Aluminum (3-mil thickness) required approximately the same energy to ablate a 1-mil diameter hole as did tungsten.

VALIDITY OF DATA

The measurements were taken indirectly, as follows:

1) The laser was fired with a given voltage applied to the capacitor bank and the energy measured with a T.R.G. *Laserater* (a ballistic thermopile).
2) The target was then inserted in the path and the laser was fired again. Care was taken to avoid variations in any parameter, especially the voltage applied to the capacitor bank. The target hole was measured and recorded.
3) Without any changes except target removal, the laser was fired again into the thermopile for energy measurement.

The energy measurement after drilling was compared to the one before drilling and, if any difference was detected, the data was discarded and a new series begun. The assumption made in these experiments was that the energy incident on the target while drilling was the same as that before and after drilling. The estimated errors were as follows:

1) The voltage applied to the capacitor bank determined the electrical energy applied to the pump. The energy U is given by $U = \frac{1}{2} CE^2$, where U is in joules, C is in farads and E is in volts. An error in E is serious since the E term is squared. This voltage was read to an estimated ± 3%. To eliminate hysteresis the voltage was brought up slowly and stopped, always approaching the reading from the same direction. Flash lamp aging was also detected by this means. Sufficient time for thermal equilibrium was allowed between shots.
2) The capacity was known to ± 10%.
3) The thermopile was estimated to be ± 10% accurate.
4) The microvoltmeter was estimated to be ± 2% (reading the thermopile).
5) The combined optical errors in reading diameter were better than ± 2%.
6) The errors in reading the thickness of the metal targets were approximately ± 0.0002 inch.

CONCLUSIONS

The energy versus hole diameter data were plotted for vacuum-deposited thin films and for various thicknesses of stainless steel. Refractory metals such as tungsten, molybdenum, and platinum were also drilled by a laser beam. The energy required for a 0.001-inch-diameter hole in a given thickness of metal, using the Q-switched beam, was relatively independent of material. When a conventional long pulse (not Q-switched) beam was used, energy dependence on material was observed. A Q-switched beam produced a clean craterless hole while a beam of longer pulse duration produced a hole with irregular sides caused by the freezing of molten metal.

Repeatability of hole location and diameter was very good.

BIBLIOGRAPHY

1. By Optical Coating Laboratory, Inc., Santa Rosa, Calif.
2. W. F. Kosonocky, *Saturable Absorber Experiments,* RCA Laboratories interim report, USAF Contract No. AF30(602)-3169, pp. 16-20.
3. *Principles of Optics,* Born & Wolf, MacMillan Company, 1959, pp. 508-522.
4. D. Gabor, *Nature,* No. 161 (1948), cit. ref. Born & Wolf, pp. 453-458.

Fig. 12—Series of holes caused by statically fired lasers in stainless steel.

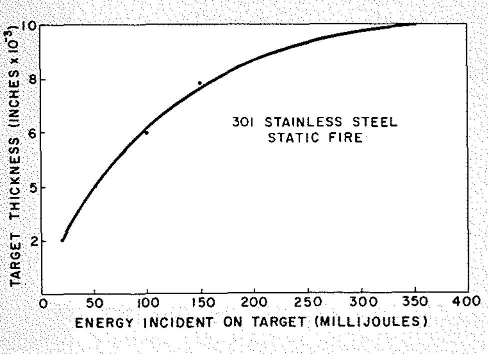

Fig. 13—Section of 0.001-inch diameter hole in 0.010-inch thick stainless steel. Non-Q-switched laser.

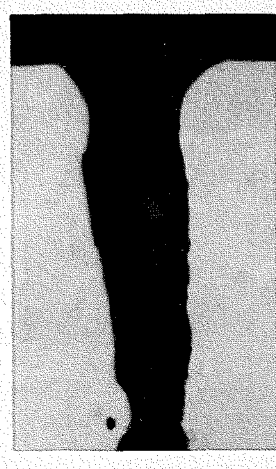

METEOROLOGICAL LASER PROBING FROM SATELLITES

Potentially, lasers are useful for remote probing of the atmosphere for meteorological purposes because of the very high power per unit bandwidth available and because of the light scattering properties of the atmosphere itself. Giant pulsed laser systems, some of which have been discussed in this issue, are available with powers of 10^9 watts in a 20-ns to 40-ns pulse, beam half-angles of a few milliradians, and bandwidths of a few angstroms. These laser characteristics, in conjunction with the light scattering properties of the atmosphere, provide a basis for remote measurement of pressure, temperature, and humidity. Initially, a simple system is envisioned. It employs a q-spoiled ruby laser system for a transmitter. The receiver consists of a mirror ($\cong 1$ m^2) in conjunction with a multiplier phototube and implemented with optical filters for appropriate frequency discrimination. Ranging is easily achieved because of the pulsed nature of the transmitter. Time gating of the multipler phototube sets resolution volume.

J. A. COONEY
Astro-Electronics Division
Princeton, N. J.

According to a theory established by Lord Rayleigh, visible light is scattered by the gaseous constituents of the atmosphere. The blue of the sky and the redness of sunsets are accounted for in Rayleigh's theory. Originally, the color of the sky was attributed to particles suspended in air. This view appears to have originated with Leonardo da Vinci. In 1873, J. C. Maxwell concluded from Lord Rayleigh's work that the air molecules themselves were the scattering particles. In 1899, Lord Rayleigh revived these ideas and formed the scattering theory which bears his name.

In 1923, Smekal, using primitive quantum considerations, discussed the effect of a light quantum of any frequency on atomic transitions, conserving the energy by means of light quanta.[1] Stimulated by Smekal's work, Kramers and Heisenberg derived, first, the classical wave theory and, then, the quantum theoretical scattering formula. The latter investigation is far more important than the particular problem dealt with, since it provided considerable impetus to modern quantum theory. For this paper, however, the work is important in that it stimulated the experimental studies of Raman and his coworkers, resulting in the verification of the presence of scattered radiation at a frequency different from the incident frequency (the so-called Raman effect). Raman scatter is significant in that it may allow unambiguous measurement of density and temperature with significant aerosol concentrations present.

Final manuscript received August 3, 1966

Da Vinci was not entirely wrong; actually, a significant fraction of the light scattered at altitudes of meteorological interest is due to scattering from the particles in the amosphere (i.e., scatter from aerosols and condensation nuclei). The fundamental analysis of this scattering process was done by G. Mie and is often referred to as Mie scattering.

These three basic scattering processes —Rayleigh, Raman, and Mie—are the physical processes of interest herein.

RAYLEIGH SCATTER

Essentially, this theory treats the gaseous molecules of the air as simple dipoles. By interaction with the dipole moment of the molecule, the incoming electromagnetic wave is scattered in space according to a dipole pattern. The analogy between this theory and the longer electromagnetic-wave and dipole-antenna theory is strong except that the wavelength is very much larger than the effective dipole length ($\cong 10^4$).

According to Rayleigh's theory, the scattering intensity increases as the fourth power of the frequency; therefore, an increase of a factor of two in frequency causes an increase in the scattering intensity by a factor of 16. Assuming a plane wave of initial intensity I_o, the variation of intensity with distance traversed is given as:

$$I = I_o \exp(\xi_R h)$$

where h is the distance traversed and ξ_R is linear extinction coefficient due to Rayleigh scattering. The formula for ξ_R, in terms of the optical refractive index of the medium traversed, is:

$$\xi_R = \frac{8\pi^3(\eta^2 - 1)^2}{3N\lambda^4}$$

where η is the optical refractive index; λ is the wavelength of the light; and N is the number of molecules in a unit volume.

Fig. 1—Vibrational-rotational energy level scheme.

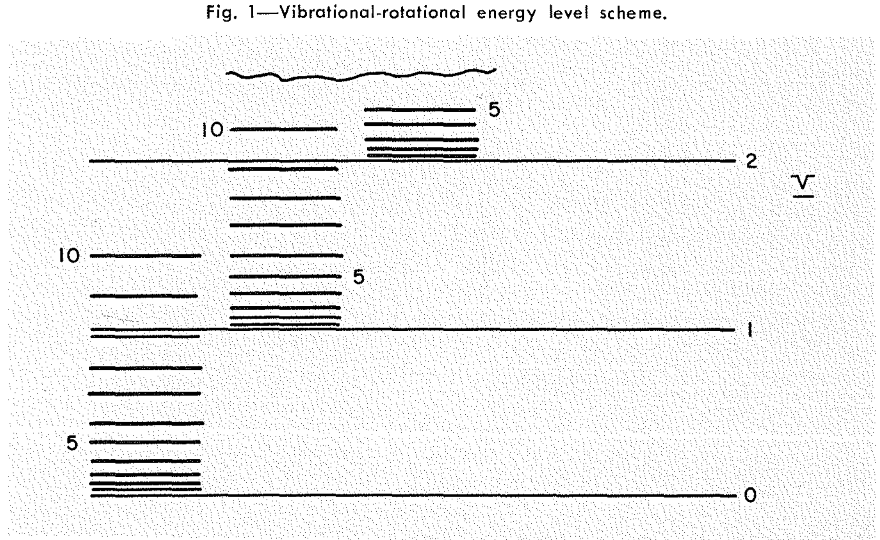

J. COONEY received a BS and MS in Physics from Fordham University in 1949 and 1950, respectively. He is presently engaged in writing a thesis for a PhD in Physics at New York University. Upon graduation in 1950, Mr. Cooney joined M. W. Kellogg Co. where he was engaged in heat transfer and flow design calculations in connection with high thrust rocket engines. In 1952, he transferred to Vitro Laboratories where he worked on systems analysis for both radar and sonar systems. In 1954, he joined the Sperry Gyroscope Co. to work in microwave tube development. In 1956, he became a member of the teaching staff at St. John's University. In 1959, he rejoined Vitro Laboratories to do work in arc and plasma physics. At Vitro, as Group Leader of the arc group, he worked on the effects on arc operation of transpiring fluid through the electrode face. This program resulted in techniques which considerably reduced the erosion of electrodes. In addition, work was performed on the development of a plasma accelerator employing a magnetic field gradient. In 1961, he joined the RCA Astro-Electronics Division and worked with RF gradient field plasma accelerators. The project converted the then existing, pulsed accelerator to continuous operation. More recently he has been engaged in the study of effects of intense magnetic fields on the acceleration and confinement of plasmas. The work dealing with confinement has resulted in a generalization of the transport coefficients of plasmas transverse to magnetic fields. Recently he has been concerned with laser scattering space applications and atmospheric scattering work. He is a member of both the American Physical Society and the American Institute of Aeronautics and Astronautics and has authored a number of publications in the field of plasma physics.

The linear extinction coefficient ξ_R can also be expressed in terms of atomic properties:

$$\xi_R = \frac{8\pi^3 N\alpha^2}{3\varepsilon_o^2\lambda^4}$$

where α is the atomic polarizability and ε_o is the dielectric constant of free space. This latter form of the linear extinction coefficient more clearly expresses the dependence of the scattering phenomenon on the number density of scattering centers.

AEROSOL SCATTER

One might expect to be able to monitor the Rayleigh return as a measure of gas density. However, recent measurements of nonresonant scatter, involving laser probing of the atmosphere above 10 km, have been made with ground-based lasers; back-scattered returns larger than the anticipated Rayleigh signal were encountered.[2,3] These returns were attributed to a high aerosol background. (As indicated above, the particulate materials suspended in the atmosphere are effective in scattering radiation.) Moreover, it is well known that in the lowest portions of the atmosphere the effective aerosol cross-sections can greatly exceed the non-resonant Rayleigh cross-sections. Thus, remotely probing the atmosphere with lasers using Rayleigh interaction at a nonresonant frequency to obtain meteorological information such as density profiles present significant problems. According to Elterman's tables, the extinction due to aerosols exceeds that due to gaseous scatter by a factor of 5 at sea level for 0.4 micrometers, and by a factor of 34 for 0.7 micrometers.[4] The Rayleigh and aerosol extinction coefficients are listed as a function of altitude in Table I.

In a classic work, Gerhard Mie solved the problem of the diffraction of a plane wave by a conducting sphere in a quite general manner. Unfortunately,[5] these solutions are very complicated and are not susceptible to simple approximations in the range of parameters of meteorological interest. Thus, the light scattering studies of the real atmosphere (e.g., solar-radiative energy balances) are burdened with an extremely cumbersome theory. One offshoot of this difficulty is that a class of "computer experiments" has arisen in an attempt to find numerical shortcuts. Slowly, the study of this problem of aerosol scattering is yielding results; however, in measurement problems it promises to remain a "thorn in the side" to those interested in the light scattering properties of this atmosphere.

RAMAN SCATTER

Presumably, the aerosol scatter on hazy days is considerably larger than that given in Table I. Thus the aerosol scatter will almost always obscure the Rayleigh scatter; however, about 0.1% to 4% of the Rayleigh scatter is frequency-shifted by the Raman effect mentioned above. This effect is due primarily to the interaction of the photons with the vibrational and rotational levels of the atmospheric molecules. As a result, the molecule undergoes a change of state and the scattered photon is frequency shifted.

In principle, the molecular changes of state may be either electronic, vibrational, or rotational. In practice, most Raman spectra are either vibrational, rotational, or some combination of both. To cite a simple and useful example, the frequency-displaced scattered radiation from an O_2 molecule will undergo a Raman shift of 1,555 cm^{-1} corresponding to a change from the $V=0$ to $V=1$ vibrational state. This is a somewhat broadened line ($\cong$ 100 angstroms at room temperature) and under high resolution exhibits a rotational fine structure with lines a few angstroms apart. At an exciting line of 5,000 angstroms, the Stokes component of the vibrational Raman line would appear at 5,421.5 angstroms. Since this is greater than a 400-angstrom shift, filtering of the exciting line is a minor problem. To see most of the details of the rotational fine structure, a resolution of 1.5 angstroms would be required. The simplified energy-level diagram is shown in Fig. 1 and a repre-

Fig. 2—Resolved rotational spectrum of O_2.

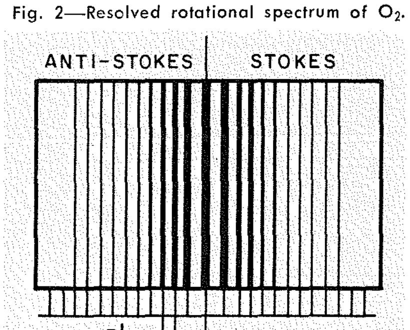

TABLE I—Comparison of the Linear Extinction Coefficients Arising From Rayleigh and Aerosol Scattering (Visibility to 20 km)

h(km)	Rayleigh Attenuation Coefficient (km^{-1})	Aerosol Attenuation Coefficient (km^{-1})
0	4.3×10^{-2}	2.0×10^{-1}
1	3.9×10^{-2}	0.9×10^{-1}
2	3.5×10^{-2}	3.8×10^{-2}
3	3.1×10^{-2}	1.6×10^{-2}
4	2.8×10^{-2}	7.2×10^{-3}
5	2.5×10^{-2}	3.2×10^{-3}
10	1.4×10^{-2}	2.6×10^{-5}
15	6.8×10^{-3}	4.2×10^{-5}
20	3.1×10^{-3}	9.0×10^{-5}
30	6.5×10^{-4}	2.0×10^{-5}

Note: $\lambda = 0.4$

Fig. 3—Satellite geometry.

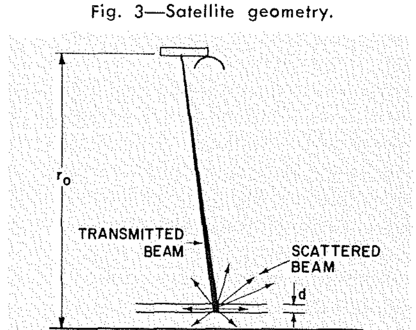

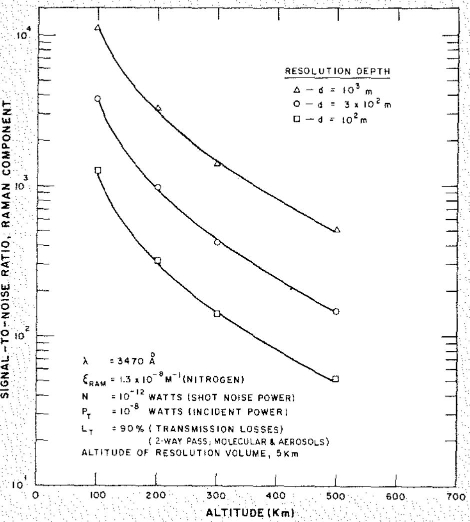

Fig. 4—Signal-to-noise ratio of Raman return as a function of altitude.

sentation of the O_2 Raman rotational spectrum is shown in Fig. 2.

To establish a somewhat better feeling as to the possibilities outlined in the above discussion, a few examples are given in Figs. 3 and 4. Along with an illustration of satellite geometry, the signal-to-noise for a Raman return is shown as a function of satellite altitude for various resolution volumes located at the 5-km altitude level. The measurement is a photon counting process, and a collector area of 1 m^2 is assumed. For a satellite altitude of 300 km and a resolution depth of 300 m, the Raman return is approximately 10^{-9} watts. In terms of the shot noise, one has a signal-to-noise ratio of $\cong$ 400. For the same signal-to-noise ratio at 25 km, a 5-km resolution depth is required. Resolution volumes should be made large enough to insure suitable averaging of the meteorological variables being measured. In these calculations, transmission losses are assumed. This is probably not accurate enough and so they may have to be measured. As can be seen by reference to available literature, this illustration uses numbers slightly beyond the present state of the art.

SYSTEM CONFIGURATION

Much laser research and development bears a strong resemblance to early microwave communications work, and so future laser systems (communication and otherwise) may well take on the sophistication of present day radar systems. However, to permit reference to present-day systems of measurement, consider a very simple system consisting of a laser transmitter and photomultiplier receiver. Basically, such a system would consist of a ruby rod mounted in a reflecting cavity. The lasing levels in the rod are light pumped by flash lamps mounted in a reflecting cavity. For the so-called Q-spoiled mode, it is possible to employ a device whose optical transparency is controllable. This is mounted in the light beam between the mirrors. The element remains essentially opaque until the rod has been fully pumped. By prearrangement the Q-spoiling device is made transparent, allowing a highly collimated burst of radiation to flow through the end mirror which has been made reasonably transparent.

As indicated above, the receiver consists simply of a large light-collecting mirror, preferably parabolic, with a photomultiplier positioned at the focus. Frequency discrimination (e.g., filters) is required at the photomultiplier input for Raman measurements.

MEASUREMENT PROBLEMS

In any practical system the measurement error is important. Thus, it is of interest to consider some sources of error which will exist for almost any measurement system. Aside from the usual systematic errors which may not necessarily be easily overcome and which will not be fully determinable until working systems are built, there are certain sources of error which are pretty much inherent in the concept and about which some preliminary statements can be made.

An important consideration in dealing with low-level signals is the error due to the statistical nature of the photoelectronic process. For example, the average fractional deviation, because Poisson statistics are involved, is proportional to the reciprocal of the square root of the average number of electrons coming from the photocathode. To obtain an average deviation of 1%, some 10^4 photoelectrons are required, and for a quantum efficiency of 0.3, approximately 3×10^4 photons are necessary at the receiver. Therefore, at present power levels, resolution depths at the lower altitudes in the nonresonant scatter mode must be approximately 1 km.

Although aerosol scattering from the resolution volume is irrelevent when monitoring Raman scatter, it is of interest because of transmission losses. Only on very clear days is it possible to ignore the effects for vertical probing, and then probably only above 10 km. Most upper-atmospheric probing measurements to date suggest that only above 30 km can one safely ignore aerosol scatter most of the time. In actual measurements, the presence of aerosols should be made apparent by an anomolous change in scale height. Thus a radar-type A-scan return would have local maxima superimposed on the signal.

Because of the complexity of the scatter pattern from aerosols, an optimum technique for measuring extinction is far from obvious. There are certain general features of aerosol scatter, however, which bear examination. To begin with, laser output can be made highly linearly polarized. Aerosols will depolarize to a much greater extent than molecules. Hence, the orthogonal component of polarization provides an index of the extent of aerosol scatter. In addition, with a laser mounted on a satellite a total atmospheric extinction coefficient measurement can be made by bouncing a signal from the earth's surface; this measurement will be somewhat uncertain, primarily because of the lack of knowledge of the surface reflection coefficient. If surface reflection were known, this along with the knowledge of differential backscatter could provide a further index, as long as the magnitude of the distribution does not change significantly with altitude.

To get some idea of the extent of the problem, consider the following equation:

$$\frac{\Delta P_r}{P_{T_h}} = \frac{1}{4\pi r_h^2} \int_h^{h+h} dh' \int_{r_1}^{r^2} i\,(r, \phi, V, m)\; n(r,h')\, dr \qquad (1)$$

where $i\ (r, \phi, v, m)$ is the Mie intensity function; $n\ (r, h')$ is the number density of aerosols as a function of particle size and altitude; r is the particle radius; ϕ is the angle of scatter; v is the frequency of radiation; m is the particle refractive index; ΔP_r is the power scattered from altitude interval Δh; and P_{T_h} is the power transmitted to altitude h.

Fig. 5—Aerosol scatter parameters.

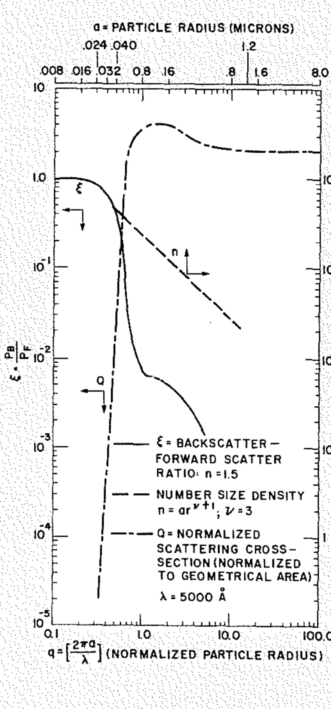

Eq. 1 shows the increment per unit time of energy scattered by aerosols. Fig. 5 presents a less mathematical but somewhat clearer idea of the nature of this problem. The curve labelled Q is measure of the total scattering efficiency normalized to geometrical area as a function of normalized particle radius, for a typical set of parameters. The curve labelled ξ shows how the backward ($\cong 180°$) to forward ($\cong 0°$) scatter ratio changes for a given abscissa. Lastly, the curve labelled n shows a particle-size distribution of aerosols, characteristic of the lower altitudes. These curves are merely representative of the atmospheric aerosols and all three curves undergo variations as a function of space and time.

The changes in values of the parameters, along with the actual fluctuations known to occur in number density, cause considerable difficulty in approximating quantitative values of total aerosol scatter. In addition, recent work[5] has brought out more clearly that natural particle distributions often occur in size groupings, contributing further to the complexity. Thus, direct assessment of the effects of aerosol scatter on transmissivity is not a simple matter. However, as the library of Mie coefficients increases to the point where the appropriate ranges of parameters as are found in the atmosphere are available, then backscatter at a number of frequencies could yield the differential aerosol scatter and give a precise measure of the transmission losses.

RESONANT SCATTER

For the upper atmosphere, and the much more highly rarefied constituents, resonance or quasi-resonance scattering is more appropriate. Molecular scattering is called resonant or non-resonant according to whether the transmitter frequency is near to, or far removed from, a resonant frequency of the molecule. It might be assumed that, if the laser frequency could be placed on a resonant line of one of the atmospheric molecules, the signal-to-noise ratio would increase due to the increased interaction cross-section. However, this is not entirely the case; the cross-section increases, giving rise to a significant increase in the backscatter from the region of interest, but the transmission path losses are also increasing. It is possible to make a quantitative estimate of an optimum cross-section.

One can assume that the atmospheric density is an exponential function of height, with regard to both the gaseous and particulate constituents. Then for satellite altitudes, an approximate expression for the ratio of transmitted to return power can be given as:

TABLE II—Optimum Cross-Sections for N_2 and O_3 Components as a Function of Altitude

$\gamma = 9.0$ km^{-1} (N_2)		$\gamma = 5.0$ km^{-1} (O_3)	
h(km)	α (m^2)	h(km)	(m^2)
0	1.78×10^{-24}	30	2.5×10^{-18}
1	1.96×10^{-24}	35	5.0×10^{-18}
2	2.14×10^{-24}	40	2.5×10^{-17}
3	2.37×10^{-24}		
5	3.0×10^{-24}		
10	5.3×10^{-24}		
20	29.5×10^{-24}		
50	265.0×10^{-24}		

Notes: γ = Number density reciprocal scale height

$n(r)$ = Number density at altitude being probed

$$\alpha = \frac{\gamma}{2n(r_o)}$$

$$\frac{P(r_o)}{P_o} = \exp\left(\frac{\alpha n_o}{\gamma}\exp\gamma r_o \frac{\beta n_o}{\delta}\exp(\delta r_o)\right. \quad (2)$$
$$\left.\frac{(CT)}{4\pi r_o^2}\left[\alpha n(r_o) + \beta N_o(r_o)\right]\right)$$

where: $P(r_o)$ is the power backscattered to the satellite from air volume at a distance r_o; P_o is the incident power; r_o is the satellite altitude; α is the Rayleigh cross-section; γ is the scale height of gas density; β is the effective aerosol cross-section; δ is the scale height of aerosol number density; n_o is the exponential gas density at satellite altitude; and N_o is the exponential aerosol density at satellite altitude.

Since, relatively speaking, appreciable interaction occurs only in the lower portions of the atmosphere, the specific assumption of the functional dependence of the gas and aerosol density with height in the upper altitudes is irrelevant, so long as it effectively indicates the absence of a measurable interaction at the upper altitudes.

It is possible to use Eq. 2 to estimate the magnitude of an optimum cross-section; Table II lists such cross-sections.

It is not surprising that the basic atmospheric scale properties help determine the optimum cross-section. The numbers in Table II suggest that it is not necessary to use a primary resonance of, say, O_2 or N_2 in order to maximize return signal. This relaxes both the requirement that the laser line fall on the center of a primary resonance and the corresponding laser stability requirements. Note also the case for a rare gas such as O_3; here, the simplified calculations imply that primary resonance is necessary to optimize return power.

The above considerations with regard to resonance probing are rather simplified and ignore features which might be usefully exploited. For example, in probing a major constituent such as N_2, the pressure broadening of the lines as a function of decreasing altitude might be utilized. Here the line width at the upper altitudes is less than that at the lower altitudes. Thus, a beam launched from a satellite at a frequency close to, but not right on, the center of a resonance line will suffer relatively smaller attenuations in the upper altitudes because of the narrowed line width. This process would allow one to get somewhat closer in frequency to the center of the resonance than the lefthand column in Table II suggests. In addition, in the course of line selection one would be required to examine the efficiency of production of fluorescence, since this in general represents a relatively broad-band return. Fluorescence would be harmful for remote probing but possibly useful for essentially *in situ* probing in the upper atmosphere.

CONCLUSION

The preceding suggestions have largely been made in terms of a satellite system; however, this is more in the nature of an ultimate goal. Present experimental plans are aimed at ground-based measurements. In fact, work is underway at the RCA Astro-Electronics Division to implement a ground-based system. Here first efforts will be devoted to determining the detailed engineering feasibility of monitoring the Raman radiation referred to above. Additionally, it might be pointed out that there are 10 or so facilities in the U.S. involving various aspects of ground-based lasers in which a variety of meteorological probings are being made.

It is by now trite to say that the laser is an answer looking for a problem. Analogously, such was the situation with traveling wave tubes at one time. As the associated component development proceeds there seems relatively little doubt that the laser will become a key component in a variety of systems. Based upon work to date, lasers systems for the sensing of meteorological state parameters seems to be a potentially fruitful application.

BIBLIOGRAPHY

1. A. Smekal, *Naturwiss*, Vol. 11, No. 873 (1923)
2. G. Fiocco and L. Smullin, "Detection of Scattering Layers in the Upper Atmosphere (60-40 km) by Optical Radar," *Nature*, Vol. 199 (1963) p. 1275
3. B. R. Climesha, G. Kent, and R. Wright, "Laser Probing the Lower Atmosphere," *Nature*, Vol. 209 (1966) p. 184
4. L. Elterman, *A Model of a Clear Standard Atmosphere in the Visible Region and Infra-Red Windows*, AFCRL-63-675, Optics Physics Laboratory, United States Air Force, Cambridge Research Laboratories, Office of Aerospace Research, Bedford, Mass.
5. R. Fenn, *Proceedings of the Conference on Atmospheric Limitations to Optical Propogation*, National Center for Atmospheric Research Report (1965)

LASERS AND HOLOGRAMS

Dennis Gabor[1], in one of his original papers on the subject, describes a hologram as a record which "contains the total information for reconstructing (an) object, which can be two-dimensional or three-dimensional". More specifically, a hologram is a recording of a standing-wave pattern formed by temporally coherent light from an object to be reproduced and from a reference source. When light from an identical reference source is incident on the developed record it gives rise to a diffracted wave identical in amplitude and phase distribution with the original wave from the object. Thus, with illumination from an appropriate reference beam, the object can either be photographed or be viewed directly by looking through the hologram.

Dr. E. G. RAMBERG

RCA Laboratories
Princeton, N.J.

GABOR demonstrated the feasibility of holography in 1948[2], using pinholes illuminated by filtered radiation from a mercury arc to obtain the required coherence. His primary objective was, however, to overcome the limitations imposed by spherical aberration on the resolution of the electron microscope[1,3]. The procedure originally suggested by him was to place the specimen in front of a fine electron probe formed by electron lenses with their inherent aberration and to record an electron hologram on a plate placed at some distance from the specimen. This was then to be scaled up optically in the ratio of a light wavelength to the electron wavelength and to be illuminated by a reference source of light with the same aberration as the electron source, scaled up in the same proportion. The specimen, scaled up in the ratio of the wavelengths or by a factor of about 100,000, should then be visible through the hologram in a location corresponding to the original specimen position.

Efforts by Haine and Mulvey[4] to exceed the resolution of the conventional electron microscope by a refined version of this technique were defeated by excessive demands on the coherence of the electron source and the stability of the entire system as well as difficulties in reconstruction. Attempts to utilize holography for x-ray microscopy by Baez[5] and El Sum[6] encountered even greater difficulties. However, the advent of the laser, providing light sources of extraordinary monochromaticity and coherence length, gave a new impulse to the field of holography. The introduction of a separate, oblique reference beam, and of diffuse illumination of the object (or diffuse scattering by the object) by Leith and Upatnieks[7,8] were particularly important steps in extending the potentialities of holography.

Final manuscript received July 11, 1966

The early work of Gabor was concerned entirely with plane holograms, i.e. records which could be regarded as planar sections through the standing-wave pattern. Three-dimensional holograms, formed in a recording medium with depth large compared to the space periods of the recorded interference patterns have quite distinctive properties, as pointed out by Denisyuk[9] and investigated in more detail by Van Heerden[10]. It will be convenient to consider these two types of holograms separately.

PLANE HOLOGRAMS

Two simple ways of recording plane holograms and reconstructing images from them are illustrated in Figs. 1 and 2. In Fig. 1a, a parallel light beam derived from a laser falls partly on a diffusely reflecting object and partly on a mirror which directs it onto the hologram plate. Here the light scattered by the object interferes with the specularly reflected parallel reference beam, forming a latent image of the hologram pattern on the plate. If the plate is developed and the resulting hologram is illuminated by a parallel laser beam of the same wavelength, the beam is diffracted by the hologram pattern so as to form two images of the original object. The light diffracted in a direction with respect to the reference beam corresponding to that of the light from the object during recording forms the primary image, whereas light diffracted in the opposite direction forms the conjugate image. If the intensity of the light from the object is comparable to that of the reference beam at the hologram plate during recording, light distributions corresponding to higher-order diffractions by the hologram pattern may be observed in addition to the two images just mentioned.

With a parallel reference beam during recording and reconstruction, the primary image is virtual and the conjugate image is real. Furthermore, if the reference beam is incident in the same direction as during recording, the virtual image appears in the same position as the object with respect to the hologram plate and, viewed through the hologram plate, is indistinguishable from the object in its full three-dimensional aspect (Fig. 1b). On the other hand, if the reference beam is incident from the opposite direction (i.e. if the effective source of the reference beam during reconstruction is a mirror image with respect to the hologram plane of that during recording) the conjugate image appears as a real, aberration-free, image in front of the hologram as shown in Fig. 1c. (Turning over the hologram, about an axis normal to the plane of the picture, and leaving the reference beam in its original position has the same effect, except that the real image appears upside down.) This image may be viewed against the hologram as a background. The remaining images—and both images for any other reference beam—are imperfect. Finally, a property which distinguishes the conjugate image from the primary image (and from the object) is that it is depth-inverted. Thus, in viewing the conjugate real image of an object, such as a human face, we see the illuminated surface from the inside. Gerritsen of RCA Labs and Rotz and Friesem[11] have demonstrated that this depth inversion can be nullified

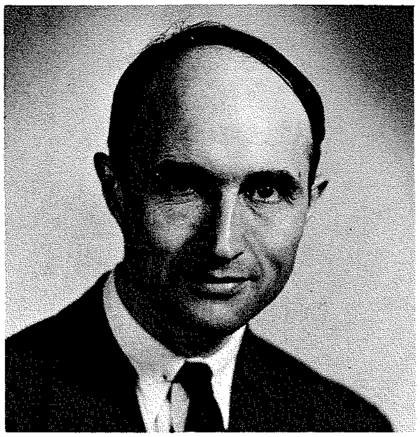

DR. EDWARD G. RAMBERG received the AB from Cornell University in 1928 and the PhD in theoretical physics from the University of Munich in 1932. After working on the theory of x-ray spectra as research assistant at Cornell, he joined the Electronic Research Laboratory of RCA in Camden in 1935. He has been associated with the RCA Laboratories in Princeton since their establishment in 1942. He has worked primarily on electron optics as applied to electron microscopy and television, various phases of physical electronics, thermoelectricity, and optics. In 1949 he was visiting professor in physics at the University of Munich and, in 1960 and 1961 Fulbright Lecturer at the Technische Hochschule, Darmstadt. Dr. Ramberg is a Fellow of the IEEE and the APS and a member of Sigma Xi and the Electron Microscope Society of America.

by forming a second hologram with the depth-inverted real image formed by a first hologram as object and observing the conjugate real image formed by the second hologram.

A hologram of a nearby object formed with a parallel reference beam is commonly designated as a Fresnel hologram. The interference pattern (i.e. the surfaces of constant path difference $n\lambda$) between the light emitted from a single object point and the reference wave is illustrated by Fig. 3c. At the left we see the intersections of the surfaces of constant path difference with the xz-plane, which is the plane of incidence of the reference beam through the object point (x_j, o, z_j) (z-axis: axis normal to hologram plane), at the right the intersection of the interference pattern with the hologram plane (the xy-plane). The surfaces of constant path difference are here paraboloids of revolution with the object point as common focus and the reference ray through the object point as axis. The hologram pattern itself is an elliptically distorted phase plate with sinusoidal intensity variation. The familiar lens properties of a phase plate account for the fact that the hologram pattern is capable of focusing parallel incident light of the reference beam into a point corresponding to the object point.

The spacing of the lines of maximum intensity on the hologram (in the xy-plane) is given by

$$D_s = \frac{\lambda}{\sin\alpha - \sin\theta_j} \qquad (1)$$

where λ is the wavelength of the light, α is the angle of incidence of the reference beam, and θ_j is the angle of incidence of the ray from the object point at any particular point on the hologram plate. In practice, the center of the phase plate pattern (corresponding to $\theta_j = \alpha$) is excluded since it would be impossible to view the object through this portion of the hologram without intercepting the direct light of the reference beam. Since for $|\alpha - \theta_j| \geq 5°$, $D_s < 0.01$ mm the hologram structure is quite generally much too fine to be resolved by direct observation; for the sake of clarity only about every 10'th line of maximum intensity is shown on the drawing.

The Fresnel hologram of a real object will consist of a complex superposition of many patterns of the type shown in Fig. 3c, all of them beyond the resolving power of the human eye. A well-prepared hologram appears thus simply as a uniformly fogged plate. However to function satisfactorily as a hologram this plate must be capable of resolving separations equal to:

$$D_{s\,min} \cong \frac{\lambda}{(\sin\alpha - \sin\theta_j)_{max}} \qquad (2)$$

Fig. 3c shows that, for a Fresnel hologram, the spacing D_s for any object point varies greatly over the hologram area. This is no longer the case if the object is translated to an infinite distance from the hologram by placing it in the focal plane of a lens interposed between the object and the hologram. The waves from any object point now become plane waves. The surfaces of path difference $n\lambda$ now are also planes and intersect the hologram plane in a series of parallel equally spaced lines. Such a hologram (Fig. 3a) is called a Fraunhofer hologram. With a reference beam incident normally on the hologram plane, the orientation of the line pattern with sinusoidal intensity variation is given uniquely by the azimuth of the object point with respect to the z-axis and the spacing

$$D_s = \frac{\lambda}{\sin\theta_j} \quad \tan\theta_j = \frac{r_j}{f} \qquad (3)$$

by the distance r_j of the object point from the axis (f = focal length of lens). Thus the intensity of any one object point in a half plane is represented by the magnitude of a corresponding two-dimensional Fourier component of the intensity at the hologram plate and the hologram pattern is a Fourier transform of the object pattern.

Very nearly the same situation exists for an object a finite distance from the hologram plane, provided that the reference beam diverges from a point in the plane of the object (Fig. 3b). The surfaces of constant path difference $n\lambda$ are now hyperboloids of revolution with the object point and the reference source as the two foci. The intersections with the hologram plane are hyperbolic arcs which are closely approximated by equispaced parallel lines. This follows from the fact that the difference in the angle of incidence on the hologram plane from the object point and the reference source is very nearly constant. Holograms prepared with the reference source in the object plane are hence commonly called Fourier-transform holograms[12].

Fourier-transform holograms possess the advantage that, for them, the interference pattern over the entire hologram is essentially the same and that, for a given image field, separation between the reference beam and the image beam can be achieved with the largest minimum spacing or least resolution capability of the hologram plate. This is obtained with the reference source at the edge of the image field (Fig. 2a). The primary and conjugate images are now obtained in the same plane—an aberration-free primary virtual image in the location of the object when the reference beam during reconstruction is identical with that during recording (Fig. 2b), an aberration-free conjugate real image, when the reference beam during reconstruction converges toward the mirror image of the source used in recording (Fig. 2c). If a reference beam is employed for reconstruction which has the same angle of incidence at the center of the hologram, but a different point of convergence, magnified or reduced images are obtained, which are free of distortion but not stigmatic (Fig. 2d). It may be shown that for very large magnification the maximum number of lines in the image which can be resolved corresponds approximately to $(z_j/\lambda)^{1/2}$, where z_j is the object distance. Thus, by choosing this distance large enough, holography may be employed for high-quality lensless microscopy.[13]

Since for a hologram prepared with a diffusely reflecting or diffusely illuminated object any portion is similar to any other, the complete image can be reproduced with any part of the hologram; the resolution is merely reduced in accord with the laws of diffraction which tell us that the least resolved distance in the image formed by a beam limited by a square aperture of side a is:

$$d_{min} = \frac{z_j\lambda}{a} \qquad (4)$$

where z_j is the image distance, which is equal to the object distance for an aberration-free hologram image. Similarly, damage to the hologram merely reduces the contrast of the image slightly, having an effect similar to inflicting similar damage to the surface of a lens of the same size forming a similar image. (For certain types of hologram damage, the effect is actually less than for a lens because of the off-axis incidence of the reference beam.)

At the same time any diffusely reflecting surface illuminated by coherent (laser) light exhibits "speckle", i.e. random brightness variations resulting from the interference of the diffusely scattered waves. This speckle is of course transferred to the image of a diffusely reflecting object formed by a hologram. The effective dimensions of the speckle grain are determined by the aperture of the imaging system and are comparable to the limit of resolution of the system. Thus, for direct observation, where the pupil of the eye definies the resolution, speckle is invariably prominent. On the other hand, if the image is recorded, speckle becomes insignificant if the hologram is chosen large enough that the effective speckle grain is smaller that the limit of resolution of the recording medium.

For an object in the form of a transparency speckle can be avoided by illuminating the transparency directly with an undiffused laser beam, as illustrated in Fig. 4. With a hologram prepared in this manner it is not possible to view the image directly, since the pupil of the eye limits the area of the image observed at any one time. Furthermore, the hologram does not possess the desirable property of redundancy, since it is in essence a shadow projection with edge diffraction fringes of the object. Accordingly dust and scratches on a transparency hologram severely affect the reproduced image.

It is of interest to compare the number of picture elements in an image which can be stored in a hologram with that which might be stored by recording the image on the hologram plate directly. Consider a square hologram with side a and a square image field with side b. If θ_p is the angle subtended by half the image side, we have (for small θ_p)

$$b = 2z_j \sin \theta_p \qquad (5)$$

For a Fourier-transform hologram with the reference source placed at the center of an edge of the image field we find in correspondence with Eq. 2:

$$D_{s\,min} = \frac{\lambda}{\sqrt{5}\ \sin \theta_p} \qquad (6)$$

The total number of picture elements which can be recorded on a hologram plate with a limiting resolution $D_{s\,min}$

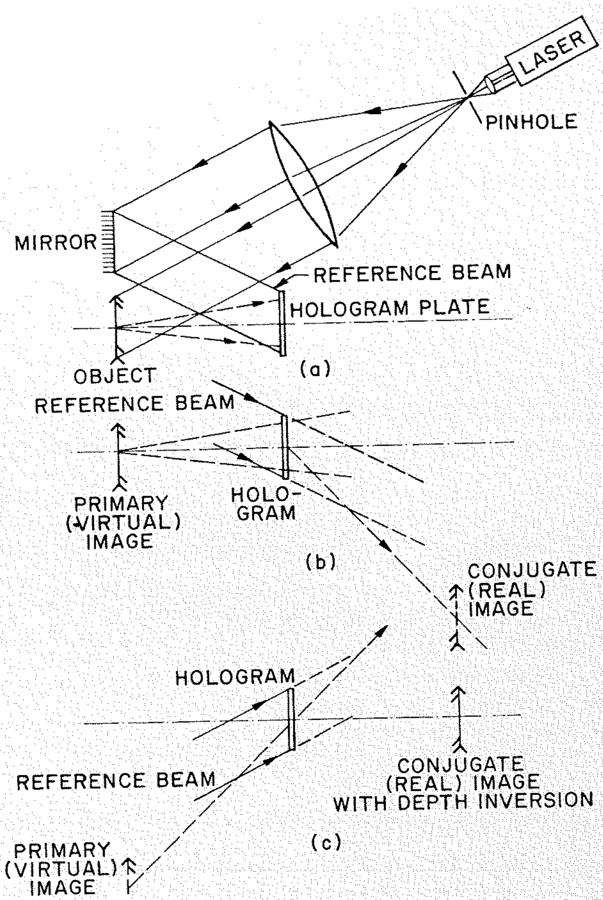

Fig. 1—Fresnel hologram.
a. Recording of hologram.
b. Reconstruction of aberration-free virtual image.
c. Reconstruction of aberration-free real image with depth inversion.

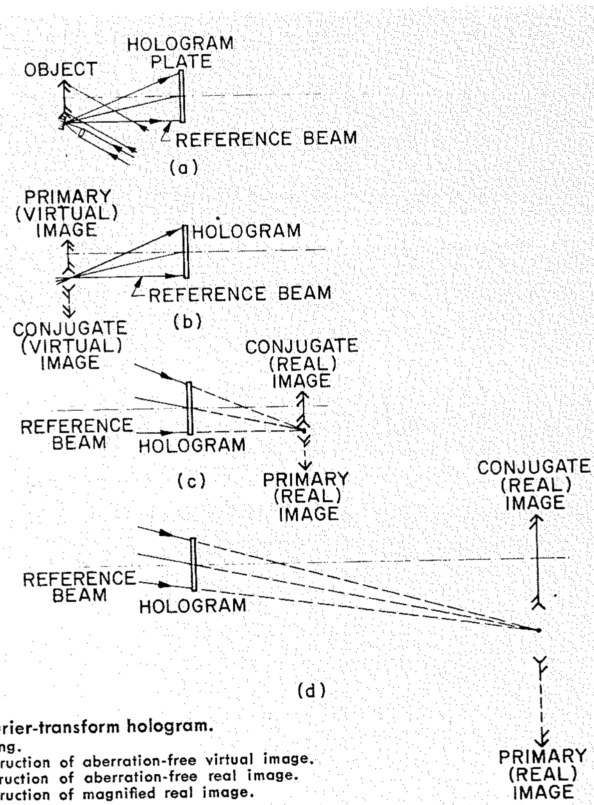

Fig. 2—Fourier-transform hologram.
a. Recording.
b. Reconstruction of aberration-free virtual image.
c. Reconstruction of aberration-free real image.
d. Reconstruction of magnified real image.

by direct photography of the object is given by:

$$N_p = \left(\frac{a}{D_{s\,min}}\right) 2 \tag{7}$$

whereas, the total number of picture elements in the hologram image is given by:

$$N_h = \left(\frac{b}{d_{min}}\right) 2 \tag{8}$$

where d_{min} is given by Eq. 4. Together, Eqs. 4 to 8 yield:

$$\frac{N_h}{N_p} = \frac{4}{5} \tag{9}$$

This would make it appear that the number of picture elements which can be recorded on a hologram is practically equal to that which can be recorded directly on a plate of the same size and resolution. It should be noted however, that the effect of the limiting resolution of the plate is quite different with direct photography and holography. In direct photography detail contrast is reduced over the entire picture area in proportion with the sine wave response $k(d)$, where d is the period of the Fourier component of the image detail considered and, approximately[14]:

$$k(d) = \frac{1}{1 + (d_o/d)^2} \tag{10}$$

The term d_o is characteristic of the emulsion and its development and is, in typical examples, about twice as large as the limiting resolution.

With the hologram, the sine-wave response of the plate has no direct effect on the detail contrast of the image. Instead, the image itself is reduced in intensity in proportion to $[k(D_s)]^2$. Since D_s decreases, in accord with Eq. 1, as the angular separation between the reference source and the image point increases, the portions of the image farthest from the reference source may become much fainter than those closer to the reference source. Thus, for reasonable uniformity of the brightness of the image, $D_{s\,min}$ should certainly not be less than d_o or twice the limiting resolution of the hologram plate. Taking this into account,

$$\frac{N_h}{N_p} = \frac{1}{5} \tag{11}$$

may be a more adequate ratio of the number of picture elements which can be stored in the hologram to that which can be stored by direct recording on the hologram plate. Increasing the hologram size to overcome the effect of speckle noise would lead to a still less favorable factor in picture element storage efficiency. However, speckle noise is not inherent in the hologram process.

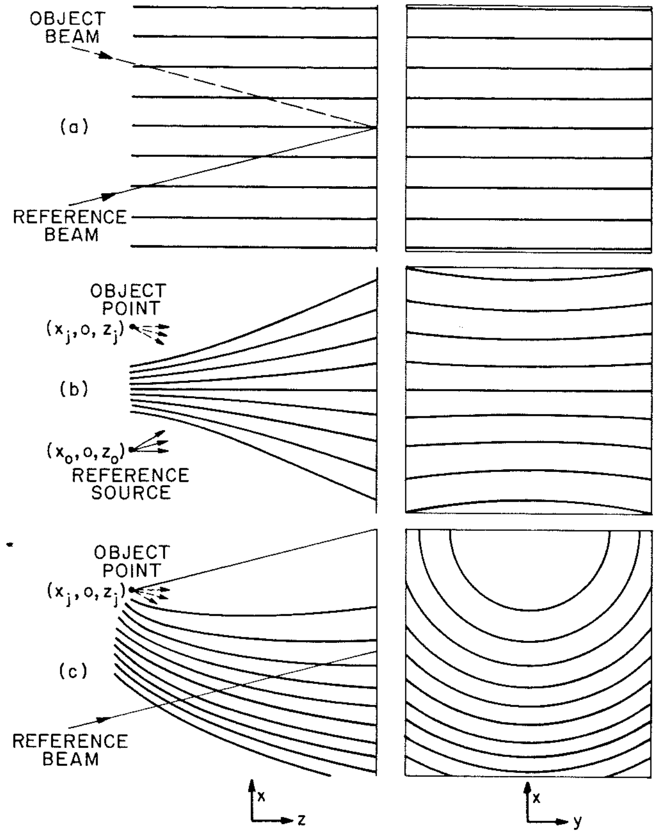

Fig. 3—Standing-wave pattern in front of hologram plate and lines of maximum intensity on hologram plate for point object (approximately every 10^4th line is indicated).
a. Fraunhofer hologram.
b. Fourier-transform hologram.
c. Fresnel hologram.

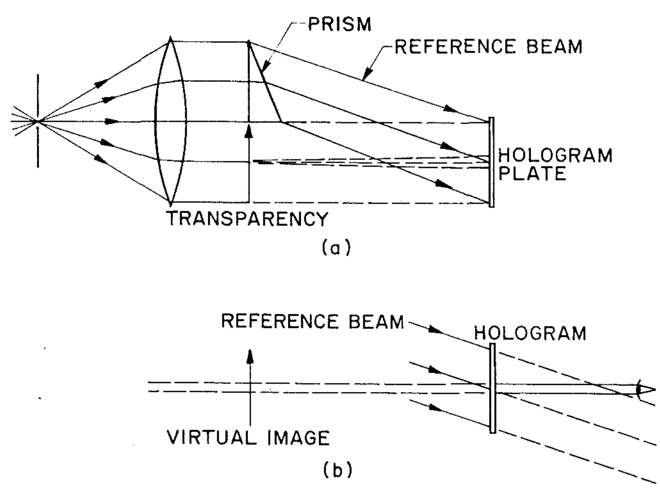

Fig. 4—Hologram of transparency prepared with undiffused illumination.
a. Recording.
b. Viewing of virtual image.

Some additional properties of the hologram which merit consideration are its ability to reproduce images of tremendous dynamic range with a medium with small photographic latitude, its capacity to store the three-dimensional aspect of any object in a plane, and the possibility of storing numerous images in superposition.

The first property becomes obvious when we consider an object consisting of a single luminous point. While, in this case, the intensity variation in the hologram plane may amount to only a few percent, corresponding to the modulation amplitude of the interference pattern, all of the diffracted light for one order may be concentrated into the diffraction disk corresponding to the object point. Under these circumstances a dynamic range of the order of 100 dB is entirely within reason.

The viewing of an object over a large solid angle with the aid of a hologram requires a hologram of large size. If the object (or image) is located at the normal viewing distance of 250 mm from the object, seeing the object with normal visual resolution from a single vantage point requires a hologram approximately a pupillar diameter ($d_p \cong 1$ mm) in size. If the object is to be viewed over a cone of half angle ω (Fig. 5) through a spherical hologram, the hologram area must be increased by a factor:

$$F = \frac{2\pi(1\text{-}\cos\omega)z_j^2}{(\pi/4)\,d_p^2} = 5 \times 10^5\,(1\text{-}\cos\omega) \tag{12}$$

For $\omega = 30°$ this is the order of 7×10^4. If the hologram information were to be transmitted electrically the bandwidth required to transmit the indicated three-dimensional information would have to be 7×10^4 times greater than that needed for transmitting the 1-mm-diameter hologram.

A number of pictures can be stored in superposition on a plane hologram by varying the direction of the reference beam of the recording wavelength. These possibilities are however quite limited if mutual interference between pictures is to be avoided. Since three-dimensional holograms possess great advantages in this respect, multiple picture storage will be discussed in connection with them.

However we must still consider the conditions which must be fulfilled in the recording of holograms and image reconstruction. Holograms may be either absorption or phase holograms, just as diffraction gratings may be either absorption or phase gratings. In an absorption hologram, variations in intensity in the interference patterns at the hologram plate are translated into variations in absorption by the plate, while in phase holograms variations of intensity are translated into variation in refractive index or thickness of a transparent medium.

The standard material for forming an absorption hologram is a fine-grained photographic plate, such as the Kodak High-Resolution Plate or the comparable red-sensitized Kodak Spectroscopic Plate, Type 649-F. Such plates have a limiting resolution which is better than 2,000 line pairs per millimeter and probably about 3,000 line pairs per millimeter. Putting $D_{s\,min} = d_o$ equal to twice the least resolvable separation and $\lambda =$ 6,328 angstroms (corresponding to a helium-neon laser) in Eq. 6 leads to permissible field angles $2\theta_p$ of 50°. Holograms with even greater field angles have been made successfully. The exposure required to record a 4x5 in² hologram on a Kodak 649-F plate with a 10-milliwatt helium-neon cw laser is of the order of a minute. With an argon laser emitting in range from 4,579 to 5,145 angstroms, the exposure may be reduced by an order of magnitude or more.

If the silver grain is bleached out of an absorption hologram a phase hologram is obtained. The optical path variations result here in part from internal variations in refractive index, in part from residual undulations of the surface which correspond to the internal developed image. Deposition of a thin reflecting layer on the surface thus results in a special type of phase hologram—a reflection or mirror hologram—for which the reconstructed images are mirror-reversed

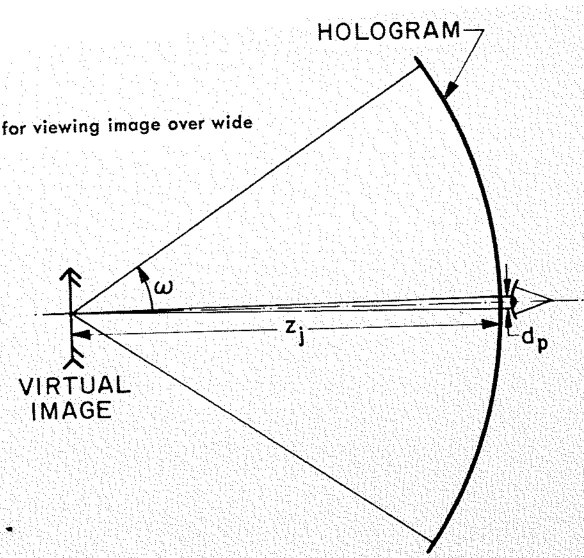

Fig. 5—Hologram for viewing image over wide angular range.

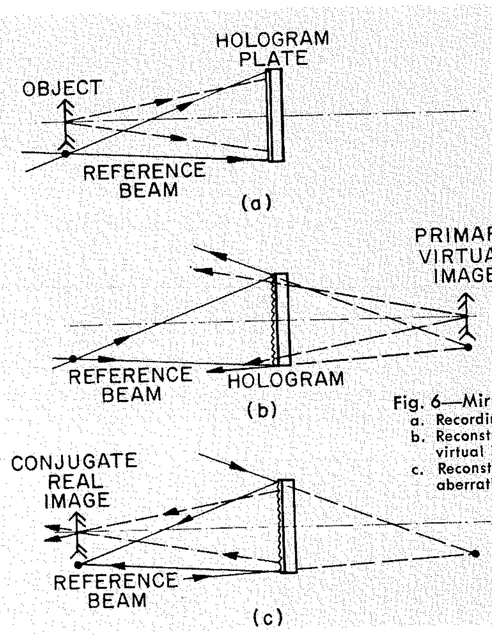

Fig. 6—Mirror hologram.
a. Recording.
b. Reconstruction of mirror-reversed aberration-free virtual image.
c. Reconstruction of mirror-reversed depth-inverted aberration-free real image.

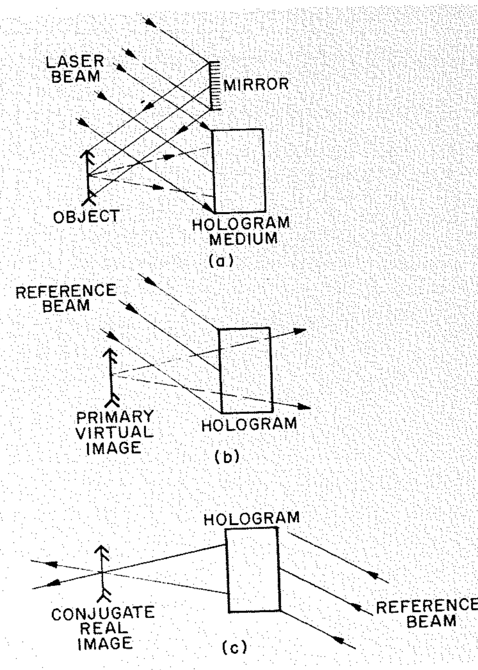

Fig. 7—Three-dimensional hologram
a. Recording.
b. Reconstruction of virtual image.
c. Reconstruction of real image.

(Fig. 6). High-quality phase holograms with pattern spacings D_s in the range from 1/200 to 1/1000 mm have also been prepared with thermoplastic-film photoconductor sandwiches[15] which possess the advantage of very low random light scattering. Their sensitivity and resolution capability is intermediate between that of special high-resolution plates and the more comventional photographic materials. Photoresist has also been shown to be useful for the preparation of phase holograms. (Private communication by F. Letton and H. J. Gerritsen of RCA Labs.)

Phase holograms have the basic advantage over absorption holograms that they are capable of directing a larger fraction of the light of the reference beam into the desired image; in typical instances this fraction has been found to be about 4% for phase holograms and less than 1% for absorption holograms (according to measurements by D. Greenaway) in good accord with the ratio 5.4 between the maximum values of these fractions for a sinusoidal phase grating and sinusoidal absorption grating.

The nature of the hologram places stringent requirements on the conditions of recording. Plate, object, and reference source should not move with respect to each other in the course of an exposure by more than a fraction of a wavelength to prevent washing out of the fine-grained hologram pattern. Thus the recording of objects in motion requires the use of Q-switched lasers, which can provide enough power for an exposure in a single pulse much less than a microsecond in length. If a light source other than a laser were to be employed, the source size would have to be less than half an interference pattern spacing D_s in size. The requirement for source monochromaticity is also stringent, since the maximum path difference Δd between interfering rays must certainly vary by less than half a wavelength. This leads to:

$$d = \frac{\lambda}{2}\,\frac{\lambda}{\Delta\lambda} \tag{13}$$

Thus, even if the maximum path difference between the interfering rays is only 1 cm, the fractional wavelength-spread of the source should not exceed $\Delta\lambda/\lambda = 3 \times 10^{-5}$.

The requirements on the size and monochromaticity of the reference source and on mechanical stability during reconstruction are much more easily satisfied. The maximum permissible source size (or the permissible mechanical displacement) corresponds simply to the maximum resolution demanded in the image. Thus the ratio of the angle subtended by the source at the hologram to that subtended by the picture diameter must be less than the reciprocal of the number of picture elements resolved along a picture diameter (i.e. the reciprocal line number $1/n$). Similarly, since the diffraction angle for the image rays is proportional to the wavelength, we must demand:

$$\frac{\Delta\lambda}{\lambda} \leq \frac{1}{n} \tag{14}$$

For a picture with television resolution ($n = 500$) this can be realized readily with continuous sources and an interference filter or gaseous discharge sources with suitable line filters. However, a laser provides the required high brightness and small source size most conveniently.

Fig. 8—Relation between unit vectors in direction of propagation of object wave (e_j), reference wave during recording (e_0), reference wave during reconstruction (e_0'), and image wave (e_2).

a. Direction of reference waves during recording and reconstruction equal or opposite.
b. Reference wave during reconstruction and object wave equal or opposite.
c. Different wavelength in recording and reconstruction.

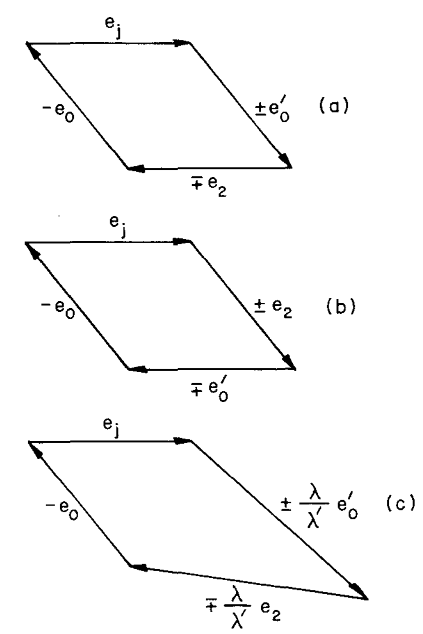

THREE-DIMENSIONAL HOLOGRAMS

The distinctive feature of three-dimensional holograms, as compared with plane holograms, is that one and only one image is formed for discrete directions of incidence uniquely related to the wavelength of the incident beam. Thus, if a hologram of an object is formed in precisely the same manner as a plane hologram, with the sole distinction that the hologram medium is very thick in comparison with the wavelength of light, a perfect three-dimensional virtual image is obtained in the position of the original object if the reference beam during reconstruction is identical with the reference beam during recording and a perfect (depth-inverted) three-dimensional real image is formed in the position of the object if the reference beam is simply reversed in direction (Fig. 7). Let us, for the sake of simiplicity, consider a Fraunhofer hologram, in which the interfering object and reference waves are plane waves and the surfaces of maximum intensity are consequently a family of equispaced planes. Light will be diffracted by such a system only if, simultaneously, the following two conditions are fulfilled: light scattered by points in any one plane is in phase in the direction of diffraction, corresponding to the condition of reflection at the plane; and light reflected by successive planes is in phase, corresponding to the Bragg condition familiar from the diffraction of x-rays by crystals. These two conditions can be combined in a single vector equation[16]:

$$e_2 - e_o' \mp (\lambda'/\lambda)\,(e_j - e_o) = 0 \tag{15}$$

Here, e_2 is the unit vector in the direction of propagation of the diffracted wave, e_o' that for the reference wave during reconstruction, e_j that for the object wave, and e_o that for the reference wave during recording. The λ' and λ are the wavelengths of the radiation used in reconstruction and recording, respectively. Eq. 15 demands that the four vectors in question form a closed (generally three-dimensional) quadrangle. Furthermore, if an extended image is to be reproduced, the condition of Eq. 15 must be preserved (for fixed e_o and e_o')

Fig. 9—Least permissible angular displacement of hologram medium with respect to reference beam for the successive recording of separate images and image movement corresponding to an equal displacement during reconstruction.

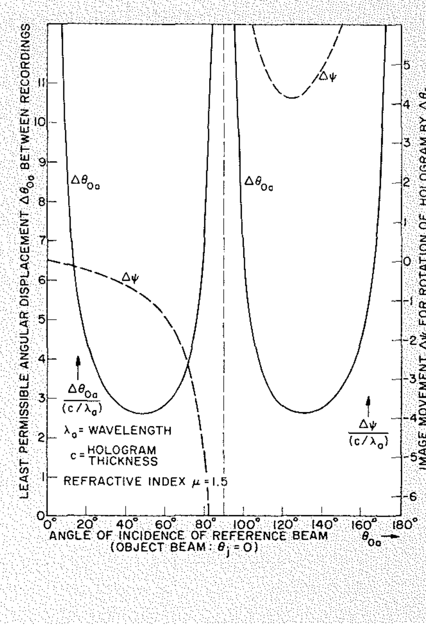

when e_j is varied over a two-dimensional angular range.

This condition can be satisfied only if $\lambda' = \lambda$ and the reference beams during reconstruction and recording have the same or opposite directions (Fig. 8a), in which case the diffracted waves also have the same or opposite directions, respectively, as the object waves. If the directions of the diffracted wave and reference wave during reconstruction are interchanged (Fig. 8b), closure can be realized only for a limited (linear) range of directions of e_j, corresponding to a rotation of the vector pair $(e_j, \pm e_2)$ around the fixed endpoints of the vector pair $(-e_o, \mp e_o')$. A similar condition prevails if the wavelength is changed between recording and reconstruction (Fig. 8c).

The maximal departures of the reference beam used in reconstruction from that used in recording in both angular orientation and in wavelength—i.e. departures from the exact fulfillment of Eq. 15—which lead to appreciable image intensity are inversely proportional to the hologram thickness (assuming this to be small compared to the lateral extend of the hologram). These departures (and the corresponding image displacements) are plotted as function of the angle of incidence of the reference beam in Figs. 9 and 10. If different images are recorded successively in a three-dimensional hologram medium with reference beams differing in angular orientation or wavelength by amounts exceeding the indicated maximal departures, they can be read out separately, without appreciable mutual interference, by changing the direction of incidence or wavelength of the reference beam used in reconstruction so as to correspond to the values used in recording the successive images. The maximum total number of pictures which can thus be stored in the three-dimensional hologram can be shown to be of the order of c/λ, where c is the hologram thickness; van Heerden[10] has shown, furthermore, that the total number of picture elements which can be stored in a three-dimensional hologram is equal to the ratio of the hologram volume to λ^3.

It should be noted that, for large angles of incidence of the reference beam, even the extra-thin photographic emulsions used for high resolution work must be regarded as thick; their thickness is commonly of the order of 4 micrometers. Consequently either the conjugate or the primary image—more generally, the off-axis image in Fig. 1—is partly suppressed. Pennington and Lin[17] have furthermore made use of the great wavelength sensitivity of a hologram prepared with a reference beam and object beam incident on opposite sides of the emulsion ($\theta_{oa} > 90°$ in Fig. 10) to reconstruct two-color images in white light. For this purpose the combined beams from a (red) helium-neon laser and a (blue) argon laser were used as reference beam and for illuminating a color transparency during recording. During reconstruction, the two superposed recorded hologram patterns select narrow wavelength bands centered about the helium-neon laser wavelength and the argon laser wavelength from the white reference beam to form the component red and blue images.

Apart from thick photographic emulsions, which pose special problems with respect to shrinkage and development in depth,[16] alkali halide crystals colored with F-centers and photochromic glasses have been considered suitable for recording three-dimensional holograms.

APPLICATIONS

Holography makes possible the compact storage of pictorial information in a form largely immune to physical damage. Its ability to reconstruct the true three-dimensional aspect of an object has been utilized for measuring the instantaneous particle distribution in an aerosol recorded by the pulse of a Q-switched laser.[18] The great sensitivity of the stored pattern to minute object displacements can be used to advantage to measure displacements of fractions of a wavelength on surfaces of arbitrary contour.[19]

Fig. 10—Least permissible wavelength difference for recording separate pictures (= half-value width of wavelength range from white-light source utilized in reconstruction) and image movement corresponding to an equal wavelength shift during reconstruction.

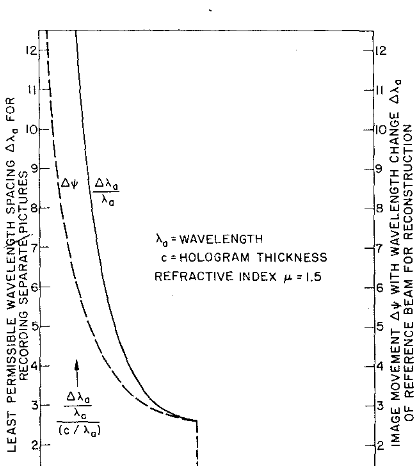

Lensless image reproduction by holography invites its application for x-ray imaging, although here the absence of sources of sufficient coherence and intensity constitutes a serious obstacle. The three-dimensional hologram, finally, presents the possibility of highly compact information storage in three dimensions, with relatively easy access for read-out.

For further detail concerning the properties and uses of holograms the reader is referred to the comprehensive bibliography recently published by Chambers and Courtney-Pratt.[20]

ACKNOWLEDGEMENT

The author has been greatly aided in all aspects of this study by Dr. H. J. Gerritsen and his associates who have carried on research on holography at RCA Laboratories.

BIBLIOGRAPHY

1. D. Gabor, "Microscopy by Reconstructed Wavefronts", *Proc. Roy. Soc.* (London) *A197*, 454-487, 1949.
2. D. Gabor, "A New Microscope Principle", *Nature 161*, 777-778, 1948.
3. D. Gabor, "Microscopy by Reconstructed Wavefronts", *Proc. Phys. Soc.* (London) *B64*, 449-469, 1951.
4. M. E. Haine and T. Mulvey, "The Formation of the Diffraction Image with Electrons in the Gabor Diffraction Microscope", *J. Opt. Soc. Am. 42*, 763-773, 1952.
5. A. V. Baez, "A Study in Diffraction Microscopy with Special Reference to X-Rays," *J. Opt. Soc. Am. 42*, 756-762, 1952.
6. H. M. A. El-Sum, *Reconstructed Wavefront Microscopy*, Ph.D. Thesis, Stanford University (University Microfilms, Inc., Ann Arbor, Mich. 1966).
7. E. N. Leith and J. Upatnieks, "Wavefront Reconstruction with Continuous-tone Objects", *J. Opt. Soc. Am. 53*, 1377-1381, 1963.
8. E. N. Leith and J. Upatnieks, "Wavefront Reconstruction with Diffused Illumination and Three-dimensional Objects", *J. Opt. Soc. Am. 55*, 1295-1301, 1965.
9. Yu. N. Denisyuk, "Photographic Reconstruction of the Optical Properties of an Object in its Own Scattered Radiation Field", *Soviet Physics—Doklady 7*, 543-545, 1962.
10. P. J. van Heerden, "Theory of Optical information Storage in Solids", *Appl. Optics 2*, 393-400, 1963.
11. F. B. Rotz and A. A. Friesem, "Holograms with Non-Pseudoscopic Real Images", *Appl. Phys. Letters 8*, 146-148, 1966.
12. G. W. Stroke, D. Brumm and A. Funkhouser, "Three-Dimensional Holography with Lensless Fourier-Transform Holograms and Coarse P/N Polaroid Film", *J. Opt. Soc. Am. 55*, 1327-1328, 1965.
13. E. N. Leith and J. Upatnieks, "Microscopy by Wavefront Reconstruction", *J. Opt. Soc. Am. 55*, 569-570, 1965.
14. R. C. Jones, "Information Capacity of Photographic Film", *J. Opt. Soc. Am. 51*, 1159-1171, 1961.
15. J. C. Urbach and R. W. Meier, "Characteristics of Thermoplastic Xerographic Holography", *Appl. Optics 5*, 666-667, 1966.
16. E. N. Leith, A. Kozma, J. Upatnieks, J. Marks and N. Massey, "Holographic data storage in three-dimensional media", *Appl. Optics 5*, 1303-1311, 1966.
17. K. S. Pennington and L. H. Lin, "Multicolor Wavefront Reconstruction", *Appl. Phys. Letters 7*, 56-57, 1965.
18. B. J. Thompson, J. Ward and W. Zinky, "Application of Hologram Techniques for Particle-Size Determinations", *J. Opt. Soc. Am. 55*, 1566, 1965.
19. K. A. Haines and B. P. Hildebrand, "Surface Deformation Measurement using the Wavefront Reconstruction Technique", *Appl. Optics 5*, 595-602, 1966.
20. R. P. Chambers and J. S. Courtney-Pratt, "Bibliography on Holograms", *J.S.M.P.T.E. 75*, 373-435, 1966.

COMPONENT PROBLEMS IN A MICROWAVE DEEP-SPACE COMMUNICATION SYSTEM

The problems associated with the development of a microwave data link system for deep-space communication are examined. Factors such as phase and frequency stability, transmitter power, low-noise receivers, and antenna systems are discussed. A system having a 10^6-bit-per-second communication rate is considered feasible within 10 years.

DR. W. T. PATTON, Ldr.
Advanced Microwave Technology
Missile and Surface Radar Division

DR. A. B. GLENN, Staff Engineer
Systems Engineering
Evaluation and Research

Moorestown, N.J.

THIS paper describes a program of research in the area of microwave technology directed toward the requirements of future deep-space communication systems. The discussion is limited largely to the spacecraft-to-Earth data link. Other communications links important to future missions include the Earth-to-spacecraft command link, spacecraft-to-probe or lander command links, return data links, and, in some systems, a link between the spacecraft and an Earth-orbiting satellite.

A deep-space communications system block diagram (Fig. 1) shows the parts of the system considered as the microwave problem. These include the spacecraft-mounted RF power amplifier with its prime power source, cooling load, and transmitting antenna; the propagation medium, consisting of solar and Earth atmospheres, linking the spacecraft with the Earth receiving terminal; and the Earth-based receiving antenna and low-noise receivers.

THE MICROWAVE PROBLEM

It is convenient to consider a microwave index of performance M for a communications link which effectively relates the communications mission and system requirements to the performance of the microwave components. The performance index is the product of the effective radiated power in watts at the transmitter and the ratio of receiver aperture area to system noise temperature.

The microwave performance index derived in Fig. 2 is simply a rearrangement of terms in the communications range equation which equates the microwave performance factors to the requirements of the communications mission. The magnitude of the microwave performance index is determined largely by the communication range, by the data rate and error probability, and, to a lesser extent, by the information-coding techniques employed. The quality of microwave system performance required in terms of coherence and stability also is determined by these factors. Values of the microwave performance index M are given in Table I for three accomplished missions, for one that is planned, and for two that indicate the requirements for future performance capabilities. The performance index listed for future missions represents a data rate of 10^6 bits per second for a Mars mission. This is about five orders of magnitude above the performance of the Mariner IV program.

The values of the microwave performance factors, plotted in Fig. 3 as a function of time, illustrate the growth trend of the performance factors. Note that the performance index increases by about 20 dB for each 5 years of research and development effort.

PHASE AND FREQUENCY STABILITY REQUIREMENTS

Before considering the means of achieving greater powers and gains in the microwave subsystem, it is important to determine the effect of signal frequency stability on data rate. An analysis of a frequency-shift-keyed (FSK) system shows (Fig. 4) that for a high-data-rate system, where the ratio of frequency instability to data rate is small, there is less than 1 dB difference in performance between coherent and noncoherent systems. As this ratio becomes large (say 1000-1) and the predetection signal-to-noise ratio is below the detector threshold, a coherent system produces signifi-

TABLE I—Typical Values of Microwave Performance Index

Program	Index M (dB)	P_t (Watts)	P_t (dB)	G_t (dB)	A_r (M²)	A_r (dB)	T_e (°K)	T_e (dB)	Freq. (MHz)
1959 Pioneer IV	−10.2	0.27	−5.7	2.5	290	24.6	1450	31.6	960
1962 Mariner II	+24	3	4.8	19	290	24.6	250	24	960
1965 Mariner IV	42	10	10	24	290	24.6	55	17.4	2290
1971 Voyager	70	50	17	34	1,770	32.5	25	14	2290
Future	90	10	10	45	63,000	48	20	13	
Future	90	100	20	40	20,000	43	20	13	

Final manuscript received May 2, 1966

Fig. 1—Block diagram of typical microwave deep-space communications system.

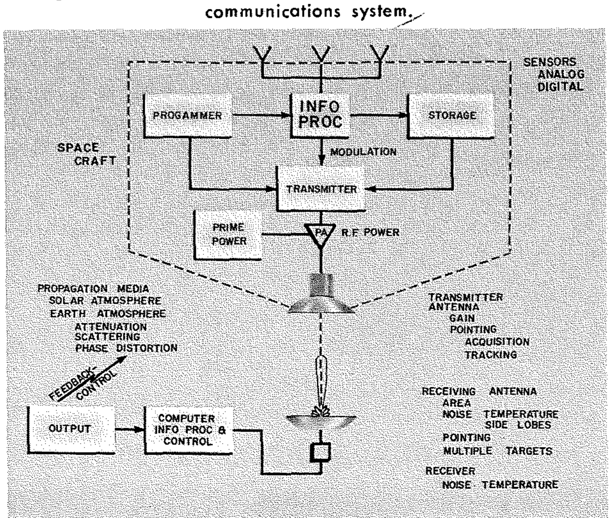

Fig. 2—Microwave performance index.

$$S = \frac{P_t G_t A_r}{4\pi R^2 L}$$

$$N = k\, T_e\, B$$

$$\frac{P_t G_t A_r}{L\, T_e} = M = S/N\ (4\pi R^2)\ kB$$

P_t = Transmitted power, watts
G_t = Gain of transmitting antenna relative to isotropic radiator
A_r = Effective aperture area of receiving antenna, meters^2
T_e = Effective system noise temperature, °K
L = System loss factor
M = Microwave index of performance, watts x meters^2/°K
S/N = Signal to noise power ratio
B = Bandwidth, Hz
k = Boltzmann's constant, 1.38 x 10^{-23} joule/°K
R = Distance between stations, meters

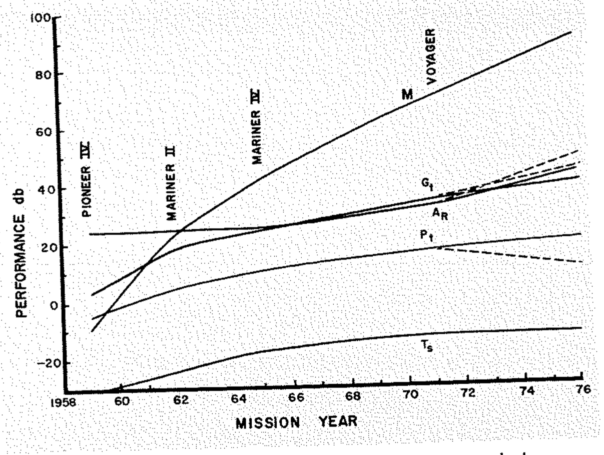

Fig. 3—Growth trend in microwave performance index.

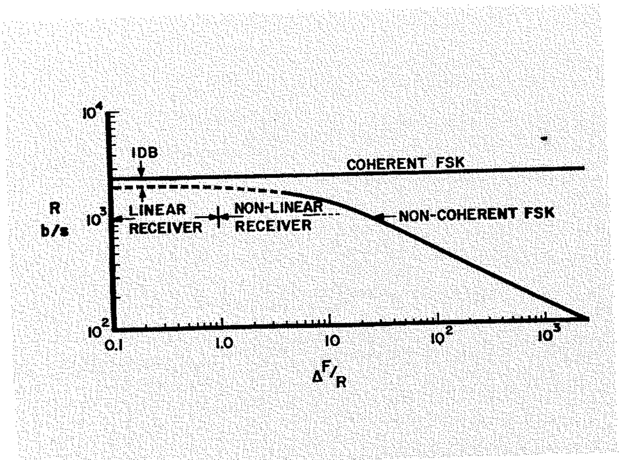

Fig. 4—Comparison between coherent and noncoherent communications systems.

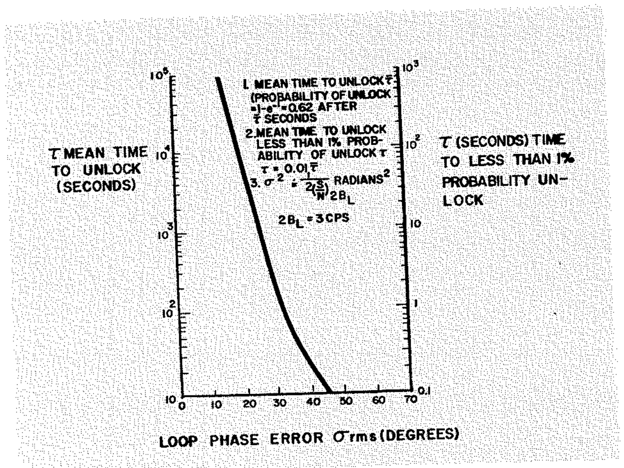

Fig. 5—Mean time to unlock vs. phase jitter for coherent system.

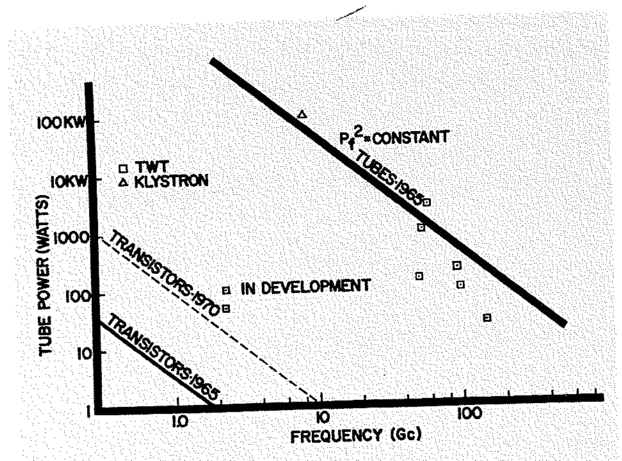

Fig. 6—Trends in microwave power sources.

cantly higher data rates than those of a noncoherent system.

State-of-the-art frequency stability is adequate for high-data-rate noncoherent systems. However, for low-data-rate coherent systems, frequency stability should be improved to reduce frequency acquisition time and to reduce doppler noise for orbit tracking purposes. At the same time, very low values of phase jitter (less than 15° RMS) are required for a high probability of maintaining phase lock over long periods of time (Fig. 5). The RMS phase noise given by note 3 of Fig. 5 is 14° for a carrier-to-noise ratio of 9 dB in a 3-Hz (cps) bandwidth. Phase noise contributed by the transmitter and by antenna and atmospheric fluctuation must be added to this. The goal of research in this area is to achieve frequency stability better than 1 part in 10^{12} and phase-locked loop bandwidths of less than 1 Hz.

TRANSMITTER POWER

There are presently available RF power sources in the 100- to 1000-watt range throughout the microwave region from 1 to 100 GHz (Gc/s). Traveling-wave tubes (RCA A-1318) delivering about 45 watts of power at 40% efficiency at about 2 GHz are presently available as space-qualified components. A space-qualified tube delivering 100 watts at 50% efficiency should be available in 1970. Efficiencies as high as 57% have been demonstrated in the laboratory.

Fig. 6 represents the state of the art in power sources in 1965. The power levels shown can presently be achieved without regard to efficiency or special packaging requirements necessary for space environment. The projected performance of transistors is based upon the present trend in doubling the available power for each year of research and development effort.

Spacecraft transmitter power is limited by the weight of the prime power source. The efficiency of the final amplifier is important not only because of prime power limitations but also because of limitations imposed by the spacecraft cooling system. It is nearly as expensive to eliminate waste power (heat) as it is to provide prime power. Prime power limitations on missions to the outer planets will dictate low transmitter powers where solar sources are used. The solar radiation intensity at Saturn orbit is about 20 dB below that at Earth orbit. However, the use of SNAP power sources, possibly for electrical propulsion, will make high-power spacecraft transmitters much more attractive.

The goal of research for spacecraft transmitters is not to increase the amount

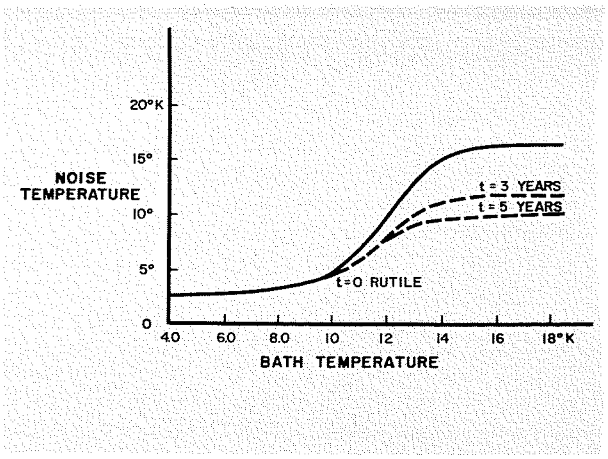

Fig. 7—Bath temperature vs. noise temperature for rutile-meander type of traveling-wave maser.

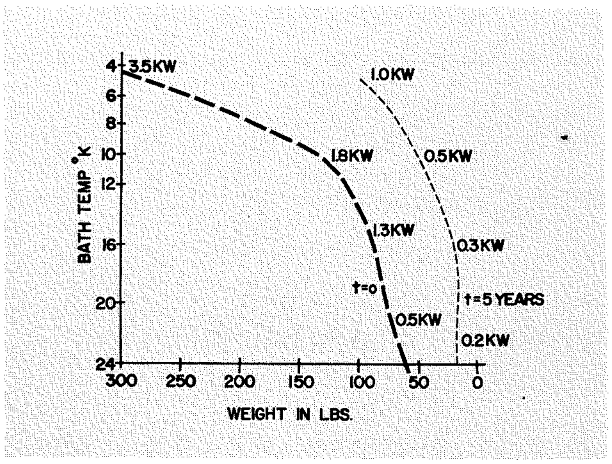

Fig. 8—Bath temperature vs. weight and primary power.

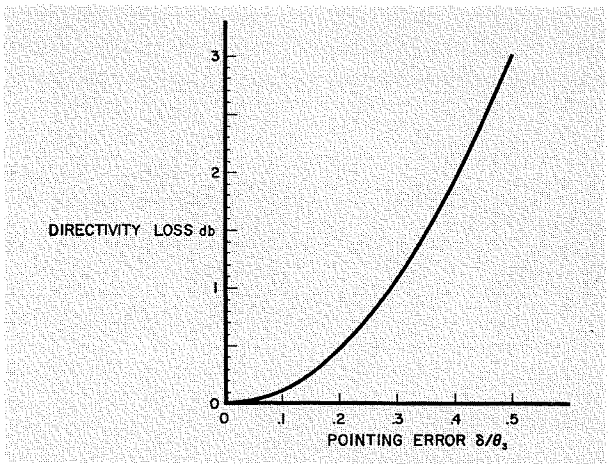

Fig. 9—Loss due to pointing error.

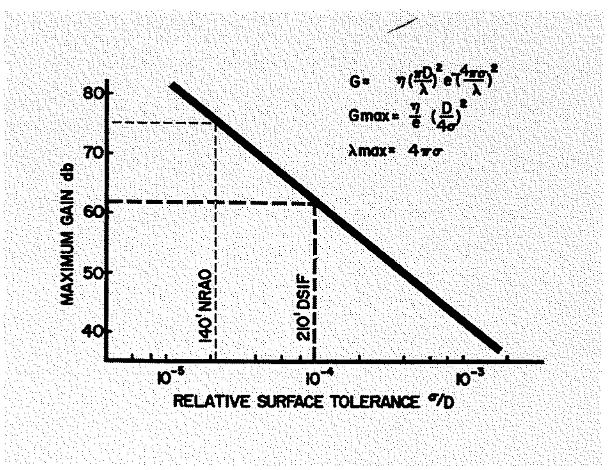

Fig. 10—Structural gain limits.

of RF power but rather to improve the quality of transmitter power. Frequency stability and phase coherence of the transmitters must be improved, particularly for relatively low data-rate missions to the outer planets; tube efficiencies must also be improved. Such techniques as beam focusing and the use of tapered helixes and multiple collectors may be used. Solid-state amplifiers should be integrated with the solar cells, antenna, and cooling structures to improve the overall efficiency of the system and minimize the weight of these components.

LOW-NOISE RECEIVERS

The present state of the art for low-noise receivers is depicted in Table II. (In Table II and Fig. 7, *bath temperature* refers to the ambient temperature at the maser.) Maser amplifiers with an effective noise temperature of 8°K are presently available for ground terminal use, and traveling-wave masers with noise temperatures of less than 4°K are under development. These temperatures are already on the order of the temperature contributed by the antenna due to atmospheric and external noise; hence, further reduction in receiver temperature will do little to increase the microwave index of performance.

The use of multi-aperture receiving arrays will require many low-noise receivers at each station. The cost and performance of this component will have a major impact on the design of the receiving antenna, determining in part the number of subapertures in the required total aperture and hence their size. The important characteristics of the receiver in this application, other than temperature, will be cost, reliability, and maintainability. The size, weight, and power demand of the device will become as important for the ground terminal as for the space terminal.

The noise temperature of the traveling-wave maser is limited by the inversion ratio in present material and by the unfavorable gain-to-loss ratio at elevated temperatures. Basic research in materials, slow-wave structures, and optimum heat stationary techniques should extend the maser art toward higher operating temperatures with small reduction in performance (Fig. 7). The need for maser operation at higher operating temperatures is shown in Fig. 8. It appears that operating temperatures between 16° and 20°K will be the optimum choice, considering the weight and power required for the refrigeration system.

The goal of research in this component should be directed toward improved maser materials and fabrication techniques as well as improved techniques

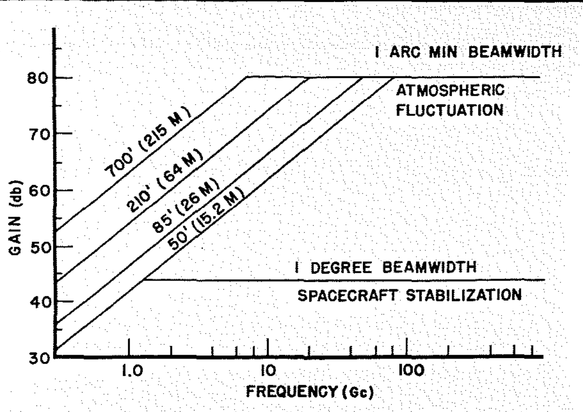

Fig. 11—Single-aperture gain limits.

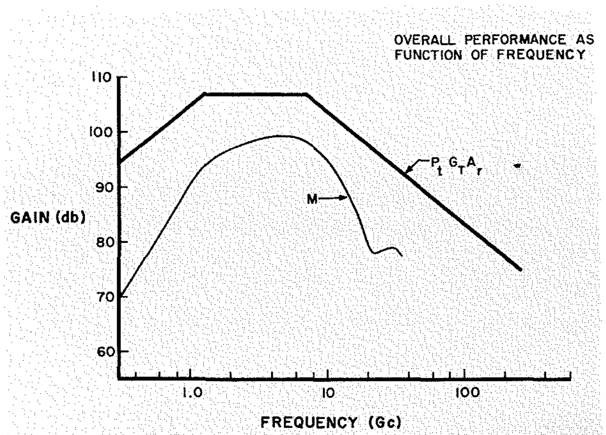

Fig. 12—Overall microwave performance as a function of frequency.

for thermal isolation between components of the system. More efficient and lighter weight closed-cycle cryogenic equipment will be required as well as more efficient RF pump sources.

TRANSMITTING ANTENNA GAIN

The principal constraints on the gain of the spacecraft transmitting antenna are pointing accuracy and surface tolerance. Pointing accuracy can be reckoned in pounds of control power, and surface tolerance in antenna structure weight. The loss in antenna gain due to pointing error is shown in Fig. 9. To limit gain loss due to pointing error to about 0.12 dB, the antenna beamwidth at the 3-dB points should be about 10 times the pointing accuracy of the antenna structure. A pointing accuracy of 1° (Mariner IV) will support an antenna beamwidth of 10° or a gain of about 24 dB.

TABLE II—Traveling-Wave Masers Operating at 4.2° K Bath Temperatures—Presently Available or Under Development

Freq. Range (MHz)	Gain (dB)	Band-width (MHz)	Noise Temp. (°K)	Packaging	Use	Comments
2.0-3.0	25	5	10	Closed-Cycle refrigerator	Classified	Superconducting (SC) magnet control center for operation 2000 ft from antenna
2.2-2.4	50	12	8	Dewar	Laboratory	For NASA
3.1-3.2	25	50	8	Dewar	Radiometer	Antenna-mounted for 150-ft dish developed for National Research Council of Canada
3.0-4.5	30	30	10	Closed-Cycle refrigerator	Classified	
4.5-6.2	30	30	10	Closed-Cycle refrigerator	Classified	
4.125	30	150	8	Closed-Cycle refrigerator	ATS satellite program	SC magnet—new refrigerator with 5000 hours MTBF
5.4-5.9	30	15	10	Dewar and refrigerator	Monopulse radar	3-channel maser; common SC magnet and pump
9.0-11.0	30	20	12	Dewar	Radiometer	For National Bureau of Standards ultrastability gain ± 0.001 dB
11.0-12.0	30	20	12	Dewar	Radiometer	For NBS ultrastability gain ± 0.001 dB
33.0-37.0	30	20	Less than 20	Dewar	Radiometer	For NBS ultrastability gain ± 0.001 dB

To minimize the acquisition problem introduced by the use of a high-gain antenna on the spacecraft, the antenna beamwidth should be of the same order as the mechanical stabilization. With RF sensing for accurate antenna pointing, a transmitting antenna beamwidth of 1° with about 44 dB gain can be achieved.

Because of the limitations imposed by pointing accuracy and acquisition, the transmitting antenna will be beamwidth limited and hence gain limited. Its diameter will be about two orders of magnitude less than that of the receiver, and its surface accuracy will be nearly equal to that of the receiver. The relative surface tolerance (σ/D) required for this antenna will therefore be about two orders of magnitude larger than that of the receiver and should not limit the design.

The goal of research in spacecraft antennas should be the development of a very lightweight antenna taking advantage of the relatively large surface tolerance. Both RF sensing and antenna beam-positioning techniques must be developed to handle beamwidths in the order of 1° or less. Single-channel RF error-sensing techniques should be developed to eliminate the need for additional receiver channels for the sensing function. In addition, techniques for integrating the transmitting antenna, RF power source, prime power source, and cooling structure should be developed to improve overall reliability and reduce the combined weight of these components.

GROUND ANTENNA SYSTEM

Finite weight and power limitations on the spacecraft make it necessary to obtain a large part of the increased performance in the communication link at the Earth terminal. This conclusion is also supported by the multiple use of these facilities, which permits cost sharing among many missions. The 210-foot reflector presently being installed at the Deep Space Instrumentation Facility (DSIF), Goldstone Lake, Calif., represents nearly an order of magnitude increase in receiver aperture over the 85-foot reflector used for the Mariner IV mission. Future missions will require an increase of at least another order of magnitude in effective receiver aperture. Disappointing results with reflectors of this size in the past suggests that a new approach is required.

The maximum gain of an antenna is determined by its relative surface tolerance (σ/D), the ratio of surface tolerance to antenna diameter (Fig. 10). A tenfold increase in effective area implies a threefold to fourfold decrease in relative surface tolerance expressed as the ratio of RMS surface tolerance to antenna diameter (σ/D). A σ/D value of 10^{-4} represents the 210-foot reflector and is consistent with a maximum gain of about 62 dB. A relative reflector tolerance of 1.7×10^{-5} has been achieved by MIT Lincoln Labs on their 120-foot Haystack antenna inside a radome. The new 140-foot radio telescope for the National Radio Astronomy Observatory at Greenbank, W. Va., has a relative surface tolerance of 2.2×10^{-5}, achieved without radome protection. Thus single reflectors (using mechanical collimation) of the requisite accuracy can be built with diameters up to about 150 feet. For much larger aperture areas, electronic collimation must be used.

To determine the optimum frequency for the communications system, careful attention must be given to the factors that limit the gain or effective area of the antenna. As an example consider a diameter of 50 feet as a practical aperture limit for future deep-space vehicles, and a diameter of about 700 feet as a limit for the ground-based aperture. Conversely we can assume that the spacecraft antenna beamwidth is limited to about 1° by stabilization requirements and the Earth antenna beamwidth is limited to about 1 arc minute by atmospheric fluctuation. The antenna gain as a function of frequency subject to these constraints is shown in Fig. 11.

The overall performance of the microwave portion of a deep-space communications system using antennas constrained as indicated above is shown as a function of frequency in Fig. 12. In this figure the frequency dependence of atmospheric loss and noise temperature has been included with that of antenna gain and receiver cross-section. Note that the microwave index of performance has a rather broad maximum between 1 and 10 GHz. With a little rain, however, the upper frequencies are rapidly attenuated. Thus the present NASA communications band is expected to see continued use into the forseeable future.

Multiple apertures have been proposed whose collected energy is summed through phase-locked loops. This technique amounts to a phased array of large elements. Note that the effective area A_e of the receiver is related to the information bandwidth (Δf), the maximum scan angle θ, the aperture efficiency η, and the velocity of light c by:

$$A_e = \frac{\eta}{4\pi}\left(\frac{c}{\Delta f \sin\theta}\right)^2$$

when maximum gain is required at the band edges. This results in an area limited to about 3×10^3 square meters for a 2-MHz bandwidth with the array steered to 60° from zenith. Since even this aperture size would produce a 4-dB droop at the band edges, and since larger apertures will be required, time-delay steering must be used to provide adequate bandwidth, perhaps using delay-locked loops.

To improve performance it is important to maintain at least the present system noise temperature, which requires very close control of the antenna side-lobe structure. Although back lobes are most important in determining the antenna noise temperature, those side-lobes that *look* through the atmosphere at the lower elevation angles can also contribute significant noise temperature. This requires very low side-lobes beyond about 20° of the main beam. Unusually high side-lobes, such as grating lobes, within 20° of the main beam can cause a serious increase in noise temperature when pointing toward some hot object in the sky. Grating lobes can be particularly troublesome when the propagation path is close to the sun.

The goal of research for an Earth-terminal antenna system should be the development of a large time-delay-collimated, multi-aperture antenna system with noise contribution from the ground and low elevation angles on the order of 4°K. The techniques developed for this application must provide an average side-lobe level of about 80 dB with peak side-lobes or grating lobes of the order of 40 dB below the main beam.

CONCLUSION

A communication rate of 10^6 bits per second from Mars is clearly feasible as a 10-year goal. The most significant step toward achieving this goal will be the development of a very-large-aperture, low-noise, electronically scanned, receiving antenna at the Earth terminal. The large number of low-noise receivers needed for such a system makes a more efficient design essential.

At the deep-space terminal, weight and power will be critical. Electronic scanning techniques will reduce the stabilization requirements on the spacecraft. Solid-state techniques must be developed for more-efficient power conversion. Integration of thermal and electrical functions in the spacecraft antenna system should provide the high effective radiated power per pound of payload weight required for future long-duration deep-space missions.

ACKNOWLEDGMENT

The authors wish to express their appreciation to L. C. Morris of Applied Research, DEP for his contributions to this paper, particularly for the preparation of Table II and Figures 7 and 8.

WILLARD T. PATTON received his BSEE and MS degrees from the University of Tennessee in 1952 and 1958, respectively. He received his PhD in Electrical Engineering from the University of Illinois in 1963. While on the staff of the University of Tennessee Experiment Station, he did research on circular arrays. He was an instructor at the University of Illinois, and he conducted research on log-periodic and simply periodic antennas at the Antenna Laboratory; he also was a consultant with the Radio Direction Finding Laboratory. For 3 years he was Ship Superintendent for DER conversions at the Boston Naval Shipyard. Since joining RCA's M&SR Div., Moorestown, N.J. in 1962, he has done research on large phased arrays. Dr. Patton is the author or coauthor of several technical publications, and he is a member of the IEEE, AAAS, Sigma Xi, Tau Beta Pi, and Eta Kappa Nu.

ALVIN B. GLENN received his BEE degree from Polytechnic Institute of Brooklyn in 1938, his MSEE from MIT in 1941, and his PhD in Electrical Engineering from Syracuse University in 1952. As an adjunct Professor at Drexel Institute of Technology, he teaches graduate courses in statistical theory of communications, information theory, and modulation theory. While with Sperry Gyroscope and Western Electric, he specialized in radio receiver design and UHF and microwave tube development. For 5 years he did advanced development and product design of TV receivers for General Electric. Since joining RCA in 1954, he has been engaged in the synthesis, analysis, and evaluation of communication systems. He is presently concerned with high-survivability satellite communication systems and interplanetary communications. Dr. Glenn is a member of Sigma Xi, Tau Beta Pi, Eta Kappa Nu, and interplanetary communications. As Staff Engineer of SEER, he acts as a consultant on communications systems for DEP. Dr. Glenn is a member of Sigma Xi, Tau Beta Pi, Eta Kappa Nu, and IEEE. He has served on and was chairman of several IEEE committees since 1959. He is listed in "American Men of Science." He has published or presented more than 40 technical papers.

DIMATE—A SPACE-AGE ROBOT

One of the most versatile of the space-age robots is a computer-controlled automatic test set developed by the Aerospace Systems Division. The test set, known as Depot Installed Maintenance Automatic Test Equipment (DIMATE), is installed at an Army Depot. This paper describes the DIMATE system and its operation.

R. L. McCOLLOR, Ldr.,
Automatic Test Equipment Programs
Aerospace Systems Div., DEP, Burlington, Mass.

THE DIMATE (Depot Installed Automatic Test Equipment), one of the family of automatic test sets developed by RCA for field and depot maintenance support of U.S. Army electronics, performs automatic inspection testing and fault isolation of all U.S. Army radio communication equipments — personal, vehicular, and airborne. DIMATE System No. 1 inspects and tests high-density radio sets.

The advantages of automatic test equipment, as compared to conventional test equipment, are as follows:

1) *Reduction in test time of 3 or more to 1.* This reduction is due to the automatic recording of test data and the elimination of manual adjustments.
2) *Reduction in number of test equipment line items required.*
3) *Standardization of test procedures and test results.* All test instructions, prerecorded on perforated or magnetic tape, are performed automatically in the same sequence for each unit under test, and all test results are automatically recorded.
4) *Reduction in operator skill level and training requirements.* Prerecorded test instructions are used. The standardization of test procedures and test results and reduced number of line items of test equipment shortens the training time required.
5) *Minimized obsolescence of test equipment.* Introduction of new prime systems into the Army inventory requires new test program tapes rather than new test equipments.
6) *Reduced calibration time and types of calibration equipments required.* DIMATE contains internal standards for self-test and calibration checks; only 19 of the 83 assemblies, or *building blocks,* require periodic calibration against external standards.

SYSTEM DESCRIPTION

The DIMATE computer-controlled automatic test set is actuated by a perforated tape, a magnetic tape, or a manual keyboard input. It is capable of automatic, semiautomatic, and manual testing of U.S. Army communication equipments and many other types of electronic, electrical, and electromechanical equipments. It consists of seven racks, an operator's control console, and a tape-preparation station containing 83 assemblies of 59 types. These assemblies are interconnected to form five functional subsystems, or groups, as follows: computer/controller group, measurements group, low-frequency stimulus group, direct-current stimulus group, and internal power supply group. Fig. 1 is a rack layout showing the location of the various assemblies, or building blocks, in the system.

Computer/Controller Group

Included in this group are the operator's control console (with controls and displays), computer, controller, printer, perforated tape reader, magnetic tape transport, manual input keyboard, and a visual instructor (microfilm viewer). An automatic typewriter with a perforated tape punch and reader is provided for off-line preparation and reproduction of program tapes. The computer/controller group performs the functions of information storage, retrieval, search, identification, selection, and interpretation. Following interpretation of the selected data, it directs and controls the programmable functions of assemblies in the other equipment groups.

The computer/controller group compares the responses of units under test (UUT's) or other assemblies of DIMATE with internal standards or programmed limit values, interprets and evaluates the comparisons, prints the results of the evaluations, and determines and directs subsequent operations.

Measurements Group

This group consists of signal-conditioning equipments, analog-to-digital converters, a time-interval and frequency converter, reference standards, switching for the selection of test points and the interconnection of the measurement assemblies, and a test-results display.

The primary function of the measurements group is to convert voltage, resistance, frequency, and time intervals to digital data. Signal-conditioning devices are provided for scaling and to convert power, impedance, or modulation characteristics to voltage and frequency for processing by the analog-to-digital converters. Programmable switches, under control of the computer/controller, select test points and route signals from the UUT's or other DIMATE assemblies to the appropriate adapters and converters for signal conditioning and conversion to digital data. A data output buffer routes the digital data to the computer/controller for processing and comparison. The data output buffer also converts the digital data to a decimal data and function for display on the test-results display.

Low-Frequency Stimulus Group

Included in this group are a frequency standard (for frequency and time base reference), a pulse generator, and AF and RF generators. These assemblies provide CW sine-wave signals from 100 Hz(c/s) to 400 MHz(Mc/s), and amplitude-, frequency-, or pulse-modulated signals with carrier frequencies from 100 kHz to 400 MHz. Programmable routing and application switches interconnect the stimulus assemblies and connect the stimuli to UUT's and assemblies in other DIMATE groups.

Direct Current Stimulus Group

This group, containing programmable, regulated DC power supplies, provides DC power of 5 to 850 volts at currents from 200 milliamperes to 20 amperes, depending upon voltage. In addition, two precision DC reference supplies provide 0 to 10 volts at currents up to 100 milliamperes. Application switches switch power or reference signals to UUT's and assemblies in other DIMATE groups.

Internal Power Supply Group

This group consists of a primary power control, DC power supplies, voltage regulators, and individual-rack power controls. It provides all DC power, both regulated and unregulated, required for the operation of DIMATE. In addition, it provides program-controlled switching to route AC and DC power from the depot power mains to a UUT.

SYSTEM OPERATION

The simplified block diagram of DIMATE in Fig. 2 shows the interfaces between the functional subsystems and the routing and distribution of power, control data, stimulus, and response signals.

The first portion of the test program is a *confidence test,* which automatically self-tests selected stimulus and measurement functions to determine if the DIMATE is within allowable tolerances

Final manuscript received January 26, 1966.

and capable of performing the required tests on the UUT.

The next portion of the test program is a series of static tests (impedance and resistance measurements) on the UUT. These static tests determine the presence of shorts or open circuits in the UUT power and input circuitry and thus prevent damage to both the UUT and the DIMATE (through application of either power or stimulus to a short or open circuit).

If both the DIMATE and the UUT are capable of further testing (as determined by the results of the confidence and static tests), the program continues into the dynamic portion of the test program. During dynamic testing, power is automatically applied to the UUT; selected stimuli are applied sequentially or simultaneously, as required, to the UUT and the response to each stimulus is measured. When required, arithmetic operations are performed on two or more responses to derive secondary measurements, e.g., gain or insertion loss, bandwidth, percent modulation, frequency deviation, and distortion. The response and computed secondary results are compared with programmed upper and lower limits in the comparator/time delay and the results are displayed to the operator by means of the test-results panel and the printer.

When operator participation is required in a test (e.g., adjustment of the UUT or manual test-point selection by means of a probe), the instructions are recorded on the program tape and printed out by the printer. Where identification of controls, parts, or test points is required, photographs or drawings are provided on microfilm and displayed on the visual instructor located above the printer on the operator's control console. Where a manual operation is required during a test, the test is automatically halted and the operator instructions are printed out. Reference to drawings, photographs, or detailed text instructions on microfilm are printed out when required. After performing the necessary adjustments or other manual operations, the operator depresses the *proceed* switch on the control panel and the test continues automatically.

Fault-isolation test routines are programmed for each probable UUT malfunction. If a test result is within programmed limits, the test is *go* and the DIMATE automatically proceeds to the next step in the program. If a test result is not within the programmed limits, the test is *no-go*. Depending upon whether the test result is a negative response, above the upper limit or below the lower limit, the DIMATE automatically selects the proper fault-isolation routine and performs the necessary tests to determine the most probable location and cause of the malfunction. Faults are isolated to one or more modules or replaceable subassemblies in modularized equipments and to one or more discrete circuit functions in nonmodularized equipments.

The value of each measurement is displayed on the test-results panel and all test numbers, test results, and operator instructions are printed out on the printer. When desirable, alignment procedures, repair instructions, and references to handbooks, drawings, and other documentation may be included on the test program tapes along with the fault-isolation routines, and these will be printed out with the appropriate fault indications.

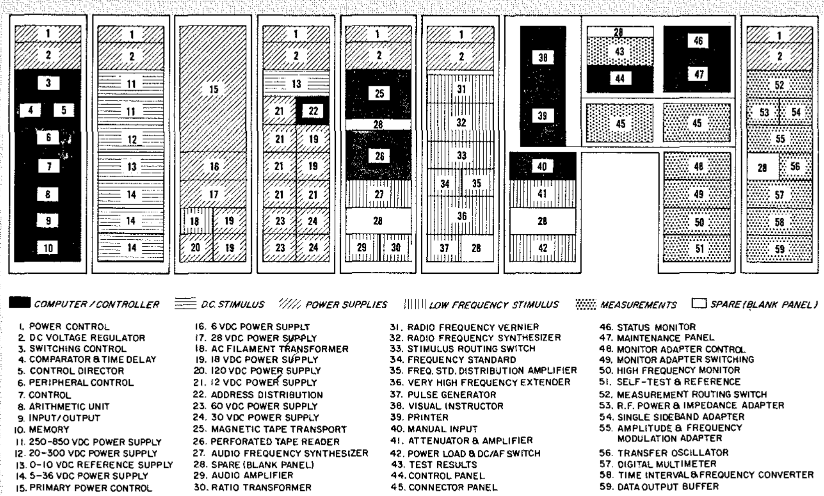

Fig. 1 — DIMATE rack layout showing location of building blocks.

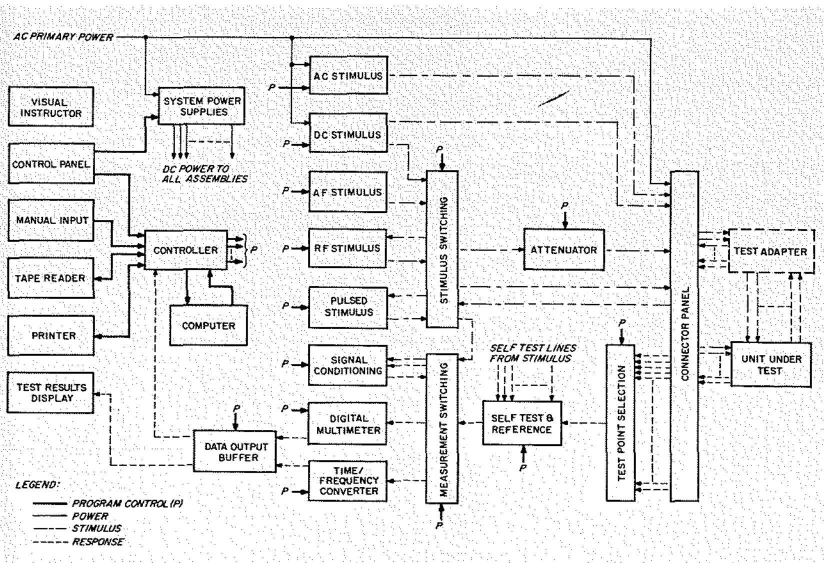

Fig. 2—Simplified block diagram of DIMATE.

ROBERT L. McCOLLOR received an associate degree in Mechanical Engineering from North Dakota Agricultural College in 1944 and a BA degree in Physics from Morningside College in 1949. Since joining RCA in March 1952, he has worked on airborne fire-control equipment, radar beacon transponders, digital-data communication system studies, and automatic test equipment (ATE). In 1954, he became a leader for MA-10 radar development. He is presently in the ATE Project Management Office, where he is responsible for system studies for the U.S. Army Electronics Command. Mr. McCollor is a member of Sigma Pi Sigma and the American Association for the Advancement of Science.

TEMPERATURE-COMPENSATED CRYSTAL OSCILLATORS

Temperature compensated crystal oscillators are finding increasing uses in place of oven controlled oscillators. Design of the TCXO is difficult and costly because of close tolerance requirements. Oscillator circuit design approaches, aimed at minimizing the design cost, are described and mathematically analyzed. Good correlation is obtained between calculated and actual performance.

P. K. MROZEK

Mobile Communications Engineering
Broadcast and Communication Products Division, Meadow Lands, Pa.

TEMPERATURE compensated oscillators (TXCO), although well known for a number of years, only recently have been gaining in popularity. This method of achieving an accurate and stable frequency source over wide temperature ranges has a number of important advantages over the better-known oven controlled oscillator; the most important are:

1) elimination of warm-up time
2) reduction of power drain and size
3) improvement in long term crystal stability because of lower average operating temperature

All TCXO's rely on compensating for crystal frequency drifts with temperature by varying the crystal load capacitance in a pre-determined manner. Accurate control of circuit components and crystal parameters is required to ensure that the compensating network temperature characteristic matches that of the crystal to the specified tolerance limits. The circuit designer will probably make use of a combination of close tolerance specifications and optimum selection of components to achieve a least costly design. There is however, one important consideration which complicates the design of TCXO. Crystal oscillators are usually provided with a trimmer capacitor (often called *warping trimmer*) which is used to reset the frequency periodically to maintain the frequency within overall specified limits. Frequency warping is necessary because changes do occur in the oscillator frequency over extended period of time due mainly to crystal aging. This trimmer may also be used to correct frequency drifts in other parts of the system. Unfortunately, the frequency compensating characteristic is dependent on the value of trimmer capacitance because of the hyperbolic relationship between crystal frequency and crystal load capacitance. Because of this *trimmer effect* on compensation, critical requirements are normally placed on crystal itself in terms of better aging and tighter tolerances. Oscillator design approaches described are aimed at minimizing this effect, and consequently, permitting the use of lower cost crystals.

Final manuscript received August 22, 1966.

OSCILLATOR ANALYSIS

The model selected for this design analysis is the Colpitts type oscillator shown in Fig. 1, where:

R_1, R_2, R_E provide conventional transistor bias.
R_3, C_3 provide by-pass and battery blocking.
C_4 is output coupling capacitor.
C_E, C_B are fixed capacitors providing correct feedback for oscillation.

In the current generator equivalent circuit of the oscillator (Fig. 2):

R_E = total parallel emitter-to-collector resistance including output resistance.
C_E = total parallel emitter to collector capacitance.
R = parallel combination of bias resistors R_1 and R_2.
g_m = transconductance.
X = crystal effective parameters, equivalent to series inductance L_x and series resistance R_x given approximately by:

$$L_x = \frac{1}{W_o^2 C_1} \frac{2\Delta f}{f_o} \frac{1}{\left(1 - \dfrac{C_o}{C_1}\dfrac{2\Delta f}{f_o}\right)} \quad (1)$$

$$R_x = \frac{R_o}{\left(1 - \dfrac{C_o}{C_1}\dfrac{2\Delta f}{f_o}\right)^2} \quad (2)$$

where: C_1 = crystal motional capacitance, C_o = crystal shunt capacitance, R_o = crystal series resistance, and f_o = crystal series resonant frequency given by:

$$W_o^2 = \frac{1}{L_1 C_1}$$

L_1 = crystal motional inductance.
$\Delta f = f - f_o$, f = frequency of oscillations.
When R_e, C_e, R_b, C_b, R_r, and C_c are the corresponding series equivalent parameters and when the ratio of parallel resistance-to-parallel reactance is assumed to be more than 10, the following conditions exist: $C_e = C_E$, $C_c = C$, and $C_b = C_B$. Under these conditions, a voltage generator equivalent circuit (Fig. 3) is obtained.

Frequency Symbols: f = frequency, ΔF = frequency change or compensation, Δf = frequency difference, and Df = frequency range.

FREQUENCY RELATIONSHIPS*

Solution of the equivalent circuit of Fig. 3 yields the approximate frequency of oscillation in parts per million (ppm) and the minimum g_m required:

$$\frac{\Delta f}{f_o} = \left(\frac{C_1 \cdot 10^6}{2(C_o + C_s)}\right)\left(1 + \frac{1}{Q_c Q_s} + \frac{1}{Q_b Q_s}\right) \quad (3)$$

$$g_{m(min)} = R_S W_o^2 C_E C_B \quad (4)$$

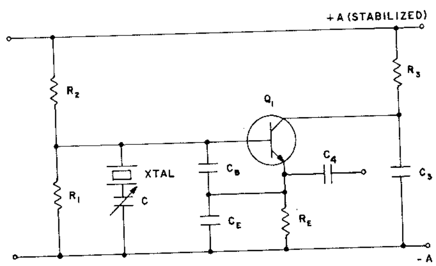

Fig. 1—Crystal oscillator.

PAWEL K. MROZEK received his BSc degree in Engineering from the University of London in 1955. After one year with British Communication Corporation in London, he joined Cossor Communication Company, also in London, where he gained extensive experience in development and design of circuits for SSB, FM, and Frequency Synthesizers. He was promoted to Senior Engineer in 1958, and became Section Leader in 1960. Since joining RCA in 1960 he has been concerned primarily with Mobile Communications.

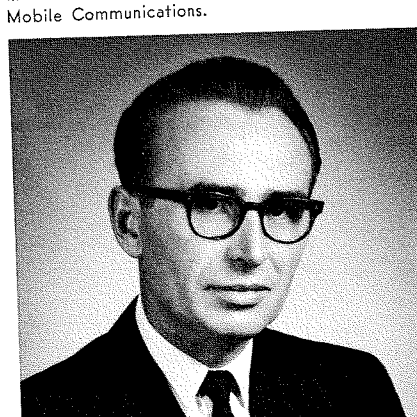

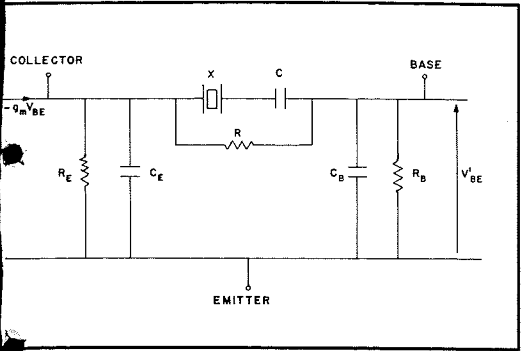

Fig. 2—Current generator equivalent circuit.

where: C_s = effective load capacitance given by:

$$\frac{1}{C_S} = \frac{1}{C_E} + \frac{1}{C_B} + \frac{1}{C}$$

$$Q_e = \frac{1}{W_oC_ER_e} = W_oC_ER_E$$

$$Q_b = \frac{1}{W_oC_BR_b} = W_oC_BR_B$$

$$Q_s = \frac{1}{W_oC_sR_s}$$

$$R_s = R_e + R_x + R_r + R_b$$
$$= \text{total circuit series resistance}$$

Equation 3 can be rewritten in terms of parallel emitter and base parameters:

$$\frac{\Delta f}{f_o} = \left(\frac{C_1 \cdot 10^6}{2(C_o + C_s)}\right)\left(1 + \frac{C_sR_s}{C_ER_E} + \frac{C_sR_s}{C_BR_B}\right) \qquad (3a)$$

FREQUENCY COMPENSATION*

Frequency compensation is achieved by varying crystal effective load capacitance C_s to compensate for crystal frequency changes with temperature.

Fig. 4 is a typical temperature-frequency characteristic of an AT-cut crystal plotted in terms of oscillator frequency change ΔF with respect to reference temperature t_o. It is convenient to express the required variations of capacitance in terms of capacitance changes ΔC_s with respect to the same reference temperature. Capacitance changes are small compared to C_S, and therefore the relationship between ΔC_s and ΔF can be obtained by differentiating Equation 3a with respect to C_s, yielding:

$$\Delta F = \rho \Delta C_S \qquad (5)$$

Where ρ = frequency sensitivity per unit capacitance obtained by differentiation (in ppm/pF).

* Note that hereafter all expressions for frequency and frequency changes are in parts per million, abbreviated by ppm.

The required ΔC_s, as a function of temperature, can be provided by a number of temperature sensitive networks, such as a thermistor-capacitor, or thermistor-voltage variable capacitor. The closeness of correlation between ΔC_s required, and ΔC_s obtained from the compensating network, will depend on the type and number of networks used.

Referring to Fig. 1, compensating networks can be connected in parallel with any of the circuit capacitors C_B, C_E, C, or in parallel with the crystal. However, since C_B and C_E are usually large, requiring large ΔC for a given ΔF, the most common connections are in parallel with C or the crystal.

TRIMMER EFFECT ON COMPENSATION

Let us consider the common case where capacitance C is made variable to obtain frequency trimming; compensation is thus applied in parallel with the trimmer capacitor (Fig. 5a).

All equations derived previously under *Oscillator Analysis* apply; from Equation 3a, it is seen that the frequency of oscillation depends also on circuit resistances. However, the effect of resistance can be made negligible by making R_EC_E and R_BC_B sufficiently large, the only limitation being the magnitude of transistor transconductance available. Under such conditions a simplified form of Equation 3a is obtained:

$$\frac{\Delta f}{f_o} = \frac{C_1 \cdot 10^6}{2(C_o + C_S)} \text{ (in ppm)} \qquad (6)$$

By differentiation, the frequency sensitivity becomes:

$$\rho c_s = \frac{-C_1 \cdot 10^6}{2C_S^2\left(1 + \frac{C_o}{C_s}\right)^2} \text{ (in ppm/pF)} \qquad (7)$$

Further, by making use of the relationship:

$$\frac{1}{C_s} = \frac{1}{C_E} + \frac{1}{C_B} + \frac{1}{C}$$

frequency sensitivity ρc to the capacitance change in parallel with C becomes:

$$\rho c = \frac{-C_1 \cdot 10^6}{2C^2\left(1 + \frac{C_o}{C_s}\right)^2} \text{ (in ppm/pF)} \qquad (8)$$

When C_o/C_s is small compared to unity (the usual case), frequency sensitivity, and therefore also the frequency compensation, ΔF of Eq. 5 will be inversely proportional to the square of the value of the trimmer capacitor; this relationship holds true for a given Δc at any temperature. When a given variable "trimmer" frequency range Df, is required with a corresponding load capacitance change DC_s, the ratio of the frequency compensation at the two trimmer capacitor extremes is given by:

$$\frac{\Delta F_1}{\Delta F_2} = 1 + \frac{2DC_S}{C_o + C_{S1}} \qquad (9)$$

where, $DC_S = C_{S2} - C_{s1} =$

$$\frac{2Df}{10^6}\,\frac{(C_o + C_{S1})^2}{C_1}$$

C_{S1} = load capacitance corresponding to high frequency

C_{s2} = load capacitance corresponding to low frequency

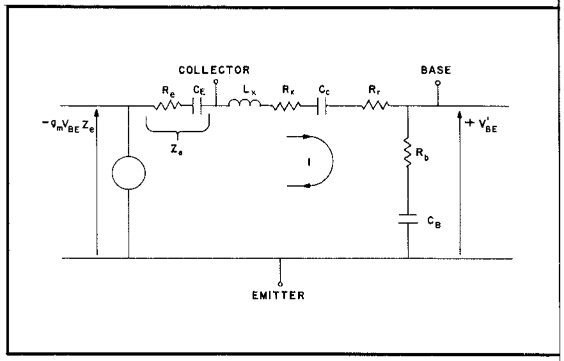

Fig. 3—Voltage generator equivalent circuit.

With a typical crystal having $C_o = 6$pF, $C_{S1} = 24$pF, $C_1 = 0.03$pF, and the trimmer capacitance range required of ± 35 ppm, i.e. $Df = 70$ ppm, the compensation change will be 28% giving a variation of

Fig. 4—Typical frequency—temperature curve of an AT cut crystal.

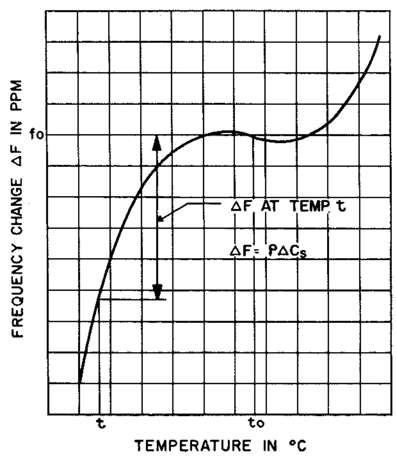

Fig. 5—Connections for compensation networks.

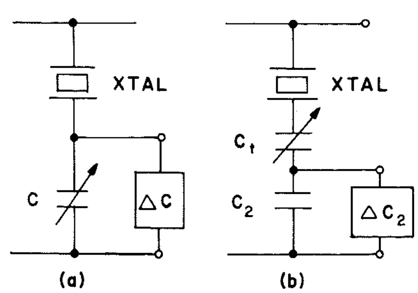

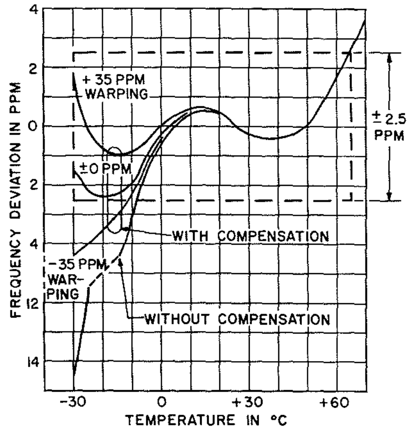

Fig. 6—Trimmer capacitor effect on compensation (commonly used method).

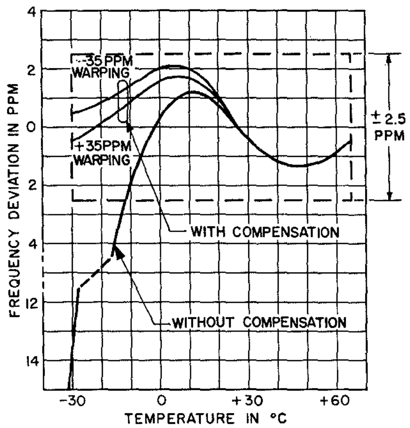

Fig. 7—Trimmer capacitor effect on compensation (case 1).

± 14% within the trimmer capacitance range. The meaning of this variation may be clearer, if one considers a given compensation of 14 ppm at a particular temperature of interest. Over an extended period of time, after the frequency of oscillation is readjusted, the compensation could change by ± 2.0 ppm which of course would add to the overall frequency tolerance of the oscillator. From Fig. 6 (curves obtained from measurements on this type of oscillator), it is clear that with an overall tolerance of ± 2.5 ppm required, the oscillator frequency would be outside the tolerance limits at one trimmer capacitor extreme.

It is possible to reduce this trimmer capacitor effect considerably, and finally to eliminate it completely. The remainder of this paper covers two cases in which this is accomplished.

Case 1: Trimmer Effect Reduction

For case I, refer to Figs. 1 and 5b in which capacitor C is divided into two series components: 1) C_t which is variable and used for trimming, and 2) fixed capacitor C_2 used for compensation so that:

$$\frac{1}{C} = \frac{1}{C_t} + \frac{1}{C_2}$$

Again, all equations derived under *Oscillator Analysis* apply for the above relationship of C in terms of C_t and C_2.

When a small ΔC_2 is introduced in parallel with C_2 rather than in parallel with C, the compensating frequency change due to a given ΔC_2 is obtained, by differentiation with respect to C_2:

$$\Delta F = \rho C_2 \Delta C_2$$

$$= \frac{-C_1 \Delta C_2 \cdot 10^6}{2C_2^2\left(1 + \frac{C_o}{C_s}\right)^2} \text{ (in ppm)}. \quad (10)$$

Since C_o/C_s is small compared with unity, the frequency change is inversely proportional to the square of the fixed capacitance, C_2 and therefore remains substantially constant within the trimming capacitor range. The amount of variation depends only on the practical value of C_o/C_s relative to unity.

If ΔF_1 and ΔF_2 are frequency changes at the two frequency trimming extremes, the ratio in this case is given approximately by:

$$\frac{\Delta F_1}{\Delta F_2} = \left(1 + \frac{2DC_s}{C_o + C_{s1}}\right)\left(\frac{1}{1 + \frac{2DC_s}{C_{s1}}}\right) \quad (11)$$

where:

$$DC_s = \frac{2Df}{10^6} \; \frac{(C_o + C_{s1})^2}{C_1}$$

With the same typical crystal and the same trimmer frequency range required as in the previous case, the compensation variation within the trimming range will be ± 2.5%.

An oscillator was built using an 8.5 MHz crystal with a thermistor-capacitor network to obtain a frequency compensation of 14 ppm at −30°C with respect to reference temperature of 25°C. The two curves, one at −35 ppm and one at +35 ppm are shown in Fig. 7. Total compensation change is seen to be ± 0.5 ppm, or ± 3.5%.

Case 2: Trimmer Effect Reduction

By making use of the resistive effects on frequency, it is possible to design an oscillator that is virtually independent of the variable trimmer capacitor. However, this applies only to such systems as the thermistor-capacitor where the compensation process includes coupling both capacitance and resistance. Both changes, ΔC_s, capacitive, and ΔR_s, resistive, can be expressed as a function of temperature. In the case of thermistor-capacitor compensation, the two functions are mutually dependent; but, it is possible to think of a network wherein the variables can be independently controlled. In such a method, a modification of Fig. 1 circuit is necessary; Fig. 8 represents this modification where:

R_1, R_2, R_E provide conventional transistor bias; but, since R_E, in this circuit is part of the compensation, the values are carefully selected according to design requirements.

C_2, C_1, C_E, C_B make up the crystal load capacitance.

C_E variable capacitor to obtain frequency trimming.

C_2 a fixed capacitor across which a temperature sensitive network C_1, R_t, is connected.

R_t Thermistor, i.e., temperature sensitive resistor.

The voltage equivalent circuit remains as shown in Fig. 3, except that a small series resistive component ΔR_s is added to indicate resistive effect of the thermistor-capacitor network (Fig. 9). Solution of this circuit gives the approximate frequency of oscillation as was done in Equation 3:

$$\frac{\Delta f}{f_o} = \left(\frac{C_1 \cdot 10^6}{2[C_o + C_s]}\right)\left(1 + \frac{C_s R_s}{C_E R_E} + \frac{C_s R_s}{C_B R_B}\right) \quad (12)$$

where, C_s is given by:

$$\frac{1}{C_s} = \frac{1}{C_E} + \frac{1}{C} + \frac{1}{C_B}$$

and $C = C_1 + C_2$ at reference temperature when R_t is small and:

$$R = R_e + R_x + R_r + R_b + \Delta R_s$$

Rewriting Equation 12, and assuming that $C_B R_B$ can be made much larger than $C_E R_E$:

$$\frac{\Delta f}{f_o} = \frac{C_1 \cdot 10^6}{2(C_o + C_s)} + \frac{C_1 \cdot 10^6}{2\left(1 + \frac{C_o}{C_s}\right)} \cdot \frac{R_s}{C_E R_E} \quad (12a)$$

Examination of Equation 12a indicates that the frequency of oscillation is made up of two parts, one dependent on C_s and independent of R_s, and the other dependent on R_s and almost independent

Fig. 8—Crystal oscillator (case 2).

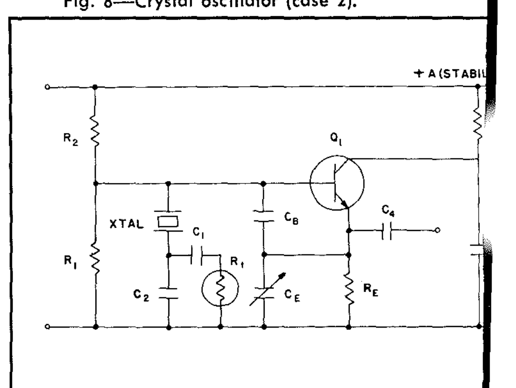

of C_s, since C_o/C_s is usually small compared to unity.

FREQUENCY COMPENSATION

As in previous cases, frequency compensation is achieved by introducing a small capacitance change ΔC controlled by the temperature sensitive thermistor. As the temperature changes from the reference temperature (t_o) where R_t is small and $C = C_1 + C_2$, to a lower temperature, the thermistor resistance increases and C is reduced by a corresponding ΔC. At the same time, the coupled resistance ΔR_s increases from a negligible value so that frequency change is brought about; the magnitude of the change is controlled by the magnitude of $1/C_E R_E$. These two effects: $\Delta F(C_s)$, the frequency change due to capacitance change; and $\Delta F(R_s)$, the frequency change due to resistance change; are used to achieve compensation independent of the trimmer capacitor.

From Eq. 12a, frequency due to C_s:

$$F(C_s) = \frac{C_1 \cdot 10^6}{2C_s\left(1 + \frac{C_o}{C_s}\right)} \qquad (13)$$

and frequency due to R_s:

$$F(R_s) = \left(\frac{C_1 \cdot 10^6}{2\left(1 + \frac{C_o}{C_s}\right)}\right)\left(\frac{R_s}{C_E R_E}\right) \qquad (14)$$

Since these two frequency components are mutually independent as far as C_s and R_s are concerned, the total frequency change, when both C_s and R_s change, can be obtained by differentiating $F(C_s)$ with respect to C_s; and $F(R_s)$ with respect to R_s, yielding the frequency change due to small ΔC_s:

$$\Delta F(C_s) = \frac{-C_1 \cdot 10^6 \Delta C_s}{2C_s^2\left(1 + \frac{C_o}{C_s}\right)^2}$$

Since compensation is applied in parallel with C, frequency change in ppm due to small ΔC:

$$\Delta F(C) = \frac{-C_1 \cdot 10^6 \Delta C}{2C^2\left(1 + \frac{C_o}{C_s}\right)^2} \qquad (15)$$

Frequency change due to small ΔR_s:

$$\Delta F(R_s) = \frac{C_1 \Delta R_s \cdot 10^6}{2\left(1 + \frac{C_o}{C_s}\right) C_E R_E} \qquad (16)$$

Now, ΔC is negative (less capacitance), when ΔR_s is positive (more resistance). Thus, when the temperature changes from the reference temperature to a lower temperature t, both changes are positive, and therefore, the total frequency change is:

$$\Delta F = \Delta F(C) + \Delta F(R_s) = \frac{C_1 \Delta C \cdot 10^6}{2C^2\left(1 + \frac{C_o}{C_s}\right)^2} + \frac{C_1}{2\left(1 + \frac{C_o}{C_s}\right)} \cdot \frac{\Delta R_s \cdot 10^6}{C_E R_E} \qquad (17)$$

The following conditions can be observed from Eq. 17 in considering the two trimmer capacitor extremes:

1) At high trimming frequency, both C_E and C_S are small; so that the first term is small and the second is large.
2) At low trimming frequency, both C_E and C_S are large; so that the first term is large and the second term is small. Therefore, within a given variable trimmer capacitance range, the change in amount of frequency compensation due to the capacitive effect is counteracted by the opposite change in compensation due to resistive effect.

Conditions for perfect cancellation of these two changes can be obtained by differentiating Eq. 17 with respect to C_E and equating to zero, which yields:

$$R_E = \frac{\Delta R_s}{2} \cdot \frac{C}{\Delta C} \cdot \frac{C}{C_o}\left(1 + \frac{2C_o}{C} + \frac{C_o}{C_E}\right) \qquad (18)$$

Thus, the required R_E is given in terms of ΔR_s, ΔC, C, C_E, and the crystal parameter. Since C_o/C_E is very small compared to unity, R_E is practically independent of C_E; therefore, an almost perfect stability of compensation is achieved within the trimmer capacitor range.

In practice, a simple thermistor capacitor compensating network ΔR_s is dependent on ΔC. Thus, when an exact ΔF is required according to design requirements, Equation 18 may be inconvenient to use. However, the resistive component of the compensation $\Delta F(R_s)$ will be usually small compared to $\Delta F(C_s)$; consequently, an approximate ΔF given by Eq. 15 can be first used to calculate the thermistor-capacitor network in terms of ΔC alone.

Emitter resistance R_E can then be selected to obtain the best results. At least two steps are usually required: 1) obtain good compensation stability within the trimmer range, and 2) make small readjustments on the thermistor-capacitor network to obtain the desired amount of compensation ΔF.

An oscillator was developed with an 8.5 MHz crystal, compensated for frequency drift in the temperature range from + 26°C to − 30°C, using a thermistor-capacitor network. The two measured curves corresponding to ± 35 ppm trimmer capacitor extremes are shown in Fig. 10. Note that the total compensation change is less than 0.25 ppm, i.e. less than ± 1.0%.

SUMMARY

Analysis of conventional crystal oscillator circuits can lead to practical modifications producing improved temperature compensated crystal oscillator performance with respect to stability of compensation over the trimmer frequency. Three

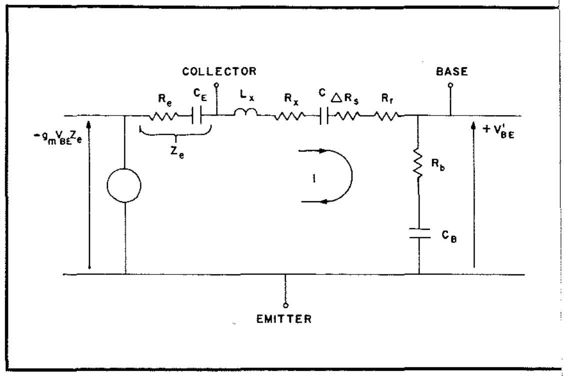

Fig. 9—Voltage generator equivalent circuit.

such oscillator circuits based on the foregoing theoretical analysis have been investigated:

1) *Conventional:* this can be considered a conventional circuit and illustrates the degree of improvement achieved in the other two oscillators. Temperature curves are shown in Fig. 6.
2) *Series oscillator circuit:* the improved results shown in Fig. 7 are achieved through making use of a series circuit that effectively reduces the variations of crystal frequency sensitivity with load capacitance.
3) *Controlled resistive effects:* this is basically the same as the series oscillator (2) where the remaining small variations in frequency sensitivity are eliminated by making use of controlled resistive effects. Temperature curves are shown in Fig. 10.

In each of the three oscillator circuits described in this paper, very good correlation has been obtained between predicted and actual oscillator performance.

ACKNOWLEDGMENTS

The author expresses his gratitude to W. J. Sweger for major assistance in the preparation of this paper, and to A. M. Missenda for contributions to the mathematical analysis. Derivations and proofs of the formulas and assumptions used in this paper will be furnished on request.

Fig. 10—Trimmer capacitor effect on compensation (case 2).

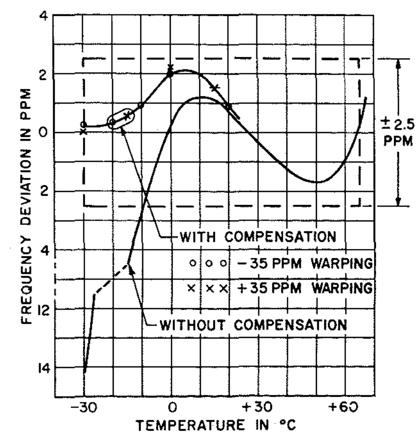

DIRECT FORCED-AIR COOLING SYSTEM FOR ELECTRONIC EQUIPMENT

This paper describes a perforated plenum technique for directing forced cooling air at equipment inside a rack enclosure. It is intended to show that this method is a relatively simple means of attaining reliable quantities of metered air directed at various levels within a rack. The data can be used in determining the applicability of this type of cooling to a particular system and to furnish information which can be applied to similar perforated-plenum configurations.

J. M. WARNICK
Aerospace Systems Div., Burlington, Mass.

As electronic packaging techniques become more sophisticated and component density increases, greater reliance is placed on the cooling system to maintain the equipment at a proper operating temperature level. In a single electronic rack enclosure where as high as 10,000 BTU's of heat per hour could be dissipated, a reliable means of cooling temperature-critical components and avoiding hot spots is necessary.

In the design of large systems consisting of many racks of electronics, as is often the case in ground support and shipboard equipment, it is usually necessary to establish the system packaging parameters at the beginning of the program. A standardization effort is made to select an overall chassis configuration, rack enclosure, and cooling system. Each item must be compatible with the others and the electronics which are to be packaged. The decision has to be made as to whether the equipment can be cooled strictly by free convection air or whether forced air is required. Consideration must also be given to the fact that many engineers will be packaging various equipment chassis, each with its own particular cooling requirements.

Final manuscript received March 7, 1966.

For high-density packaging, free convection throughout the rack usually is not sufficient. Forcing air through the rack is a minimum requirement. Where temperature-sensitive components are involved, there still may not be enough movement of air in the component area to carry away the heat. Although the air forced into the rack moves around the outside of the chassis, the heat-sensitive components inside may have to depend upon free convection. In such a case it would be advantageous to locate these components close to an air source so that the air can wash directly over them. A known quantity of metered air available at a known location would enable the packaging engineer to cope with this and similar situations.

PERFORATED-PLENUM CONFIGURATION

The plenum is a hollow pressurized duct which can be installed in the side of a rack, using the rack side cover as one of the plenum sides. The holes in the side of the plenum facing the equipment can be located to direct forced air at specific areas, thus providing cooling to nearby hot spots and other areas which are discussed later.

A typical 0.06-inch-thick, sheet-aluminum plenum containing eight rows of 0.375-inch-diameter orifice holes is shown

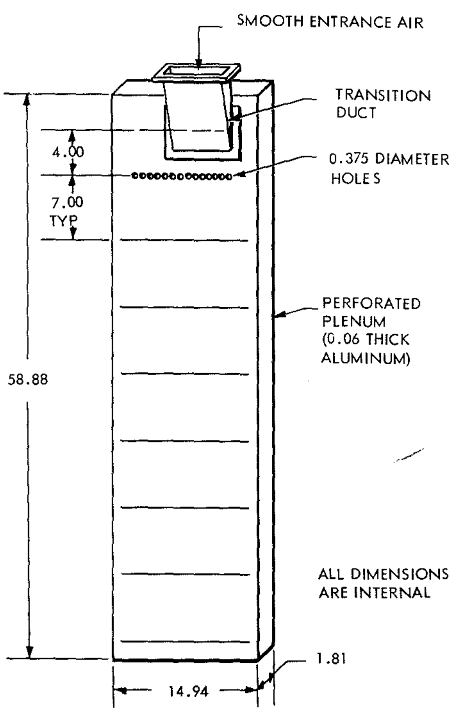

Fig. 1—Plenum and transition duct assembly.

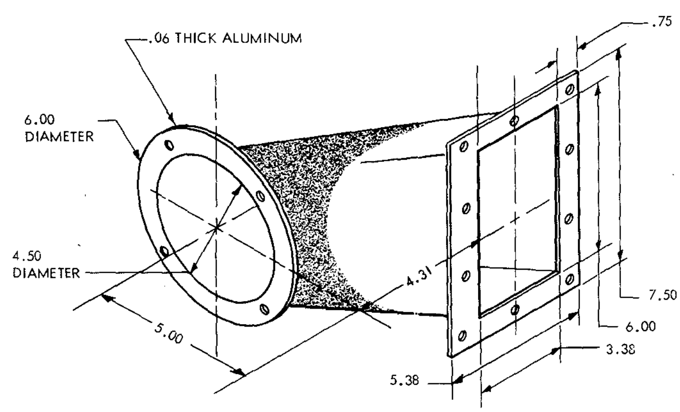

Fig. 2—Transition duct.

JOSEPH M. WARNICK received a certificate in Electrical Engineering from Wilkes College and a BSME in 1955 from Pennsylvania State University. He subsequently joined Goodyear Tire and Rubber Co., where he participated in development of airspring suspension systems. In 1958 he joined RCA and was assigned to the design of signal monitoring equipment for BMEWS. He later was responsible for all mechanical engineering on part C of the Stellarator Timer Project. Since being assigned to ground support equipment, he has developed the rack housing scheme and cooling techniques for Multisystem Test Equipment. Mr. Warnick is a member of Phi Kappa Tau and is a registered professional engineer in Pa. and Mass.

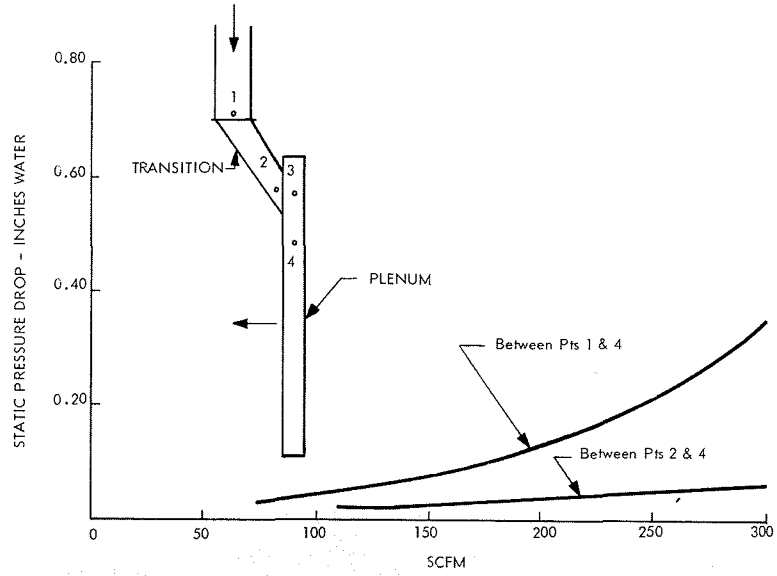

Fig. 3—Pressure drop vs. specific ft^3/min (SCFM) for rack ducting without screen.

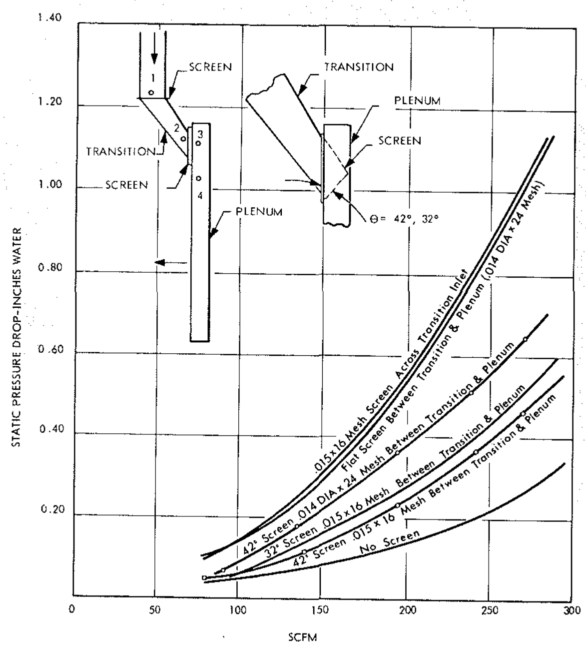

Fig. 4—Pressure drop between points 1 and 4 for various RFI screen configurations.

in Fig. 1. Since part of the rack frame structure would ordinarily be directly above the plenum installed in the side, a transition duct is required to supply air to the face of the plenum. The transition duct shown in Figs. 1 and 2 gradually angles into the plenum to minimize entrance pressure losses. Air can be furnished to this duct directly from a blower mounted on top or from an overhead air-conditioning header duct.

ORIFICE HOLE CHARACTERISTICS

The orifice holes are punched in the plenum. Since it is common shop practice to deburr the sharp side of such holes, consideration should be given to the effect on the hole coefficient of discharge. The coefficient of discharge C_D is based on the relationship

$$\text{Flow} = C_D A \sqrt{2\,gh}$$

where A is the orifice area; g, the acceleration of gravity; and h, the pressure differential across the orifice in the height of the fluid. With typical shop-deburred hole edges upstream to the direction of air flow, and with smooth air entry directly into the hole, C_D is 0.71 for 0.06-inch-thick aluminum. For the deburred edges downstream, C_D is 0.65. For undeburred holes, C_D is 0.65 for the burred edges downstream and 0.63 for the burred edges upstream. It is apparent that since C_D is the same when the punched edges of the holes are upstream, regardless of whether the downstream edges are deburred or not, more consistent results will be obtained by punching the plenum from the upstream side.

The plenum in Fig. 1 has its holes punched from the upstream condition. However, since the main flow of air within the plenum is at right angles to the flow through the holes, C_D is reduced to 0.61. Subsequent curves, where applicable, are based on this coefficient of discharge.

PRESSURE-DROP CHARACTERISTICS

The pressure drops through the transition duct and plenum are shown in Figs. 3 and 4. In many applications radio frequency interference (RFI) must be prevented from entering or leaving the rack enclosure. Fig. 4 shows pressure-drop curves for various configurations of protective screens. It is apparent from these curves that screens angling into the plenum almost normal to the direction of the air flow, and with a larger area exposed (Fig. 5), have the lower pressure drop.

A variety of air entrance conditions into the transition duct is possible, depending on the blower used, the size of the overhead header duct, and whether turning vanes are used in the header duct. Figs. 3 and 4 are, therefore, based upon smooth entrance conditions. If an additional pressure loss results from the particular air entrance situation, it can be added to the losses shown in these figures. If a lower pressure drop is desired across the protective screen, other commercially available shielding materials, such as honeycomb-type material, can be substituted, but usually at higher cost and space consumption.

PLENUM AIR-FLOW PATTERNS

In Fig. 6 the air-flow gradient along the various levels of the plenum is shown. At the higher flow rates the static pressure regain is demonstrated at the bottom of the plenum, causing higher flow through the port holes. Conversely, at the top of the plenum a decrease in static pressure is demonstrated as the air moves past the holes with a higher velocity, causing slightly less air to go through the holes. At lower to moderate overall flow rates the flow through the holes at each level is essentially constant, and slight fluctuations for practical purposes can be ignored. In light of the appreciable pressure drop at the plenum entrance, together with the flow patterns shown in Fig. 6, the pressure drop between the plenum top and bottom can be considered negligible. It should be noted that this data is not only applicable to the specific configuration shown in Fig. 1; it can also be applied to similar systems where favorable aspect ratios are maintained and abrupt air pattern changes are minimized.

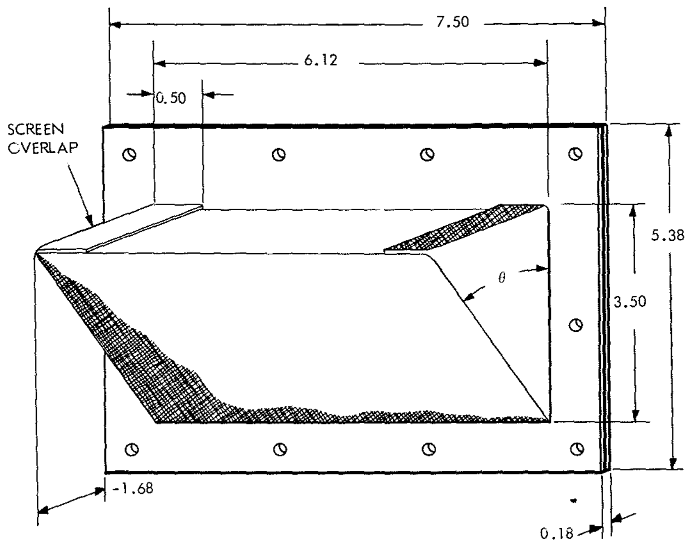

Fig. 5—Angled-type RFI screen.

METERED AIR COOLING CHARACTERISTICS

The cooling capacity in watts/hole for a 0.375-inch-diameter hole is shown in Fig. 7. It is applicable for any case where the hole coefficient of discharge is close to 0.61. For example, if a rack of equipment has heat dissipation of 1 kW and the overall temperature rise is limited to 30° F, this would correspond to a cooling air rate of 7.9 lb/min/kW. For a plenum pressurized at 1.0 inch of water above rack pressure, each hole would have a cooling capacity of 17.8 watts. Therefore, for 1 kW of heat dissipation, 1000/17.8 or 56 holes are required.

At 1.0 inch of water pressure it can be seen from the relationship

$$\text{Velocity} = C_V \sqrt{2\,gh},$$

where the velocity coefficient C_V equals 0.97, that the air exit velocity from the plenum holes is 3890 ft/min. The depth of penetration of this air into a chassis of equipment depends upon the particular equipment configuration and the airflow resistance that the configuration causes. When this resistance is appreciable, the air can be expected to penetrate past the heat-critical components part way into the equipment. It then is carried into the surrounding air paths by free convection. In other cases where suitable paths are set up, the air can move straight across to the opposite side of the rack. In most applications of this type of cooling, the entire rack is maintained at a slight positive pressure, resulting in a general movement of air to an exhaust opening and overall removal of the heat.

CONCLUSION

The perforated-plenum cooling system can be applied to most cases where forced air is used for cooling electronic rack enclosures. The major advantages of this type of system are listed below.

1) Air openings can be located to direct air where it will do the most good.
2) The air is reliably metered so that a known quantity of air can be made available from specific locations for particular chassis cooling needs.
3) Flexibility is provided, since an equipment chassis can be flushed with cooling air around the outside and also penetrated.
4) Air that has not been preheated by other components is available for cooling properly located temperature-critical components.
5) The need for auxiliary blowers and heat sinks within a chassis is minimized.
6) The need for baffles for directing air flow within a rack is minimized.

Disadvantages of the perforated-plenum cooling system that should be considered are as follows:

1) Additional cost of ducting within the rack.
2) Additional blower capacity required to maintain the positive plenum pressure.
3) Possible blower noise if blowers are not carefully selected.

The advantages and disadvantages noted above are useful in comparing this system with the other two most common types of air cooling: completely free convection within the rack, and air flushed directly through the rack. These two cooling methods usually are adequate for low to medium heat dissipation by loosely packaged equipment. For high-density, high-heat-dissipating equipments, however, the advantages of the perforated-plenum technique are more apparent.

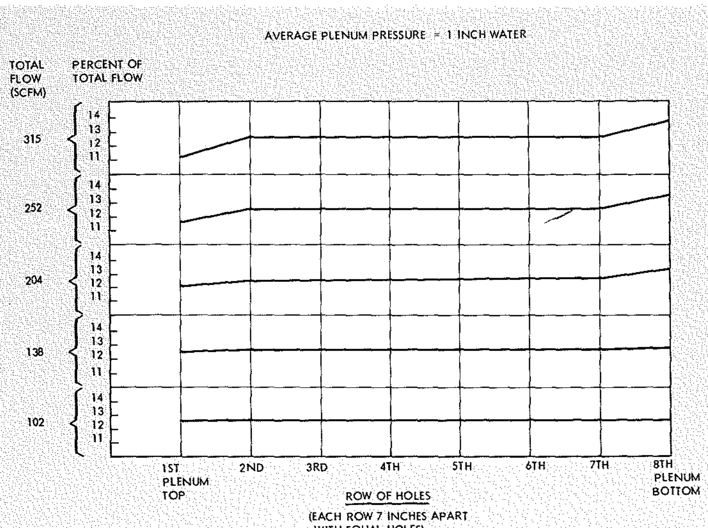

Fig. 6—Variation of flow through orifice holes along length of plenum.

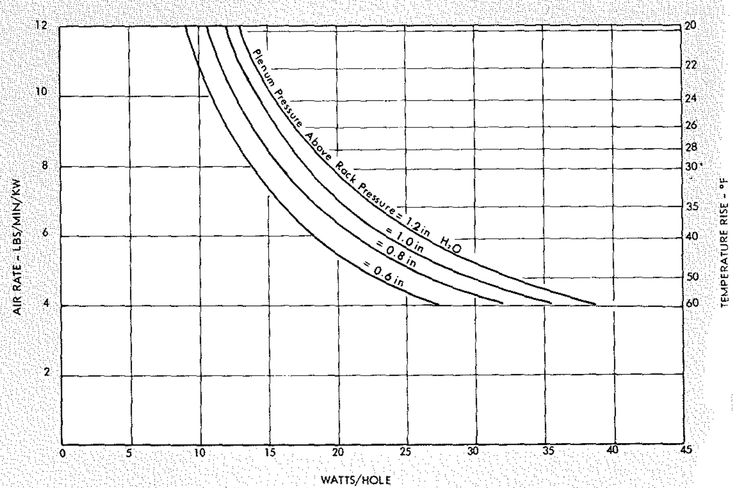

Fig. 7.—Cooling capacity of 0.375-inch-diameter hole (C_D=0.61).

Engineering and Research NOTES

BRIEF TECHNICAL PAPERS OF CURRENT INTEREST

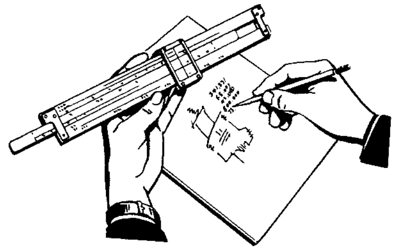

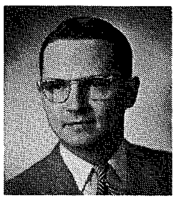

Laser Radiation Nomograph

D. J. Blattner, *Electronic Components and Devices, Princeton, N. J.*

Final manuscript received June 13, 1966

The phenomenal development of the laser has combined techniques from optics, spectroscopy, physics, and electronics. Small wonder, therefore, that laser radiation is variously reported in terms of wavelength, wave number, frequency, and photon energy. However, any one of these terms can be converted to the others by use of a straightedge and the nomograph shown in Fig. 1. For example, light at a wavelength of 0.5 μm can also be specified as having the following parameters:

wavelength = 5,000 angstroms
frequency = 6×10^{14} hertz or 600 terahertz
wave number = 20,000 cm.$^{-1}$
photon energy = 2.48 electron-volts

As other examples, a glance across the chart shows that electrons with an energy of 4 volts radiate at 3,100 angstroms, and that light at 200 terahertz produce conduction in semiconductors that have bandgaps up to 0.82 volt. *Keep this nomograph handy!*

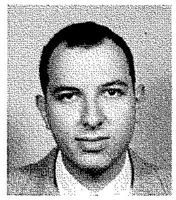

Laser User's Guide

D. Blattner and R. Wasserman, *Electronic Components and Devices, Princeton, N. J.*

Final manuscript received Sept. 14, 1966

Here is a helpful chart (Fig. 1) that shows at a glance the wavelength, frequency, color, and photon energy of radiation from various laser materials. The lasers listed on the chart are only a few of the many types reported; however, the chart itself, which illustrates the conversions from frequency to wavelength or from wavelength to energy, can be used for any laser. Detectors for each region of the spectrum are also indicated on the chart. Semiconductor detectors are useful over the entire range shown. Intrinsic semiconductors are available for energies greater than 0.2 eV; for detection of wavelengths farther out in the infrared, the semiconductor must be doped. For short wavelengths ($\lambda < 0.7$ μm) phototubes offer the advantages of amplification by electron multipliers and higher speed. Bolometers (heat detectors) also cover the whole range, and although they have less speed and sensitivity than quantum detectors, they have the advantage of responding to power regardless of wavelength.

Fig. 1—Laser radiation nomograph.

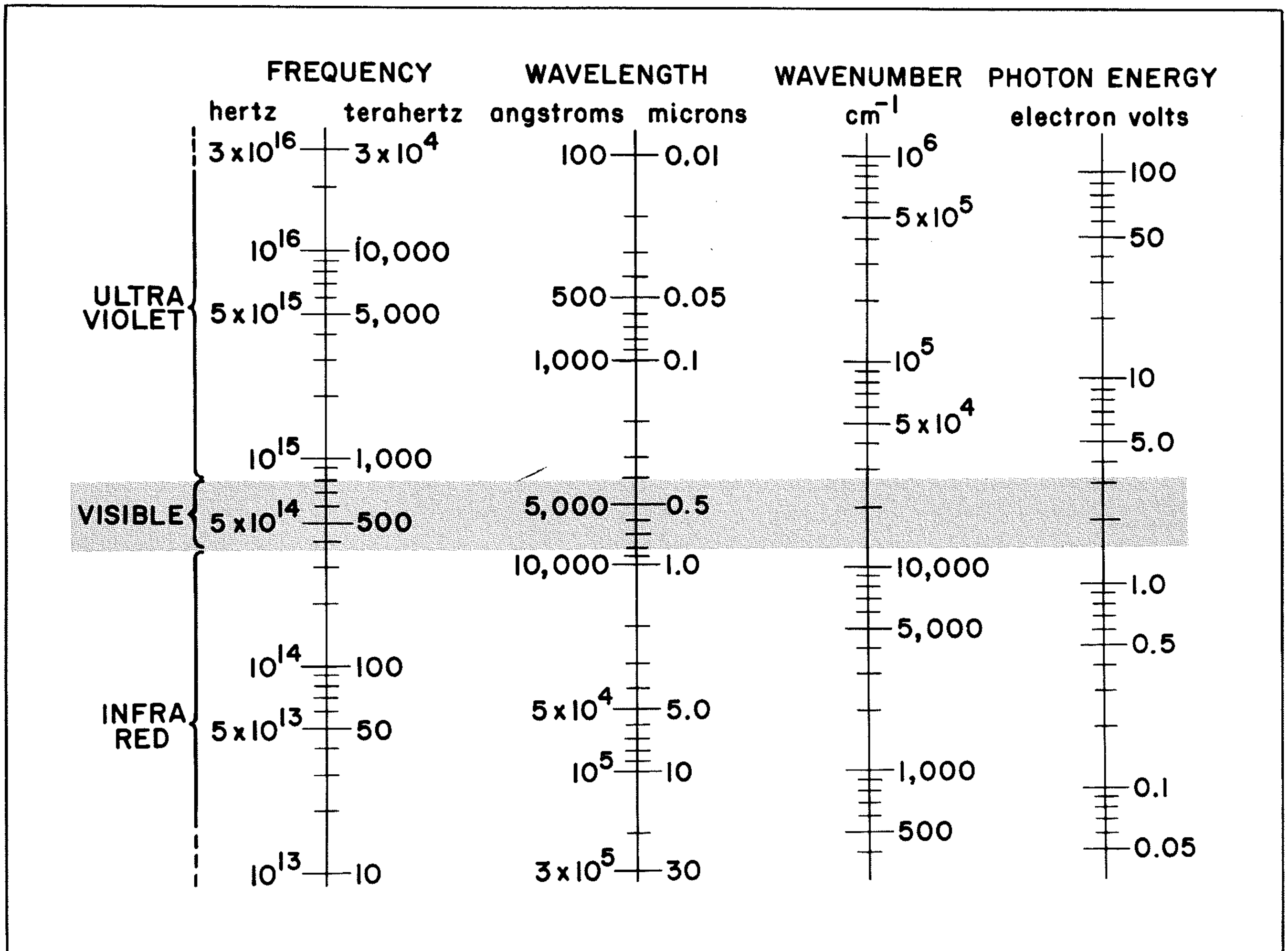

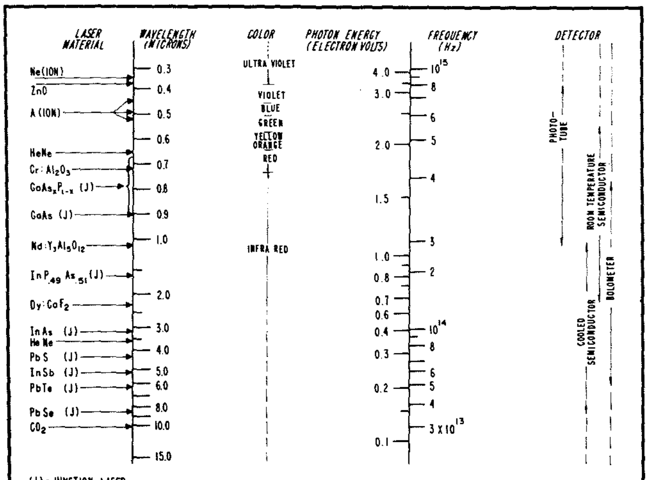

Fig. 1—Laser user's guide.

Flexible-Film Interconnection and Packaging (FFIP) of Integrated-Circuit Flatpacks

B. Matonick, *Astro-Electronics Division,*

Princeton, N. J.

Final manuscript received July 13, 1966

A search for a suitable electronic packaging technique for spacecraft application resulted in the development at the Astro-Electronics Division of a unique method for achieving high-density packaging of flatpack integrated circuits and miniature components. The flexible-film interconnection and packaging (FFIP) scheme has enabled an increase in logic-module density of from 0.54 module per cubic inch for conventional miniature packaging to 120 modules per inch for FFIP. The FFIP scheme eliminates many connectors, contacts, and hand-wired harnesses between connectors; thus, reliability and the probability of survival are increased. Because of the high packaging density on a single substrate, most interconnections remain on the substrate as reliable printed-circuit connections.

The FFIP scheme can be used with newer high-density modules as they become available. Since FFIP enables compact, three-dimensional packaging without plug-type interconnections, it can be used to interconnect metal-oxide-semiconductor (MOS) transistor arrays, thin-film transistor (TFT) memory elements, conventional integrated-circuit flatpacks, and discrete miniature components, each of which may have a large range of internal packing densities. It is also possible with FFIP to interconnect the different types of arrays not possible with most other array fabrication techniques. The FFIP scheme will thus increase in value as newer technologies evolve.

The FFIP comprises the mounting of integrated circuits and miniature components on a flexible printed-circuit dielectric film 0.002-inch thick, with one-ounce copper conductor on both sides. The width of the conductor line is approximately 0.012 inch, permitting a flexible printed-circuit assembly to be rolled or otherwise shaped and packaged in various configurations. Fig. 1 illustrates the evolution of the packaging techniques and the impact upon size, weight, and power requirements. The striking improvement in the most significant parameter, the number of logic modules per cubic inch, is shown. Data in Figure 1 indicates that, with conventional packaging, a density of 0.54 module per cubic inch was achieved; with integrated circuits on printed-circuit boards, a density of 5.9 modules per cubic inch was provided; and with the new FFIP configuration, a density of 120 modules per cubic inch was achieved.

Fig. 2 shows a mounting case, an interface printed-edge board, and two FFIP films containing 45 integrated-circuit flatpacks with provision for mounting seven discrete components. The printed-edge board (made of 0.032-inch-thick epoxy-bonded Fiberglas with one-ounce copper laminated on both sides) is used as an interface between the two flexible film strips and as a male member of a standard printed-circuit-type connector. The assembly is enclosed in a rectangular case, with the center board designed to transmit the insertion and removal loads (i.e., the forces required to insert and remove the printed-circuit boards into and from the mating connector) to both the base and the cover of the one-piece enclosure. The center board is bonded to the cover, which is in turn bonded to the one-piece enclosure. The enclosure is designed for screw mounting, but may be adapted for clip mounting; depending upon its intended use, it may be made of either metal or plastic. The advantage of anchoring the center board to the enclosure is that in the event of a malfunction, the bonded section can be separated and the board assembly removed for repairs.

The mounting of the components (Fig. 2) was done with the impulse-soldering technique developed at RCA. This technique, presently used for flight equipment, accomplishes electrical junctions by means of a reflow soldering process whereby presoldered component leads are joined to solder-plated, printed-circuit boards. Standard, parallel-gap welding equipment is used, with the electrodes modified for the soldering process. This process enables the production of a high yield of quality terminations without damage to the dielectric between the laminated conductors or to the components by excessive heat. The heat applied to melt the solder at the junction can be controlled (as can the dwell time, electrode pressure, applied energy, amount of solder and flux, heat-sinking, and soldering cycle) to provide a solder connection of the quality required for spacecraft application.

By the use of multicircuit flatpacks, a larger number of functions can be packaged in the same volume. This packaging technique can therefore be described as a method of compact *interfacing* as well as a high-density packaging technique.

The flexible-film technique affords large savings in cost of procurement and manufacturing, as compared with the conventional method of packaging electronic circuitry. The reduction of the parts required (e.g., harness boards, interface connectors, and hardware), the reduction of container size, and the elimination of manual soldering and "hard" wiring all contribute to the cost savings. The cost of manufacturing and assembling the micropackage, integrated-circuit unit shown in Fig. 1 is approximately one-seventh that of the conventional unit and approximately one-fourth that of the integrated-circuit unit.

A comparative cost is not given for the test cycle; however, the location of malfunctioning equipment may be simplified by the addition of convenient test pads. The defective components can be replaced by removing the flexible film from the container and expanding it to expose the area to be reworked. Flatpacks and discrete components can be removed by lifting and shearing the solder connections with a sharp knife. If jumpers must be added for circuit changes, insulated nickel ribbon 0.003-inch thick by 0.010-inch wide may be used. This ribbon can be routed as required and joined by impulse-soldering.

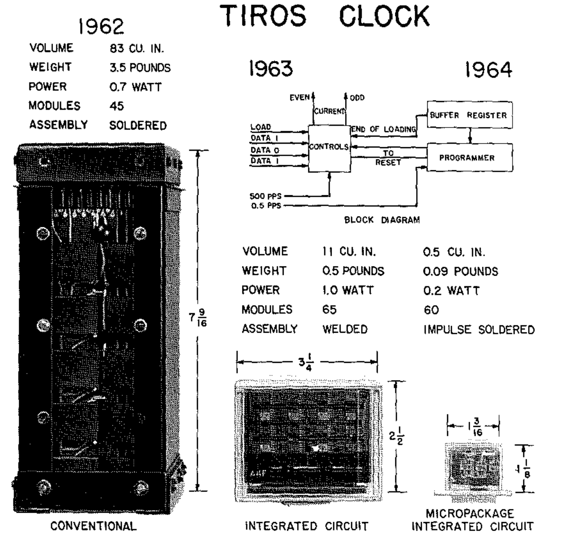

Fig. 1—Comparison of (l. to r.) conventional, integrated-circuit, and flexible-film-interconnection packaging (FFIP).

Fig. 2—FFIP mounting case, printed-edge board, and two films.

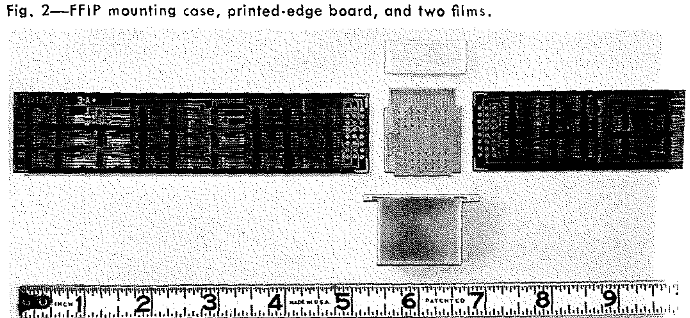

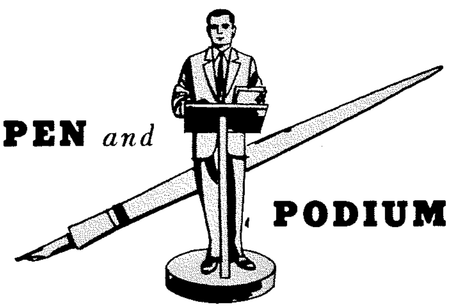

COMPREHENSIVE SUBJECT-AUTHOR INDEX
to
RECENT RCA TECHNICAL PAPERS

Both published papers and verbal presentations are indexed. To obtain a published paper, borrow the journal in which it appears from your library, or write or call the author for a reprint. For information on unpublished verbal presentations, write or call the author. (The author's RCA Division appears parenthetically after his name in the subject-index entry.) For additional assistance in locating RCA technical literature, contact: **RCA Staff Technical Publications, Bldg. 2-8, RCA, Camden, N. J. (Ext. PC-4018).**

This index is prepared from listings provided bimonthly by RCA Division Technical Publications Administrators and Editorial Representatives—who should be contacted concerning errors or omissions (see inside back cover).

Subject index categories are based upon the Thesaurus of Engineering Terms, Engineers Joint Council, N. Y., 1st Ed., May 1964.

SUBJECT INDEX

Titles of papers are permuted where necessary to bring significant keyword(s) to the left for easier scanning. Authors' division appears parenthetically after his name.

AIRCRAFT INSTRUMENTS

ALTIMETER ACCURACY DEGRADATION (J_1) from Transmission Line Reflections and Circular Leakage—S. L. Goldman (ASD, Burl.) *MS Thesis,* Univ. of Pa., Phila., Pa., Feb. 1966

AMPLIFICATION

HF POWER AMPLIFIER Design, Semiconductor—R. Minton (ECD, Som) *WESCON Preprint,* Aug. 1966

TRANSISTOR (FIELD-EFFECT) Amplifiers—R. W. Ahrons (ECD, Som) WESCON, L. A., Calif., Aug. 23-26, 1966; *WESCON Preprint*

TRANSISTOR (RF) Power Amplifiers, Design Trade-Offs for—R. Minton (ECD, Som) WESCON, L. A., Calif., Aug. 23-26, 1966; *WESCON Preprint*

ANTENNAS

DIELECTRIC ANTENNA, A Wide-Beam—J. J. Brumbaugh (MSR, Mrstn) *MSEE Thesis,* Villanova Univ., May 16, 1966

PHASED-ARRAY Radar Orientation to Minimize Average Scanning Loss—J. L. Worst (MSR, Mrstn) *MSEE Thesis,* Univ. of Penna., June 1966

BIONICS

(POSTGANGLIONIC WAVEFORMS): The Use of Fourier Waveform Analysis to Conform the Differentiability Preganglionic Slow Potentials into Slow Potential Postganglionic Waveforms—D. B. Mayer (MSR, Mrstn) Rochester Conf. on Data Acquisition and Processing in Biology and Medicine, July 25-27, 1966; *Conf. Proc.*

CIRCUITS, INTEGRATED

CONSUMER PRODUCTS, Integrated Circuits in—R. C. Smith (ServCo) Booklet for Internal RCA Svc. Co. Distribution.

FM RECEIVER, Integrated Circuits Make Low-Cost—R. L. Sanquini (ECD, Som) *Electronics,* August 8, 1966

THIN-FILM Integrated Arrays—W. Y. Pan (CSD, Cam) Seminar on Modern Eng. Tech., Gaiwan, China, June 27-July 6, 1966

TRANSISTORS (FIELD-EFFECT) Based on Silk-Screened CdS Layers—W. Witt, F. Huber, W. Laznovsky (DME, Som) *Proc. of IEEE,* Vol. 54, Pg. 898, June 1966

(TRANSISTORS, THIN-FILM): Reversible Gate Insulator Instabilities in TFT's—R. Schelhorn (DME, Som) 5th Ann. Symp. on Microelectronics, IEEE, July 17-20, 1966, St. Louis, Mo.; *Conf. Proc.*

CIRCUITS, PACKAGED

WELDED CONSTRUCTION and Repair, Microelectronic—R. G. Clark and J. W. Kaufman (CSD, Cam) *Assembly Engineering,* June 1966

COMMUNICATIONS COMPONENTS
(equipment subsystems)

(MIXERS): Rid Mixers of Spurious Signals—D. H. Westwood (CSD, Cam) *Electronic Design,* Aug. 16, 1966

MULTIPLIERS (Microwave Solid-State) for Space Systems—W. J. Dodds (ECD, Hr) WESCON, L. A., Calif., Aug. 23-26, 1966; *WESCON Preprint*

PHOTOPARAMETRIC DETECTORS With Internal Current Multiplication—F. Sterzer, J. R. Collard (ECD, Pr) Electron Device Res. Conf., Pasadena, Calif., June 27, July 1, 1966

ROCKETSONDE TRANSMITTER, A New Low-Cost Solid-State—R. E. Askew (ECD, Hr) *Electronic Communicator,* July-August, 1966

VARACTOR MULTIPLIERS and High-Power Microwave Varactors—J. Collard, C. Sun, T. E. Walsh (ECD, Pr) WESCON, L. A., Calif., Aug. 23-26, 1966; *WESCON Preprint*

VFO ELEMENT Using the Field-Effect Transistor as a—G. D. Hanchett (ECD, Som) Club de Radio Experimentadores, New Laredo, Mexico, Aug. 13, 1966

COMMUNICATIONS SYSTEMS

MULTILINGUAL TROOPS, Message Sent in Symbols Will Link—H. R. Gutsmuth (CSD, Cam) *Electronics,* July 25, 1966

PUBLIC NAVIGATION SYSTEM—J. N. Breckman (SEER, Mrstn) *Space and Aeronautics,* July 1966

SPACE ENVIRONMENT, Satellite Communications and the—R. B. Marsten (AED, Pr) The Franklin Inst., Phila., Penna., July 26, 1966

COMMUNICATION, VOICE
(equipment & techniques)

TRANSISTORS (RF POWER) in Vehicular Radio Communications Equipment—S. Matyckas (ECD, Som) WESCON, L. A., Calif., Aug. 23-26, 1966; *WESCON Preprint*

COMPUTER APPLICATIONS

PERT TIME & PERT COST in Marketing to the Department of Defense, Use and Assumed Value of—J. F. Blair (ASD, Burl) *MS Thesis,* Drexel Inst. of Tech., College of Business Administration, Phila., Penna., Apr. 1966

COMPUTER COMPONENTS
(subsystems & peripheral equip.)

REVIEW OF: "Recertification of Instrumentation Tape," General Kinetics, Inc.—F. H. Fowler, Jr. (CSD, Cam) *Computing Reviews,* May-June 1966

REVIEW OF: "The Tape Management Program," General Kinetics, Inc.—F. H. Fowler, Jr. (CSD, Cam) *Computing Reviews,* May-June 1966

REVIEW OF: "The Technology of Tape Preventive Maintenance," General Kinetics, Inc.—F. H. Fowler, Jr. (CSD, Cam) *Computing Reviews,* May-June 1966

REVIEW OF: "Why is Tape Preventive Maintenance Needed?", General Kinetics, Inc.—F. H. Fowler, Jr. (CSD, Cam) *Computing Reviews,* May-June 1966

COMPUTER STORAGE

COMPLEMENTARY MOS Memories, High-Speed—J. R. Burns, J. J. Gibson (Labs, Pr) Natl. Aeronautical Electronics Conf., Dayton, Ohio, May 16-18, 1966

INTEGRATED MEMORY Combining Monolithic Ferrite and MOS Transistor Arrays—J. W. Tuska (Labs, Pr) Informal talk at Lake Arrowhead, IEEE Computer Group Workshop, Aug. 31-Sept. 2, 1966

INTEGRATED MEMORY Using Complementary Field-Effect Transistors—J. R. Burns, J. J. Gibson, A. Harel, K. C. Hu, R. A. Powlus (Labs, Pr) Intl. Solid-State Circuits Conf., *Digest of Tech. Papers,* Feb. 1966

DOCUMENTATION
(& information science)

TECHNICAL INFORMATION SERVICES (Advances in)—Some Implications for Engineering Managers—E. R. Jennings (Staff Prod. Engrg., Cam) Joint Engrg. Mgmt. Conf., Sept. 26-27, 1966, Washington, D.C.; in: *JEMC Conf. Proceedings—Creating Second Sources of Engineering Manpower,* IEEE, N.Y., 1966.

TECHNICAL MANUALS vs. the Military Status Report (Project 5), NASA Requirements for—R. E. Patterson (CSD, Cam) Military/NASA/Industry Symp., Anaheim, Calif., May 25-26, 1966

EDUCATION
(& training)

ELECTRONIC TECHNICIAN, Aim for a Job as an—J. E. Keefe (ServCo) To be pub. (Book Form) by Richard Rosen Press, for the author, June 22, 1966

STUDENT CONTRIBUTION to Science—J. C. Flint (ASD, Burl) Medford High School Science Club, March 16, 1966

ELECTROMAGNETIC WAVES
(theory & phenomena)

PROPAGATION of Waves in a Bounded Solid-State Plasma in Transverse Magnetic Fields—R. Hirota, K. Suzuki (Labs, Pr) *J. of the Phys. Society of Japan,* Vol. 21, No. 6, June 1966

ELECTRO-OPTICS
(systems & techniques)

IMAGE SENSOR, A Thin-Film Solid-State—P. K. Weimer, G. Sadasiv, H. Borkan, L. Meray-Horvath, F. V. Shallcross, J. Meyer, Jr. (Labs, Pr) Intl. Solid-State Circuits Conf., *Digest of Tech. Papers,* Feb. 1966

MODULATOR (Gallium Arsenide Electro-Optic) for the 10.6-Micron CO_2 Laser—T. E. Walsh (ECD, Pr) Electron Device Research Conf., Pasadena, Calif., June 27-July 1, 1966

ENERGY CONVERSION
(& power sources)

PHOTOVOLTAICS for Space Applications—P. Rappaport (Labs, Pr) AIChE, Chem. Eng. Symp. Series, No. 5, London, June 13-17, 1965

SOLAR CELL Output Characteristics, Temperature, Illumination Intensity, and Degradation-Factor Effects on—R. Rasmussen, H. Harmon (AED, Pr) IEEE Aerospace Systems Conf., Seattle, Wash., July 13, 1966; *Conf. Proc.*

SOLAR CELLS, Lithium-Doped Radiation-Resistant Silicon—J. J. Wysocki (Labs, Pr) IEEE Nuclear & Space Radiation Effects Conf., Palo Alto, Calif., July 18-22, 1966

SOLAR CELLS, Low-Energy Proton Bombardment of GaAs and Si—J. J. Wysocki, P. Rappaport, E. Davison, J. J. Loferski (Labs, Pr) *IEEE Trans. on Electron Devices,* Vol. ED-13, No. 4, P. 420, Apr. 1966

SPACECRAFT POWER Systems, The Comparison of—L. Pessin, D. Rusta (AED, Pr) IEEE Aerospace Systems Conf., Seattle, Wash., July 12-13, 1966; *Conf. Proc.*

THERMIONIC CONVERTER, The Development of a Reservoirless—F. G. Block, W. E. Harbaugh, A. Basiulis (ECD, Lanc) *Journal of the Amer. Inst. of Astronautics and Aeronautics,* June 7, 1966

THERMOELECTRIC Power Generation, Ge-Si Alloys for—A Review—F. D. Rosi, J. P. Dismukes (Labs, Pr) AIChE, Chem. Eng. Symp. Series, No. 5, London, June 1965

ENVIRONMENTAL ENGINEERING

LEAK TESTING and Acceptance of Clean Areas—E. L. Romero (ECD, Lanc) Northeast Chapter of Amer. Assoc. for Contamination Control, Boston, Mass., June 22, 1966

FILTERS, ELECTRIC

DISHAL METHOD of Adjusting Multiple-Resonant Circuit Filters, A Note Regarding the—J. H. Pratt (WCD, Van Nuys) *Proc. of IEEE,* Apr. 1966

FOUR-RESONATOR Filters, General—R. M. Kurzrok (CSD, Cam) *Electrical Design News,* July 1966

GEOPHYSICS

SEISMOMETER-AMPLIFIER COUPLING for Maximum Signal-to-Noise Ratio—D. S. McCoy (Labs, Pr) *IEEE Trans. on Geoscience Electronics,* Vol. GE-4, No. 1, June 1966

INTERFERENCE
(& noise)

(MIXERS): Rid Mixers of Spurious Signals—D. H. Westwood (CSD, Cam) *Electronic Design,* Aug. 16, 1966

LABORATORY EQUIPMENT
(& techniques)

ABSORPTION-TYPE RESERVOIR for Gas Tubes—K. G. Hernqvist, J. D. Levine (Labs, Pr) *RCA Review,* XXVII, No. 1, Mar. 1966

ELECTRON MICROSCOPY of Solid-State Materials—M. D. Coutts (Labs, Pr) EMSA 24th Mtg., San Francisco, Calif., Aug. 25, 1966

MASS SPECTROMETRY in Color-Television Picture Tubes, Chemical Applications of—J. J. Moscony (ECD, Lanc) Chemistry Dept. Sem., Univ. of Maine, July 27, 1966

POINT-DEFECT DISLOCATION Interactions and Frictional Stresses in Nickel Using Microstrain Measurements, A Study of—H. Kressel (ECD, Som) ASM Symp. on Precision Mechanical Property Measurements, Atlantic City, N. J., June 27, 1966

SEISMOMETER-AMPLIFIER COUPLING for Maximum Signal-to-Noise Ratio—D. S. McCoy (Labs, Pr) *IEEE Trans. on Geoscience Electronics,* Vol. GE-4, No. 1, June 1966

X-RAY SECONDARY-EMISSION SPECTROMETER, A New Slit Aperture and a Comparison of Four Slit Apertures for Selected-Area Analysis with the—E. P. Bertin (ECD, Hr) Seminar on X-Ray Spectrometric Analysis, Stevens Inst., Hoboken, N. J., June 20, 1966

X-RAY SPECTROMETRIC ANALYSIS (Specimen Preparation Methods for) and X-Ray Spectrometric Analysis of Small Selected Areas—E. P. Bertin (ECD, Hr) X-Ray Spectrometry Clinic, N. Y. State Univ., Albany, N. Y., Aug. 22-27, 1966

X-RAY SPECTROMETRY, Chemical Analysis by—Principles, Instrumentation, Methods, Measurements, and Specimen Preparation—E. P. Epstein (ECD, Hr) Seminar on X-Ray Spectrometric Analysis, Stevens Inst., Hoboken, N. J., June 20, 1966

LASERS

INJECTION LASERS, Dislocations and Precipitates in GaAs—M. S. Abrahams, C. J. Buiocchi (Labs, Pr) *J. of App. Phys.*, Vol. 37, No. 5, Apr. 1966

MODULATOR (Gallium Arsenide Electro-Optic) for the 10.6-Micron CO_2 Laser—T. E. Walsh (ECD, Pr) Electron Device Research Conf., Pasadena, Calif., June 27-July 1, 1966

NOBLE GAS ION LASERS, Plasma Aspects of—K. G. Hernqvist (Labs, Pr) Seminar at Royal Inst. of Tech., Stockholm, Sweden, Aug. 23, 1966

ROOM-TEMPERATURE Pulse-Operated GaAs Injection Laser, Optimum Design for a—A. Akselrad (Labs, Pr) *App. Phys. Ltrs.*, Vol. 8, No. 10, May 15, 1966

SURFACE LASER of $BaTiO_3$—D. R. Callaby (Labs, Pr) *J. of App. Phys.*, Vol. 37, No. 6, May 1966

THERMAL RESISTANCE of GaAs Laser Diodes—M. F. Lamorte, S. Caplan, T. Gonda, P. Nyul (ECD, Som) Tech. Conf. on Preparation and Properties of Electronic Matls. for the Control of Radiative Processes, Boston, Mass., Aug. 22-31, 1966

VAPOR-PHASE GROWTH of $GaAs_{1-x}P_x$ Room-Temperature Injection Lasers—J. J. Tietjen, J. I. Pankove, I. J. Hegyi, H. Nelson (Labs, Pr) Conf. on Electronic Matls., Boston, Mass., Aug. 29-31, 1966

VAPOR PHASE GROWTH of GaP Electro-Optic Modulator—D. Richman, J. J. Tietjen (Labs, Pr) Conf. on Electronic Mtals., Boston, Mass., Aug. 29-31, 1966

WAVELENGTH CHANGES (LARGE) with Cavity Q in Injection Lasers—G. C. Dousmanis, D. L. Staebler (Labs, Pr) *J. of App. Phys.*, Vol. 37, No. 6, May 1966

MANAGEMENT

ENGINEERING COMMUNICATION, The Need for Better—J. Gillespie (CSD, Cam) Phila. Exchange Club, Phila., Pa., July 19, 1966

PERT TIME & PERT COST in Marketing to the Department of Defense, Use and Assumed Value of—J. F. Blair (ASD, Burl) *MS Thesis*, Drexel Inst. of Tech., College of Business Administration, Phila., Pa., Apr. 1966

RESEARCH, ENGINEERING, and the Profession—A. A. Wolf (ASD, Burl) Graduate Eng. Students at Boston Univ., May 5, 1966

TECHNICAL INFORMATION SERVICES (Advances in)—Some Implications for Engineering Managers—E. R. Jennings (Staff Prod. Engrg., Cam) Joint Engrg. Mgmt. Conf., Sept. 26-27, 1966, Washington, D.C.; in: *JEMC Conf. Proceedings—Creating Second Sources of Engineering Manpower*, IEEE, N.Y., 1966.

MASERS

SOLID-STATE CW Optically Pumped Microwave Maser—E. S. Sabisky, C. H. Anderson (Labs, Pr) *App. Phys. Ltrs.*, Vol. 8, No. 11, June 1, 1966

MEDICAL ELECTRONICS

(POSTGANGLIONIC WAVEFORMS): The Use of Fourier Waveform Analysis to Conform the Differentiability Preganglionic Slow Potentials into Slow-Potential Postganglionic Waveforms—D. B. Mayer (MSR, Mrstn) Rochester Conf. on Data Acquisition and Processing in Biology and Medicine, July 25-27, 1966; *Conf. Proc.*

OPTICS

CENTRAL FOVEAL PHOTOCHROMATIC INTERVAL, Implications of a—B. M. Hillman (ASD, Burl) Optical Soc. of Amer., Wash., D. C., Mar. 15, 1966

PLASMA PHYSICS

MICROPLASMA OBSERVATIONS in Silicon Junctions Using a Scanning Electron Beam—J. W. Gaylord (Labs, Pr) *J. of Electro-Chem. Soc.*, Vol. 113, No. 7, July 1966

NOBLE GAS ION LASERS, Plasma Aspects of—K. G. Hernqvist (Labs, Pr) Seminar at Royal Inst. of Tech., Stockholm, Sweden, Aug. 23, 1966

PROPAGATION of Waves in a Bounded Solid-State Plasma in Transverse Magnetic Fields—R. Hirota, K. Suzuki (Labs, Pr) *J. of the Phys. Society of Japan*, Vol. 21, No. 6, June 1966

PROPERTIES, ATOMIC

EMISSION (Nd^{+3}) and Excitation in $ZnSe_xTe_{1-x}$ Host, Characteristics of—W. H. Fonger (Labs, Pr) Conf. on Electronic Materials, Boston, Mass., Aug. 29-31, 1966

INFRARED RADIATION from Bulk GaAs—K. K. N. Chang, S. G. Liu, H. J. Prager (Labs, Pr) *App. Phys. Ltrs.*, Vol. 8, No. 8, p. 196, Apr. 15, 1966

MICROWAVE EMISSION from Indium Antimonide—R. D. Larrabee, W. D. Hicinbothem, Jr. (Labs, Pr) Gordon Res. Conf., Crystal Mountain, Washington, Aug. 8-12, 1966

MOBILITY of Electrons and Holes in Anthracene—J. Dresner (Labs, Pr) Amer. Phys. Soc. (invited paper), Mexico City, Aug. 29, 1966

PROPERTIES, MOLECULAR (& crystalography)

INJECTION LASERS, Dislocations and Precipitates in GaAs—M. S. Abrahams, C. J. Buiocchi (Labs, Pr) *J. of App. Phys.*, Vol. 37, No. 5, Apr. 1966

VAPOR-PHASE GROWTH and Properties of GaAs Gunn Devices—R. E. Enstrom, C. C. Peterson (Labs, Pr) Conf. on Electronic Matls. for Control of Radiative Processes, Boston, Mass., Aug. 29-31, 1966

VAPOR-PHASE GROWTH of $GaAs_{1-x}P_x$ Room-Temperature Injection Lasers—J. J. Tietjen, J. I. Pankove, I. J. Hegyi, H. Nelson (Labs, Pr) Conf. on Electronic Matls., Boston, Mass., Aug. 29-31, 1966

VAPOR PHASE GROWTH of GaP Electro-Optic Modulator—D. Richman, J. J. Tietjen (Labs, Pr) Conf. on Electronic Matls., Boston, Mass., Aug. 29-31, 1966

PROPERTIES, SURFACE (& thin films)

ELECTRICAL CONDUCTIVITY of 0-2 Monolayers of Cesium on Sapphire at 77°K—J. D. Levine (Labs, Pr) *J. of App. Phys.*, Vol. 37, No. 5, Apr. 1966

SURFACE LASER of $BaTiO_3$—D. R. Callaby (Labs, Pr) *J. of App. Phys.*, Vol. 37, No. 6, May 1966

VAPOR-DEPOSITED EPITAXIAL $GaAs_{1-x}P_x$ Using Arsine and Phosphine, The Preparation and Properties of—J. J. Tietjen, J. A. Amick (Labs, Pr) *J. of Electro-Chem. Soc.*, Vol. 133, No. 7, July 1966

PROPERTIES, CHEMICAL

SOLVENT GROWTH (Lateral Traveling) in Indium Arsenide—H. P. Kleinknecht (Labs, Pr) *J. of App. Phys.*, Vol. 37, No. 5, Apr. 1966

STABILIZATION OF GERMANIUM (II) by Complex Formation in Iodimetric Titration of Germanium—K. L. Cheng (Labs, Pr) *Analytica Chimica Acta*, Vol. 35, No. 3, July 1966

X-RAY SPECTROMETRY, Chemical Analysis by—Principles, Instrumentation, Methods, Measurements, and Specimen Preparation—E. P. Epstein (ECD, Hr) Seminar on X-Ray Spectrometric Analysis, Stevens Inst., Hoboken, N. J., June 20, 1966

PROPERTIES, ELECTRICAL

ELECTRONIC PROPERTIES in the System $BaO-TiO_2-BaF_2$, Investigation of the—F. E. Richter (H. I. Indpls) Elec. Div. Amer. Ceramic Soc. Natl. Conv., May 10, 1966

SUBCRITICAL CURRENTS, RF Resistance in the Mixed State for—J. I. Gittleman, B. Rosenblum (Labs, Pr) *Phys. Rev. Ltrs.*, Vol. 16, No. 17, Apr. 25, 1966

PROPERTIES, MAGNETIC

FLUX FLOW and Flux Pinning, R. F Studies of—J. I. Gittleman, B. Rosenblum (Labs, Pr) 10th Intl. Conf. on Low-Temperature Physics, Moscow, Aug. 31-Sept. 6, 1966

FLUX PINNING in Nb_3Sn by Grain Boundaries—J. J. Hanak, R. E. Enstrom (Labs, Pr) 10th Intl. Conf. on Low-Temperature Physics, Moscow, Aug. 31-Sept. 6, 1966

MAGNETIZATION STUDIES of Single Crystals of Nb_3Sn—J. J. Hanak, J. J. Halloran, G. D. Cody (Labs, Pr) 10th Intl. Conf. on Low-Temperature Physics, Moscow, Aug. 31-Sept. 6, 1966

PROXIMITY EFFECTS in Magnetic Fields—G. Fischer, R. Klein (Labs, Pr) 10th Intl. Conf. on Low-Temperature Physics, Moscow, Aug. 31-Sept. 6, 1966

PROPERTIES, MECHANICAL

POINT-DEFECT DISLOCATION Interactions and Frictional Stresses in Nickel Using Microstrain Measurements, A Study of—H. Kressel (ECD, Som) ASM Symp. on Precision Mechanical Property Measurements, Atlantic City, N.J., June 27, 1966

PROPERTIES, OPTICAL

ELECTROLUMINESCENCE in II-VI Compounds—A. G. Fischer (Labs, Pr) Intl. Conf. on Luminescence, Budapest, Hungary, Aug. 23-30, 1966

EXCITED STATE LIFETIMES in Phthalocyanines—S. E. Harrison, W. F. Kosonocky (Labs, Pr) Intl. Conf. on Luminescence, Budapest, Hungary, Aug. 23-30, 1966

FLUORESCENSE of Ternary Sulfides and Selenides—L. Krausbauer, R. Nitsche, P. Wild (Labs, Pr) Intl. Conf. on Luminescence, Budapest, Hungary, Aug. 23-30, 1966

GROUP II-VI PHOSPHORS with Rare-Earth Activators—S. Larach (Labs, Pr) Intl. Conf. on Luminescence, Budapest, Hungary, Aug. 8-23, 1966

IMAGE SENSOR, A Thin-Film Solid-State—P. K. Weimer, G. Sadasiv, H. Borkan, L. Meray-Horvath, F. V. Shallcross, J. Meyer, Jr. (Labs, Pr) Intl. Solid-State Circuits Conf., *Digest of Tech. Papers*, Feb. 1966

RADAR

ORBITING BODIES, The Radar Acquisition of—L. E. Kitchens (MSR, Mrstn) *MSEE Thesis*, Villanova Univ., June 1966

PHASED-ARRAY Radar Orientation to Minimize Average Scanning Loss—J. L. Worst (MSR, Mrstn) *MSEE Thesis*, Univ. of Penna., June 1966

RADAR VIDEO—A New Dimension in Data Analysis—S. F. Cohen (MSR, Mrstn) IEEE Aerospace System Conf., Seattle, Wash., July 11-15, 1966; *Conf. Proc.*

RADIATION EFFECTS

CAPACITORS (MOS): Irradiation of MOS Capacitors with High-Energy Electrons—K. H. Zaininger (Labs, Pr) IEEE Conf. on Nuclear and Space Radiation Effects, Palo Alto, Calif., July 18-22, 1966

COMMENT ON: "Radiation Resistance of Linear Current Filament in a Simple Anisotropic Medium"—H. Staras (Labs, Pr) *IEEE Trans. on Antennas and Propagation*, Vol. AP-14, No. 3, May 1966

SOLAR CELL Output Characteristics, Temperature, Illumination Intensity, and Degradation-Factor Effects on—R. Rasmussen, H. Harmon (AED, Pr) IEEE Aerospace Systems Conf., Seattle, Wash., July 13, 1966; *Conf. Proc.*

SOLAR CELLS, Lithium-Doped Radiation-Resistant Silicon—J. J. Wysocki (Labs, Pr) IEEE Nuclear & Space Radiation Effects Conf., Palo Alto, Calif., July 18-22, 1966

SOLAR CELLS, Low-Energy Proton Bombardment of GaAs and Si—J. J. Wysocki, P. Rappaport, E. Davison, J. J. Loferski (Labs, Pr) *IEEE Trans. on Electron Devices*, Vol. ED-13, No. 4, P. 420, Apr. 1966

TRANSISTORS (MOS) Radiation Induced Instability in—W. Dennehy, G. Brucker, A. Holmes-Siedle (AED, Pr) 1966 IEEE Annual Conf. on Nuclear and Space Radiation Effects, Palo Alto, Calif., July 18, 1966

RADIO RECEIVERS (mass-media)

INTEGRATED CIRCUITS Make Low-Cost FM Receiver—R. L. Sanquini (ECD, Som) *Electronics*, Aug. 8, 1966

RECORDING (techniques & materials)

DIELECTRIC TAPE Camera System for Meteorological Applications—L. Freedman (AED, Pr) IEEE Aerospace Systems Conf., Seattle, Wash., July 13, 1966; *Conf. Proc.*

RECORDING, DIGITAL (equipment)

REVIEW OF: "Recertification of Instrumentation Tape," General Kinetics, Inc.—F. H. Fowler, Jr. (CSD, Cam) *Computing Reviews*, May-June 1966

REVIEW OF: "The Tape Management Program," General Kinetics, Inc.—F. H. Fowler, Jr. (CSD, Cam) *Computing Reviews*, May-June 1966

REVIEW OF: "The Technology of Tape Preventive Maintenance," General Kinetics, Inc.—F. H. Fowler, Jr. (CSD, Cam) *Computing Reviews*, May-June 1966

REVIEW OF: "Why is Tape Preventive Maintenance Needed"?, General Kinetics, Inc.—F. G. Fowler, Jr. (CSD, Cam) *Computing Reviews*, May-June 1966

SOLID-STATE DEVICES

CAPACITORS (MOS): Irradiation of MOS Capacitors with High-Energy Electrons—K. H. Zaininger (Labs, Pr) IEEE Conf. on Nuclear and Space Radiation Effects, Palo Alto, Calif., July 18-22, 1966

ELECTRON MICROSCOPY of Solid-State Materials—M. D. Coutts (Labs, Pr) EMSA 24th Mtg., San Francisco, Calif., Aug. 25, 1966

FERROELECTRIC Field-Effect Device—P. M. Heyman, G. H. Heilmeier (Labs, Pr) *Proc. of IEEE*, Vol. 54, No. 6, June 1966

TRANSISTOR (FIELD-EFFECT) Amplifiers—R. W. Ahrons (ECD, Som) WESCON, L. A., Calif., Aug. 23-26, 1966; *WESCON Preprint*

MICROPLASMA OBSERVATIONS in Silicon Junctions Using a Scanning Electron Beam—J. W. Gaylord (Labs, Pr) *J. of Electro-Chem. Society*, Vol. 113, No. 7, July 7, 1966

PHOTOPARAMETRIC DETECTORS with Internal Current Multiplication—F. Sterzer, J. R. Collard (ECD, Pr) Electron Device Res. Conf., Pasadena, Calif., June 27-July 1, 1966

TRANSISTOR (RF) Power Amplifiers, Design Trade-Offs for—R. Minton (ECD, Som) WESCON, L. A., Calif., Aug. 23-26, 1966; *WESCON Preprint*

TRANSISTORS (FIELD-EFFECT) Based on Silk-Screened CdS Layers—W. Witt, F. Huber, W. Laznovsky (DME, Som) *Proc. of IEEE*, Vol. 54, Pg. 898, June 1966

TRANSISTORS, Microwave Power—H. C. Lee (ECD, Som) WESCON, L. A., Calif., Aug. 23-26, 1966; *WESCON Preprint*

TRANSISTORS (MOS), Radiation Induced Instability in—W. Dennehy, G. Brucker, A. Holmes-Siedle (AED, Pr) 1966 IEEE Annual Conf. on Nuclear and Space Radiation Effects, Palo Alto, Calif., July 18, 1966

TRANSISTORS (RF POWER) in Vehicular Radio Communications Equipment—S. Matyckas (ECD, Som) WESCON, L. A., Calif., Aug. 23-26, 1966; *WESCON Preprint*

(TRANSISTORS, THIN-FILM): Reversible Gate Insulator Instabilities in TFT's—R. Schelhorn (DME, Som) 5th Ann. Symp. on Microelectronics, IEEE, July 17-20, 1966, St. Louis, Mo.; *Conf. Proc.*

TUNNEL DIODES, Selecting—R. M. Minton (ECD, Som) *Electronics World*, July 1966

VARACTOR MULTIPLIERS and High-Power Microwave Varactors—J. Collard, C. Sun, T. E. Walsh (ECD, Pr) WESCON, L. A., Calif., Aug. 23-26, 1966; *WESCON Preprint*

SPACE COMMUNICATION (mass-media & scientific)

DECENTRALIZED CONTROL for an Advanced Communication Satellite System—J. C. Bry, K. Solomon (SEER, Mrstn) AIAA, Wash., D.C., May 2, 1966

EARTH STATION, Canada's Communication Satellite—D. Jung (RCA Ltd., Montreal) IEEE 1966 Intl. Communications Conf., Phila., Penna., June 17, 1966

LEM COMMUNICATIONS Systems—R. E. Davis (ASD, Burl) IEEE Aerospace Systems Conf., Seattle, Wash., July 14, 1966; *Conf. Proc.*

MARS-LANDER Direct Communication Link—Dr. A. B. Glenn (SEER, Mrstn) Natl. Electronics Conf., Chicago, Oct. 4-6, 1966; *Conf. Record*

PCM TELEMETRY Data, Burst Retransmission of—H. W. Trigg (MSR, Mrstn) IEEE Aerospace Systems Conf., Seattle, Wash., July 11-15, 1966; *Conf. Proc.*

ROCKETSONDE TRANSMITTER, A New Low-Cost Solid-State—R. E. Askew (ECD, Hr) *Electronic Communicator*, July-August 1966

SATELLITE COMMUNICATIONS and the Space Environment—R. B. Marsten (AED, Pr) The Franklin Inst., Phila., Penna., July 26, 1966

SPACE COMMUNICATION, Modern Techniques for—W. Y. Pan (CSD, Cam) Seminar on Modern Eng. Tech., Taiwan, China, June 27-July 9, 1966

SPACE NAVIGATION (& tracking)

ATTITUDE and Spin Control for TIROS Wheel—W. Lindorfer, L. Muhlfelder (AED, Pr) AIAA Guidance and Control Specialist Conf., Seattle, Wash., Aug. 15-17, 1966

GUIDANCE and Control in Space—T. Furia (AED, Pr) Aerospace Education Workshop for Teachers, Ambler Campus of Temple Univ., Phila., Pa., Aug. 22, 1966

REENTRY CAPSULE SURVEILLANCE and Tracking, HF Applications to—M. H. Lowe (MSR, Mrstn) IEEE Aerospace Systems Conf., Seattle, Wash., July 1966

SPACECRAFT (& space missions)

ELECTRONIC SYSTEMS Management in Space Vehicles—J. F. Gardiner (ASD, Burl) Moderator of Panel Discussion, IEEE Aerospace Systems Conf., Seattle, Wash., July 11-15, 1966; *Conf. Proc.*

LEM COMMUNICATIONS Systems—R. E. Davis (ASD, Burl) IEEE Aerospace Systems Conf., Seattle, Wash., July 14, 1966; *Conf. Proc.*

PUBLIC NAVIGATION SYSTEM—J. N. Breckman (SEER, Mrstn) *Space and Aeronautics*, July 1966

REENTRY CAPSULE SURVEILLANCE and Tracking, HF Applications to—M. H. Lowe (MSR, Mrstn) IEEE Aerospace Systems Conf., Seattle, Wash., July 1966

SPACECRAFT POWER Systems, The Comparison of—L. Pessin, D. Rusta (AED, Pr) IEEE Aerospace Systems Conf., Seattle, Wash. July 12-13, 1966; *Conf. Proc.*

SPACECRAFT INSTRUMENTATION

ALTIMETER ACCURACY DEGRADATION (J_1) from Transmission Line Reflections and Circular Leakage—S. L. Goldman (ASD, Burl) *MS Thesis*, Univ. of Pa., Phila., Pa., Feb. 2, 1966

DIELECTRIC TAPE Camera System for Meteorological Applications—L. Freedman (AED, Pr) IEEE Aerospace Systems Conf., Seattle, Wash., July 13, 1966; *Conf. Proc.*

MULTIPLIERS (Microwave Solid-State) for Space Systems—W. J. Dodds (ECD, Hr) WESCON, L. A., Calif., Aug. 23-26, 1966; *WESCON Preprint*

PHOTOVOLTAICS for Space Applications—P. Rappaport (Labs, Pr) AIChE, Chem Eng. Symp. Series, No. 5, London, June 13-17, 1965

SUPERCONDUCTIVITY (& cryoelectrics)

ELECTRICAL CONDUCTIVITY of 0-2 Monolayers of Cesium on Sapphire at 77°K—J. D. Levine (Labs, Pr) *J. of App. Phys.*, Vol. 37, No. 5, April 1966

FLUX FLOW and Flux Pinning, RF Studies of—J. I. Gittleman, B. Rosenblum (Labs, Pr) 10th Intl. Conf. on Low-Temperature Physics, Moscow, Aug. 31-Sept. 6, 1966

FLUX PINNING in Nb Sn_3 by Grain Boundaries—J. J. Hanak, R. E. Enstrom (Labs, Pr) 10th Intl. Conf. on Low-Temperature Physics, Moscow, Aug. 31-Sept. 6, 1966

MAGNETIC TRANSITIONS (Parallel and Perpendicular) of Superconducting Films and Foils of Lead—G. D. Cody, R. E. Miller (Labs, Pr) *Phys. Rev. Ltrs.*, Vol. 16, No. 16-18 April 18, 1966

MAGNETIZATION STUDIES of Single Crystals of Nb_3Sn—J. J. Hanak, J. J. Halloran, G. D. Cody (Labs, Pr) 10th Intl. Conf. on Low-Temperature Physics, Moscow, Aug. 31-Sept. 6, 1966

PROXIMITY EFFECTS in Magnetic Fields—G. Fischer, R. Klein (Labs, Pr) 10th Intl. Conf. on Low-Temperature Physics, Moscow, Aug. 31-Sept. 6, 1966

SUPERCONDUCTING CONTACTS, A New Effect at—J. I. Pankove (Labs, Pr) 10th Intl. Conf. on Low-Temperature Physics, Moscow, Aug. 31-Sept. 6, 1966

TELEVISION BROADCASTING (mass-media)

NTSC & PAL COLOR STANDARDS, A Comparison of Color TV Cameras for—A. H. Line (BCD, Cam) SMPTE Spring Conf. on Broadcast & TV Receivers, Chicago, Ill., June 14, 1966

TELEVISION EQUIPMENT (non-mass-media)

IMAGE SENSOR, A Thin-Film Solid-State—P. K. Weimer, G. Sadasiv, H. Borkan, L. Merey-Horvath, F. V. Shallcross, J. Meyer, Jr. (Labs, Pr) Intl. Solid-State Circuits Conf., *Digest of Tech. Papers*, Feb. 1966

TRANSMISSION LINES (& waveguides)

WAVEGUIDE CAVITY RESONATOR, Comments on Loaded Q of a—R. M. Kurzrok (CSD, Cam) *IEEE Trans. Corres.*, July 28, 1966

TUBE COMPONENTS (materials & fabrication)

LEAK TESTING and Acceptance of Clean Areas—E. L. Romero (ECD, Lanc) Northeast Chapter of Amer. Assoc. for Contamination Control, Boston, Mass., June 22, 1966

MASS SPECTROMETRY in Color-Television Picture Tubes, Chemical Applications of—J. J. Moscony (ECD, Lanc) Chemistry Dept. Sem., Univ. of Maine, July 27, 1966

AUTHOR INDEX

Subject listed opposite each author's name indicates where complete citation to his paper may be found in the subject index. Where an author has more than one paper, his name is repeated for each.

PRODUCT ENGINEERING (STAFF)

BROADCAST AND COMMUNICATIONS PRODUCTS DIVISION

RCA SERVICE COMPANY

RCA VICTOR COMPANY, LTD.

DEFENSE MICROELECTRONICS

COMMUNICATIONS SYSTEMS DIVISION

MISSILE AND SURFACE RADAR DIVISION

SYSTEMS ENGINEERING, EVALUATION AND RESEARCH

ASTRO-ELECTRONICS DIVISION

AEROSPACE SYSTEMS DIVISION

WEST COAST DIVISION

RCA VICTOR HOME INSTRUMENTS DIVISION

ELECTRONIC COMPONENTS AND DEVICES

RCA LABORATORIES

S/C/A/P/C

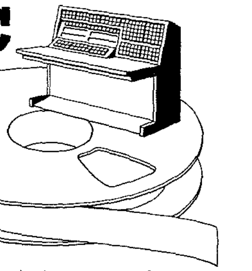

Scientific
Computer
Applications
Program
Catalog

Data sheets added to SCAPC are published when received from R. Gildea, ASD, Burlington, who coordinates SCAPC. Data sheets contain an abstract describing the program and its status. The following engineers maintain SCAPC data sheets for reference.

AEDH	R. Goerss, AED, Prin., N.J.	EDPS	L. Stuart, EDP, Cher. Hill, N.J.
ASDB	J. L. Richmond, ASD, Burl., Mass.	LABS	R. W. Klopfenstein, RCA Labs, Princeton, N.J.
BCDM	F. M. Brock, Broadcast Microwave Eng., Cam., N.J.	M&SR	R. Faust, M&SR Div., Mrstn., N.J.
CSDC	H. Jacobowitz, CSD, Cam., N.J.	VICM	G. Payette, RCA Victor Co., Ltd., Montreal, Can.
DEPA	R. D. Smith, Appl. Res., Cam., N.J.	WCDV	A. E. Cressey, West Coast Div., Van Nuys, Calif.
EDPP	S. Heiss, EDP, W. Palm Beach, Fla.		

SCAPC INDEX: Entries below consist of: the key words identifying the application (boldface type), **program title** (quoted italics), **computer language**, **name(s)** of program **contributor(s)**, and SCAPC **program number** (including location symbol from above list).

DOCUMENTATION GENERATOR (& Dewey Decimal Paragraph Numbering): *"Semiautomatic Documentation Generator"*—Fortran II; A. L. Pires, ASDB-0006

ANTENNA ELEMENTS (& SAM-D, & Array Elements & Array Spacing Optimization): *"SAM-D Array Element Spacing Optimization"*—Fortran IV; D. Shanken, M&SR-0002

CURVE FIT (& Least Squares, & Orthogonal Polynomials): *"Least Squares Curve Fit Via Orthogonal Polynomials"*—Fortran IV and Taissit; D. H. Shanken, R. D. Wattis, M&SR-0003

Patents Granted

TO RCA ENGINEERS

As Reported By RCA Domestic Patents, Princeton

RCA VICTOR HOME INSTRUMENTS

RCA LABORATORIES

Direct-Current Restorer System for Color Television Receiver—W. H. Moles, R. N. Rhodes (Labs, Pr) U.S. Pat. 3,272,914, September 13, 1966

Integrated Electrical Circuit—M. E. Sekely (Labs, Pr) U.S. Pat. 3,272,989, September 13, 1966

Television Tuner—M. A. Leedom (Labs, Pr) U.S. Pat. 3,270,571, September 6, 1966

Tunable Semiconductor Optical Modulator—B. Rosenblum (Labs, Pr) U.S. Pat. 3,259,-016, July 5, 1966

Power Semiconductor Assembly Including Heat Dispersing Means—M. W. Green (Labs, Pr) U.S. Pat. 3,259,814, July 5, 1966

Magnetic Memory Employing Anisotropy—R. H. Cornely, W. F. Kosonocky (Labs, Pr) U.S. Pat. 3,259,888, July 5, 1966

Threshold Circuit Utilizing Field Effect Transistors—J. R. Burns, R. A. Powlus (Labs, Pr) U.S. Pat. 3,260,863, July 12, 1966

Radiation Powered Semiconductor Devices—P. Rappaport, E. Pasierb, Jr. (Labs, Pr) U.S. Pat. 3,263,085, July 26, 1966

Cryoelectric Logic Circuits—R. A. Gange (Labs, Pr) U.S. Pat. 3,264,490, August 2, 1966

Heat Responsive Variable Characteristic Semiconductor Device—J. O. Kessler (Labs, Pr) U.S. Pat. 3,264,532, August 2, 1966

System for the Retrieval of Information from a Content Addressed Memory and Logic Networks Therein—H. Weinstein (Labs, Pr) U.S. Pat. 3,264,624, August 2, 1966

Deposition of Crystalline Niobium Stannide—J. J. Hanak, J. L. Cooper (Labs, Pr) U.S. Pat. 3,268,362, August 23, 1966

Thermionic Energy Converter—K. G. Hernqvist (Labs, Pr) U.S. Pat. 3,267,308, August 16, 1966

Device for Producing Recombination Radiation—A. G. Fischer (Labs, Pr) U.S. Pat. 3,267,317, August 16, 1966

Cathode Ray Tube—J. J. Thomas (Labs, Pr) U.S. Pat. 3,265,915, August 9, 1966

Variable Impedance Device for Transistor Automatic Gain Control—W. B. Guggi (Labs, Pr) U.S. Pat. 3,264,564, August 2, 1966

Method for Preparing Rare Earth Activated Zinc Sulfide Phosphors and Products Thereof—P. N. Yocom, S. Larach (Labs, Pr) U.S. Pat. 3,269,956, August 30, 1966

Multi-Layer Semiconductor Electroluminescent Output Device—E. E. Loebner (Labs, Pr) U.S. Pat. 3,270,235, August 30, 1966

Cyclotron Wave Double-Stream Devices—B. Vural (Labs, Pr) U.S. Pat. 3,270,241, August 30, 1966

Laser Control Device Using A Saturable Absorber—W. F. Kosonocky (Labs, Pr) U.S. Pat. 3,270,291, August 30, 1966

ELECTRONIC COMPONENTS AND DEVICES

Method of Making Luminescent Screens for Cathode Ray Tubes—T. A. Saulnier (ECD, Lanc) U.S. Pat. 3,269,838, August 30, 1966

Method of Fabricating Semiconductor Devices—G. T. Elie (ECD, Som) U.S. Pat. 3,264,707, August 9, 1966

Method of and Apparatus for Sealing Glass-Type Envelopes—J. Lysak (ECD, Hr) U.S. Pat. 3,266,124, August 16, 1966

Logic Circuits—B. Zuk (ECD, Som) U.S. Pat. 3,267,295, August 16, 1966

Apparatus for Manufacturing Reed Switches—H. L. Blust (ECD, Hr) U.S. Pat. 3,268,317, August 23, 1966

Plural Electron Gun Assembly and Magnetic Convergence Cage—R. H. Hughes (ECD, Lanc) U.S. Pat. 3,268,753, August 23, 1966

Plural Electrode Unit Electron Tube—R. A. Bonnette, T. E. Deegan (ECD, Hr) U.S. Pat. 3,268,760, August 23, 1966

Method of Making Modules—W. L. Oates (ECD, Som) U.S. Pat. 3,263,303, August 2, 1966

Cathode Ray Tube Fabrication—C. T. Lattimer (ECD, Marion) U.S. Pat. 3,264,157, August 2, 1966

Control System—R. W. Sonnenfeldt, L. M. Glickman (ECD, Natick) U.S. Pat. 3,264,397, August 2, 1966

Stereophonic FM Receivers—R. Santilli, L. Plus (ECD, Som) U.S. Pat. 3,264,414, August 2, 1966

Line Voltage Reenergized Transistor Signal Amplifier Including a High Voltage Stage and a Low Voltage Stage—H. M. Kleinman (ECD, Som) U.S. Pat. 3,262,063, July 19, 1966

Electron Discharge Tube Having a Diode Built Therein—T. M. De Muro (ECD, Hr) U.S. Pat. 3,263,108, July 26, 1966

Data Storage Systems—A. Harel (ECD, Natick) U.S. Pat. 3,263,214, July 24, 1966

Color Cathode Ray Tube With Index Stripes on Ultra-Violet-Emitting Phosphor Layer—H. B. Law (ECD, Pr) U.S. Pat. 3,271,610, September 6, 1966

Printed Circuit Assemblies of Magnetic Cores—H. P. Lemaire, L. B. Smith (ECD, Needham Hts) U.S. Pat. 3,273,134, September 13, 1966

RCA VICTOR HOME INSTRUMENTS

Color Television Receiver Including Transistorized Color Killer—G. E. Theriault (HI, Indpls) U.S. Pat. 3,272,915, September 13, 1966

Enclosure for High Voltage Apparatus—J. Stark, Jr., B. E. Denton, J. W. McLeod, Jr. (HI, Indpls) U.S. Pat. 3,273,021, September 13, 1966

Positioning Mechanism—D. R. Andrews (HI, Indpls) U.S. Pat. 3,271,034, September 6, 1966

Field Effect Transistor Translating Circuit—G. E. Theriault (HI, Indpls) U.S. Pat. 3,260,948, July 12, 1966

Parametric Amplifier Frequency—L. A. Harwood, T. Murakami (HI, Indpls) U.S. Pat. 3,261,981, July 19, 1966

Automatic Frequency Control—J. Stark, Jr. (HI, Indpls) U.S. Pat. 3,264,408, August 2, 1966

Transistor Clamp Circuit—J. O. Schroeder, J. F. Merritt (HI, Indpls) U.S. Pat. 3,268,658, August 23, 1966

Insulated-Gate Field-Effect Transistor Amplifier Having Means to Reduce High Frequency Instability—D. J. Carlson, G. E. Theriault (HI, Indpls) U.S. Pat. 3,268,827, August 23, 1966

Color Kinescope Operating and Testing Arrangements—G. E. Kelly, P. E. Crookshanks (HI, Indpls) U.S. Pat. 3,270,125, August 30, 1966

Color Matrix Including Negative Feed Back and A Cross-Feed Connection—P. E. Crookshanks, T. C. Jobe (HI, Indpls) U.S. Pat. 3,270,126, August 30, 1966

Power Supply Protection Arrangement—J. Stark, Jr. (HI, Indpls) U.S. Pat. 3,270,128, August 30, 1966

Ultra High Frequency Transistor Oscillator—L. A. Harwood (HI, Indpls) U.S. Pat. 3,270,292, August 30, 1966

FM Stereophonic Receiver Using an Insulated-Gate-Field-Effect Transistor for Combining the Subcarrier and Composite Waves—J. F. Merritt (HI, Indpls) U.S. Pat. 3,264,413, August 2, 1966

BROADCAST AND COMMUNICATIONS PRODUCTS DIVISION

Automatic Exciter Lamp Changer—B. F. Floden (BCD, Cam) U.S. Pat. 3,269,795, August 30, 1966

Servo System with Plural Reference Signals—R. N. Hurst, R. A. Dischert (BCD, Cam) U.S. Pat. 3,270,130, August 30, 1966

Frequency Modulated Oscillator—A. Lochanko (BCD, Cam) U.S. Pat. 3,263,190, July 26, 1966

Frequency Insensitive Phase Measuring by Averaging the Imbalance of a Wheatstone Bridge—R. N. Hurst (BCD, Cam) U.S. Pat. 3,259,843, U.S. Pat. 3,259,843, July 5, 1966

Phase Inverter and Automatic Frequency Control Stabilizer for a Frequency Modulator System—A. H. Bott (BCD, Cam) U.S. Pat. 3,259,856, July 5, 1966

COMMUNICATIONS SYSTEMS DIVISION

Signal Limiter—W. Y. Pan (CSD, N.Y.) U.S. Pat. 3,272,996, September 13, 1966

Variable Attenuator—J. F. McSparran (CSD, N.Y.) U.S. Pat. 3,273,084, September 13, 1966

Matrix Printer Employing Print—E. D. Simshauser (CSD, Cam) U.S. Pat. 3,267,845, August 23, 1966

APPLIED RESEARCH

Inverter Circuit in Which a Coupling Transistor Functions Similar to Charge Storage Diode—A. Feller (AppRes, Cam) U.S. Pat. 3,265,906, August 9, 1966

Balanced Current Pumped Parametric Converter—E. P. McGrogan, Jr. (AppRes, Cam) U.S. Pat., 3,264,488, August 2, 1966

Tunnel Diode Circuit—M. Cooperman (AppRes, Cam) U.S. Pat. 3,260,862, July 12, 1966

WEST COAST DIVISION

Data Processing—L. W. Bleiman (WCD, VanNuys) U.S. Pat. 3,266,497, August 16, 1966

Means for Returning a Record Card to Its Stack—L. W. Bleiman (WCD, VanNuys) U.S. Pat. 3,266,798, August 16, 1966

MISSILE AND SURFACE RADAR DIVISION

Analog-to-Digital Converter—D. J. Coyle, E. D. Grim (MSR, Mrstn) U.S. Pat. 3,268,885, August 23, 1966

RCA VICTOR RECORD DIVISION

Brake Member for a Tape Cartridge—S. W. Liddle (Rec, Indpls) U.S. Pat. 3,259,331, July 5, 1966

ELECTRONIC DATA PROCESSING

Document Stacking Device—U. Germen (EDP, Fla) U.S. Pat. 3,271,026, September 6, 1966

Tape Transport—S. Baybick, R. H. Jenkins (EDP, Cam) U.S. Pat. 3,259,330, July 5, 1966

Coaxial Cable Terminal Connection and Method—S. M. Shelley (EDP, Cam) U.S. Pat. 3,260,791, July 12, 1966

Binary Coded Decimal Counter Circuits—A. Prieto (EDP, Fla) U.S. Pat. 3,264,567, August 2, 1966

Timing Pulse Generator Having Selective Pulse Spacing—E. L. Newman, Fuh-Lin Wang (EDP, Cam) U.S. Pat. 3,268,820, August 23, 1966

Timing or Clock Pulse Generator Employing Plural Counters Capable of Being Selectively Gated—Fuh-Lin Wang (EDP, Cam) U.S. Pat. 3,268,821, August 23, 1966

Electrical Connectors—M. Silverberg (EDP, Cam) U.S. Pat. 3,268,849, August 23, 1966

Mechanical Movement—H. M. Wellers, J. G. Seymour (EDP, Fla) U.S. Pat. 3,266,329, August 16, 1966

Meetings

DEC. 1-2, 1966: **Vehicular Comm. Conf.,** IEEE, G-EMB, ISA, ASME, Queen Elizabeth Hotel, Montreal, Canada. **Prog. Info.:** H. Stewart, Dept. of Transport, Hunter Bldg., Ottawa, Ontario, Canada.

DEC. 5-7, 1966: **Int'l Antennas & Propagation Symposium,** IEEE, G-AP, Cabana Motor Hotel, Palo Alto, Calif. **Prog. Info.:** R. L. Leadabrand, Stanford Res. Inst., Menlo Park, Calif.

DEC. 7-8, 1966: **Fall URSE-IEEE Meeting,** URSE-IEEE, Stanford Univ., Stanford, Calif. **Prog. Info.:** IEEE Headquarters, 345 E. 47th St., N.Y., N.Y. 10017.

JAN. 4-7, 1967: **Solid-State Physics,** Inst. of Physics and Physical Soc.; **Prog. Info.:** Meetings Officer, IPPS, 47 Belgrave Sq., London SW1, England.

JAN. 9-11, 1967: **Electrical & Electronic Meas. Test Instrument Conf.** (EEMTIC), IEEE, Ottawa Section, Ottawa, Ontario, Canada; **Prog. Info.:** J. H. Bradley, Material Command, Canadian Forces Base, Rockcliffe, Ottawa, Ontario.

JAN. 10-12, 1967: **Symp. on Reliability,** G-R, ASQC, et al.; Sheraton Park Hotel, Washington, D.C. **Prog. Info.:** H. D. Hulme, Westinghouse R&D Center Bldg., 601-1B46, Pittsburgh, Penna. 15235.

JAN. 29-FEB. 3, 1967: **Winter Power Meeting,** G-P, Statler Hilton Hotel, New York. **Prog. Info.:** E. C. Day, IEEE, 345 E. 27th St., New York, N.Y. 10017.

FEB. 7-9, 1967: **Winter Convention on Aerospace & Electronic Systems,** G-AES, L.A. District, International Hotel, Los Angeles, Calif. **Prog. Info.:** IEEE Headquarters, 345 E. 47th St., New York, N.Y. 10017.

FEB. 15-17, 1967: **Int'l Solid State Circuits Conference,** G-CT, Phila. Section, Univ. of Penn. Sheraton Hotel, Philadelphia, Pa. **Prog. Info.:** J. S. Mayo, Bell Tel. Labs. Room 3F332, Holmdel, New Jersey.

MARCH 20-22, 1967: **Physical Process in the Lower Atmosphere,** U. of Michigan American Meteorological Soc. **Prog. Info.:** A. C. Wiin-Nielsen, Meteorology and Oceanography Dept., U. of Michigan, 2038 East Engineering Bldg., Ann Arbor, Mich.

PROFESSIONAL MEETINGS

DATES *and* DEADLINES

Be sure deadlines are met—consult your Technical Publications Administrator or your Editorial Representative for the lead time necessary to obtain RCA approvals (and government approvals, if applicable). Remember, abstracts and manuscripts must be so approved BEFORE sending them to the meeting committee.

APRIL 17-19, 1967: **Thermal Balance of Spacecraft,** American Inst. of Aeronautics and Astronautics, Nat'l Bureau of Standards, Air Force. **Prog. Info.:** Y. S. Touloukian, Thermophysical Properties Research Center, Purdue U., 2595 Yeager Rd., Lafayette, Ind.

Calls for Papers

APR. 5-7, 1967: **Int'l Magnetics Conference** (INTERMAG), G-Mag, Shoreham Hotel, Wash., D.C. **Deadline Info.:** R. F. Elfant, IBM, Yorktown Heights, New York.

APR. 18-19, 1967: **Electronics & Instrumentation Conf. & Exhibition,** IEEE Cincinnati Sec., ISA, Carousel Inn, Cincinnati Gardens, Cincinnati, Ohio. **Deadline Info.:** IEEE Headquarters, 345 E. 47th St., N.Y., N.Y. 10017.

APR. 18-20, 1967: **Spring Joint Computer Conf.,** IEEE, AFIPS, Chalfonte-Haddon Hall, Atlantic City, N.J. **Deadline Info.:** AFIPS Headquarters, 211 E. 43rd St., New York, N.Y. 10017.

APR. 19-21, 1967: **Southwestern IEEE Conf. & Elec. Exhibition** (SWIEECO), IEEE Region 5, Dallas Memorial Auditorium, Dallas, Texas. **Deadline Info.:** IEEE Headquarters, 345 E. 47th St., N.Y., N.Y. 10017.

APR. 19-22, 1967: **Semiconductor Device Research Conf.,** IEEE Region 8 et al., Bad Nauheim, Germany. **Deadline:** (Abstract) **12/15/66** TO: Prof. W. J. Kleen, 8 Munchen 8 (F.R. Germany) Balanstr. 73.

MAY 3-5, 1967: **Joint Parts, Materials & Packaging Conf.** (formerly the Electronic Components Conf.), IEEE, G-PMP, EIA, Marriott Motor Hotel, Washington, D.C. **Deadline Info.:** C. K. Morehouse, Globe Union Inc., Box 591, Milwaukee, Wisc.

MAY 3-6, 1967: **Rare Earths,** Oak Ridge Nat'l Lab, Air Force Office of Scientific Research. **Deadline Info.:** (Abstract) **12/1/66** TO: W. C. Koehler, ORNL, Oak Ridge, Tenn.

MAY 15-17, 1967: **IEEE Aerospace Elc. Conv.** (NAECON), IEEE Dayton Sec., G-AES, Dayton, Ohio. **Deadline Info.:** IEEE Headquarters, Dayton Office, 1414 E. 3rd St., Dayton 3, Ohio.

MAY 16-18, 1967: **Nat'l Telemetering Conf.,** IEEE, AIAA, ISA, San Francisco Hilton Hotel, San Francisco, Calif. **Deadline Info.:** IEEE Headquarters, 345 E. 47th St., N.Y., N.Y. 10017.

MAY 18-19, 1967: **10th Midwest Symp. on Circuit Theory,** IEEE, G-CT & Purdue Univ., Purdue Univ., Lafayette, Ind. **Deadline Info.:** IEEE Headquarters, 345 E. 47th St., N.Y., N.Y. 10017.

MAY 22-25, 1967: **Spring URSI-IEEE Mtg.,** URSI-IEEE, Ottawa, Ontario, Canada. **Deadline Info.:** IEEE Headquarters, 345 E. 47th St., N.Y., N.Y. 10017.

MAY, 1967: **Int'l Symp. on Microwave Theory & Techniques,** IEEE, G-MTT, Boston, Mass. **Deadline Info.:** IEEE Headquarters, 345 E. 47th St., N.Y., N.Y. 10017.

JUNE 5-9, 1967: **Joint Automatic Control Conference,** IEEE, AACC, Univ. of Penna., Phila., Penna. **Deadline Info.:** IEEE Headquarters, 345 E. 47th St., N.Y., N.Y. 10017.

JUNE 12-14, 1967: **IEEE Int'l Communications Conf.,** IEEE G-Com. Tech. Twin Cities Sect., Radisson Hotel, Minneapolis, Minn. **Deadline Info.:** R. J. Collins, Univ. of Minnesota, Dept. of E.E., Minneapolis, Minn. 55455.

JUNE 19-21, 1967: **San Diego Symp. for Biomedical Engrg.,** IEEE, U.S. Naval Hospital et al., San Diego, Calif. **Deadline:** (Abstract) **4/12/67** TO: D. L. Franklin, Scripps Clinic & Res. Foundation, LaJolla, Calif.

JULY 9-14, 1967: **Summer Power Mtg.,** IEEE G-P, Portland Hilton Hotel, Portland, Oregon. **Deadline:** (Abstract) **4/10/67** TO: E. C. Day, IEEE, 345 E. 47th St., N.Y., N.Y. 10017.

JULY 18-20, 1967: **9th Electromagnetic Compatibility Symposium,** IEEE G-EMC, Shoreham Hotel, Washington, D.C. **Deadline Info.:** F. T. Mitchell, Atlantic Res. Corp., Shirley Hwy. & Edsall Rd., Alexandria, Va.

AUG. 22-25, 1967: **Western Electronic Show & Convention (WESCON),** IEEE-WEMA, Cow Palace, San Francisco, Calif. **Deadline:** (Abstract) **5/15/67** TO: WESCON, 3600 Wilshire Blvd., Los Angeles, Calif.

SEPT. 11-15, 1967: **Int'l Symp. on Info. Theory,** IEEE, G-IT, Athens, Greece, **Deadline:** (Abstract) **5/1/67** TO: IEEE, 345 E. 47th St., N.Y., N.Y. 10017.

SEPT. 13-14, 1967: **8th Biennial Elec. Heating Conf.,** IEEE, G-IGA, Statler Hilton Hotel, Detroit, Mich. **Deadline:** (Abstract) **12/29/66** TO: IEEE, 345 E. 47th St., N.Y., N.Y. 10017.

SEPT. 24-28, 1967: **Joint Power Generation Conf.,** IEEE, G-P et al., ASME, Statler Hilton Hotel, Detroit, Mich. **Deadline:** (Abstract) **4/1/67** TO: IEEE, 345 E. 47th St., N.Y., N.Y. 10017.

OCT. 9-10, 1967: **Joint Engineering Management Conf.,** IEEE-ASME et al., Jack Tar Hotel, San Francisco, Calif. **Deadline:** (Paper) **4/1/67** TO: IEEE, 345 E. 47th St., N.Y., N.Y. 10017.

OCT. 15-19, 1967: **7th Nat'l Electrical Insulation Conf.,** G-EI, NEMA; Palmer House, Chicago, Illinois. **Deadline Info.:** John Lenkey, Anaconda, 605 3rd Ave., New York, N.Y.

OCT. 16-18, 1967: **Convention on Aerospace & Electronic Systems,** G-AES, Sheraton Park Hotel, Washington, D.C. **Deadline Info.:** IEEE Headquarters, 345 E. 47th St., N.Y., N.Y. 10017.

OCT. 16-18, 1967: **Fall URSI-IEEE Meeting,** URSI-IEEE, Ann Arbor, Mich. **Deadline Info.:** IEEE Headquarters, 345 E. 47th St., N.Y., N.Y. 10017.

OCT. 18-20, 1967: **Int'l Symp. on Antennas & Propagation,** G-AP, Rockham Bldg., Univ. of Mich., Ann Arbor, Mich. **Deadline Info.:** R. Hiatt, Radiation Lab., Univ. of Mich., Ann Arbor, Mich.

OCT. 23-25, 1967: **Nat'l Electronics Conf.,** IEEE et al., McCormick Pl., Chicago, Ill. **Deadline Info.:** Nat'l Electronics Conf., 228 N. LaSalle St., Chicago, Illinois.

OCT. 1967: **Electron Devices Meeting,** G-ED, Washington, D.C. **Deadline Info.:** IEEE Headquarters, 345 E. 47th St., N.Y., N.Y.

NOV. 1-3, 1967: **Northeast Research & Eng. Meeting** (NEREM), New England Section, Boston, Mass. **Deadline:** (Abstract) **6/15/67** TO: IEEE Boston Office, 31 Channing St., Newton, Mass.

Engineering NEWS *and* HIGHLIGHTS

SALUTE TO DAVID SARNOFF

The electronics and communications industries paid tribute to RCA Chairman **David Sarnoff** in commemoration of the 60th anniversary of the start of his career in communications. Three national organizations—the Electronics Industries Association, the Institute of Electrical and Electronics Engineers, and the National Association of Broadcasters—co-sponsored the "Salute to David Sarnoff" at New York's Waldorf-Astoria Hotel on September 30, the exact day 60 years ago when General Sarnoff started working for a telegraph company.

Frederick R. Kappel, Chairman of the Board of the American Telephone and Telegraph Co., served as program chairman at the dinner, and **Lowell Thomas,** noted author, commentator, and explorer acted as toastmaster. Approximately 1,700 people, including national government leaders and eminent Americans in all walks of life, attended.

ASD TECHNICAL EXCELLENCE AWARD WINNERS

Recipients of *Technical Excellence Awards* at the Aerospace Systems Division, Burlington, Mass., for the second quarter of 1966 include: **Angelo Muzi, Robert Piper,** and **John J. Cadigan.** They were cited for outstanding performance in the following areas: Mr. Muzi—mechanical design of automated production test equipment; Mr. Piper—Lunar Module radar test facility; and Mr. Cadigan—DIMATE AM/FM adapter. In addition, a 19-man ASD team was honored for the design, development, test, and delivery on schedule of the Land Combat Support System.

M&SR TECHNICAL EXCELLENCE AWARD WINNERS

Winners of the Technical Excellence Awards at the RCA Missile and Surface Radar Division, Moorestown, N.J., for the second quarter of 1966 and their areas of achievement are: **J. D. Frattura**—data handling; **J. F. Herbert**—configuration management; **H. J. Kishi**—electrical configuration of 2-pound radar; **E. A. Mechler**—signature analysis; **R. F. Pavley**—new smoothing technique based on invariant imbedding principle; **C. E. Profera**—monopulse antenna feed horns using multimode techniques; **H. Ravitch**—analysis of AN/FPS-92 Category II test results; **Dr. M. Weiss**—thermal design and analysis for the Lunar Module.

CSD NAMES W. KIRKPATRICK V.P., MARKETING

Appointment of **William B. Kirkpatrick** as Division Vice President, Marketing Department, of the RCA Communications Systems Division, Camden, has been announced by **Joseph M. Hertzberg,** Division Vice President and General Manager. Mr. Kirkpatrick had been Marketing Manager of CSD. Mr. Kirkpatrick, who joined RCA in 1947, served earlier with the U.S. Army Signal Corps and Air Force. With the Air Force he was a Project Officer responsible for the design, development and testing of airborne radar equipment at Wright Field, Ohio. Mr. Kirkpatrick received a BSEE from the University of Pennsylvania.

DR. ENGSTROM, E. BERTERO, AND V. DUKE HONORED BY SMPTE

Dr. Elmer W. Engstrom, RCA Chief Executive Officer, and two NBC engineers were honored by the Society of Motion Picture and Television Engineers at the SMPTE 100th Semiannual Technical Conference in Los Angeles. The two NBC engineers are **Vernon J. Duke** and **Edward Bertero.**

Dr. Engstrom was given the Honorary Membership Award presented to *"living pioneers whose basic contributions . . . represent a substantial forward step in the recorded history of the arts and sciences with which the Society is most concerned."* Mr. Duke received the Herbert T. Kalmus Gold Medal Award *"for outstanding contributions in the development of color films, processes, techniques or equipment useful in making color motion pictures for theater or television use."* Mr. Bertero was given Fellow Membership *"awarded to active members who by proficiency and contributions have attained outstanding rank among engineers or executives in the disciplines with which the Society is most concerned."*

FIRST VIDEOCOMP INSTALLATION

The first installation of a new RCA electronic type composition system has been announced by Poole Bros., Inc., of Chicago. The pioneering project, scheduled to begin operations this fall at Poole Bros. typesetting division, the Poole Clarinda Co., includes the first RCA Videocomp 70/820, and an RCA Spectra 70/45 computer.

RCA COMMUNICATIONS EXPANDS SERVICES

A major expansion in the Southeast Asia telecommunications network of RCA Communications, Inc., has been announced by **Howard R. Hawkins,** President. The Company will use circuits in the recently completed segment of the SEACOM (Southeast Asian Commonwealth) Cable System. The first segment of the new cable links Guam, Hong Kong, Singapore and Malaysia. At Guam, SEACOM connects with RCA's facilities in the Transpacific Cable System, thereby providing access to the world wide RCA Telecommunications radio and cable network. Another leg of the SEACOM Cable System, which is being constructed by the Commonwealth Cable Partners, will be added early next year, directly linking Guam and Australia. RCA will use a large number of channels in SEACOM to provide message telegram, telex (teleprinter exchange) and leased channel service. RCA will operate many of these channels to provide direct cable service from the United States to Hong Kong, Singapore and Malaysia. RCA initially also will use eight wideband cable circuits providing direct public telephone service between the Philippines and Hong Kong, Malaysia and Singapore.

RCA already has a large network of more than 60 wideband cable circuits in the Transpacific Cable System, which links the U.S. Mainland with Hawaii, Midway, Wake, Guam, the Philippines and Japan. Each wideband 3-kHz cable circuit is capable of being used for alternate voice-date service or subdivided into 22 separate narrowband telegraph channels. The company also offers a variety of telecommunications services throughout the Pacific area over radio facilities.

DR. HAROLD B. LAW HONORED AT NEC

The 1966 Consumer Electronics *Outstanding Contribution Award* of the National Electronics Conference was presented to **Dr. Harold B. Law** on October 3, 1966. A former Fellow of the Technical Staff, RCA Laboratories, he is now director of the EC&D Television Picture Tube Division's Materials and Display Devices Laboratory at The David Sarnoff Research Center, Princeton, N.J.

In his research on single-tube color displays, Dr. Law was instrumental in adapting the shadow-mask principle for use in color television picture tubes. All shadow mask tubes depend on basic principles of phosphor screen printing that he developed. His invention of the photo deposition method of color tube screening made possible the utilization of the present shadow mask tube with phosphors deposited directly on the faceplate.

Dr. Law was a co-recipient of the *Television Broadcasters Association Award* in 1946. The *IEEE Vladimir K. Zworykin Television Prize* was presented to him in 1955, and in 1961 he was a co-recipient of the *David Sarnoff Outstanding Team Award* for contributions to electron optics.

RCA VICTOR, LTD., ESTABLISHES SPACE SYSTEMS ORGANIZATION

Following the successful completion of the Mill Village Communications Earth Station by RCA Victor Company, Ltd., of Montreal, **J. G. Sutherland,** Vice President, Technical Products, has announced the formation of a Space Systems activity to design and build earth stations and scientific satellites in the Canadian and International markets. RCA Victor, Ltd., already is prime contractor for the ALOUETTE and ISIS satellite series.

B. MacKimmie heads up Space Systems with **J. A. Collins** in charge of Marketing. **A. Lovas** is Program Manager for earth station work, and **J. M. Stewart** is in charge of aerospace activity.

The Mill Village units in which significant advances in the state of the art were achieved are: a highly efficient, wideband multimode feed system and a broadband liquid helium, closed cycle parametric amplifier with a noise temperature of 13°K. The measured antenna gain of the station is 58.9 dB and 61.0 dB at 4.1 GHz and 6.2 GHz, respectively, including losses on the feed, duplexer, and radome. The overall system noise temperature is 60°K at 7.5° elevation angle.

The Mill Village station joins the select family of stations—Andover, Goonhilly, Plemeu Badou, and Raisting—that have pioneered advances in earth station technology that are being applied to the network of commercial stations. Mill Village is classified as experimental because it can participate in experimental work with NASA's Advanced Technological Satellite (ATS) as well as provide commercial operation with INTELSAT I, II, and III satellite systems.

Mr. Lovas was the RCA Program Manager for the Mill Village project; **D. Jung** was the Chief Systems Engineer, and **P. Foldes** was responsible for the development and supply of the Special Feed System.

... PROMOTIONS ...

to Engineering Leader & Manager

As reported by your Personnel Activity during the past two months. Location and new supervisor appear in parentheses.

Electronic Components and Devices

C. W. Bell, Jr.: from Assoc. Eng. to *Mgr., Standardizing* (R. W. Osborne, Marion)

J. Evans, Jr.: from Sr. Eng. to *Engrg. Ldr. Product Dev.* (Mgr., Product Engrg., Lancaster)

RCA Service Company

R. L. Howland: from Systems Serv. Engr. to *Ldr. Systems Service Engr.* (C. M. Fisher, Alexandria, Va.)

Home Instruments Engineering Division

P. G. McCabe: from Member Engr. to *Ldr. Electrical Design* (G. E. Kelly, Indpls.)

P. Crookshanks: from Mbr. Engr. to *Ldr. Electrical Design* (G. E. Kelly, Indpls.)

E. Lemke: from Mbr. Engr. to *Ldr. Electrical Design* (G. E. Kelly, Indpls.)

J. W. McLeod: from Mbr. Engr. to *Ldr. Mechanical Design* (G. E. Kelly, Indpls.)

E. S. Maris: from Mbr. Engr. to *Ldr. Mechanical Design* (G. E. Kelly, Indpls.)

G. L. Roth: from Mbr. Engr. to *Ldr. Mechanical Design* (G. E. Kelly, Indpls.)

G. F. Schmitt: from Mbr. Engr. to *Ldr. Mechanical Design* (G. E. Kelly, Indpls.)

L. R. Wolter: from Mbr. Engr. to *Ldr. Electrical Design* (R. J. Lewis, Indpls.)

P. C. Wilmarth: from Mbr. Engr. to *Ldr. Electrical Design* (R. J. Lewis, Indpls.)

M. Garlotte: from Mbr. Engr. to *Ldr. Mechanical Design* (R. J. Lewis, Indpls.)

G. Shilling: from Mbr. Engr. to *Ldr. Mechanical Design* (R. J. Lewis, Indpls.)

J. J. Legault: from Sr. Liaison Engr. to *Ldr. Liaison* (E. J. Evans, Indpls.)

Broadcast and Communications Products Division

K. C. Shaver: From Eng. Design and Development to *Ldr. Design and Development* (H. S. Wilson, New York)

Missile & Surface Radar Division

J. S. Williams: from Ldr. Engrg. Sys. Proj. to *Mbr. Program Mgt. Staff* (W. V. Goodwin. Mrstn.)

K. C. Eddy: from Cl. "A" Eng. to *Ldr., D & D Engrs.* (N. Lesso, Mrstn.)

E. E. Fox: from Cl. "A" Eng. to *Ldr., D & D Engrs.* (E. Hatcher Mrstn.)

J. S. Daglian: from Cl. "B" Eng. to *Cl. "A" Engr.* (E. S. Lewis Mrstn.)

D. R. Higgs: from Cl. "A" Eng. to *Ldr., D & D Engr.* (W. L. Hendry, Mrstn.)

J. C. Kohr: from Log. Coord. to *Cl. "A" Engr.* (D. L. Lundgren, Mrstn.)

Systems Engineering, Evaluation, and Research

C. L. Moye: from Cl. "AA" Eng. to *Ldr., Sys. Engrg.* (E. E. Roberts, Mrstn.)

W. A. Triplett: from Cl. "AA" Eng. to *Ldr., Sys. Engrg.* (T. M. Johnston, Mrstn.)

Communications Systems Division

S. J. Davis: from AA Engr. to *Ldr. Systems Proj.* (K. Miller, Camden)

J. J. Davaro: from A Engr. to *Ldr. Engrg. Systems Proj.* (K. Miller, Camden)

Aerospace Systems Division

W. Moon: from Sr. Mbr. Auto. Test Equip. to *Adm., Advanced Techniques* (Mgr., Planning & Adv. Technology, Burl.)

H. K. Schlegelmilch: from Ldr. Radar Engr. to *Mgr., RF & Microwave* (Mgr., Radar Engineering, Burl.)

TUITION LOAN AND REFUND PLAN IMPROVED FOR GRADUATE STUDIES

The RCA Tuition Loan and Refund Program has been improved to provide increased financial assistance for approved graduate degree programs. The change, effective August 1, 1966 provides that the yearly loan or refund for RCA employees working toward advanced degrees under provisions of the plan is the actual tuition cost up to $300, plus 50% of the tuition cost above that amount up to a maximum of $500. (The previous maximum had been $325.)

The change was effected because: 1) Costs for graduate degree courses in many areas of the country have increased significantly in the past few years. 2) Continuing education, especially for those in the physical sciences, engineering, mathematics, and other professional fields, has become increasingly important.

No change has been made in the $225 maximum for undergraduate study.

Under the plan, RCA loans money to qualified employees to cover tuition costs for approved study courses. The loan is deducted in installments from the employee's pay, but the money is refunded upon successful completion of the course. For additional information about the Tuition Loan and Refund Program, contact the Personnel activity at your location.

NEW ENGLISH COLOR TUBE PLANT

The formation of *RCA Colour Tubes Limited* to manufacture RCA color TV picture tubes in England for the British and export markets has been announced by RCA and Radio Rentals Limited, one of Britain's leading manufacturers and distributors of television sets. The new company is owned two-thirds by RCA Great Britain Limited, the wholly owned British subsidiary of RCA, and one-third by Radio Rentals Limited. It will have production facilities at Skelmersdale, Lancashire, in a new plant to be completed for the start of operations in mid-1967.

NEW TECHNICAL EDUCATION COMMITTEE AT CSD-NY LABS

The CSD Advanced Communications Laboratory (ACL), New York, has established a Technical Education Committee to keep ACL engineers and scientists abreast of the state of the art in the various programs at ACL. The committee has scheduled a series of lunch-hour lectures by in-house speakers. The subjects include: ACL Communications, Trends in Technology; The Marketing-Engineering Team; FM Threshold Extension; Secure Voice Communications; Advanced Filter Techniques; Superconducting Resonators, and Microwave Power Sources.

PROGRAM TO TRAIN COMPUTER PERSONNEL

The first state supported program set up exclusively to train computer programmers and systems analysts through the use of an elaborate data communications network has been announced by the Oklahoma State Board for Vocational Education. Dr. Oliver Hodge, State Superintendent of Public Instruction, said the system, designed to alleviate the critical need for trained data processing personnel, initially will include nine RCA computers—one RCA Spectra 70/35 and eight RCA 301 systems, and peripheral equipment.

DME CUSTOM CIRCUIT FACILITY

The Defense Microelectronics (DME) activity has established a High Performance Custom Circuits (HPCC) facility at Somerville, N.J. The objective of HPCC is to provide defense engineering activities with: 1) Small quantities of custom microelectronic circuits for developmental work in which it is not technically and/or economically feasible to use available monolithic integrated circuits. 2) Production quantities of microelectronic circuits with performance characteristics not available in monolithic circuits.

In producing a circuit, HPCC's approach is to etch resistor-interconnect patterns on precoated substrates and then add available monolithic integrated-circuit chips and individual component chips. HPCC can provide larger value thin- and thick-film resistors and higher value (ceramic and MOS) capacitors than are available in ICs. Also, coils, transformers, and other special components not available in monolithics can be utilized in the special custom circuits.

Because HPCC, in effect, acts as the DEP central purchasing coordinating activity for microelectronic chip components (from RCA or other sources, if necessary), it is able to purchase them at quantity prices and to stock them. Thus, when a DEP activity orders a particular custom circuit, the availability of the materials at Somerville plus HPCC's simple, fast interconnection and bonding techniques makes it possible for HPCC to provide the special circuits quickly and relatively inexpensively. When circuits are needed in production quantities, HPCC will either produce them or arrange to produce them.

HPCC engineers, who have prepared approximately 50 different types of special circuits, estimate that currently available monolithic circuits can be used for approximately 70% of the microelectronic requirements in digital work, while custom circuits can be used for the remainder as well as for some analog applications.

In meeting specific requirements, HPCC custom circuits offer advantages over monolithic ICs such as: higher frequencies, higher power, denser array packaging, higher precision components, and better temperature stability with reliability equivalent to ICs inasmuch the same bonding techniques are employed.

Although the EC&D Special Electronic Components Division (SECD), which produces large quantities of monolithic ICs at the Somerville plant, is primarily concentrating its development work, as well as its production, on monolithics, SECD engineers and production personnel have provided appreciable support and assistance to HPCC personnel in the development and fabrication of the custom circuits. SECD and other EC&D activities are, of course, major suppliers of the components employed.

RCA TO SUPPLY LARGEST 2-WAY MOBILE RADIO SYSTEM

RCA Broadcast & Communications Products Division, Meadow Lands, Pa., has received a $4.2 million award from the New York City Transit Authority to provide the world's largest two-way mobile radio system for public transportation control and communications. RCA will supply 4,734 mobile radio units for buses and other vehicles, and 21 base stations and associated equipment over an 18-month period.

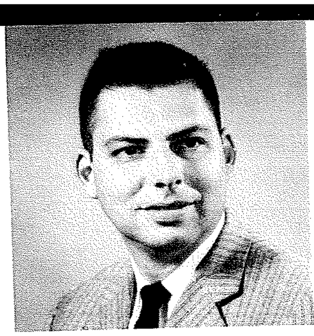

M. B. ALEXANDER, NEW ECD INDUSTRIAL SEMICONDUCTORS ED. REP.

Marvin B. Alexander, recently named RCA ENGINEER Editorial Representative for Industrial Semiconductor Engineering, Somerville, received a BA degree in Economics from Rutgers University in 1956 and subsequently did graduate work at Stevens Institute of Technology toward an MS degree in Industrial Management. After graduation in 1956, he joined Curtiss-Wright Corporation where he worked in the Quality Control Department. In 1958, Mr. Alexander joined RCA Semiconductor and Materials Division, as a Technical Writer. His responsibility in this area included rewriting and supervising the publication of Government Proposals and Reports. Mr. Alexander left RCA in 1960 to join Aero-projects, Incorporated as Senior Technical Writer where he was responsible for the preparation and publication of Government contract reports. In early 1961, he rejoined RCA as Coordinator, Technical Publications. He served in this capacity until May 1966 when he was appointed Engineering Administrator, Industrial Semicondutor Engineering Department.

CORRECTIONS:

In the article by **J. E. Volkmann** in the Aug-Sept 1966 issue, the graph appearing above the caption marked *Fig. 6* should have appeared above the caption marked *Fig. 4*, and vice versa. (on p. 42).

In the article by **J. W. Whelan** in the Feb-Mar 1966 issue, the photos comprising *Figs. 6c* and *6d* should be interchanged, the captions remaining as is (on p. 58).

—The Editors

PROFESSIONAL ACTIVITIES

Product Engineering Staff, Camden. **Al Pinsky** (Editor of *RCA Trend*) is serving as a member of the Executive Committee of the IEEE Philadelphia Section, and as Publicity Chairman, with responsibility for the section publication, *IEEE Almanac.*

Missile Test Project, Cape Kennedy, Fla.: **R. P. Murkshe** has been named both National President and Chairman of the Board of Governors at SPIE's 11th Technical Symposium in St. Louis in August. During the past year he was Executive Vice President. During the conference, Mr. Murkshe also served as chairman of the Range Instrumentation technical papers session. Assisting him as co-chairman of the session was **E. N. Bowker.**

Frank W. Hopkins, Jr., has been elected president of the Canaveral Chapter of the American Institute of Industrial Engineers. He previously has served the organization as Director and as a member of its local conference committee.

Two members of the RCA Missile Test Project have been elected President and Vice President of the Cape Kennedy Quality Control and Reliability Club. **Paul E. Bedard** will fill the presidency for the coming year, and **Kingsley E. Forry** will serve as Vice President.

Robert A. Mennella is serving as Assistant Planning Director and consultant for a Science Center to be established near Cape Kennedy by the Brevard County, Florida, Board of Public Instruction. Mr. Mennella will lend particular assistance in the area of instrument requirements and design. The Science center will include a planetarium, observatory, laboratory, optics workshop and other related facilities.

Some 41 members of the Missile Test Project's Data Processing and Systems Analysis organizations made presentations during the recent Seventh Range Users Data Conference held by the Air Force Eastern Test Range at Orlando AFB, Florida. The conference is an annual event sponsored by the Air Force in coordination with RCA MTP to acquaint Range Users with the capabilities available from the AFETR.

W. M. Sheahan, Manager of Range Photography for the Missile Test Project, has been elected a Governor of the Southeastern Region of the Society of Motion Picture and Television Engineers. Active in SMPTE for many years, Mr. Sheahan is a Fellow of the Society.

—T. L. Elliott, Jr.

Record Division, Indpls. **Robert C. Moyer** was chairman of the symposium on Automotive Tape Cartridge Systems Oct. 11 at the Audio Engineering Soc. meeting in New York.

DEP Central Engineering, Camden **M. S. Gokhale** participated in a Conference on Standardization organized by the Metropolitan New York Section of the Standards Engineers Society, at Saddle Brook, New Jersey on June 10, 1966. Presentation by Mr. Gokhale consisted of data on various aspects of "Budgeting for a Standards Department", based on an objective analysis of the problem without reference to any one industry. Data on "Cost Avoidance through Standardization" was also presented by him as a basis for discussion on this subject. At the invitation of the U.S. Department of State, Agency for International Development (USAID) and the Rensselaer Polytechnic Institute (RPI) School of Management, Mr. Gokhale also made a presentation on the importance of Standardization to a group of visitors from various industries in the Developing Countries, meeting in Troy, New York, during June.

ECD, Somerville, N.J.: **Dr. H. S. Veloric** is serving as Membership Chairman, N.Y. Area IEEE Electron Device Group.

—P. Farina

MSR, Moorestown, N.J.: **Ulrich Frank** has been appointed Chairman, Program Committee, IEEE professional group for Parts, Materials, and Packaging for the Philadelphia Chapter.

—L. W. Lazarick

ECD, Harrison, N.J.: **Robert McMurrough** was made chairman of the New York Section of the Electron Devices group of the IEEE. This includes No. N.J., N.Y.C., L.I, and Westchester.

—H. Wolkstein

ECD, Lancaster, Pa.: **L. D. Miller,** Dept. 980, attended the 14th National Iris Symposium held at Ft. Monmouth, New Jersey, on June 1-2. **A. G. Nekut** and **H. R. Krall,** Dept. 987 attended the Federation of American Societies for Experimental Biology meeting in Atlantic City, New Jersey, on April 17.

—R. L. Kauffman

Jules M. Forman, P.E., a past president of Lincoln Chapter, was recently appointed by the new President of Lincoln Chapter, PSPE, as the 1966-1967 Chairman of a Long Range Planning Committee. This special committee will be composed of only past presidents of Lincoln Chapter and the Chapter State Director. The committee will attempt to formulate improved plans and directions to strengthen the Chapter and enhance the concepts of professionalism. Mr. Forman, also was recently appointed by the State Society President-Elect, Mr. **R. L. Reitinger,** P.E., to serve as a member of the State Examination Committee for the Pennsylvania Society of Professional Engineers. Committee efforts will be applied to the strengthening of the examination phase of professionalism while aiding the State Registration Board.

—G. G. Thomas

CSD, Camden, N.J.: **David Shore** CSD Chief Engineer will be Chairman of the 1968 International Communication Conference to be held in Philadelphia in June of 1968.

—D. G. Hymas

Dr. Richard Guenther was Program Vice Chairman of the IEEE International Communications Conference held in Philadelphia on June 15-17, 1966.

Wes Fields is serving as Chairman, Philadelphia Chapter of IEEE-GEWS, Editor of the GEWS national *Newsletter*, and as a member of the GEWS Administrative Committee. In addition, he is Editor of *Standards Engineering* magazine, the journal of the Standards Engineering Society.

CSD, New York: **Seymour Krevsky,** CSD Advanced Communications Lab., N.Y., was elected Chairman of the New Jersey Coast Chapter, Communication Technology Group, IEEE.

M. P. Rosenthal completed Technical Writer's Institute, Rensselaer Polytech. Inst., Troy, N.Y. June 13-17, 1966.

—C. W. Fields

RCA Labs., Princeton, N.J.: In the Princeton Section of IEEE, from RCA Labs. the new officers (July 1966-June 1967) are: Chairman, **B. J. Lechner;** Vice Chairman, **G. B. Herzog;** Secretary-Treasurer, **H. L. Cooke;** and Editor of *PS*, Section Newsletter, **S. F. Dierk.**

—C. W. Sall

ASD, Burlington, Mass.: **David B. Dobson** was Chairman of the *Conference Record* Committee of the 1966 Aerospace and Electronic Systems Convention held at the Sheraton Park Hotel, Washington, D.C. on October 3, 4, 5, 1966. Mr. Dobson is Executive Editor of the *IEEE Transactions on Aerospace and Electronic Systems* and former Editor of *IEEE Transactions on Aerospace.* He also was Guest Editor of the July 1962 issue of the *IRE Transactions on Military Electronics* which was devoted to Automatic Testing Techniques.